

SCALING LIMIT OF THE COLORED ASEP AND STOCHASTIC SIX-VERTEX MODELS

AMOL AGGARWAL^{1,2}, IVAN CORWIN¹, MILIND HEGDE¹

¹ *Department of Mathematics, Columbia University, New York, NY USA.*

² *Clay Mathematics Institute, Denver, Colorado USA.*

ABSTRACT. We consider the colored asymmetric simple exclusion process (ASEP) and stochastic six vertex (S6V) model with fully packed initial conditions; the states of these models can be encoded by 2-parameter height functions. We show under Kardar-Parisi-Zhang (KPZ) scaling of time, space, and fluctuations that these height functions converge to the Airy sheet.

Several corollaries follow. For ASEP and the S6V model under the basic coupling, we consider the 4-parameter height function at position y and time t , with a step initial condition at position x and time $s < t$. Under KPZ scaling, we deduce its convergence to the directed landscape. We further prove that ASEP's under the basic coupling, with multiple general initial data, converge to KPZ fixed points coupled through the directed landscape. We moreover show that the colored ASEP stationary measures converge to the stationary horizon.

The starting point for our Airy sheet convergence result is an embedding of these colored models into a larger structure—a color-indexed family of coupled line ensembles with an explicit Gibbs property, i.e., a colored Hall-Littlewood line ensemble. The core of our work then becomes to develop a framework to analyze the edge scaling limit of these ensembles.

CONTENTS

1. Introduction	2
2. Models and statements of results	11
3. Colored q -Boson model, line ensembles, and Gibbs properties	24
4. Approximate LPP representation	38
5. Properties of ASEP and S6V	46
6. Preliminaries for line ensemble tightness	49
7. Airy sheet and tightness of S6V sheet	55
8. Weak monotonicity statements for one path	62
9. Lower tail estimates	66
10. Uniform separation of curves	76
11. Partition function and non-intersection probability estimates	88
12. Brownian Gibbs property in the limit	91
Appendix A. The Yang-Baxter equation, S6V, and the q -Boson model	94
Appendix B. Proofs of miscellaneous lemmas	99
Appendix C. LPP maximizer location asymptotics	105
Appendix D. Directed landscape and KPZ fixed point convergence	110
References	119

E-mail address: amolagga@gmail.com, ivan.corwin@gmail.com, mh4259@columbia.edu.

1. INTRODUCTION

1.1. **Preface.** The asymmetric simple exclusion process (ASEP) was introduced by MacDonald-Gibbs-Pipkin [MGP68] in 1968 in the biology literature, and by Spitzer [Spi70] in 1970 in the probability literature. The stochastic six-vertex (S6V) model was introduced in 1992 by Gwa-Spohn [GS92] in the physics literature (as a Markovian analog of the square ice model introduced by Pauling in 1935 in the chemistry literature [Pau35]). Interest in these models has come from applications across science, as well as connections to areas of mathematics such as interacting particle systems, conservation law differential equations, random matrix theory and quantum integrable systems.

In this paper we focus on the colored (also called multi-species, -type, or -class) versions of the above models, in which each particle is assigned an integer “color” (or “priority”). The colored ASEP was introduced soon after its uncolored version, arising naturally from the basic coupling developed by Liggett and Harris in the 1970s [Lig76, Har78]. Since then, colored ASEP has been intensely investigated, both as a means to analyze uncolored ASEP and as a multi-component lattice gas of intrinsic interest (including as an archetypal model for understanding nonlinear fluctuating hydrodynamics; see the survey of Spohn [Spo14b]). The colored S6V model weights were introduced in the 1980s by Bazhanov [Baz85] and Jimbo [Jim86], which were used to define a Markov process more recently by Kuniba-Mangazeev-Maruyama-Okado [KMMO16] and Borodin-Wheeler [BW22].

A basic question about both systems is to understand their limiting fluctuations, after being run for a long time. Especially over the past decade, a fairly complete answer to this question has been attained for uncolored ASEP. This topic has an extensive history (dating at least back to the physics work of van Beijeren-Kutner-Spohn [BKS85]). The first one-point fluctuation results under step initial conditions were proven by Johansson [Joh00] for the uncolored totally asymmetric simple exclusion process (TASEP) and by Tracy-Widom [TW09] for uncolored ASEP. The most general results now known have identified the full scaling limit for the fluctuations of uncolored ASEP under arbitrary initial conditions, after dividing time by a large parameter t , space by $t^{2/3}$, and fluctuations by $t^{1/3}$; these are commonly called the Kardar-Parisi-Zhang (KPZ) [KPZ86] exponents in one dimension (see the surveys of Corwin [Cor12] and Quastel-Spohn [QS15]). This was shown for uncolored TASEP in [MQR21] by Matetski-Quastel-Remenik, where the scaling limit was introduced and named the KPZ fixed point, using exact determinantal formulas for TASEP due to Borodin-Ferrari-Prähofer-Sasamoto [BFPS07]. Quastel-Sarkar later extended this to the uncolored ASEP (and KPZ equation) in [QS22], by a careful comparison of its generator to that of uncolored TASEP (for the KPZ equation, a different proof was also given by Virág [Vir20]).

Less is known for the uncolored S6V model. One-point fluctuation results were proven by Borodin-Corwin-Gorin [BCG16] under step initial conditions, by adapting the coordinate Bethe ansatz analysis implemented in [TW09] for ASEP. This exact analysis was later extended by Dimitrov [Dim23] to obtain the scaling limit of its two-point height fluctuations (assuming the S6V asymmetry parameter $q \in [0, 1)$ is sufficiently small).

In spite of considerable activity in recent years, progress on the colored ASEP and S6V model has been more limited. Stochastic dualities for them were uncovered by Belitsky-Schütz [BS18], Kuan [Kua18], and Chen-de Gier-Wheeler [CGW20]. Explicit formulas for (q -deformed) moments of their height functions were found by Borodin-Wheeler [BW20], Bufetov-Korotkikh [BK21], and de Gier-Mead-Wheeler [GMW23]. However, even for colored TASEP, it remains open how to extract asymptotics from these results (outside of work by Chen-de Gier-Hiki-Sasamoto-Usui [CGHSU22] proving one-point convergence for a different colored TASEP model from the one studied here). Instead, the most fruitful way of obtaining fluctuation results for colored models had previously been through matching results, identifying certain marginals of the colored model with those of the uncolored ones; see the works of Borodin, Bufetov, Galashin, Gorin, Wheeler, and Zhang [BW22,

BB21, BGW22, Gal21, Zha23]. This matching framework is potent but, since it can only capture specific marginals of the colored models, it cannot identify their full universal scaling limit.

Even from a conjectural standpoint, what this universal scaling limit should exactly be has only come into focus within the past few years. It is given by the Airy sheet and directed landscape, introduced in 2018 by Dauvergne-Ortmann-Virág [DOV22]. These objects were originally constructed in a different context, namely, as scaling limits for Brownian last passage percolation (LPP). This is a model on $\mathbb{R} \times \mathbb{N}$, in which one has a notion of directed paths and an environment of independent Brownian motions $\mathbf{B} = (B_1, B_2, \dots)$; for each k , we view B_k as associated with the k^{th} row of the system. Any directed path is assigned a random weight, given by an integral of the noise along it. The LPP value between two given points (x, i) and (y, j) , denoted by $\mathbf{B}[(x, i) \rightarrow (y, j)]$, is the maximum weight over all directed paths connecting them; all of these LPP values between different pairs of points are coupled through the common random environment \mathbf{B} . The Airy sheet $\mathcal{S} : \mathbb{R}^2 \rightarrow \mathbb{R}$ is then the random function prescribing the $n \rightarrow \infty$ limit, under KPZ scaling, of these coupled LPP values across all pairs of points on the 1^{st} and n^{th} rows. Specifically, setting $\varepsilon = n^{-1}$,

$$\varepsilon^{1/3} \left(\mathbf{B}[(2\varepsilon^{-2/3}x, \varepsilon^{-1}) \rightarrow (2\varepsilon^{-2/3}y + \varepsilon^{-1}, 1)] - 2\varepsilon^{-1} + 2(x - y)\varepsilon^{-2/3} \right) \text{ converges to } \mathcal{S}(x, y),$$

as $\varepsilon \rightarrow 0$. The directed landscape is more generally the joint KPZ scaling limit of this coupling of LPP values across all possible pairs of points in the system (on possibly different pairs of rows).

The Airy sheet and directed landscape have since been shown to be scaling limits for various other solvable LPP and polymer models. These include Poissonian, exponential, and geometric LPP, and the Seppäläinen-Johansson and Poisson lines models, by Dauvergne-Nica-Virág [DNV23, DV21b], as well as the KPZ equation by Wu [Wu23]. These works all use the Robinson-Schensted-Knuth (RSK) correspondence (or its geometric analog due to Noumi-Yamada [NY04]) to equate the original LPP (or polymer) model with a “dual” one, whose environment is given by an ensemble of correlated random curves (such as Dyson Brownian motion in the case of Brownian LPP). In the dual model, all LPP values happen to be asymptotically determined by only the environment given by the curves near the top of the ensemble. The ensemble’s top edge converges to a universal scaling limit called the Airy line ensemble, which was originally introduced by Prähofer-Spohn [PS02] in terms of its finite-dimensional distributions, and later realized as an ensemble of continuous random curves by Corwin-Hammond [CH14]. This suggests that the scaling limit of the original model is given by an LPP across the Airy line ensemble; indeed, this is how the Airy sheet was defined in [DOV22].

While this RSK framework is well-suited to (solvable) LPP and polymer models, the Airy sheet and directed landscape are also believed to arise as scaling limits for other models in the KPZ universality class. This particularly includes colored interacting particle systems, such as ASEP and S6V. However, an appropriate variant of the RSK correspondence has not been found in such contexts; in fact, the relevant hypothetical output of such a correspondence, an exact representation for the system as a “dual” LPP or polymer, is not known (or really expected) to exist for colored ASEP or S6V in general. Partly for this reason, until now there had been no proof of convergence to the Airy sheet or directed landscape for any colored interacting particle system.

The purpose of this paper is to provide one for the colored ASEP and S6V.

1.2. Sample result. Here we state one of our results for the colored ASEP; our conventions for this system are as follows. Across every bond of \mathbb{Z} , independently and in continuous time, we swap colors at rates 1 or $q \in [0, 1)$ depending on whether the colors along the bond are in reverse order (e.g., 2—1) or order (e.g., 1—2), respectively; see Figure 1. We start under the “packed” initial condition, with site k occupied by a particle of color $-k$, for each $k \in \mathbb{Z}$; this is equivalent to infinitely many uncolored ASEPs, the k^{th} one with a step initial condition at $-k \in \mathbb{Z}$, evolving jointly under the

basic coupling. The colored ASEP height function $h(x, 0; y, t)$ is defined as the number of particles of color at least $-x$, whose location at time t exceeds y . See Figure 2 for a simulation.

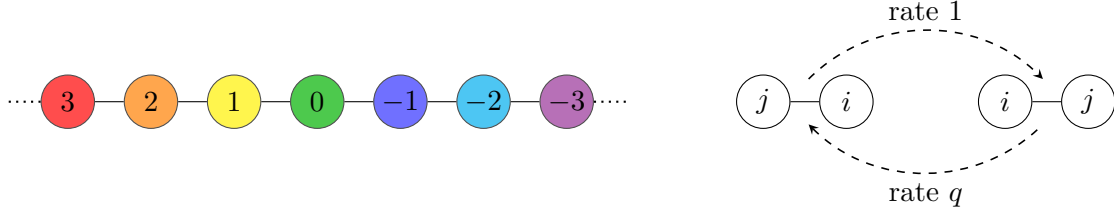


FIGURE 1. The colored ASEP. On the left is the packed initial condition; the number inside the circle is the color of the particle. On the right are the transition rates, where $i < j$.

One of our main results states that, after KPZ rescaling, the colored ASEP height function $h(\cdot, 0; \cdot, t)$ converges to the Airy sheet \mathcal{S} (see Definition 2.3 for its precise description). To lighten the notation in this introductory section, we only state a special case of that result (corresponding to the choice $\alpha = 0$ for the velocity in the rarefaction fan); this will make the underlying normalization constants as simple as possible. For the most general version of the below result, see Theorem 2.8.

Theorem 1.1 (Theorem 2.8, $\alpha = 0$ case). *Fix $q \in [0, 1)$. The rescaled colored ASEP height function*

$$\varepsilon^{1/3} \left(\varepsilon^{-1} + 2(x - y)\varepsilon^{2/3} - 2h(2\varepsilon^{-2/3}x, 0; 2\varepsilon^{-2/3}y, 2\varepsilon^{-1}(1 - q)^{-1}) \right) \text{ converges to } \mathcal{S}(x, y),$$

where $\mathcal{S}(x, y)$ is the Airy sheet, weakly as $\varepsilon \rightarrow 0$ as continuous functions on \mathbb{R}^2 , under the topology of uniform convergence on compact sets.

All other results about ASEP that we prove herein follow as quick corollaries of this theorem (sometimes, together with existing results in the literature). First, while the above result states a scaling limit in space, it directly implies that the space-time scaling limit for the colored ASEP under packed initial conditions is given by the directed landscape (Corollary 2.12 (1)). It follows by projection (also called color merging) that for any $k \geq 1$ the space-time scaling limit of ASEP with k colors under step initial condition is (a marginal of) the directed landscape (Corollary 2.12 (2) and Remark 2.13). Second, we generalize the initial conditions of these results by combining

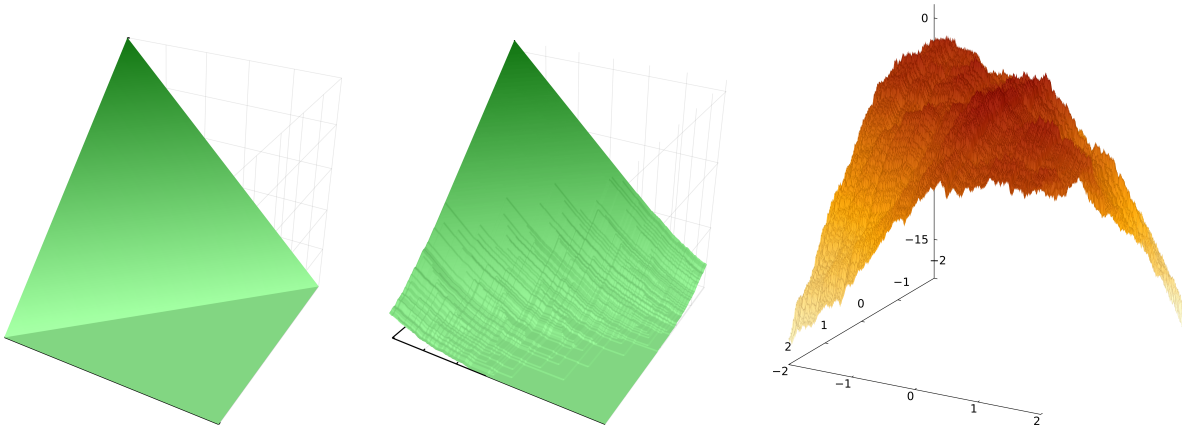


FIGURE 2. Simulations of the colored ASEP height function $(x, y) \mapsto h(x, 0; y, t)$ under packed initial conditions, with $q = 0.3$. The vertical axis is the height, and the other two axes are the x and y coordinates. On the left is the height function at $t = 0$, and in the middle is its crop at $t \approx 300$. On the right is its KPZ rescaling, on $[-2, 2]^2$ and at time $t = 4000$.

them with those in [QS22] that showed KPZ fixed point convergence for a single uncolored ASEP under arbitrary initial conditions; we deduce (Corollary 2.12 (3)) that multiple uncolored ASEPs under the basic coupling, each started from an arbitrary initial condition, converge to KPZ fixed points coupled through the directed landscape. Third, by combining this with results of Busani-Seppäläinen-Sørensen [BSS22, BSS23], we deduce (Corollary 2.14) that the colored ASEP stationary measures converge to the stationary horizon, a limit introduced by Busani in [Bus24].

For the colored S6V model, we similarly prove its height function converges to the Airy sheet, after KPZ rescaling; see Theorem 2.18. The directed landscape space-time scaling limits under packed initial data (Corollary 2.20) then follows in a similar way as for ASEP. The stationary measures for the colored S6V coincide with those of the colored ASEP, so the stationary horizon convergence of the latter implies the same for the former. We do not prove the S6V analogs of convergence from general initial data under the basic coupling, as we do not currently have a S6V counterpart of the result from [QS22].

To briefly describe the proofs of our results, we focus on the colored S6V model, whose discrete structure enables a more direct analysis. Our results on colored S6V can then be transferred to colored ASEP through an effective coupling between ASEP and S6V (see Lemma 5.2).

The starting point for analyzing the colored S6V with $n \geq 1$ colors is an embedding, originally due to Aggarwal-Borodin [AB24], of its height function as the top curves of a structure that we call a “colored Hall-Littlewood line ensemble.” In [AB24] this was proved as a consequence of the Yang-Baxter equation (we also provide a short, self-contained explanation here in Appendix A, tailored to our special case), extending prior works of Borodin-Bufetov-Wheeler [BBW24], Bufetov-Mucciconi-Petrov [BP19, BMP21], and Aggarwal-Borodin-Bufetov [ABB19] proving similar results in the uncolored case.

The colored Hall-Littlewood line ensemble is a family of n line ensembles, one indexed by each color, where a “line ensemble” is a random infinite collection of Bernoulli paths; see the right side of Figure 3, where $n = 2$ (and only the top three walks in each ensemble are depicted). The law of this colored line ensemble is described through certain local and explicit Boltzmann weights, which provide it with a Gibbs property that gives the law of its paths (of every color) in any given interval, conditional on the colored line ensemble outside of that interval. This couples its n constituent line ensembles (of all colors) in a concrete but highly nontrivial way. We refer to any such structure as a “colored Gibbsian line ensemble” (see [AB24] for other examples).

Due to this embedding, to identify the scaling limit of the colored S6V model, it suffices to pinpoint the scaling limit for the top curves of the colored Hall-Littlewood line ensemble. Most of this paper is devoted to this task. Over the past decade, a substantial theory has developed around the asymptotic analysis of Gibbsian line ensembles that are uncolored (that is, have $n = 1$ colors), since the papers [CH14, CH16] initiating a framework for proving their tightness. That uncolored context differs from our colored one, in that we must now understand how the n lines ensembles in our colored family asymptotically couple together, as opposed to only understanding how any individual line ensemble in the family behaves marginally.

To do so, we will address these two issues separately, by proving the following two statements.

- (1) *Identifying the coupling* (Theorem 3.20): All of the line ensembles in the colored family are approximately determined via an LPP problem across just one of them (namely, the line ensemble indexed by the minimal color).
- (2) *Airy limit of the determining ensemble* (Theorem 3.19): This “determining” line ensemble converges around its top edge to the parabolic Airy line ensemble.

Hence, the other colored line ensembles converge to limits determined by LPP problems in the parabolic Airy line ensemble; as discussed above, this is how the Airy sheet was defined [DOV22].

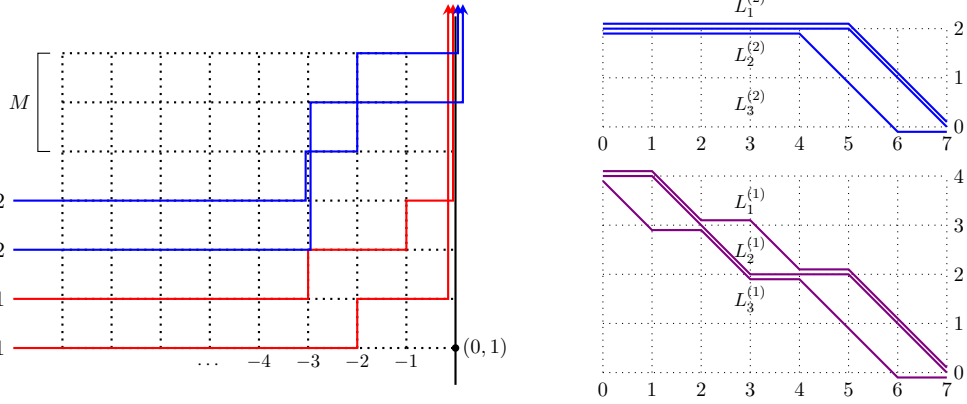


FIGURE 3. On the left is a colored q -Boson model (where color 1 is red and color 2 is blue). On the right is its associated colored line ensemble $L = (L^{(1)}, L^{(2)})$ (where $L^{(1)}$ is purple, and $L^{(2)}$ is blue).

Let us briefly comment on the two statements above. The first can be viewed as a substitute for the above-mentioned “dual” LPP (or polymer) representation that was used in [DOV22, DNV23, DV21b, Wu23] to analyze LPP (and polymer) models, though now its underlying algebraic source is the Yang-Baxter equation instead of the RSK correspondence. Indeed, it enables the colored S6V (and ASEP) height functions to be interpreted as LPP values across a dual environment given by the determining line ensemble in the colored family, but now only approximately (instead of exactly).

On the second statement, this determining line ensemble can be shown to marginally have the structure of an uncolored Gibbsian line ensemble that was first studied by Corwin-Dimitrov [CD18]; they observed that it does not satisfy the Fortuin-Kasteleyn-Ginibre (FKG) inequality, i.e., does not admit monotone couplings. To prove its tightness (which is the main new input needed to access its edge scaling limit, due to characterization results of Dimitrov-Matetski [DM21] or Aggarwal-Huang [AH23b]), we must thus circumvent many prior uses of monotonicity, which requires an appreciable reworking of the theory developed in [CH14, CH16]. See Section 1.3.3 for further discussion.

Before proceeding, let us make two remarks. First, as shown in [AB24, Figure 1], the structure of colored Gibbsian line ensembles is common to a wide class of stochastic models studied in integrable probability. These colored ensembles are of differing complexities but are likely to be of a similar qualitative nature to the colored Hall-Littlewood line ensemble studied here. Thus, this paper could serve as a blueprint for accessing the Airy sheet scaling limits for these other models (where the strong characterization result for the Airy line ensemble proven in [AH23b] is likely to play a more vital role). Second, the approximate LPP representation of the colored line ensembles in terms of a “determining” one applies for quite general initial data, not only the packed one; this might serve as a starting point for the direct analysis of these models from general initial conditions. We do not pursue either of these points further here and leave them as future directions.

The remainder of this section is a more detailed proof outline, to act as an informal guide (focusing on the main ideas and intuition) for readers examining the arguments of this paper in greater detail.

1.3. Proof outline.

1.3.1. Colored Hall-Littlewood line ensemble. The colored S6V model (see Section 2.3 for a precise definition) is a system of up-right directed random paths, each assigned an integer color. At every vertex, a weight is assigned depending on the configuration of colored paths adjacent to it. Given parameters $q \in [0, 1)$ and $z \in (0, 1)$, these weights are depicted below, where we assume $i < j$:

1	$\frac{q(1-z)}{1-qz}$	$\frac{1-z}{1-qz}$	$\frac{1-q}{1-qz}$	$\frac{z(1-q)}{1-qz}$

These weights satisfy a Yang-Baxter equation that relates them to those of a different system called the (discrete) colored q -Boson model. This is also a system of colored paths, but where vertical edges may now accommodate arbitrarily many colored arrows (while horizontal edges still accommodate at most one); see the left side of Figure 3. The explicit forms for its weights, which are not stochastic, lead to the colored Hall-Littlewood Gibbs property; the probability of a configuration of paths in this model is equal to the product of all vertex weights, suitably normalized. These vertex weights are given below, where we again assume $i < j$, and we let $A_{[k,\ell]}$ denote the number of arrows of color in the interval $[k, \ell]$ that are vertically entering the vertex (writing A_k if $k = \ell$):

1	$(1 - q^{A_i})q^{A_{[i+1,N]}}$	1	$(1 - q^{A_j})q^{A_{[j+1,N]}}$	0	$q^{A_{[i+1,N]}}$

In [AB24] the Yang-Baxter equation was shown to imply a distributional match between the colored S6V model and a colored q -Boson model on the negative quadrant $\mathbb{Z}_{<0} \times \mathbb{Z}$ (see the left side of Figure 3), identifying the law of the former’s height function with the marginal law of the latter’s rightmost column; this colored q -Boson model is also sometimes called a “colored Hall-Littlewood process” [BW22, Section 1.6]; the $n = 1$ case of this object (with just one color) is called an uncolored Hall-Littlewood process. The paper [AB24] developed these types of matching results for considerably more general fused vertex models. Here, we only require the colored S6V model special case of that framework, whose Yang-Baxter equation origin is relatively quick to explain conceptually. Appendix A provides a self-contained proof of the result we use from [AB24].

The colored q -Boson model on the negative quadrant gives rise in a fairly direct way to a colored line ensemble, which we call the colored Hall-Littlewood line ensemble (see Section 3.2). Specifically, we set the location of the i^{th} curve of the color j line ensemble at site y to be the number of paths in the colored q -Boson model of color at least j that pass strictly above the point $(-i, y)$; see Figure 3. The fact that the colored q -Boson model is prescribed by local Boltzmann weights implies a local Gibbs property for the full color-indexed collection of line ensembles. However, each constituent line ensemble in this colored family (except for the “first” one corresponding to all the colors in the system) will usually not marginally satisfy a Gibbs property on its own.

This correspondence identifies the rightmost column of the colored q -Boson model with the first (topmost) curves of the n line ensembles in the colored family. Therefore, the distributional match described above implies that the height function of the colored S6V model embeds as the first curves in the colored line ensemble (see Proposition 3.12). Extracting the large scale limit for the colored S6V model thus reduces to doing so for the above colored Gibbsian line ensemble around its (top) edge. This task simplifies considerably when $q = 0$, so we will first discuss that case (where our results are still new). We then explain what must be done to extend our results to all $q \in [0, 1)$.

1.3.2. *Simplifications and asymptotics when $q = 0$.* The weights of the colored (and uncolored) q -Boson model simplify when $q = 0$ to be either zero or one. This has several useful consequences.

First, in the case of only one color, the uncolored Hall-Littlewood line ensemble (i.e., uncolored Hall-Littlewood process), whose topmost curve encodes the uncolored S6V height function, becomes at $q = 0$ an ensemble of independent Bernoulli random walks conditioned on not intersecting. This is a Schur process, which is known to be a determinantal point process by work of Okounkov-Reshetikhin [OR03]. The finite-dimensional distributions around the top edge of the ensemble can therefore be computed exactly and shown to converge as $t \rightarrow \infty$ to those of the Airy line ensemble. The convergence can then be upgraded to functional convergence of the curves by use of the non-intersecting Gibbs property and existing techniques in the theory of Gibbsian line ensembles, facilitated by the key property of monotone coupling that holds in this $q = 0$ case: Gibbs measures with ordered boundary conditions can likewise be stochastically ordered.

Now we pass to multiple colors. The colored $q = 0$ S6V height function is again related to the top curves of a colored line ensemble, consisting of a collection of several line ensembles indexed by color. The line ensemble corresponding to the lowest color in this family, which we assume to be 1 (as we may, by a color merging projection), has the marginal law of an uncolored line ensemble, in this case the above Schur process (Proposition 3.17). The other line ensembles in the colored family are nontrivially coupled to this 1-colored one via the colored $q = 0$ Boson weights. Let us explain how to extract the joint asymptotics for the 1-colored and 2-colored line ensembles; the case for more colors then follows inductively.

We begin by examining the 1-colored line ensemble and conclude (as described above) that it marginally converges around its top edge to the parabolic Airy line ensemble. Next, conditioned on the 1-colored line ensemble, we study the 2-colored one. As all $q = 0$ Boson weights are either zero or one, this second line ensemble is seen to be determined completely by the first one. We then prove (Theorem 3.20), through a careful inspection of these $q = 0$ Boson weights, that the 2-colored line ensemble can be realized as an LPP problem (via a suitable ‘‘Pitman transform’’) across the 1-colored one. Therefore, the first and second line ensembles jointly converge in the scaling limit to a parabolic Airy line ensemble and an LPP problem across it, giving the Airy sheet.

Turning this back into the $q = 0$ colored S6V model, this implies the convergence of its height function under KPZ scaling to the Airy sheet. In the limit to ASEP, this shows that the height function for the colored TASEP under packed initial condition also converges to the Airy sheet.

When $q > 0$, there are two obstructions in implementing the approach sketched above. The first is in extracting the edge limit of the uncolored Hall-Littlewood line ensemble; the second is in extracting the joint limit of the coupled line ensembles.

1.3.3. *Edge limit for uncolored line ensembles ($q > 0$).* For $q > 0$ the basic input in Section 1.3.2, the convergence of the uncolored Hall-Littlewood line ensemble to the parabolic Airy one, is no longer known; the reason is that the former (and likewise, S6V and ASEP) is not determinantal.

Hence, we adopt a more probabilistic route, by showing that any subsequential edge limit of the Hall-Littlewood line ensemble is Brownian Gibbsian; this means that it satisfies the Gibbs property for non-intersecting Brownian bridges, called the Brownian Gibbs property. This, with the recent strong characterization for Brownian Gibbsian line ensembles established in [AH23b], would then uniquely identify the limit as the parabolic Airy line ensemble. For ASEP, the use of [AH23b] can be bypassed by instead using results in [QS22, DM21] (though one must still verify the Brownian Gibbs property); see Remark 6.7.

Assuming tightness under KPZ scaling of the Hall-Littlewood line ensemble around its top edge, the Brownian Gibbs property for subsequential limits follows from the Gibbs property of prelimits, along with Kolmós-Major-Tusnády type couplings between random walks and Brownian bridges.

The main effort therefore rests in proving this tightness; the inputs we will need to do this are its Gibbs property and known [BCG16] one-point asymptotics for its top curve.

Previous works establishing full tightness for Gibbsian line ensembles all make substantial use of a monotonicity property (FKG inequality), stating that if one increases the boundary data then all of its paths stochastically increase. This monotonicity property is false for the Hall-Littlewood line ensemble, a fact originally observed in [CD18], where this Gibbs property was first studied. That work showed tightness of the top curve of the Hall-Littlewood line ensemble by way of a much weaker form of monotonicity wherein, upon changing boundary conditions, certain one-point probabilities change monotonically up to a large constant. In order to extend tightness to an arbitrary number of curves, one could pursue such a weak form of monotonicity involving more curves. We were unable to produce a suitable generalization.

To explain the method we instead use, we first informally describe the Hall-Littlewood Gibbs property (see Section 3.3 for a more precise definition). It states that the law of the top k curves on a spatial interval (a, b) conditioned on the entire external state of the ensemble only depends on the boundary data, i.e., the height of the top k curves at $\{a, b\}$ and that of the $(k + 1)^{\text{st}}$ curve on $[a, b]$. The conditioned law is given explicitly by a reweighting of the law for k Bernoulli random walk bridges with the same boundary data, conditioned to neither intersect each other nor the $(k + 1)^{\text{st}}$ curve. The weight is proportional to a product of factors (one for each position) equal to either 1 or $1 - q^d$, where d is the distance between two consecutively labeled curves at that position. The latter factor only occurs when the height difference between two consecutive curves decreases by 1.

Now, to establish tightness of our line ensemble, we show that it suffices to *a priori* demonstrate a reasonable degree of separation between its curves. Indeed, since q is fixed, the factors $1 - q^d$ approach 1 as the distances d between the curves grows; although many such factors may exist in the product (up to the size of the spatial interval, of order $t^{2/3}$), if we can show a separation of $d \gg \log t$ with high probability, then the reweighting factor becomes very close to 1. We therefore incur little error by replacing these factors by 1, after which the tightness analysis follows from arguments similar to those used in previously studied models.

It therefore suffices to show this *a priori* separation between curves. This is the primary technical component of the proof for tightness and is done by induction. Using the Gibbs property and the one-curve weak monotonicity (a minor refinement of that in [CD18]), we first prove that the k^{th} curve in the line ensemble is uniformly bounded below, assuming that the first $k - 1$ curves are uniformly separated (which holds trivially at $k = 1$); then we show that the first k curves are likely separated at one spatial coordinate, using the control on how far down the k^{th} curve can be; and finally we conclude that the first k curves are uniformly separated across the full spatial interval. See Section 9 for further details.

1.3.4. *Approximate LPP representation for other colors ($q > 0$).* As with the uncolored Gibbs property, the colored Gibbs property becomes more involved when $q > 0$; its weights are not all equal to zero or one. So, the 2-colored line ensemble in the family is now not deterministic upon conditioning on the 1-colored one (which has the marginal law of an uncolored Hall-Littlewood line ensemble; see Proposition 3.17). In particular, the representation of the former as an LPP problem across the latter is no longer exactly true when $q > 0$.

We instead prove that this LPP representation remains approximately true with high probability for any $q \in [0, 1)$; see Theorem 3.20. Our proof of this fact is combinatorial. While the colored q -Boson weights are not all equal to zero or one conditional on the 1-colored line ensemble, they involve certain powers of q (namely, factors of $q^{A[k, \ell]}$). We show that these powers become quite large, thereby exponentially penalizing the 2-colored line ensemble, if the latter substantially differs from being an LPP problem across the 1-colored one. Since $q < 1$, this can be used to prove the above approximate LPP representation; see Section 4 for more details.

Using this approximate LPP representation, and the convergence of the uncolored Hall-Littlewood line ensemble to the parabolic Airy one, our Airy sheet limit results follow just as in the $q = 0$ case.

Notation. For $a, b \in \mathbb{Z}$ with $a < b$, $\llbracket a, b \rrbracket := \{a, \dots, b\}$, $\llbracket a, \infty \rrbracket := \{a, a + 1, \dots\}$, and $\llbracket -\infty, a \rrbracket := \{a, a - 1, \dots\}$. Symbols written in bold face such as \mathbf{A} or \mathbf{v} will represent vectors or tuples. For a finite set A , $\#A$ will denote its cardinality. For $a, b \in \mathbb{R}$, $a \wedge b$ is shorthand for $\min(a, b)$.

For random objects X and Y taking values in some measurable space, $X \stackrel{d}{=} Y$ means that their distributions are the same; we will often omit explicitly specifying the σ -algebra on the target space, but will specify its topology (in which case we endow the space with the associated Borel σ -algebra). For random objects X_n and X taking values in some common topological space, $X_n \xrightarrow{d} X$ means that X_n converges weakly to X ; the topological space will be specified or obvious in the context. We will sometimes abuse notation and say $X_n \xrightarrow{d} \mu$ for some probability measure μ on the same space. The space of continuous functions from a topological space \mathcal{X} to \mathbb{R} will be denoted $\mathcal{C}(\mathcal{X}, \mathbb{R})$. $\mathcal{N}(m, \sigma^2)$ will denote the normal distribution with mean m and variance σ^2 . For a σ -algebra \mathcal{F} , $\mathbb{P}_{\mathcal{F}}$ and $\mathbb{E}_{\mathcal{F}}$ are shorthand for the conditional probability and conditional expectation given \mathcal{F} . Events will be written in sans serif font, e.g., \mathbf{E} , and \mathbf{E}^c will denote the complement of \mathbf{E} .

We will sometimes write $f(\cdot)$ for a function of the variable \cdot , and sometimes $x \mapsto f(x)$. For $\mathbf{f} = (f_1, f_2, \dots)$ a collection of continuous functions, $\mathbf{f}[(\cdot, \cdot) \rightarrow (\cdot, \cdot)]$ will denote the last passage percolation values in the environment given by \mathbf{f} , and is defined ahead in Definition 2.2.

Organization of paper. Section 2 precisely defines our models and states our main results. Section 3 introduces the colored q -Boson model and colored Hall-Littlewood line ensemble; explains the latter's relation to the colored S6V model; sets up a framework for the convergence of the uncolored line ensemble to the parabolic Airy line ensemble (Theorem 3.19); and states the approximate last passage percolation representation of the colored Hall-Littlewood line ensemble (Theorem 3.20). Section 4 proves the latter result. Section 5 explains how to fit ASEP into the vertex model framework of the other arguments. Section 6 begins setting up the ingredients for the proof of Theorem 3.19 and gives its proof assuming them. Section 7 gives the proofs of our main results. Sections 8–12 concern the proofs of the ingredients of Theorem 3.19: Section 8 explains the weak monotonicity property our arguments rely on; Sections 9 and 10 contain the inductive argument yielding lower tail control of lower curves in the line ensemble as well as their uniform separation; Section 11 uses these to obtain control on the partition function; and Section 12 uses the same to establish all subsequential limits of the uncolored line ensembles have the Brownian Gibbs property.

There are also four appendices. Appendix A gives a self-contained proof of the mapping from [AB24], between the colored S6V model and the colored q -Boson model, using the Yang-Baxter equation. Appendices B and C give routine proofs of certain miscellaneous lemmas and of asymptotics of last passage percolation and maximizer values across the parabolic Airy line ensemble. Appendix D gives the proofs of convergence results of the colored ASEP to the directed landscape and coupled KPZ fixed point and colored S6V to the directed landscape, using an idea communicated to us by Shalin Parekh, combined with an approximate monotonicity result in the S6V case.

Code for simulations. Code for simulations of the ASEP sheet (as in the third panel of Figure 2) is available in the arXiv source for this article.

Acknowledgements. The authors wish to thank Shalin Parekh for explaining an approach to arrive at directed landscape (and coupled KPZ fixed points) convergence from our main result of Airy sheet convergence (which, with his gracious permission, we have included in this text); Evan Sorensen for discussions related to the stationary horizon and his work [BSS23]; and Alexei Borodin for discussions about colored stochastic vertex models and for helpful comments on an earlier draft of this manuscript. Amol Aggarwal was partially supported by a Packard Fellowship for Science

and Engineering, a Clay Research Fellowship, by the NSF through grant DMS-1926686, and by the IAS School of Mathematics. Ivan Corwin was partially supported by the NSF through grants DMS-1937254, DMS-1811143, DMS-1664650, by the Simons Foundation through an Investigator Award and through the W.M. Keck Foundation through a Science and Engineering Grant. Milind Hegde was partially supported by the NSF grant through grant DMS-1937254.

2. MODELS AND STATEMENTS OF RESULTS

Here we define our limiting objects (Section 2.1) and the models of study in this article and state our results (Section 2.2 for ASEP and Section 2.3 for stochastic six-vertex).

2.1. The Airy line ensemble, Airy sheet, and directed landscape. In this section we define our limiting objects. We start with the parabolic Airy line ensemble, which is needed to give the definitions of the Airy sheet and the directed landscape.

2.1.1. Parabolic Airy line ensemble.

Definition 2.1 (Parabolic Airy line ensemble). The *parabolic (and stationary) Airy line ensembles* $\mathcal{P}, \mathcal{A} : \mathbb{N} \times \mathbb{R} \rightarrow \mathbb{R}$ are \mathbb{N} -indexed families of random non-intersecting continuous curves $(\mathcal{P}_i(\cdot))_{i \in \mathbb{N}} := (\mathcal{P}(i, \cdot))_{i \in \mathbb{N}}$ and $(\mathcal{A}_i(\cdot))_{i \in \mathbb{N}} := (\mathcal{A}(i, \cdot))_{i \in \mathbb{N}}$, related by

$$\mathcal{P}_i(x) := \mathcal{A}_i(x) - x^2.$$

The finite-dimensional distributions of \mathcal{A} are determinantal with kernel the extended Airy kernel $K_{\text{Ai}}^{\text{ext}}$ given by

$$K_{\text{Ai}}^{\text{ext}}((x, t); (y, s)) := \begin{cases} \int_0^\infty e^{-\lambda(t-s)} \text{Ai}(x + \lambda) \text{Ai}(y + \lambda) d\lambda & t \geq s \\ - \int_{-\infty}^0 e^{-\lambda(t-s)} \text{Ai}(x + \lambda) \text{Ai}(y + \lambda) d\lambda & t < s, \end{cases}$$

where Ai is the classical Airy function. This means the following (adopting the notation $(t_j, y_j) \in \mathcal{A}$ for the existence of some k such that $\mathcal{A}_k(t_j) = y_j$ and $d\mathbb{P}$ for the density with respect to Lebesgue measure): for every $m \in \mathbb{N}$ and $(t_1, y_1), \dots, (t_m, y_m) \in \mathbb{R}^2$,

$$d\mathbb{P}\left((t_j, y_j) \in \mathcal{A} \text{ for } j = 1, \dots, m\right) = \det\left[K_{\text{Ai}}^{\text{ext}}((y_i, t_i); (y_j, t_j))\right]_{1 \leq i, j \leq m} \prod_{j=1}^m dy_j. \quad (2.1)$$

These finite-dimensional distributions were first discovered in [PS02] (see also [Joh03]), and the existence of such an ensemble was shown in [CH14, Theorem 3.1] (and the uniqueness follows from the prescription (2.1) of the finite-dimensional distributions).

The distribution of $\mathcal{A}_1(0)$ is known as the *GUE Tracy-Widom distribution* (discovered much earlier in random matrix theory [TW94]).

An alternative, more probabilistic, description of the Airy line ensemble is that it is the unique [AH23b] family of continuous random curves satisfying what is known as the Brownian Gibbs property; see Definition 6.4 and Proposition 6.6 for more details.

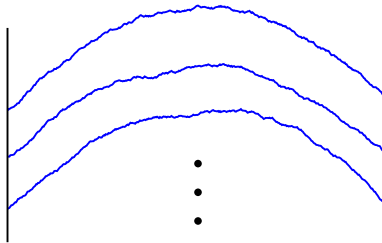


FIGURE 4. A depiction of the parabolic Airy line ensemble.

2.1.2. *Last passage percolation.* We next introduce the notion of a last passage percolation (LPP) problem; this will be needed in defining the Airy sheet, as well as in some of our proofs.

Definition 2.2 (Last passage percolation). Given real numbers $u < v$, a sequence of continuous functions $\mathbf{f} = (f_1, f_2, \dots, f_n)$ with $f_i : [u, v] \rightarrow \mathbb{R}$ for each $i \in \llbracket 1, n \rrbracket$, and natural numbers $j < k \leq n$, we define the LPP value from (u, k) to (v, j) in the environment given by \mathbf{f} by (where $t_{j-1} = v$ and $t_k = u$)

$$\mathbf{f}[(u, k) \rightarrow (v, j)] = \sup_{t_k < \dots < t_{j-1}} \sum_{i=j}^k (f_i(t_{i-1}) - f_i(t_i)). \quad (2.2)$$

2.1.3. *Airy sheet, directed landscape, and KPZ fixed point.* The Airy sheet is defined via a coupling with the parabolic Airy line ensemble.

Definition 2.3 (Airy sheet, [DOV22, Definition 8.1]). The *Airy sheet* $\mathcal{S} : \mathbb{R}^2 \rightarrow \mathbb{R}$ is the unique (in law) random continuous function such that:

- (i) *Stationarity:* \mathcal{S} has the same law as $\mathcal{S}(\cdot + x, \cdot + x)$ for all $x \in \mathbb{R}$; and
- (ii) *Coupling with \mathcal{P} :* \mathcal{S} can be coupled with a parabolic Airy line ensemble \mathcal{P} such that $\mathcal{S}(0; \cdot) = \mathcal{P}_1(\cdot)$ and for all $(x, y, z) \in \mathbb{Q}_{>0} \times \mathbb{Q}^2$, almost surely,

$$\mathcal{S}(x; y) - \mathcal{S}(x; z) = \lim_{k \rightarrow \infty} \left(\mathcal{P}[(-\sqrt{k/2x}, k) \rightarrow (y, 1)] - \mathcal{P}[(-\sqrt{k/2x}, k) \rightarrow (z, 1)] \right). \quad (2.3)$$

The existence and uniqueness of the Airy sheet is established in [DOV22, Proposition 8.2 and Theorem 8.3].

The Airy sheet can be thought of as a marginal of a four-parameter space-time object (the parameters being a pair of space-time coordinates) when the two time coordinates are set to be 0 and 1. This four-parameter object is known as the directed landscape and is in fact constructed from the Airy sheet in a manner analogous to the construction of Brownian motion from the Gaussian distribution. We turn to defining it next. In what follows, we let $\mathbb{R}_+^4 := \{(x, s; y, t) \in \mathbb{R}^4 : s < t\}$.

Definition 2.4 (Directed landscape, [DOV22, Definition 10.1]). The *directed landscape* is the unique (in law) random continuous function $\mathcal{L} : \mathbb{R}_+^4 \rightarrow \mathbb{R}$ that satisfies the following properties.

- (i) *Airy sheet marginals:* For any $s \in \mathbb{R}$ and $t > 0$ the increment over time interval $[s, s + t)$ is a rescaled Airy sheet:

$$(x, y) \mapsto \mathcal{L}(x, s; y, s + t) \stackrel{d}{=} (x, y) \mapsto t^{1/3} \mathcal{S}(xt^{-2/3}; yt^{-2/3}).$$

- (ii) *Independent increments:* For any $k \in \mathbb{N}$ and disjoint time intervals $\{(s_i, t_i) : i \in \llbracket 1, k \rrbracket\}$, the random functions

$$(x, y) \mapsto \mathcal{L}(x, s_i; y, t_i)$$

are independent as $i \in \llbracket 1, k \rrbracket$ varies.

- (iii) *Metric composition law:* Almost surely, for any $r < s < t$ and $x, y \in \mathbb{R}$,

$$\mathcal{L}(x, r; y, t) = \max_{z \in \mathbb{R}} \left(\mathcal{L}(x, r; z, s) + \mathcal{L}(z, s; y, t) \right).$$

The existence and uniqueness of the directed landscape is proved in [DOV22, Theorem 10.9].

We also need to introduce height functions from general initial conditions in the directed landscape.

Definition 2.5 (KPZ fixed point). Let UC be the space of upper semi-continuous functions $f : \mathbb{R} \rightarrow \mathbb{R} \cup \{-\infty\}$ satisfying $f(x) \leq m|x| + c$ for some $m, c < \infty$ and all $x \in \mathbb{R}$. For a function

$\mathfrak{h}_0 \in \text{UC}$, and $t > 0$, define the *KPZ fixed point* $(y, t) \mapsto \mathfrak{h}(\mathfrak{h}_0; y, t) : \mathbb{R} \times (0, \infty) \rightarrow \mathbb{R}$ started from \mathfrak{h}_0 at time 0 by

$$\mathfrak{h}(\mathfrak{h}_0; y, t) := \sup_{x \in \mathbb{R}} \left(\mathfrak{h}_0(x) + \mathcal{L}(x, 0; y, t) \right). \quad (2.4)$$

The KPZ fixed point was first defined in [MQR21] as a Markov process on UC (with the topology of local UC convergence, i.e., local Hausdorff convergence of hypographs; see [MQR21, Section 3.1]) by specifying its transition kernel through explicit formulas. This was later shown to be equivalent to (2.4), which arises as a scaling limit of solvable last passage percolation models, in [NQR20, Corollary 4.2]. Note that a natural coupling of $\mathfrak{h}(\mathfrak{h}_0^{(j)}; y, t)$ for different initial conditions $\mathfrak{h}_0^{(j)}$ is obtained by using the same directed landscape \mathcal{L} in the variational formula.

2.2. Colored ASEP. The colored (also called multi-species, -type, or -class) asymmetric simple exclusion process is an interacting particle system on \mathbb{Z} , where each particle has an associated *color*, which is an integer (multiple particles may share the same color). There is also an asymmetry parameter $q \in [0, 1)$ which is fixed. At time zero, we have a particle of some color at each site of \mathbb{Z} , which is encoded by the configuration $\eta_0 = (\eta_0(i))_{i \in \mathbb{Z}} \in \mathbb{Z}^{\mathbb{Z}}$, where $\eta_0(i)$ is the color of the particle at site i . The state at any later time t will be denoted by η_t .

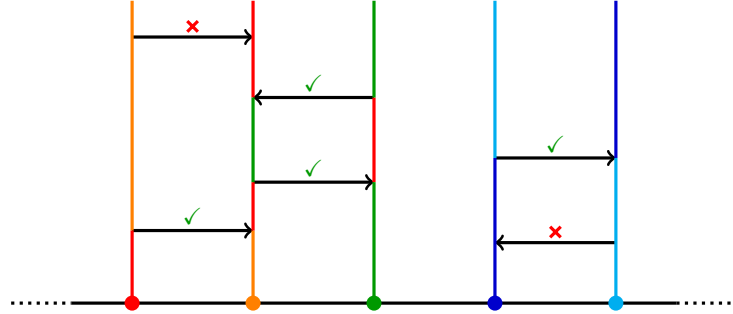


FIGURE 5. A depiction of the graphical construction of colored ASEP. In this illustration, initially particles are in decreasing color from left to right. The arrows indicate the times where a left clock ξ_x^L or right clock ξ_x^R rang. If an arrow goes from site x to site y at time t and the color at time t^- of the particle at x is greater than that of the particle at y , the particles swap positions at time t (indicated by a green check mark); if not, nothing happens (red cross).

2.2.1. The dynamics. We may construct the dynamics of colored ASEP using a variant of Harris' graphical construction [Har78] (see Figure 5). Fix a family of independent Poisson clocks $\xi = \{\xi_x^L, \xi_x^R\}_{x \in \mathbb{Z}}$, one pair for each site in \mathbb{Z} , with ξ_x^L of rate q and ξ_x^R of rate 1. Given the randomness of the clocks, the dynamics are deterministic. When the clock ξ_x^L rings, the particle at site x attempts a jump to the left by one site, and when ξ_x^R rings, it attempts a jump to the right by one site. The attempt succeeds if the particle at the target site is of color lower than the particle attempting to jump, and fails otherwise. If the attempt succeeds, the two particles swap positions. The well-definedness of this description follows from [Har78, Section 10]. Note that higher colors have higher priority, in contrast to the dynamics in terms of “classes”, where typically particles of higher class have lower priority (e.g., second class particles in comparison to first class particles). Our convention is consistent with behavior of higher color arrows in the colored S6V model that we will shortly introduce.

The *uncolored (or single-species) ASEP* corresponds to the case when there are only two colors in the system; in the typical terminology, the particles of higher color are referred to as particles, while the particles of lower color are referred to as holes.

Remark 2.6. An important property of colored ASEP is known as *color merging*. It says that one can project colored ASEP onto one of fewer colors by declaring all particles of color lying in a given interval $I \subseteq \mathbb{Z}$ to be the same color (which is itself an element of I , or, more generally, lies between the largest color below I in the system and the smallest color above I in the system); that this holds is readily apparent from the above description of the dynamics. Equivalently, any function $f : \mathbb{Z} \cup \{-\infty\} \rightarrow \mathbb{Z} \cup \{-\infty\}$ which is weakly monotone commutes with the Markov semigroup of the process; in particular, after merging colors we may relabel the groups in such a way that the relabeling maintains the order of the groups. The case of obtaining uncolored ASEP from colored ASEP is a particular example of color merging.

2.2.2. Packed and step initial conditions. The initial condition we will work with from now on unless otherwise specified is the *packed initial condition*, where we have a particle of color i at site $-i$ for each $i \in \mathbb{Z}$. By color merging, we can easily obtain the case of *step initial condition* for finitely many colors (and thus uncolored ASEP in the case of two colors): for integers $\ell_k < \dots < \ell_1$, we merge the colors in $[-\infty, \ell_k]$ to have color k ; those in $[\ell_{i+1} + 1, \ell_i]$ to have color i for $i = 1, \dots, k - 1$; and those in $[\ell_1 + 1, \infty)$ to have color 0.

We note that under the packed initial condition, η_t is a permutation on \mathbb{Z} (i.e., $\eta_t : \mathbb{Z} \rightarrow \mathbb{Z}$ is a bijection), and thus colored ASEP can be thought of as a Markov chain on such permutations in which transpositions are applied at rate q or 1 depending on whether the entries are sorted or not respectively. In this sense, our results can be understood as a scaling limit for this infinite random transposition model.

2.2.3. The ASEP sheet. As mentioned, we are now working with the packed initial condition. The first observable of ASEP that we study, called the *colored height function* is defined, for $t \geq 0$, by

$$h^{\text{ASEP}}(x, 0; y, t) := \#\{z > y : \eta_t(z) \geq -x\}, \quad (2.5)$$

or, in words, it is the number of particles of color greater than or equal to $-x$ which are strictly to the right of y at time t . Equivalently, it is the number of particles that were initially at or to the left of x which are strictly to the right of y at time t . It can also be thought of as a collection indexed by $x \in \mathbb{Z}$ of coupled copies of the uncolored ASEP's height function or current under step initial condition from x (i.e., a particle at every site at or to the left of x), by writing it as $(h^{\text{ASEP}}(x, 0; \cdot, t))_{x \in \mathbb{Z}}$. We will refer to this coupling as the *colored coupling*; it agrees with the well-known basic coupling, which we will introduce in more detail in Section 2.2.6.

Our results concern the scaling limit of this collection of height functions, which we define next. Let $\gamma = 1 - q$ and fix $\alpha \in (-1, 1)$. Let $\mu^{\text{ASEP}}(\alpha)$ and $\sigma^{\text{ASEP}}(\alpha)$ be defined by

$$\mu(\alpha) = \mu^{\text{ASEP}}(\alpha) := \frac{1}{4}(1 - \alpha)^2 \quad \text{and} \quad \sigma(\alpha) = \sigma^{\text{ASEP}}(\alpha) := \frac{1}{2}(1 - \alpha^2)^{2/3}, \quad (2.6)$$

and let the spatial scaling factor $\beta^{\text{ASEP}}(\alpha)$ be given by

$$\beta(\alpha) = \beta^{\text{ASEP}}(\alpha) := \frac{2\sigma(\alpha)^2}{|\mu'(\alpha)|(1 - |\mu'(\alpha)|)} = 2(1 - \alpha^2)^{1/3}. \quad (2.7)$$

Definition 2.7 (ASEP sheet). For $\varepsilon > 0$, we define the *ASEP sheet* $\mathcal{S}^{\text{ASEP}, \varepsilon} : \mathbb{R}^2 \rightarrow \mathbb{R}$, for x and y such that the arguments of h^{ASEP} below are integers, by

$$\begin{aligned} \mathcal{S}^{\text{ASEP}, \varepsilon}(x; y) := & \sigma(\alpha)^{-1} \varepsilon^{1/3} \left(\mu(\alpha) 2\varepsilon^{-1} + \mu'(\alpha) \beta(\alpha) (y - x) \varepsilon^{-2/3} \right. \\ & \left. - h^{\text{ASEP}}(\beta(\alpha) x \varepsilon^{-2/3}, 0; 2\alpha \varepsilon^{-1} + \beta(\alpha) y \varepsilon^{-2/3}, 2\gamma^{-1} \varepsilon^{-1}) \right); \end{aligned} \quad (2.8)$$

the values at all other x, y are determined by linear interpolation.

Thus the ASEP sheet captures the spatial scaling limit of the colored ASEP at time $2\gamma^{-1}\varepsilon^{-1}$.

2.2.4. *An explanation of the scalings.* Let us say a few words on a heuristic to understand the scalings in Definition 2.7. The $\varepsilon^{-2/3}$ spatial scaling and $\varepsilon^{1/3}$ factor outside come from the KPZ universality class scaling exponents (see the surveys [Cor12, QS15]). We evaluate the height function at time $2\gamma^{-1}\varepsilon^{-1}$ for the following reasons. The factor of 2 is essentially just a convention; it allows us to include fewer constant factors in the definition of $\mathcal{S}^{\text{ASEP},\varepsilon}$ to ensure that it will converge to \mathcal{S} and matches the conventions in earlier works such as [MQR21, QS22]. On the other hand, the factor of γ^{-1} is important as it allows all other scaling constants to not depend on q ; in other words, by speeding up the process by the single particle drift, all ASEP (i.e., corresponding to different values of q) look the same on the fluctuation scale, a fact which was previously known for various marginals. Finally, α controls the macroscopic velocity of the particles around which we look, and the range $(-1, 1)$ of α corresponds to the full “rarefaction” fan of the step initial condition’s hydrodynamic limit shape (as given by $\mu(\alpha)$).

Next we explain the definitions of $\mu(\alpha)$ and $\sigma(\alpha)$ from (2.6) and $\beta(\alpha)$ from (2.7), as well as their role in (2.8). Essentially, the latter two are chosen such that in the limit, the local diffusion rate and parabolic curvature of $y \mapsto \mathcal{S}^{\text{ASEP},\varepsilon}(0; y)$ are 2 and 1 respectively, matching those of the parabolic Airy line ensemble (Definition 2.1). More precisely, it is known [Ros81, BF87, Rez91] (see also [TW09, Theorem 3] or [BO17, Theorem 11.3]) that the first order behavior of $h^{\text{ASEP}}(0, 0; 2\alpha\varepsilon^{-1}, 2\gamma^{-1}\varepsilon^{-1})$ is $\mu(\alpha) \cdot 2\varepsilon^{-1} = \frac{1}{4}(1 - \alpha)^2 \cdot 2\varepsilon^{-1}$ (i.e., $\mu(\alpha) = \lim_{\varepsilon \rightarrow 0} \varepsilon h^{\text{ASEP}}(0, 0; \alpha\varepsilon^{-1}, \gamma^{-1}\varepsilon^{-1})$); thus, locally, one would expect the process to behave like a Bernoulli random walk (with increments of 0 or -1) with drift $\mu'(\alpha) = \frac{d}{d\alpha} \frac{1}{4}(1 - \alpha)^2 = -\frac{1}{2}(1 - \alpha)$, which must be subtracted off to see the fluctuations. Finally, note that the local curvature of the limit profile is $\frac{1}{2}\mu''(\alpha) = \frac{1}{2} \frac{d^2}{d\alpha^2} \frac{1}{4}(1 - \alpha)^2 = \frac{1}{4}$ and the approximately Bernoulli random walk behavior has increment variance $|\mu'(\alpha)|(1 - |\mu'(\alpha)|) = \frac{1}{4}(1 - \alpha^2)$. The spatial scaling factor of $\beta(\alpha)$ and the external factor of $\sigma(\alpha)^{-1}$ are chosen such that

$$\beta(\alpha)|\mu'(\alpha)|(1 - |\mu'(\alpha)|)\sigma(\alpha)^{-2} = 2 \quad \text{and} \quad \frac{1}{4}\beta(\alpha)^2\mu''(\alpha)\sigma(\alpha)^{-1} = 1, \quad (2.9)$$

i.e., the local diffusion rate is 2 and the local curvature is 1; for the latter relation, note that there is an extra factor of $\frac{1}{2}$ compared to the curvature discussion above. This arises because we are looking at the process with an extra factor of 2 in the time coordinate; more precisely, it arises because we expect $\mathcal{S}^{\text{ASEP},\varepsilon}(0; y)$ to be approximately

$$\begin{aligned} & \mu \left(\frac{1}{2\varepsilon^{-1}}(2\alpha\varepsilon^{-1} + \beta(\alpha)y\varepsilon^{-2/3}) \right) \cdot 2\varepsilon^{-1} \\ & \approx \left(\mu(\alpha) + \beta(\alpha)\mu'(\alpha)y\varepsilon^{-2/3} \cdot (2\varepsilon^{-1})^{-1} + \frac{1}{2}\mu''(\alpha)\beta(\alpha)^2y^2\varepsilon^{-4/3} \cdot \frac{1}{(2\varepsilon^{-1})^2} \right) \cdot 2\varepsilon^{-1}, \end{aligned}$$

and we see the factor of $\frac{1}{2}$ coming from simplifying $(2\varepsilon^{-1})/(2\varepsilon^{-1})^2$ in the last term.

These scaling coefficients can also be derived from the general KPZ scaling theory explained in [Spo14a], which makes use of information about the stationary measures of the system (and indeed the above explanation shares many features with this theory). Thus we expect relations of the form (2.9), which allows one to derive $\sigma(\alpha)$ from an expression for the law of large numbers $\mu(\alpha)$, to hold in greater generality.

2.2.5. *Main result for ASEP.* Our main result for colored ASEP is proven in Section 7.1.

Theorem 2.8 (Airy sheet convergence for ASEP). *Fix any asymmetry $q \in [0, 1)$ and any velocity $\alpha \in (-1, 1)$ in the rarefaction fan. Then, as $\varepsilon \rightarrow 0$, $\mathcal{S}^{\text{ASEP},\varepsilon} \xrightarrow{d} \mathcal{S}$ weakly in $\mathcal{C}(\mathbb{R}^2, \mathbb{R})$ under the topology of uniform convergence on compact sets.*

In the rest of Section 2.2, we give various consequences of Theorem 2.8 (some of which are obtained on combining with existing results in the literature). This requires us to first introduce the basic coupling.

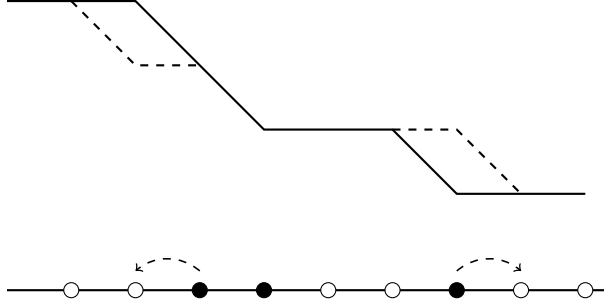


FIGURE 6. A depiction of a Bernoulli path h_0 and the associated particle configuration η_{h_0} . The dashed portions of the path illustrate the definition of the new height function, under the corresponding displayed particle movements.

2.2.6. *The basic coupling.* The graphical construction of ASEP provided in Section 2.2.1 provides a natural way to couple together the evolution of uncolored ASEP from all choices of initial conditions—this is also called the *basic coupling*.

Consider countably many initial conditions $\eta_0^{(1)}, \eta_0^{(2)}, \dots \in \{0, 1\}^{\mathbb{Z}}$, where $\eta_0^{(j)}(i)$ represents the state at location i in the j^{th} initial condition, with 0 for a hole and 1 for a particle. To define the basic coupling, as in Section 2.2.1, we fix a family of independent Poisson clocks $\xi = \{\xi_x^L, \xi_x^R\}_{x \in \mathbb{Z}}$. Then we evolve $\eta_0^{(j)}$ for each j according to the dynamics described in Section 2.2.1, where we use the same family of clocks ξ for all $j \in \mathbb{N}$. For example, if ξ_x^L rings at time t , then the particle at location x in the configuration $\eta_t^{(j)}$ attempts a jump to the left for each $j \in \mathbb{N}$.

We observe that this coupling recovers the colored coupling in the case that the set of particle locations in $\eta_0^{(j+1)}$ is a subset of those in $\eta_0^{(j)}$ for each j , i.e., $\eta_0^{(j+1)}(x) = 1$ implies $\eta_0^{(j)}(x) = 1$; in colored ASEP, this corresponds to the initial condition with the particle at site x having color $\min\{j \geq 0 : \eta_0^{(j+1)}(x) = 0\} = \#\{j : \eta_0^{(j)}(x) = 1\}$. Of course, the basic coupling itself is more general since it allows the coupling of arbitrary initial conditions.

We also note that we may consider the same evolution, using the fixed Poisson clocks, of an initial condition started at time $s > 0$, i.e., we set the configuration at time s to be some η and apply the dynamics from Section 2.2.1 from there. In this way the basic coupling gives a coupling of initial conditions started at different times as well.

Using the basic coupling, we can define a four parameter process extending the ASEP sheet, which we call the ASEP landscape; here, the two additional parameters arise from allowing the time at which the colored height function is evaluated, as well as the time at which the evolution from the step initial condition is begun, to vary. We first define the evolution of the uncolored ASEP height function from an arbitrary initial condition or an initial height function; this definition is more general than (2.5) in that it allows initial particle configurations which are not right-finite, i.e., it is possible to have infinitely many particles initially to the right of zero.

Definition 2.9 (Bernoulli path). Let $\Lambda \subseteq \mathbb{Z}$ be a (possibly infinite) interval. We say a function $\gamma : \Lambda \rightarrow \mathbb{Z}$ is a *Bernoulli path* if $\gamma(x+1) - \gamma(x) \in \{0, -1\}$ for all x with $x, x+1 \in \Lambda$.

Let $h_0 : \mathbb{Z} \rightarrow \mathbb{Z}$ be a Bernoulli path. We define an associated configuration η_{h_0} by

$$\eta_{h_0}(y) := h_0(y-1) - h_0(y); \quad (2.10)$$

see Figure 6. Note that, in the case that $h_0(y) = 0$ for all large enough y , h_0 is related to η_{h_0} by $h_0(y) = \sum_{i=y+1}^{\infty} \eta_{h_0}(i)$; this is exactly the case of a right-finite initial condition.

For $h_0 : \mathbb{Z} \rightarrow \mathbb{Z}$ a Bernoulli path and $s \geq 0$, define the (uncolored) height function $(y, t) \mapsto h^{\text{ASEP}}(h_0, s; y, t)$ for $t > s$ and $y \in \mathbb{Z}$ as follows (see also Figure 6). For a function f with left limits, we use the notation $f(r^-) := \lim_{s \uparrow r} f(s)$; note that this does not require $f(r)$ to be defined.

Start ASEP under basic coupling at time s with initial particle configuration η_{h_0} . Whenever a particle jumps from y to $y + 1$ at time $r > s$, define $h^{\text{ASEP}}(h_0, s; y, r) = h^{\text{ASEP}}(h_0, s; y, r^-) + 1$ (and $h^{\text{ASEP}}(h_0, s; x, r) = h^{\text{ASEP}}(h_0, s; x, r^-)$ for all $x \neq y$), and whenever a particle jumps from y to $y - 1$ at time r , define $h^{\text{ASEP}}(h_0, s; y - 1, r) = h^{\text{ASEP}}(h_0, s; y - 1, r^-) - 1$ (and $h^{\text{ASEP}}(h_0, s; x, r) = h^{\text{ASEP}}(h_0, s; x, r^-)$ for all $x \neq y - 1$). The utility of the definition of $h^{\text{ASEP}}(h_0, s; y, t)$ is that, while the ASEP dynamics only sees the discrete derivative of h_0 (through η_{h_0}), here we keep track of the constant shift in h_0 as well.

For multiple initial conditions $(h_0^{(j)})_{j=1}^\infty$ and times $s_j > 0$, we couple the height functions $(y, t) \mapsto h^{\text{ASEP}}(h_0^{(j)}, s_j; y, t)$ using the basic coupling for the underlying ASEP dynamics.

2.2.7. The ASEP landscape. Now we may define the unscaled version of the ASEP landscape. For $x, y \in \mathbb{Z}$ with $x < y$ and $0 < s < t$, we overload the notation and define

$$h^{\text{ASEP}}(x, s; y, t) := h^{\text{ASEP}}(h_{0,x}, s; y, t),$$

coupled via the basic coupling, where

$$h_{0,x}(z) := (x - z)\mathbb{1}_{z \leq x}.$$

In words, we start the ASEP under basic coupling at time s with a step initial condition at x , and then evaluate the height function at location y at time t .

It follows immediately that this definition generalizes the definition of $h^{\text{ASEP}}(x, 0; y, t)$ from (2.5) as a process in x , y , and t . We also note that $h^{\text{ASEP}}(\cdot, s; \cdot, \cdot)$ corresponds to starting colored ASEP with packed initial condition at time s , coupled (for different values of s) to the same environment of Poisson clocks.

We now define the ASEP landscape and the scaled general initial condition height function.

Definition 2.10 (ASEP landscape). Recall $\mu(\alpha)$, $\sigma(\alpha)$, and $\beta(\alpha)$ from (2.6) and (2.7). For $\varepsilon > 0$, the *ASEP landscape* is defined by

$$\begin{aligned} \mathcal{L}^{\text{ASEP}, \varepsilon}(x, s; y, t) := & \sigma(\alpha)^{-1} \varepsilon^{1/3} \left(\mu(\alpha)(t - s) \cdot 2\varepsilon^{-1} + \mu'(\alpha)\beta(\alpha)(y - x)\varepsilon^{-2/3} \right. \\ & \left. - h^{\text{ASEP}}(\beta(\alpha)x\varepsilon^{-2/3}, 2\gamma^{-1}\varepsilon^{-1}s; 2\alpha(t - s)\varepsilon^{-1} + \beta(\alpha)y\varepsilon^{-2/3}, 2\gamma^{-1}\varepsilon^{-1}t) \right). \end{aligned}$$

As in the case of $\mathcal{S}^{\text{ASEP}, \varepsilon}$ in (2.8), this definition is for those x, y such that the arguments of h^{ASEP} are integers, and the value at all other x, y are determined by linear interpolation.

Definition 2.11. For general initial condition h_0 , we define a scaled version of $h^{\text{ASEP}}(h_0, 0; y, t)$

$$\begin{aligned} \mathfrak{h}^{\text{ASEP}, \varepsilon}(h_0; y, t) := & \sigma(\alpha)^{-1} \varepsilon^{1/3} \left(\mu(\alpha)t \cdot 2\varepsilon^{-1} + \mu'(\alpha)\beta(\alpha)y\varepsilon^{-2/3} \right. \\ & \left. - h^{\text{ASEP}}(h_0, 0; 2\alpha t\varepsilon^{-1} + \beta(\alpha)y\varepsilon^{-2/3}, 2\gamma^{-1}\varepsilon^{-1}t) \right), \end{aligned}$$

for y such that the argument of h^{ASEP} is an integer, and by linear interpolation elsewhere.

The next corollary of Theorem 2.8 gives the scaling limit of the ASEP landscape, as well as of the height functions under general initial conditions coupled via the basic coupling. This will be proven in Appendix D, using an idea communicated to us by Shalin Parekh. For a set \mathcal{T} , we define $\mathcal{T}_<^2 := \{(s, t) \in \mathcal{T}^2 : s < t\}$. Below, for a topological space \mathcal{X} and a set A , $\mathcal{C}(\mathcal{X}, \mathbb{R})^A$ is endowed the product topology (across A) of the topology on $\mathcal{C}(\mathcal{X}, \mathbb{R})$ of uniform convergence on compact sets.

Corollary 2.12 (Directed landscape and KPZ fixed point convergence for ASEP). *Fix $q \in [0, 1)$ and a countable set $\mathcal{T} \subseteq [0, \infty)$. Then, the following limits hold as $\varepsilon \rightarrow 0$.*

(1) (Directed landscape). *For any velocity $\alpha \in (-1, 1)$, in $\mathcal{C}(\mathbb{R}^2, \mathbb{R})^{\mathcal{T}_<^2}$,*

$$\left(\mathcal{L}^{\text{ASEP}, \varepsilon}(\cdot, s; \cdot, t) \right)_{(s,t) \in \mathcal{T}_<^2} \xrightarrow{d} \left(\mathcal{L}(\cdot, s; \cdot, t) \right)_{(s,t) \in \mathcal{T}_<^2}.$$

(2) As a special case, for any $\alpha \in (-1, 1)$, $k \in \mathbb{N}$ and $x_k < \dots < x_1$, in $\mathcal{C}(\mathbb{R}, \mathbb{R})^{\llbracket 1, k \rrbracket \times \mathcal{T}}$,

$$\left(\mathcal{L}^{\text{ASEP}, \varepsilon}(x_i, 0; \cdot, t)\right)_{i \in \llbracket 1, k \rrbracket, t \in \mathcal{T}} \xrightarrow{d} \left(\mathcal{L}(x_i, 0; \cdot, t)\right)_{i \in \llbracket 1, k \rrbracket, t \in \mathcal{T}}.$$

(3) (Coupled KPZ fixed point). Fix $\alpha = 0$. For each $i \in \{1, \dots, k\}$, suppose $h_0^{(i), \varepsilon} : \mathbb{Z} \rightarrow \mathbb{Z}$ is a sequence of (possibly random, and independent of the ASEP dynamics) Bernoulli paths and $\mathfrak{h}_0^{(i)} : \mathbb{R} \rightarrow \mathbb{R}$ is a (possibly random, and independent of \mathcal{L}) continuous function. Assume they satisfy $\mathfrak{h}_0^{(i)}(x) \leq C(1 + |x|^{1/2})$ for some $C < \infty$ almost surely for all $x \in \mathbb{R}$ and $i \in \llbracket 1, k \rrbracket$, such that $x \mapsto \mathfrak{h}_0^{(i), \varepsilon}(x) := -2\varepsilon^{1/3}(h_0^{(i), \varepsilon}(2x\varepsilon^{-2/3}) + x\varepsilon^{-2/3})$ converges to $\mathfrak{h}_0^{(i)}$ as $\varepsilon \rightarrow 0$ for $i = 1, \dots, k$ jointly in distribution under the topology of uniform convergence on compact sets (where we regard $\mathfrak{h}_0^{(i), \varepsilon}(\cdot)$ as a continuous function by linear interpolation). Then, in $\mathcal{C}(\mathbb{R}, \mathbb{R})^{\llbracket 1, k \rrbracket \times \mathcal{T}}$,

$$\left(\mathfrak{h}^{\text{ASEP}, \varepsilon}(h_0^{(i), \varepsilon}; \cdot, t)\right)_{i \in \llbracket 1, k \rrbracket, t \in \mathcal{T}} \xrightarrow{d} \left(\mathfrak{h}(\mathfrak{h}_0^{(i)}; \cdot, t)\right)_{i \in \llbracket 1, k \rrbracket, t \in \mathcal{T}},$$

where the lefthand side is coupled via the basic coupling and the righthand side is coupled as in (2.4) under the same directed landscape \mathcal{L} .

Item (3) is stated only for $\alpha = 0$ as its proof will use the marginal convergence (i.e., for each j separately) of $\mathfrak{h}^{\text{ASEP}, T}(h_0^{(j)}; y, t)$ to $\mathfrak{h}(\mathfrak{h}_0^{(j)}; y, t)$ from [QS22], which is stated and proved therein only for $\alpha = 0$.

Note that the convergence to the directed landscape and KPZ fixed point stated here is for times in a fixed countable set, and not uniform convergence as a continuous function for all times in an interval. Obtaining the latter form of convergence would require proving certain tightness estimates on ASEP as a temporal process that we do not pursue here.

Remark 2.13 (Scaling limit of ASEP with finitely many colors). By color merging, Corollary 2.12 (2) is equivalent to the following statement on the space-time scaling limit of colored ASEP with finitely many colors. Let $k \in \mathbb{N}$, $\alpha \in (-1, 1)$, and fix real numbers $x_k < \dots < x_1$. Consider colored ASEP with initial condition of holes (or particles of color zero) at locations $\llbracket \lfloor \beta(\alpha)x_1\varepsilon^{-2/3} \rfloor + 1, \infty \rrbracket$; particles of color k at locations $\llbracket -\infty, \lfloor \beta(\alpha)x_k\varepsilon^{-2/3} \rfloor \rrbracket$; and particles of color i at all locations in $\llbracket \lfloor \beta(\alpha)x_{i+1}\varepsilon^{-2/3} \rfloor + 1, \lfloor \beta(\alpha)x_i\varepsilon^{-2/3} \rfloor \rrbracket$ for $i = 1, \dots, k-1$. By color merging, $(y, t) \mapsto (\mathcal{L}^{\text{ASEP}, \varepsilon}(x_1, 0; y, t), \dots, \mathcal{L}^{\text{ASEP}, \varepsilon}(x_k, 0; y, t))$ is exactly a centered and rescaled version of the height functions associated to ASEP with k different colors, evaluated around the location $2\alpha t\varepsilon^{-1}$ and, by Corollary 2.12 (2), they converge to the directed landscape.

2.2.8. *Convergence to stationary horizon.* Introduced in [Bus24], the *stationary horizon* $G = (G_\xi)_{\xi \in \mathbb{R}}$ is the unique process (under certain slope conditions) [BSS24] taking values in $\mathcal{C}(\mathbb{R}, \mathbb{R})$ of jointly invariant initial conditions for the KPZ fixed point under the directed landscape coupling (2.4). A precise definition of the process can be found, for example, in [BSS22, Appendix D]. It is expected to be the universal scaling limit of multi-type invariant distributions in the KPZ universality class.

By combining Corollary 2.12 with recent results of [BSS23], we can obtain weak convergence to the stationary horizon for the (rescaled) height function corresponding to the stationary colored ASEP. In the case of colored TASEP, this was proven (under a stronger topology) in [BSS22], using detailed information of the structure of the multi-species invariant measure [FM07]. For colored ASEP, these stationary measures have been the topic of several recent studies [EPM09, CGW15, Mar20, CMW22, ANP23], and their structure is considerably more involved. While a direct proof of their convergence to the stationary horizon might take some effort, here we deduce it as a quick consequence of a different convergence statement (Corollary 2.12).

Now we give the setup for stating this stationary horizon convergence. First, given $k \in \mathbb{N}$ and a sequence of densities $\boldsymbol{\rho} = (\rho_1, \dots, \rho_k) \in (0, 1)^k$ such that $\sum_{i=1}^k \rho_i \leq 1$, there exists a unique translation-invariant stationary distribution $\mu_{\boldsymbol{\rho}}$ for colored ASEP with colors $1, \dots, k$ such that the

marginal distribution of the particle configuration obtained by considering only particles of colors j through k (i.e., merging colors j through k and regarding particles of lower colors as holes) is product Bernoulli with density $\sum_{i=j}^k \rho_i$ [Mar20, Theorem 3.2].

In order to obtain the stationary horizon scaling limit, we need the component densities of $\boldsymbol{\rho}$ to be perturbed on the diffusive scale around density $\rho = \frac{1}{2}$; this choice of density corresponds to the choice of slope $\alpha = 0$ in Corollary 2.12 (3), and the extension to general ρ would require an extension of the results of [MQR21, QS22] to general α . More precisely, let ε be a scaling parameter and $\boldsymbol{\xi} = (\xi_1, \dots, \xi_k) \in \mathbb{R}^k$ with $\xi_1 < \dots < \xi_k$. Consider $\boldsymbol{\rho} = \boldsymbol{\rho}_{\boldsymbol{\xi}}^\varepsilon = (\rho_1, \dots, \rho_k)$ with $\rho_k = \frac{1}{2} + \frac{1}{2}\xi_1\varepsilon^{1/3}$ and $\rho_{k-i} = \frac{1}{2}(\xi_{i+1} - \xi_i)\varepsilon^{1/3}$ for $i = 1, \dots, k-1$. Let $\eta \in \llbracket 0, k \rrbracket^{\mathbb{Z}}$ (0 for holes) be a particle configuration sampled according to $\mu_{\boldsymbol{\rho}}$. Define the initial conditions $h_0^{(j),\varepsilon}$ for $j = 1, \dots, k$ by

$$h_0^{(j),\varepsilon}(0) = 0 \quad \text{and} \quad h_0^{(j),\varepsilon}(x-1) - h_0^{(j),\varepsilon}(x) = \mathbb{1}_{\eta(x) \geq j}.$$

By the stationarity of η , $(h_0^{(j),\varepsilon})$ satisfies $h^{\text{ASEP}}(h_0^{(j),\varepsilon}, 0; \cdot, t) - h^{\text{ASEP}}(h_0^{(j),\varepsilon}, 0; 0, t) \stackrel{d}{=} h_0^{(j),\varepsilon}(\cdot)$ jointly over $j = 1, \dots, k$. Further, for each j , $h_0^{(j),\varepsilon}$ is marginally distributed as a two-sided Bernoulli random walk with drift $-\frac{1}{2} - \frac{1}{2}\xi_j\varepsilon^{1/3}$. Below we regard $h_0^{(j),\varepsilon}$ as a continuous function on \mathbb{R} by linear interpolation.

Corollary 2.14 (Stationary horizon convergence for ASEP). *Fix $k \in \mathbb{N}$, $\xi_1 < \dots < \xi_k$, and let $h_0^{(j),\varepsilon}$ be as above. As $\varepsilon \rightarrow 0$, in the topology of uniform convergence on compact sets,*

$$\left(x \mapsto -2\varepsilon^{1/3} \left(h_0^{(j),\varepsilon}(2x\varepsilon^{-2/3}) + x\varepsilon^{-2/3}\right)\right)_{j=1}^k \xrightarrow{d} (G_{\xi_j})_{j=1}^k. \quad (2.11)$$

Proof. This is an immediate consequence of Corollary 2.12 (3) combined with [BSS23, Theorem 2.4]. Assumption 1 of the latter is satisfied by the fact that the i^{th} component of the lefthand side of (2.11) converges to a Brownian motion of drift $2\xi_i$, for each i ; Assumption 2 is merely that we consider the jointly invariant distribution; and Assumption 3 is satisfied due to Corollary 2.12 (3). \square

2.3. Colored stochastic six-vertex model. The colored stochastic six-vertex model (S6V) we consider is defined on the domain $\mathbb{Z}_{\geq 1} \times \llbracket -N, \infty \rrbracket$ for some choice of $N \in \mathbb{N}$. The model has two parameters: a quantization (or asymmetry) parameter $q \in [0, 1)$ and a rapidity (or spectral) parameter $z \in (0, 1)$, which are both fixed.

2.3.1. Configurations and weights. A configuration of the model is described as follows. First, an *arrow configuration* is a tuple $(a, i; b, j)$ such that $i, j, a, b \in \mathbb{Z} \cup \{-\infty\}$ and $\{i, a\} = \{j, b\}$; see the left panel of Figure 7. Under this notation, i, a, j , and b can be interpreted as the *colors* of the arrows horizontally entering, vertically entering, horizontally exiting, and vertically exiting the vertex, respectively. Here, an arrow of color $-\infty$ may be viewed as the absence of an arrow along an edge. The condition $\{i, a\} = \{j, b\}$ is called *colored arrow conservation*, i.e., the number of incoming arrows of each color is equal to the number of outgoing arrows of the same color.

A configuration of the model consists of an assignment of arrow configurations, one to each vertex v of the domain $\mathbb{Z}_{\geq 1} \times \llbracket -N, \infty \rrbracket$; we will denote the arrow configuration at v by $(a_v, i_v; b_v, j_v)$. We require that the arrow configurations are *consistent*: $i_{(x,y)} = j_{(x-1,y)}$ and $a_{(x,y)} = b_{(x,y-1)}$, i.e., an arrow of color k is horizontally entering at (x, y) if and only if an arrow of color k is horizontally exiting at $(x-1, y)$, and similarly an arrow of color k is vertically entering at (x, y) if and only if an arrow of color k is vertically exiting at $(x, y-1)$. We will refer to the colors of the arrows entering and exiting a vertex v (horizontally and vertically) as the incoming and outgoing arrow configurations at v respectively, and the combined set of incoming and outgoing arrows as the arrow configuration at v . One consequence of this description is that the colored arrows form up-right paths; see the right panel of Figure 7.

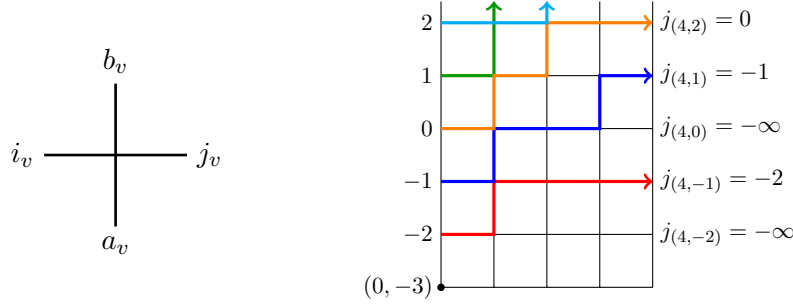


FIGURE 7. Left: a depiction of the labels for the arrow configuration at a vertex v . Right: A sample configuration of the colored stochastic six-vertex model with $N = 2$ and the packed boundary condition, i.e., $\sigma(k) = k$ for $k \in \llbracket -N, N \rrbracket$. The numbers on the left boundary next to an arrow is the color of the arrow. Any edges without arrows should be interpreted as an arrow with color $-\infty$, i.e., a color lower than the colors of all the other arrows in the system.

The *boundary condition* of the model is specified as follows. Let $\sigma : \llbracket -N, N \rrbracket \rightarrow \mathbb{Z} \cup \{-\infty\}$. Then the colored S6V model with boundary condition σ is defined as the model where an arrow of color $\sigma(k)$ enters horizontally at $(1, k)$ (i.e., $i_{(1,k)} = \sigma(k)$) for $k \in \llbracket -N, N \rrbracket$, and an arrow of color $-\infty$ enters vertically at $(\ell, -N)$ (i.e., $a_{(\ell,-N)} = -\infty$) for $\ell \in \mathbb{N}$; see the right panel of Figure 6. Note that arrows enter only at heights in $\llbracket -N, N \rrbracket$, so there are only finitely many arrows in the system.

Remark 2.15. The restriction that we impose of no arrows entering above height N is to make the upcoming definition (2.12) of the colored height function simpler (because of the just noted finiteness); we will soon restrict our attention to the height function’s behavior in $\mathbb{Z}_{\geq 1} \times \llbracket -N, N \rrbracket$, where the entrance of arrows above height N would have no distributional effect anyway. Allowing arrows to enter on $\llbracket -N, N \rrbracket$ allows us to consider arrows of negative color without recentering, which will make our height function definition simpler, and will later allow us to couple directly with colored ASEP on all of \mathbb{Z} .

The probability measure on configurations is defined by the following sampling procedure. We start at the vertex $(1, -N)$. Here there is a horizontally incoming arrow determined by the boundary condition σ and no vertically entering arrow. We determine the outgoing arrow configuration by choosing each of the two possible configurations (whether the horizontally incoming arrow exits vertically or horizontally) with probability equal to the vertex weight read from Figure 8; note that this uses that the vertex weights are *stochastic*, i.e., non-negative and for a given incoming arrow configuration, the sum of the weights of the possible outgoing arrow configurations satisfying arrow conservation is 1. We then proceed iteratively in a Markovian fashion: if the outgoing arrow configuration at all vertices in the domain $\mathcal{D}_n = \{(x, y) \in \mathbb{Z}_{\geq 1} \times \llbracket -N, \infty \rrbracket : x + y < n\}$ has been determined, the configuration for vertices on the line $x + y = n$ is determined by picking the outgoing

1	$\frac{q(1-z)}{1-qz}$	$\frac{1-z}{1-qz}$	$\frac{1-q}{1-qz}$	$\frac{z(1-q)}{1-qz}$

FIGURE 8. The weights for colored S6V written for colors i and j satisfying $i < j$.

arrow configuration at each vertex independently with probability equal to that vertex's weight (again regarding an absence of an arrow along an edge as an arrow of color $-\infty$); note that the incoming arrows configuration at each such vertex is already determined by the requirement of consistency of the overall configuration, and that the order in which the outgoing arrow configurations are sampled does not matter.

The *uncolored stochastic six vertex model* corresponds to the case of colored S6V with two colors: the arrows of lower color are typically not drawn, leaving only arrows of a single color which may then be regarded as uncolored.

Remark 2.16. Like the colored ASEP, the colored S6V model also satisfies color merging: we can project onto a colored S6V model with fewer colors by declaring all arrows of color lying in an interval $I \subseteq \mathbb{Z}$ to be the same color, which is an element of I . Equivalently, the Markov semigroup of the process (viewed as a Markov chain on configurations on vertical lines $x = t$ indexed by the time parameter t) commutes with any weakly monotone function $\mathbb{Z} \cup \{-\infty\} \rightarrow \mathbb{Z} \cup \{-\infty\}$. That this is true follows from the observation that the vertex weights in Figure 8 are determined by only the order relation of the colors of the incident arrows and not their precise value. The uncolored S6V model can again be obtained from the colored one via color merging.

2.3.2. *The S6V sheet.* Recall the notation j_v from Section 2.3.1 for the color of the arrow horizontally exiting the vertex v . Fix a boundary condition $\sigma : \llbracket -N, N \rrbracket \rightarrow \llbracket -N, N \rrbracket$. We define the *colored height function*

$$h^{\text{S6V}}(x, 0; y, t) := \#\{k > y : j_{(t,k)} \geq x\} \quad (2.12)$$

for $x \in \llbracket -N, N \rrbracket$, $y \in \llbracket -N, \infty \rrbracket$, and $t \in \mathbb{N}$. In words, $h^{\text{S6V}}(x, 0; y, t)$ is the number of arrows of color at least x that exit horizontally from some vertex in $\{t\} \times \llbracket y + 1, \infty \rrbracket$.

Note that we did not include the boundary condition σ in the notation (2.12). The boundary configuration we primarily work with is the *packed boundary condition* (see right panel of Figure 7), though some of our results will hold for general boundary conditions as well (see Sections 3.2 and 3.4). The packed boundary condition corresponds to $\sigma(k) = k$, i.e, the arrows entering each vertex on the left boundary of the domain have color decreasing by 1 from top to bottom. We will restrict to the packed boundary condition in the rest of this article unless explicitly mentioned otherwise.

In terms of starting position under packed boundary condition, $h^{\text{S6V}}(x, 0; y, t)$ above is the number of arrows of any color entering horizontally at a vertex $(1, k)$ for some $k \in \llbracket x, N \rrbracket$ that exit horizontally from $\{t\} \times \llbracket y + 1, \infty \rrbracket$. As suggested by the notation, the horizontal coordinate should be thought of as time. Note that $h^{\text{S6V}}(x, 0; y, t)$ is finite since we started with finitely many arrows on the left boundary. Note also that though the distribution of h^{S6V} depends on N , we omit it from the notation (though as alluded to earlier in Remark 2.15, the distribution of $h^{\text{S6V}}(x, 0; y, t)$ jointly over $x, y \in \llbracket -N, N \rrbracket$ and $t \in \mathbb{N}$ will not depend on N).

As in the colored ASEP, the collection $(h^{\text{S6V}}(x, 0; \cdot, t))_{x \in \llbracket -N, N \rrbracket}$ is a coupled collection of copies of the height functions under *step initial condition* from x for uncolored S6V, which means arrows enter at all heights in $\llbracket x, N \rrbracket$ (again recalling from Remark 2.15 that the N cutoff is irrelevant for the domain where we will consider the colored height function). We again refer to this coupling as the *colored coupling*.

Now we define a rescaled version of the height function, which we will call the S6V sheet. Fix $q \in [0, 1)$, $z \in (0, 1)$ and a velocity $\alpha \in (z, z^{-1})$ (which corresponds to the full rarefaction fan). Define $\mu(\alpha)$ and $\sigma(\alpha)$ by

$$\begin{aligned} \mu(\alpha) = \mu^{\text{S6V}}(\alpha) &:= -\frac{(\sqrt{\alpha} - \sqrt{z})^2}{1 - z} \quad \text{and} \\ \sigma(\alpha) = \sigma^{\text{S6V}}(\alpha) &:= \frac{\alpha^{-1/6} z^{1/6} (1 - \sqrt{z\alpha})^{2/3} (\sqrt{\alpha} - \sqrt{z})^{2/3}}{1 - z}; \end{aligned} \quad (2.13)$$

these are exactly the limit shape and fluctuation scale expressions as first proven in [BCG16]. Next define the spatial scaling factor $\beta(\alpha) = \beta^{\text{S6V}}(\alpha)$ by

$$\beta(\alpha) = \beta^{\text{S6V}}(\alpha) := \frac{2\sigma(\alpha)^2}{|\mu'(\alpha)|(1 - |\mu'(\alpha)|)}. \quad (2.14)$$

Definition 2.17 (S6V sheet). For $\varepsilon > 0$, we define the *S6V sheet* $\mathcal{S}^{\text{S6V},\varepsilon} : \mathbb{R}^2 \rightarrow \mathbb{R}$, in the case that $|x|, |y| \leq \varepsilon^{-1/6}$ and the arguments of h^{S6V} below are integers, by

$$\begin{aligned} \mathcal{S}^{\text{S6V},\varepsilon}(x; y) := & \sigma(\alpha)^{-1} \varepsilon^{1/3} \left(h^{\text{S6V}}(\beta(\alpha)x\varepsilon^{-2/3}, 0; \alpha\varepsilon^{-1} + \beta(\alpha)y\varepsilon^{-2/3}, \lfloor \varepsilon^{-1} \rfloor) \right. \\ & \left. + \beta(\alpha)x\varepsilon^{-2/3} - N - \mu(\alpha)\varepsilon^{-1} - \mu'(\alpha)\beta(\alpha)(y-x)\varepsilon^{-2/3} \right); \end{aligned} \quad (2.15)$$

for $|x|, |y| \in [-\varepsilon^{-1/6}, \varepsilon^{-1/6}]$ where the arguments of h^{S6V} are not integers we define $\mathcal{S}^{\text{S6V},\varepsilon}(x; y)$ by linear interpolation so that $\mathcal{S}^{\text{S6V},\varepsilon}$ is continuous on $[-\varepsilon^{-1/6}, \varepsilon^{-1/6}]^2$, and we define it on $\mathbb{R}^2 \setminus ([-\varepsilon^{-1/6}, \varepsilon^{-1/6}]^2)$ in an arbitrary way such that the resulting function is again continuous.

The choice of $[-\varepsilon^{-1/6}, \varepsilon^{-1/6}]$ is merely to ensure that h^{S6V} is well-defined, i.e., its arguments fall within its domain (for all $\varepsilon > 0$); this is true under the assumption we will later adopt that N is at least of order ε^{-1} . The value of $\mathcal{S}^{\text{S6V},\varepsilon}$ outside $[-\varepsilon^{-1/6}, \varepsilon^{-1/6}]^2$ will not be relevant for our results which will only concern uniform convergence on compact sets as $\varepsilon \rightarrow 0$. Note that again we omit N from the notation. The choice of scalings (i.e., $\beta(\alpha)$ and $\sigma(\alpha)$) can be understood by the same heuristics as in Section 2.2.4. We also observe that this definition differs qualitatively slightly from that of the ASEP sheet in Definition 2.7 in that $\mathcal{S}^{\text{S6V},\varepsilon}$ involves h^{S6V} without a negative sign, unlike in ASEP, and there is an extra additive term of $\beta(\alpha)x\varepsilon^{-2/3}$ here. The first is because the proof of Theorem 2.8 will be via a limit of h^{S6V} (as mentioned before), based on a matching between $h^{\text{S6V}}(x, 0; y, t)$ and $-h^{\text{ASEP}}(-x, 0; -y, t)$ (omitting some terms; see (5.3) for more precision), and relying on a symmetry of the Airy sheet: $\mathcal{S}(x; y) \stackrel{d}{=} \mathcal{S}(-x; -y)$ as processes. The introduction of the $\beta(\alpha)x\varepsilon^{-2/3}$ term is to ensure $\mathcal{S}^{\text{S6V},\varepsilon}(\cdot; \cdot) \stackrel{d}{=} \mathcal{S}^{\text{S6V},\varepsilon}(\cdot + r; \cdot + r)$, since $h^{\text{S6V}}(\cdot, 0; \cdot, t)$ does not itself have this property; the term is absent in $\mathcal{S}^{\text{ASEP},\varepsilon}$ since $h^{\text{ASEP}}(\cdot, 0; \cdot, t)$ does have this property.

Our main result for the colored stochastic six-vertex model is the following, where recall we work with the packed boundary condition. It is proved in Section 7.1.

Theorem 2.18 (Airy sheet convergence for S6V). *Fix any asymmetry $q \in [0, 1)$, spectral parameter $z \in (0, 1)$, and velocity $\alpha \in (z, z^{-1})$ in the rarefaction fan. Assume $N \geq 2\alpha\varepsilon^{-1}$. Then, as $\varepsilon \rightarrow 0$, $\mathcal{S}^{\text{S6V},\varepsilon} \xrightarrow{d} \mathcal{S}$ weakly in $\mathcal{C}(\mathbb{R}^2, \mathbb{R})$ with the topology of uniform convergence on compact sets.*

The lower bound on N in Theorem 2.18 is merely to ensure that $\mathcal{S}^{\text{S6V},\varepsilon}$ is well-defined.

2.3.3. The basic coupling for S6V. We next give an analog of ASEP's basic coupling for S6V, which again corresponds to using the same randomness for the evolution of different initial conditions. This will allow us to define the S6V landscape which we show converges to the directed landscape. We work in the model of uncolored S6V, or, equivalently, colored S6V with two colors, which we take to be 1 and $-\infty$, where as usual $-\infty$ represents the absence of an arrow (as discussed in Section 2.3.1).

Consider finitely many initial conditions $\eta_0^{(1)}, \dots, \eta_0^{(K)} \in \{-\infty, 1\}^{\llbracket -N, \infty \rrbracket}$ where $\eta_0^{(j)}(x)$ represents the presence or absence of a horizontal arrow at location $(1, x)$, i.e., $i_{(1,x)} = \eta_0^{(j)}(x)$. As a notational convention, we will use η for uncolored initial conditions (as opposed to σ for colored initial conditions as in Section 2.3.1).

Let $b^\uparrow = q(1-z)/(1-qz)$ and $b^\rightarrow = (1-z)/(1-qz)$ which, from Figure 8, are the probabilities of the arrow of higher color going straight through a vertex vertically or horizontally, respectively. We start with a collection of independent 0-1 Bernoulli random variables $\{X_v^\uparrow, X_v^\rightarrow\}_{v \in \mathbb{Z}_{\geq 1} \times \llbracket -N, \infty \rrbracket}$, where $\mathbb{P}(X_v^\uparrow = 1) = b^\uparrow$ and $\mathbb{P}(X_v^\rightarrow = 1) = b^\rightarrow$ for each $v \in \mathbb{Z}_{\geq 1} \times \llbracket -N, \infty \rrbracket$.

Given this randomness, the configuration is specified deterministically from the initial condition as follows. For any vertex $(x, y) \in \mathbb{Z}_{\geq 1} \times \llbracket -N, \infty \rrbracket$ such that the incoming arrow configuration has been assigned to the vertex at (x, y) (either by the boundary conditions or by the assignment of outgoing arrow configurations to the vertices at $(x-1, y)$ and $(x, y-1)$, along with consistency), let $I_{\rightarrow}, I_{\uparrow} \in \{-\infty, 1\}$ respectively be $i_{(x,y)}$ and $a_{(x,y)}$, the colors of the horizontally and vertically incoming arrows at (x, y) respectively. The colors $O_{\rightarrow}, O_{\uparrow} \in \{-\infty, 1\}$ of the horizontally and vertically outgoing arrows from (x, y) (i.e., $j_{(x,y)}$ and $b_{(x,y)}$), respectively are defined by:

- (1) If $I_{\rightarrow} = I_{\uparrow}$, then $O_{\rightarrow} = O_{\uparrow} = I_{\rightarrow} = I_{\uparrow}$.
- (2) If $(I_{\rightarrow}, I_{\uparrow}) = (-\infty, 1)$, then $(O_{\rightarrow}, O_{\uparrow}) = (-\infty, 1)$ if $X_{(x,y)}^{\uparrow} = 1$ and $(O_{\rightarrow}, O_{\uparrow}) = (1, -\infty)$ if $X_{(x,y)}^{\uparrow} = 0$.
- (3) If $(I_{\rightarrow}, I_{\uparrow}) = (1, -\infty)$, then $(O_{\rightarrow}, O_{\uparrow}) = (1, -\infty)$ if $X_{(x,y)}^{\rightarrow} = 1$ and $(O_{\rightarrow}, O_{\uparrow}) = (-\infty, 1)$ if $X_{(x,y)}^{\rightarrow} = 0$.

Note that for any times $s_j \in \mathbb{N}$, we may also specify (horizontally entering) boundary data $\eta_0^{(j)}$ at vertices on a vertical line (s_j, i) , $i \in \llbracket -N, \infty \rrbracket$ and obtain the evolution of the arrows to the right using this definition, i.e., we may couple together the evolutions starting from different initial conditions at different times (by using the same randomness $(X_v^{\uparrow}, X_v^{\rightarrow})_v$).

We observe as in the case of the ASEP that the basic coupling specializes to the colored coupling in the case that the set of arrows in $\eta_0^{(j+1)}$ is a subset of those in $\eta_0^{(j)}$ for each j , i.e., $\eta_0^{(j+1)}(x) = 1$ implies $\eta_0^{(j)}(x) = 1$ for any $x \in \llbracket -N, \infty \rrbracket$.

Next we define the S6V height function when started from a general initial height function. Let $h_0 : \llbracket -N-1, \infty \rrbracket \rightarrow \mathbb{Z}$ be a Bernoulli path such that $h_0(x) = 0$ for all large enough x . As in ASEP (recall (2.10)), we define an associated arrow configuration $\eta_{h_0} \in \{-\infty, 1\}^{\llbracket -N, \infty \rrbracket}$ by

$$\eta_{h_0}(x) := \begin{cases} 1 & h_0(x-1) - h_0(x) = 1 \\ -\infty & h_0(x-1) - h_0(x) = 0. \end{cases} \quad (2.16)$$

The assumption of h_0 being asymptotically zero implies that η_{h_0} consists of only finitely many arrows (note that we did not assume the analogous condition of right-finiteness for ASEP from a general height function, but it will be convenient to impose this condition for S6V).

Now, for such a Bernoulli path h_0 and $s \in \mathbb{N}$, consider the S6V model with initial condition η_{h_0} started at time $s \in \mathbb{N} \cup \{0\}$ (i.e., η_{h_0} is the configuration on $\{s\} \times \llbracket -N, \infty \rrbracket$), and let $j_{(x,y)}$ be the arrow exiting horizontally from (x, y) . Define the height function $(y, t) \mapsto h^{\text{S6V}}(h_0, s; y, t)$ for $t > s$ (with $s, t \in \mathbb{N} \cup \{0\}$) and $y \in \llbracket -N, \infty \rrbracket$ by

$$h^{\text{S6V}}(h_0, s; y, t) := \#\{k > y : j_{(t,k)} = 1\}. \quad (2.17)$$

For multiple initial conditions $(h_0^{(k)})_{k=1}^K$ and times $s_k > 0$, the height functions $(y, t) \mapsto h^{\text{S6V}}(h_0^{(k)}, s_j; y, t)$ are coupled together via the basic coupling for S6V.

2.3.4. The S6V landscape. Using this coupling we may define the S6V landscape. As in the ASEP case, we start with a precursor: for $x, y \in \llbracket -N, N \rrbracket$ with $x < y$ and $0 \leq s < t \in \mathbb{N}$, we overload the notation and define

$$h^{\text{S6V}}(x, s; y, t) := h^{\text{S6V}}(h_{0,x}, s; y, t)$$

coupled via the basic coupling, where, for $z \in \llbracket -N-1, \infty \rrbracket$,

$$h_{0,x}(z) = (x-z) \mathbb{1}_{z \leq x};$$

note that this function is zero for all large z . It follows that $h^{\text{S6V}}(x, s; y, t)$ generalizes $h^{\text{S6V}}(x, 0; y, t)$ as a process in x, y , and t .

Definition 2.19 (S6V landscape). Recall $\mu(\alpha)$, $\sigma(\alpha)$, and $\beta(\alpha)$ from (2.13) and (2.14). We define the *S6V landscape* for $\varepsilon > 0$ by

$$\begin{aligned} \mathcal{L}^{\text{S6V},\varepsilon}(x, s; y, t) := & \sigma(\alpha)^{-1} \varepsilon^{1/3} \left(h^{\text{S6V}}(\beta(\alpha)x\varepsilon^{-2/3}, \lfloor s\varepsilon^{-1} \rfloor; \alpha(t-s)\varepsilon^{-1} + \beta(\alpha)y\varepsilon^{-2/3}, \lfloor t\varepsilon^{-1} \rfloor) \right. \\ & \left. + \beta(\alpha)x\varepsilon^{-2/3} - N - \mu(\alpha)(t-s)\varepsilon^{-1} - \mu'(\alpha)\beta(\alpha)(y-x)\varepsilon^{-2/3} \right); \end{aligned}$$

again this definition is for $|x|, |y| \leq \varepsilon^{-1/6}$ such that the arguments of h^{S6V} are integers, under the assumption that N is at least of order ε^{-1} . For all other x, y , the function is defined by linear interpolation so that it is continuous in x and y .

We now state the convergence result for $\mathcal{L}^{\text{S6V},\varepsilon}$, which is proved in Appendix D by using an approximate monotonicity estimate for the S6V model under basic coupling (Proposition D.3) together with an idea communicated to us by Shalin Parekh. Recall that for a set \mathcal{T} , $\mathcal{T}_{<}^2 = \{(s, t) \in \mathcal{T}^2 : s < t\}$.

Corollary 2.20 (Directed landscape convergence for S6V). *Fix $q \in [0, 1)$, $z \in (0, 1)$, $\alpha \in (z, z^{-1})$, and a countable set $\mathcal{T} \subseteq [0, \infty)$. Assume $N \geq 2\alpha\varepsilon^{-1}$. Then, the following limits hold as $\varepsilon \rightarrow 0$.*

- (1) $(\mathcal{L}^{\text{S6V},\varepsilon}(\cdot, s; \cdot, t))_{(s,t) \in \mathcal{T}_{<}^2} \xrightarrow{d} (\mathcal{L}(\cdot, s; \cdot, t))_{(s,t) \in \mathcal{T}_{<}^2}$ in $\mathcal{C}(\mathbb{R}^2, \mathbb{R})^{\mathcal{T}_{<}^2}$ under the topology of uniform convergence on compact sets.
- (2) As a special case, for $k \in \mathbb{N}$ and $x_k < \dots < x_1$,

$$(\mathcal{L}^{\text{S6V},\varepsilon}(x_i, 0; \cdot, t))_{i \in [1, k], t \in \mathcal{T}} \xrightarrow{d} (\mathcal{L}(x_i, 0; \cdot, t))_{i \in [1, k], t \in \mathcal{T}}$$
 in $\mathcal{C}(\mathbb{R}, \mathbb{R})^{[1, k] \times \mathcal{T}}$ under the topology of uniform convergence on compact sets.

Remark 2.21 (Scaling limit of S6V with finitely many colors). Analogous to the ASEP case (Remark 2.13), Corollary 2.20 (2) can be interpreted as a scaling limit result for the S6V with finitely many $k \geq 1$ colors via color merging. More precisely, fix real numbers $x_k < \dots < x_1$. Consider colored S6V with initial condition of arrows of color k at locations $\llbracket \lfloor \beta(\alpha)x_1\varepsilon^{-2/3} \rfloor + 1, N \rrbracket$; arrows of color 0 at locations $\llbracket -N, \lfloor \beta(\alpha)x_k\varepsilon^{-2/3} \rfloor \rrbracket$; and arrows of color $k-i$ at all locations in $\llbracket \lfloor \beta(\alpha)x_{i+1}\varepsilon^{-2/3} \rfloor + 1, \lfloor \beta(\alpha)x_i\varepsilon^{-2/3} \rfloor \rrbracket$ for $i = 1, \dots, k-1$. Then, by color merging, $(\mathcal{L}^{\text{S6V},\varepsilon}(x_1; \cdot), \dots, \mathcal{L}^{\text{S6V},\varepsilon}(x_k; \cdot))$ is exactly a centered and rescaled version of the height functions associated to the colored S6V with k different colors and, by Corollary 2.20 (2), they converge to the directed landscape.

Remark 2.22. As mentioned in Section 1.2, we do not pursue a S6V version of Corollary 2.12 (3), i.e., joint convergence of multiple initial conditions to the KPZ fixed point (though we expect such a result still holds). This is because there is not currently a S6V analog of the work of [QS22], i.e., convergence from a single general initial condition to the KPZ fixed point.

However, the stationary measures for the colored S6V coincide with those of the colored ASEP (as is a consequence of the convergence of the former to the latter; see [AB24, Proposition B.2]); so, the stationary horizon convergence of the colored ASEP (Corollary 2.14) implies the same for the colored S6V.

3. COLORED q -BOSON MODEL, LINE ENSEMBLES, AND GIBBS PROPERTIES

As we saw in Definition 2.3, the Airy sheet is given in terms of a last passage percolation problem in the parabolic Airy line ensemble \mathcal{P} . As outlined in Section 1.3.2, the starting point of our proof is a prelimiting analog of this relation, in terms of a certain colored line ensemble, called the *colored Hall-Littlewood line ensemble*, that is associated to the colored S6V model and was recently introduced in [AB24] (we reproduce the argument for the relation between the colored line ensemble and the colored S6V model in Appendix A). This line ensemble is defined in terms of an auxiliary vertex model which we refer to as the *colored q -Boson model*, and we introduce it in Section 3.1. We will then introduce the colored Hall-Littlewood line ensemble and its Gibbs property in Section 3.2.

Section 3.3 states the convergence of uncolored line ensembles to \mathcal{P} . Section 3.4 states the precise prelimiting LPP representation of higher color height functions.

3.1. Colored q -Boson model. The *colored and uncolored q -Boson models* we are introducing are vertex models on the domain $\mathbb{Z}_{\leq 0} \times \llbracket 1, N + M \rrbracket$ for $N, M \in \mathbb{N}$; note that this is different from the domain for the colored stochastic six-vertex model, and we will make the connection between the two in Proposition 3.12. As in the stochastic six vertex model introduced in Section 2.3, there are two parameters: a *quantization parameter* $q \in [0, 1)$ and a *spectral parameter* $z \in (0, 1)$, both of which are held fixed. We will focus on the colored model for the time being. Again as in the colored S6V model, informally (see the next paragraph for a more precise description), a configuration of the model consists of colored arrows, with the color of an arrow being an integer in $\llbracket 1, N \rrbracket$. These arrows enter the domain at the left boundary and move through the domain forming up-right paths, satisfying colored arrow conservation at each vertex; we will specify the colors of these arrows via a boundary condition σ shortly (Section 3.1.2). There is also an exiting boundary condition: all arrows in the system exit vertically from $(0, N + M)$.

An important difference compared to the colored S6V model is that here an arbitrary number of arrows may occupy the same vertical edge (though horizontal edges are still restricted to at most 1 arrow), as well as the fact that the weights (as will be introduced ahead in Figure 10) are not stochastic, i.e., do not sum to 1 when summing over all possible outgoing vertex configurations for fixed incoming vertex configuration; thus the model’s probability distribution is defined via a product of vertex weights with an additional non-trivial normalization factor. Finally, note that in the colored q -Boson model we allow arrows to have only positive colors.

3.1.1. Arrow configurations. More formally, for a vertex $v \in \mathbb{Z}_{\leq 0} \times \llbracket 1, N + M \rrbracket$, we denote the arrow configuration at v by a tuple $(\mathbf{A}_v, i_v; \mathbf{B}_v, j_v)$, where $i_v, j_v \in \llbracket 0, N \rrbracket$ and $\mathbf{A}_v, \mathbf{B}_v \in \mathbb{Z}_{\geq 0}^N$ are vectors $(A_{v,1}, \dots, A_{v,N})$ and $(B_{v,1}, \dots, B_{v,N})$, such that $A_{v,k} + \mathbb{1}_{i_v=k} = B_{v,k} + \mathbb{1}_{j_v=k}$ for each $k \in \llbracket 1, N \rrbracket$. Here i_v and j_v represent the colors of the horizontally incoming and outgoing arrows at v , respectively, while $A_{v,k}, B_{v,k}$ represent the number of arrows of color k vertically entering and exiting at v , respectively, for $k \in \llbracket 1, N \rrbracket$. For this model, color 0 will represent no arrow (unlike the colored S6V model in Section 2.3.1, where $-\infty$ did). The condition $A_{v,k} + \mathbb{1}_{i_v=k} = B_{v,k} + \mathbb{1}_{j_v=k}$ is that of *colored arrow conservation*. A configuration of the model is an assignment of arrow configurations to all

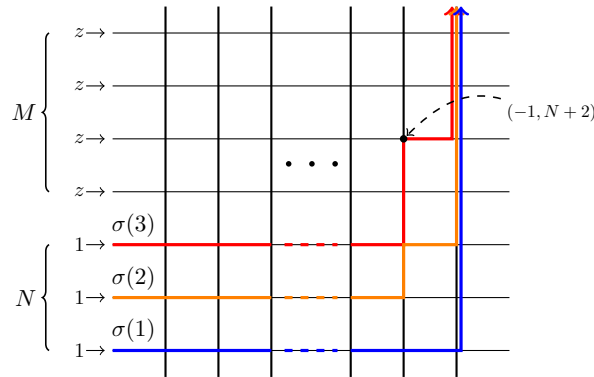


FIGURE 9. The colored q -Boson model. The $z \rightarrow$ and $1 \rightarrow$ at the left indicate the spectral parameters of the L weights associated to vertices in the corresponding rows, the expressions above the entry point of the arrows indicate the corresponding arrow’s color, and the \dots indicate that there are infinitely many columns, though, by definition of the boundary conditions, the arrows travel purely horizontally except until finitely many columns from the right.

vertices of $\mathbb{Z}_{\leq 0} \times \llbracket 1, N + M \rrbracket$ that is *consistent*, i.e., the arrows entering a vertex horizontally or vertically are respectively the same as the arrows horizontally exiting the vertex immediately to the left or vertically exiting the vertex immediately below.

3.1.2. Boundary conditions. Let $\sigma : \llbracket 1, N \rrbracket \rightarrow \llbracket 1, N \rrbracket$ be a function. The boundary condition σ of arrows is specified as follows: informally, at $(-\infty, i)$ for $i \in \llbracket 1, N \rrbracket$ an arrow of color $\sigma(i)$ enters and moves purely horizontally for all but finitely many edges, and no arrow enters at row i for $i \in \llbracket N + 1, N + M \rrbracket$; further, all arrows which originally entered the system vertically exit at $(0, N + M)$. More formally, the arrow configuration at $v = (-K, i)$ is given by $(0^N, \sigma(i); 0^N, \sigma(i))$ for $i \in \llbracket 1, N \rrbracket$ and by $(0^N, 0; 0^N, 0)$ for $i \in \llbracket N + 1, N + M \rrbracket$, for all large enough K , and no arrows vertically enter the system through the bottom boundary $\mathbb{Z}_{\leq 0} \times \{1\}$. Further, the configuration of arrows vertically exiting $(0, N + M)$ is $(\#\sigma^{-1}(\{j\}))_{j=1}^N$, and no arrows horizontally or vertically exit the system elsewhere. We emphasize that we only consider boundary conditions σ taking values at least 1; in other words, we require that an arrow enters the i^{th} row for each $i \in \llbracket 1, N \rrbracket$.

	$(\mathbf{A}, 0; \mathbf{A}, 0)$	$(\mathbf{A}, 0; \mathbf{A}_i^-, i)$	$(\mathbf{A}, i; \mathbf{A}_i^+, 0)$	$(\mathbf{A}, i; \mathbf{A}_{ij}^{+-}, j)$	$(\mathbf{A}, j; \mathbf{A}_{ji}^{+-}, i)$	$(\mathbf{A}, i; \mathbf{A}, i)$
1	$u(1 - q^{A_i})q^{A_{[i+1, N]}}$	1	$u(1 - q^{A_j})q^{A_{[j+1, N]}}$	0	$uq^{A_{[i+1, N]}}$	

FIGURE 10. The L_u weights for $1 \leq i < j \leq N$. Here for $\mathbf{A} \in \mathbb{Z}_{\geq 0}^N$ and $i \in \llbracket 1, N \rrbracket$, $A_{[i, N]} = \sum_{j=i}^N A_j$. The notation \mathbf{A}_ℓ^+ and \mathbf{A}_ℓ^- respectively means the vector obtained by increasing or decreasing the ℓ^{th} component of \mathbf{A} by 1; similarly $\mathbf{A}_{k\ell}^{+-}$ is the vector obtained by increasing the k^{th} component of \mathbf{A} by 1 and decreasing the ℓ^{th} component by 1.

3.1.3. The colored q -Boson weights and probability measure. The weight of a configuration is given by the product of the vertex weights at each vertex of the domain. The vertex weights are specified as follows. First we define the L_u weights in Figure 10, which will also be called the *colored q -Boson weights* (and are the same as the ones in [BW22, eq. (1.2.2)] or [AB24, Figure 5], with $s = 0$). The vertex weights in our model are of two types, coming from the weights in Figure 10 with two different values of u : those on the bottom N rows, i.e., on $\mathbb{Z}_{\leq 0} \times \llbracket 1, N \rrbracket$, are given by the L_u weights with $u = 1$, while those on the top M rows, i.e., on $\mathbb{Z}_{\leq 0} \times \llbracket N + 1, N + M \rrbracket$, are given by the same with $u = z$ as fixed above; see Figure 9.

Definition 3.1. Fix a boundary condition $\sigma : \llbracket 1, N \rrbracket \rightarrow \llbracket 1, N \rrbracket$. This specifies a collection of consistent configurations that satisfy this boundary condition and which have positive weight. We may define a probability measure supported on this collection, which we call the *colored q -Boson measure* with boundary condition σ . The measure is defined by specifying that

$$\begin{aligned} &\text{the probability of a given configuration is proportional to its weight;} \\ &\text{the normalization constant is finite and equals } \left(\frac{1-qz}{1-z}\right)^{NM}. \end{aligned} \tag{3.1}$$

The *uncolored q -Boson model* is the case where only arrows of color 1 are present, i.e., $\sigma(k) = 1$ for all $k \in \llbracket 1, N \rrbracket$ (and thus there is no boundary condition to be specified, i.e., there is only one choice for σ).

The normalization constant in (3.1) is the sum of weights of all configurations and its expression is derived in [AB24, Lemma 2.9] via the Yang-Baxter equation relating the colored q -Boson and colored S6V weights; equivalently, this can be seen as a Cauchy identity for certain functions associated to the vertex model. We reproduce the former argument in Appendix A.

3.1.4. Color merging. The colored q -Boson model satisfies a form of color merging, like the colored S6V model (Remark 2.16). Take the colored q -Boson measure with boundary condition σ and identify any interval $I \subseteq \llbracket 1, N \rrbracket$ of colors with an element of I , and if desired relabel all the colors in a weakly increasing way (preserving the original orderings). The resulting projection is the colored q -Boson measure with boundary condition σ' obtained by performing the same color identification and relabeling in σ . A more precise statement is as follows.

Lemma 3.2. *Let $N, M \in \mathbb{N}$ and $\sigma : \llbracket 1, N \rrbracket \rightarrow \llbracket 1, N \rrbracket$. Let $\tau : \llbracket 0, N \rrbracket \rightarrow \llbracket 0, N \rrbracket$ be non-decreasing and such that $\tau^{-1}(\{0\}) = \{0\}$. Then $(j_v)_{v \in \mathbb{Z}_{\leq 0} \times \llbracket 1, N+M \rrbracket}$ under the colored q -Boson measure with boundary condition $\tau \circ \sigma$ has the same distribution as $(\tau(j_v))_{v \in \mathbb{Z}_{\leq 0} \times \llbracket 1, N+M \rrbracket}$ under the colored q -Boson measure with boundary condition σ .*

In particular, defining τ by $\tau(0) = 0$ and $\tau(j) = 1$ for $j \in \llbracket 1, N \rrbracket$, we see that the colored q -Boson model with all colors ignored (i.e., only total arrow counts are observed) yields the uncolored q -Boson model.

That this color merging property holds is not as immediate as in the case of colored S6V. Indeed, in the latter it was a consequence of the vertex weights being determined by the relative order of the colors of arrows and not their precise values; this implicitly used that the normalization constant or partition function for the measure is 1 (or, rather, independent of the boundary condition), since the weights are stochastic, i.e, for a fixed incoming arrow configuration, summing the weights over all valid outgoing arrow configurations yields 1. In contrast, the L_u weights are not determined purely by the relative order and are also not stochastic.

Proof of Lemma 3.2. The verification of color merging requires the following fact. First, for $\tau : \llbracket 0, N \rrbracket \rightarrow \llbracket 0, N \rrbracket$ non-decreasing with $\tau^{-1}(\{0\}) = \{0\}$, define $\rho_\tau : \mathbb{Z}_{\geq 0}^N \rightarrow \mathbb{Z}_{\geq 0}^N$ by the following: for $\mathbf{A} \in \mathbb{Z}_{\geq 0}^N$ and $k \in \llbracket 1, N \rrbracket$, $(\rho_\tau(\mathbf{A}))_k = \sum_{i \in \tau^{-1}(\{k\})} A_i$. Then, it is a straightforward calculation that for $\mathbf{A}_v \in \mathbb{Z}_{\geq 0}^N$, $i_v \in \llbracket 0, N \rrbracket$, $\tilde{\mathbf{B}}_v \in \rho_\tau(\mathbb{Z}_{\geq 0}^N)$, and $\lambda \in \tau(\llbracket 0, N \rrbracket)$,

$$\sum_{\substack{\mathbf{B}_v, j_v: \tau(j_v) = \lambda, \\ \rho_\tau(\mathbf{B}_v) = \tilde{\mathbf{B}}_v}} L_u(\mathbf{A}_v, i_v; \mathbf{B}_v, j_v) = L_u(\rho_\tau(\mathbf{A}_v), \tau(i_v); \tilde{\mathbf{B}}_v, \lambda). \quad (3.2)$$

In words, if we fix the incoming arrow configurations and sum the vertex weight over all outgoing arrow configuration under the constraint that the outgoing arrow colors, on merging according to τ , are fixed, we obtain the vertex weight with the colors merged according to τ . That the L_u weights have this property has been observed a number of times in the literature; see, for example, [AB24, eq. (4.9)], or [BW22, Proposition 2.4.2] or [FW13] in the case of merging all colors with color 1.

Fix a configuration ω of the colored q -Boson model with boundary condition $\tau \circ \sigma$. Repeatedly applying (3.2) implies that the weight of ω is the same as the sum of the weights of all configurations of the colored q -Boson model with boundary condition σ such that one obtains ω on color merging according to τ . Next, repeatedly applying the special case of (3.2), with $\tau(k) = 1$ for all $k \in \llbracket 1, N \rrbracket$ and $\tau(0) = 0$, yields that the partition functions for the models with boundary conditions σ and $\tau \circ \sigma$, respectively, are the same. These two inferences complete the proof by recalling the definition (3.1) of the colored q -Boson measure. \square

Remark 3.3. Unlike the colored S6V model, in the colored q -Boson model one cannot merge colors with color zero (no arrows). This is a consequence of the L_u weights not being stochastic. It can be

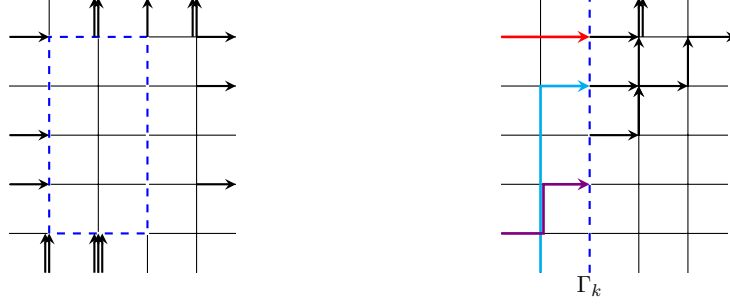


FIGURE 11. Left: The setup for the Gibbs property in the uncolored q -Boson model. Outgoing arrow counts outside the region Λ outlined in blue are conditioned upon, and arrows have been displayed in this depiction if the arrow count is non-zero and has been conditioned on. Arrow counts entering the blue region are conditioned on due to consistency, but those exiting it are not. Right: The setup for the Gibbs property in the colored q -Boson model. Horizontally outgoing colored arrows counts are conditioned on strictly to the left of the blue dashed line (which extends to the ends of the domain in both directions), while only total outgoing arrow counts (depicted in black) are conditioned on to the right (including on Γ_k).

seen by the fact that the analog of (3.2) for merging with 0 (i.e., $\tau^{-1}(0)$ contains a non-zero integer) does not hold.

3.1.5. *Gibbs property for q -Boson models.* Next we discuss two Gibbs properties, one each for the colored and uncolored q -Boson models, that are consequences of the above description, and which will be used in later arguments. By Gibbs property, we mean a spatial Markov property: informally, for a domain Λ , the conditional distribution of the configuration strictly inside Λ , given the configuration on the boundary of Λ as well as outside Λ , is explicit and depends only on the configuration on the boundary of Λ .

We start with the uncolored Gibbs property. We may write the arrow configuration at a vertex v as $(A_v, i_v; B_v, j_v)$ where $i_v, j_v \in \{0, 1\}$ (presence of arrow) and $A_v, B_v \in \mathbb{Z}_{\geq 0}$ (number of arrows). Because of the form of the weight of a configuration as a product of vertex weights, that this model enjoys a Gibbs property is immediate; the dependency of the conditional distribution on the configuration on the boundary of the domain is imposed via the requirement of consistency and arrow conservation. To state the Gibbs property more precisely, fix a rectangle $\Lambda := \llbracket -k, -\ell \rrbracket \times \llbracket a, b \rrbracket \subseteq \mathbb{Z}_{\leq 0} \times \llbracket 1, N+M \rrbracket$, let $\Lambda^c = \mathbb{Z}_{\leq 0} \times \llbracket 1, N+M \rrbracket \setminus \Lambda$, and let $\mathcal{F}_{\Lambda^c}^{\text{uB}}$ (“uB” short for uncolored q -Boson) be the σ -algebra (where $\sigma(\cdot)$ for \cdot some collection of random variables means the σ -algebra generated by that collection)

$$\mathcal{F}_{\Lambda^c}^{\text{uB}} := \sigma(\{j_v : v \in \Lambda^c\}); \quad (3.3)$$

note that, by consistency, for every v in the left boundary of Λ , it holds that i_v is $\mathcal{F}_{\Lambda^c}^{\text{uB}}$ -measurable, and by consistency along with arrow conservation, for every v in the bottom boundary of Λ , it holds that A_v is $\mathcal{F}_{\Lambda^c}^{\text{uB}}$ -measurable. This implies that, for v the top left corner of Λ , B_v is $\mathcal{F}_{\Lambda^c}^{\text{uB}}$ -measurable and, iteratively, that the same holds for every v in the top boundary of Λ . Continuing reasoning in this way, we see that B_v is $\mathcal{F}_{\Lambda^c}^{\text{uB}}$ -measurable for every v in $\mathbb{Z}_{\leq 0} \times \llbracket 1, N+M \rrbracket \setminus (\llbracket -k, -\ell+1 \rrbracket \times \llbracket a, b-1 \rrbracket)$. See the left panel of Figure 11.

For the statement of the Gibbs property, we adopt the notation $L_{z,v}$ for the vertex weights in the model: $L_{z,v} = L_1$ for $v \in \mathbb{Z}_{\leq 0} \times \llbracket 1, N \rrbracket$ and $L_{z,v} = L_z$ for $v \in \mathbb{Z}_{\leq 0} \times \llbracket N+1, N+M \rrbracket$.

Lemma 3.4 (Uncolored q -Boson Gibbs property). *Let $\Lambda = \llbracket -k, -\ell \rrbracket \times \llbracket a, b \rrbracket$ and $\mathcal{F}_{\Lambda^c}^{\text{uB}}$ be as in (3.3). Under the uncolored q -Boson measure, the conditional distribution of $((A_v, i_v; B_v, j_v) : v \in \Lambda)$*

given $\mathcal{F}_{\Lambda^c}^{\text{uB}}$ is supported on tuples $((A'_v, i'_v; B'_v, j'_v) : v \in \Lambda)$ such that arrow conservation and consistency are satisfied inside Λ and with respect to the boundary conditions; call the (random) set of such tuples Supp^{uB} . Further, the conditional probability that $((A_v, i_v; B_v, j_v) : v \in \Lambda) = ((A'_v, i'_v; B'_v, j'_v) : v \in \Lambda)$, for any fixed (i.e., deterministic) selection of the righthand side, is proportional to $\prod_{v \in \Lambda} L_{z,v}(A'_v, i'_v; B'_v, j'_v) \mathbb{1}_{(A'_v, i'_v; B'_v, j'_v)_{v \in \Lambda} \in \text{Supp}^{\text{uB}}}$.

Proof. This follows from the form of the uncolored q -Boson measure as a product of vertex weights. \square

Next we turn to a Gibbs property for the colored q -Boson model. Informally, it explains how to “reveal” colored arrow counts, conditional on total arrow counts. Fix $k \in \mathbb{N}$. Let $\Lambda_k = (-\infty, -k] \times \llbracket 1, N+M \rrbracket$ and $\Gamma_k = \{-k\} \times \llbracket 1, N+M \rrbracket$, and let $\mathcal{F}_k^{\text{cB}}$ (“cB” short for colored q -Boson) be the σ -algebra

$$\mathcal{F}_k^{\text{cB}} := \sigma \left(\{ \mathbb{1}_{i_v \geq 1} : v \in \mathbb{Z}_{\leq 0} \times \llbracket 1, N+M \rrbracket \} \cup \{ i_v : v \in \Lambda_k \} \right). \quad (3.4)$$

For $\mathbf{A} \in \mathbb{Z}_{\geq 0}^N$, let $|\mathbf{A}| := \sum_{i=1}^N A_i$. Note that by colored arrow conservation and consistency, the collection of random variables $\{(|\mathbf{A}_v|; |\mathbf{B}_v|, \mathbb{1}_{j_v \geq 1}) : v \in \mathbb{Z}_{\leq 0} \times \llbracket 1, N+M \rrbracket\}$ and $\{(\mathbf{A}_v; \mathbf{B}_v, j_v) : v \in \Lambda_{k+1}\}$ is $\mathcal{F}_k^{\text{cB}}$ -measurable. Thus, in words, $\mathcal{F}_k^{\text{cB}}$ contains the information of the incoming colored arrow counts at Γ_k , incoming and outgoing total arrow counts of every vertex in the domain, and incoming and outgoing colored arrow counts of every vertex in Λ_{k+1} . See the right panel of Figure 11.

The following is the Gibbs property when conditioning on $\mathcal{F}_k^{\text{cB}}$; because of the heterogeneous nature of the random variables being conditioned (a mixture of colored and total arrow counts), its proof is slightly more complicated than that of Lemma 3.4. Recall the definition of $L_{z,v}$ from before Lemma 3.4.

Lemma 3.5 (Colored q -Boson Gibbs property). *Fix $k \in \mathbb{N}$ and $\sigma : \llbracket 1, N \rrbracket \rightarrow \llbracket 1, N \rrbracket$, and let Γ_k and $\mathcal{F}_k^{\text{cB}}$ be as in (3.4). Under the colored q -Boson measure with boundary condition σ , the conditional distribution of $((\mathbf{A}_v; \mathbf{B}_v, j_v) : v \in \Gamma_k)$ given $\mathcal{F}_k^{\text{cB}}$ is supported on tuples $((\mathbf{A}'_v; \mathbf{B}'_v, j'_v) : v \in \Gamma_k)$ such that (i) $\mathbb{1}_{j'_v \geq 1} = \mathbb{1}_{j_v \geq 1}$ for all $v \in \Gamma_k$ and (ii) colored arrow conservation and consistency are satisfied. Call the (random) set of all such tuples Supp^{cB} . Further, the conditional probability that $((\mathbf{A}_v; \mathbf{B}_v, j_v) : v \in \Gamma_k) = ((\mathbf{A}'_v; \mathbf{B}'_v, j'_v) : v \in \Gamma_k)$, for any fixed (i.e., deterministic) selection of the righthand side, is proportional to $\prod_{v \in \Gamma_k} L_{z,v}(\mathbf{A}'_v, i'_v; \mathbf{B}'_v, j'_v) \mathbb{1}_{(\mathbf{A}'_v; \mathbf{B}'_v, j'_v)_{v \in \Gamma_k} \in \text{Supp}^{\text{cB}}}$.*

Proof. Let $\Lambda_k^c := \mathbb{Z}_{\leq 0} \times \llbracket 1, N+M \rrbracket \setminus \Lambda_k = \llbracket -k+1, 0 \rrbracket \times \llbracket 1, N+M \rrbracket$. Let $\boldsymbol{\omega} = ((\mathbf{A}'_v; \mathbf{B}'_v, j'_v) : v \in \Gamma_k)$ and let $\text{Val}_k(\boldsymbol{\omega})$ (for “valid”) be the collection of configurations $(\mathbf{A}'_v, i'_v; \mathbf{B}'_v, j'_v)_{v \in \Lambda_k^c}$ which satisfy colored arrow conservation and consistency as well as the following:

- $i'_{(-k+1,x)} = j'_{(-k,x)}$ for $x \in \llbracket 1, N+M \rrbracket$ (consistency of incoming arrows to Γ_{k-1} with outgoing arrows from Γ_k as given by $\boldsymbol{\omega}$),
- $\mathbf{B}'_{(0,N+M)} = (\#\sigma^{-1}(\{j\}))_{j=1}^N$ (all arrows exit vertically from the rightmost column), and
- $\mathbb{1}_{i'_v \geq 1} = \mathbb{1}_{i_v \geq 1}$, $\mathbb{1}_{j'_v \geq 1} = \mathbb{1}_{j_v \geq 1}$, $|\mathbf{A}'_v| = |\mathbf{A}_v|$, and $|\mathbf{B}'_v| = |\mathbf{B}_v|$ for all $v \in \Lambda_k^c$ (respecting the total arrow counts conditioned on).

It is immediate from the definition of the colored q -Boson measure that the $\mathcal{F}_k^{\text{cB}}$ -conditional probability of the event $\{((\mathbf{A}_v; \mathbf{B}_v, j_v) : v \in \Gamma_k) = \boldsymbol{\omega}\}$ is proportional to

$$\prod_{v \in \Gamma_k} L_{z,v}(\mathbf{A}'_v, i'_v; \mathbf{B}'_v, j'_v) \cdot \left(\sum_{(\mathbf{A}'_v, i'_v; \mathbf{B}'_v, j'_v)_{v \in \Lambda_k^c} \in \text{Val}_k(\boldsymbol{\omega})} \prod_{w \in \Lambda_k^c} L_{z,w}(\mathbf{A}'_w, i'_w; \mathbf{B}'_w, j'_w) \right). \quad (3.5)$$

To absorb the factor in parentheses into the normalization constant, we must show that it is $\mathcal{F}_k^{\text{cB}}$ -measurable. The lemma will therefore be implied by the following claim: that factor’s value depends

only on $((|\mathbf{A}_v|, \mathbb{1}_{i_v \geq 1}; |\mathbf{B}_v|, \mathbb{1}_{j_v \geq 1}) : v \in \Lambda_k^c)$, which has been conditioned upon (it is determined by $(\mathbb{1}_{i_v \geq 1} : v \in \Lambda_k^c)$ by consistency and arrow conservation). This claim in turn follows by applying (3.2) (with $\tau(k) = 1$ for all $k \in \llbracket 1, N \rrbracket$ and $\tau(0) = 0$) iteratively for each factor in the second product in (3.5) (i.e., for each vertex in Λ_k^c); notice that the sum in (3.5) is over $\text{Val}_k(\omega)$, which fixes the total arrow counts at each vertex according to $((|\mathbf{A}_v|, \mathbb{1}_{i_v \geq 1}; |\mathbf{B}_v|, \mathbb{1}_{j_v \geq 1}) : v \in \Lambda_k^c)$. This yields that the parenthetical quantity in (3.5) equals the partition function for the uncolored q -Boson measure on configurations $(\tilde{A}_v, \tilde{i}_v; \tilde{B}_v, \tilde{j}_v)_{v \in \Lambda_k^c}$ (where $A_v, B_v \in \mathbb{Z}_{\geq 0}$ and $i_v, j_v \in \{0, 1\}$ represent total arrow counts, as in the beginning of Section 3.1.5) constrained to satisfy the uncolored analogs of the three bullet points above, namely, $\tilde{i}_{(-k+1, x)} = \mathbb{1}_{j_{(-k, x)} \geq 1}$ for $x \in \llbracket 1, N + M \rrbracket$; $\tilde{B}_{(0, N+M)} = N$; and $\tilde{i}_v = \mathbb{1}_{i_v \geq 1}, \tilde{j}_v = \mathbb{1}_{j_v \geq 1}, \tilde{A}_v = |\mathbf{A}_v|$, and $\tilde{B}_v = |\mathbf{B}_v|$ for all $v \in \Lambda_k^c$ (this actually includes the first point since $\mathbb{1}_{j_{(-k, x)} \geq 1} = \mathbb{1}_{i_{(-k+1, x)} \geq 1}$). This verifies the claim and completes the proof. \square

3.2. Colored Hall-Littlewood line ensemble. Next we define a rewriting of a configuration sampled from the colored q -Boson measure in a more probabilistically appealing form, namely, the colored line ensemble. First we specify what we mean by a discrete line ensemble.

Definition 3.6 (Discrete line ensemble). Fix a (possibly infinite) interval $\Lambda \subseteq \mathbb{Z}$. A Λ -indexed discrete line ensemble $\mathbf{L} = (L_1, L_2, \dots)$ is a random variable defined on a probability space $(\Omega, \mathcal{F}, \mathbb{P})$ taking values in the space of functions $\mathbb{N} \times \Lambda \rightarrow \mathbb{Z}$ (here the first argument is written as a subscript, i.e., $L_i(\cdot) := \mathbf{L}(i, \cdot)$), endowed with the discrete topology, such that: (i) $L_i(y + 1) - L_i(y) \in \{0, -1\}$ for any $i \in \mathbb{N}$ and y such that $y, y + 1 \in \Lambda$, and (ii) $L_i(y) \geq L_{i+1}(y)$ for any $y \in \Lambda$ and $i \in \mathbb{N}$.

Note that we take discrete line ensembles, and all the line ensembles we work with in this paper, to have an infinite number of curves. This differs slightly from some previous studies focused on tightness of line ensembles (e.g., [CH14, CH16, CD18]).

We will refer to the set of vertices $\{-k\} \times \llbracket 1, N + M \rrbracket$ in the domain $\mathbb{Z}_{\leq 0} \times \llbracket 1, N + M \rrbracket$ of the colored q -Boson model as the k^{th} column. The colored line ensemble will be given in terms of colored arrow counts in columns at a finite distance from the rightmost (zeroth) column. Recall that, in the notation from Section 3.1.1, for $y \in \llbracket 1, N + M \rrbracket$, and $k \in \mathbb{N}$, $j_{(-k, y)}$ is the color of the arrow exiting horizontally from vertex $(-k, y)$; and $j_{(-k, y)} = 0$ if there is no such arrow.

Definition 3.7 (Colored and uncolored Hall-Littlewood line ensembles). Let $\sigma : \llbracket 1, N \rrbracket \rightarrow \llbracket 1, N \rrbracket$ and let $\{(\mathbf{A}_v, i_v; \mathbf{B}_v, j_v) : v \in \mathbb{Z}_{\leq 0} \times \llbracket 1, N + M \rrbracket\}$ be a configuration sampled from the colored q -Boson measure with boundary condition σ (from Section 3.1.2). For each $k \in \llbracket 1, N \rrbracket$, we define the discrete line ensemble $\mathbf{L}^{\text{cHL}, (k)} = (L_1^{\text{cHL}, (k)}, L_2^{\text{cHL}, (k)}, \dots) : \mathbb{N} \times \llbracket 0, N + M \rrbracket \rightarrow \mathbb{Z}$ by letting $L_i^{\text{cHL}, (k)}(y)$ be the number of arrows of color at least k which exit horizontally in the i^{th} column strictly above row y , i.e.,

$$L_i^{\text{cHL}, (k)}(y) := \#\{y' > y : j_{(-i, y')} \geq k\}. \quad (3.6)$$

The object $\mathbf{L}^{\text{cHL}} = (\mathbf{L}^{\text{cHL}, (1)}, \mathbf{L}^{\text{cHL}, (2)}, \dots, \mathbf{L}^{\text{cHL}, (N)})$ is called the *colored Hall-Littlewood line ensemble* with boundary condition σ (see Figure 3). The line ensemble $\mathbf{L}^{\text{cHL}, (1)}$ is called the *uncolored Hall-Littlewood line ensemble*.

Remark 3.8. The terminology comes from the fact that, if one interprets the colored Hall-Littlewood line ensemble as random sequences of compositions (see [AB24, Definition 4.1]), the resulting process is the same as the colored Hall-Littlewood process introduced in [BW22, Section 1.6] (though we do not need or prove this).

We call $\mathbf{L}^{\text{cHL}, (1)}$ the uncolored Hall-Littlewood line ensemble as it is determined purely by total arrow counts in the colored q -Boson model. As in the uncolored q -Boson model, there is no boundary condition to be specified for the uncolored Hall-Littlewood line ensemble. Analogous to the colored case, the uncolored Hall-Littlewood line ensemble is associated to the (uncolored) Hall-Littlewood process (see e.g., [BC14, Dim18]), a collection of measures on sequences of partitions that is specified

by a choice of specializations and a down-right path. The specializations (in some cases) can be thought of as our choices of spectral parameters, and the down-right path as the choice of boundary conditions of the uncolored q -Boson model (allowing arrows to horizontally enter only at rows with spectral parameter 1, but which may be different than the bottom N rows as we have fixed here; see also [AB24, Remark 3.11]). The choice of boundary condition and spectral parameters we have fixed (and the only one considered in this article) is equivalent to the ‘‘ascending Hall-Littlewood process’’ with a homogeneous choice of specializations.

Note that we do not include σ in the notation for the colored Hall-Littlewood line ensembles, but we will specify σ in the relevant statements. Next we record some simple consequences of Definition 3.7.

Lemma 3.9. *Fix $\sigma : \llbracket 1, N \rrbracket \rightarrow \llbracket 1, N \rrbracket$, and for each $k \in \llbracket 1, N \rrbracket$, let $\mathbf{L}^{\text{cHL},(k)} = (L_1^{\text{cHL},(k)}, L_2^{\text{cHL},(k)}, \dots)$ be defined as in (3.6) with boundary condition σ . It holds deterministically that, for any $i \in \mathbb{N}$ and $y \in \llbracket 0, N + M - 1 \rrbracket$,*

$$\begin{aligned} (i) \quad & L_i^{\text{cHL},(k)}(y) \geq L_i^{\text{cHL},(k+1)}(y), \\ (ii) \quad & L_i^{\text{cHL},(k)}(y) \geq L_{i+1}^{\text{cHL},(k)}(y), \text{ and} \\ (iii) \quad & L_i^{\text{cHL},(k)}(y+1) - L_i^{\text{cHL},(k)}(y) = -\mathbb{1}_{j(-i, y+1) \geq k} \in \{0, -1\}. \end{aligned} \tag{3.7}$$

Proof. The first and third points are immediate from the definition. The second relies on the fact that arrows can only move up and to the right, so that any arrow exiting the $(i+1)^{\text{st}}$ column at a row higher than y must exit the i^{th} column at a row higher than y . \square

We next record a statement of color merging for the colored Hall-Littlewood line ensemble.

Lemma 3.10 (Color merging for \mathbf{L}^{cHL}). *Fix $\sigma : \llbracket 1, N \rrbracket \rightarrow \llbracket 1, N \rrbracket$ and $k \in \llbracket 1, N \rrbracket$, and let $\tau : \llbracket 1, N \rrbracket \rightarrow \llbracket 1, k \rrbracket$ be surjective and non-decreasing. Let $\mathbf{L}^{\text{cHL},\sigma}$ and $\mathbf{L}^{\text{cHL},\tau \circ \sigma}$ be the colored Hall-Littlewood line ensembles with boundary conditions σ and $\tau \circ \sigma$ as in Definition 3.7, respectively. For $j \in \llbracket 1, k \rrbracket$, let $t_j = \min \tau^{-1}(\{j\})$. Then*

$$(\mathbf{L}^{\text{cHL},\sigma,(t_j)})_{j \in \llbracket 1, k \rrbracket} \stackrel{d}{=} (\mathbf{L}^{\text{cHL},\tau \circ \sigma,(j)})_{j \in \llbracket 1, k \rrbracket}.$$

In particular, defining τ by $\tau(j) = 1$ for all $j \in \llbracket 1, N \rrbracket$, it follows that $\mathbf{L}^{\text{cHL},\sigma,(1)}$ under any boundary condition σ has the same distribution as $\mathbf{L}^{\text{cHL},\sigma',(1)}$ with $\sigma'(j) = 1$ for all $j \in \llbracket 1, N \rrbracket$, i.e., the colored line ensemble associated with the uncolored q -Boson model.

Proof. This is an immediate consequence of combining Definition 3.7 with the color merging statement Lemma 3.2. \square

3.2.1. Restricting the domain. We need to connect the top curve of $\mathbf{L}^{\text{cHL},(j)}$ for different j with the height function of the colored S6V model (we focus on S6V since we will ultimately deal with ASEP via a limit to it from the former; see Section 5). To do so, we must first modify the setup of the colored S6V model slightly. Recall from (2.12) that the prelimiting analog $\mathcal{S}^{\text{S6V},\varepsilon}$ of \mathcal{S} concerns counts of the number of arrows above a varying vertex on the vertical line $x = \lfloor \varepsilon^{-1} \rfloor$, and that arrows horizontally enter the system from the left side at coordinates $(1, i)$ for $i \in \llbracket -N, N \rrbracket$. In the packed boundary condition, the arrow entering horizontally at $(1, i)$ has color i , and thus all arrow colors entering at or below the x -axis are not positive. In contrast, note that the colored Hall-Littlewood line ensemble we defined are associated with only positive colors. (We needed to allow arrows of negative color in the colored S6V model, as $\mathcal{S}^{\text{S6V},\varepsilon}$ needs to allow negative values in the first argument.)

We first record a consequence of color merging (of the colored S6V model) that says that, when considering the height function for colors 1 or higher, we may restrict the domain to $\mathbb{Z}_{\geq 1} \times \llbracket 1, N \rrbracket$

without changing the distribution of the colored height function. This will address the discrepancy pointed out in the previous paragraph.

Lemma 3.11. *Fix $N \in \mathbb{N}$ and let $\sigma : \llbracket -N, N \rrbracket \rightarrow \llbracket -\infty, N \rrbracket \cup \{-\infty\}$, $\sigma_{\geq 1} : \llbracket 1, N \rrbracket \rightarrow \llbracket 1, N \rrbracket$ be such that $\sigma(k) = \sigma_{\geq 1}(k) \geq 1$ for $k \in \llbracket 1, N \rrbracket$ and $\sigma(k) \leq 0$ for $k \in \llbracket -N, 0 \rrbracket$. Consider the colored S6V model on the domains $\mathbb{Z}_{\geq 1} \times \llbracket -N, \infty \rrbracket$ and $\mathbb{Z}_{\geq 1} \times \llbracket 1, \infty \rrbracket$ with boundary conditions σ and $\sigma_{\geq 1}$, respectively (i.e., an arrow of color $\sigma(k)$ or $\sigma_{\geq 1}(k)$ enters horizontally at $(1, k)$ for $k \in \llbracket -N, N \rrbracket$ and $\llbracket 1, N \rrbracket$, respectively), and let h^{S6V} and $h_{\geq 1}^{\text{S6V}}$ be their respective colored height functions as defined in (2.12). Then $(h^{\text{S6V}}(x, 0; y, t))_{x, y, t \in \mathbb{N}} \stackrel{d}{=} (h_{\geq 1}^{\text{S6V}}(x, 0; y, t))_{x, y, t \in \mathbb{N}}$.*

Proof. This is an immediate consequence of color merging for colored S6V (Remark 2.16): in the colored S6V model on $\mathbb{Z}_{\geq 1} \times \llbracket -N, \infty \rrbracket$ with boundary condition σ in the statement, we merge the colors $\llbracket -\infty, 0 \rrbracket \cup \{-\infty\}$ with $-\infty$ and thus obtain the colored S6V model on $\mathbb{Z}_{\geq 1} \times \llbracket 1, \infty \rrbracket$ with boundary condition $\sigma_{\geq 1}$. \square

As noted, the convergence of the S6V and ASEP sheets to \mathcal{S} is a statement about the colored height functions at a fixed time, so to prove Theorems 2.8 and 2.18 we can restrict our attention to the colored height function at time M for fixed M , i.e., $h^{\text{S6V}}(\cdot, 0; \cdot, M)$. Note that we switched the notation for the time argument from t to M ; this is so as to match the notation of the colored q -Boson model as well as [AB24].

3.2.2. *Relation to colored S6V.* With these preliminaries, we may state the crucial link between the colored Hall-Littlewood line ensemble and the height functions in colored S6V. Its proof, originally due to [AB24], relies on the Yang-Baxter equation of colored S6V and the colored q -Boson model. Because our arguments fundamentally rely on this result, we give a self-contained proof in Appendix A.

Proposition 3.12 ([AB24, Theorem 4.7]). *Fix $N, M \in \mathbb{N}$, $\sigma : \llbracket 1, N \rrbracket \rightarrow \llbracket 1, N \rrbracket$, $q \in [0, 1)$, and $z \in (0, 1)$. Let h^{S6V} be the height function associated with the colored S6V on $\mathbb{Z}_{\geq 1} \times \llbracket 1, \infty \rrbracket$ as in (2.12) and $\mathbf{L}^{\text{cHL},(j)}$ be as in Definition 3.7 (with the associated colored q -Boson model on domain $\mathbb{Z}_{\leq 0} \times \llbracket 1, N + M \rrbracket$), both with boundary condition σ . We have the equality in distribution of $(h^{\text{S6V}}(k, 0; y, M))_{y \in \llbracket 1, N-1 \rrbracket, k \in \llbracket 1, N \rrbracket}$ and $(L_1^{\text{cHL},(k)}(y))_{y \in \llbracket 1, N-1 \rrbracket, k \in \llbracket 1, N \rrbracket}$.*

Next we move to describing a Gibbs property of the colored Hall-Littlewood line ensemble.

3.2.3. *Colored Hall-Littlewood Gibbs property.* From the definition of the colored Hall-Littlewood line ensemble in terms of the colored q -Boson model, and the Gibbs property of the latter recorded in Lemma 3.5, we obtain a Gibbs property for the former. We restrict ourselves to stating the case where the system contains only two colors, i.e., $\sigma : \llbracket 1, N \rrbracket \rightarrow \llbracket 1, 2 \rrbracket$, as this will turn out to suffice for our purposes (by performing a color merging later, see Section 4), though more general Gibbs properties involving more colors also hold. In this case, $\mathbf{L}^{\text{cHL},(1)}$ and $\mathbf{L}^{\text{cHL},(2)}$ determine the colored arrow configurations at all vertices in the system via Definition 3.7. Let $\mathcal{F}_k^{\text{cHL}}$ (“cHL” short for colored Hall-Littlewood) be the σ -algebra

$$\mathcal{F}_k^{\text{cHL}} = \sigma \left(\{ L_i^{\text{cHL},(1)}(x), L_j^{\text{cHL},(2)}(x) : i \in \mathbb{N}, j \in \llbracket k+1, \infty \rrbracket, x \in \llbracket 0, N+M \rrbracket \} \right); \quad (3.8)$$

in words, we condition on all curves of the line ensemble $\mathbf{L}^{\text{cHL},(1)}$, and the curves indexed $k+1$ or larger of $\mathbf{L}^{\text{cHL},(2)}$. We now state the Gibbs property of the colored Hall-Littlewood line ensemble that we will need. Recall the notation $\mathbf{L}_{z,v}$ from before Lemma 3.4.

Lemma 3.13 (Colored Hall-Littlewood Gibbs property). *Under the colored Hall-Littlewood line ensemble measure (with boundary condition $\sigma : \llbracket 1, N \rrbracket \rightarrow \llbracket 1, 2 \rrbracket$), the conditional distribution of $L_k^{\text{cHL},(2)}(\cdot)$ given $\mathcal{F}_k^{\text{cHL}}$ is supported on the collection of Bernoulli paths $L' : \llbracket 0, N+M \rrbracket \rightarrow \mathbb{Z}$ such*

that (i) $L_k^{\text{cHL},(1)}(\cdot) - L'(\cdot)$ is a Bernoulli path and (ii) $L'(\cdot) \geq L_{k+1}^{\text{cHL},(2)}(\cdot)$ with $L'(N+M) = 0$ and $L'(0) = L_{k+1}^{\text{cHL},(2)}(0)$; call the (random) set of such Bernoulli paths Supp^{cHL} .

For such a Bernoulli path L' , let $(\mathbf{A}'_v, i'_v; \mathbf{B}'_v, j'_v)_{v \in \Gamma_k}$ be the associated tuple determined by $L'(\cdot)$, $L_k^{\text{cHL},(1)}(\cdot)$, $L_{k+1}^{\text{cHL},(1)}(\cdot)$, and $L_{k+1}^{\text{cHL},(2)}(\cdot)$ on the event that $L_k^{\text{cHL},(2)}(\cdot) = L'(\cdot)$ (we write i'_v and not i'_v as it has no dependence on $L'(\cdot)$). The condition $L'(\cdot) \in \text{Supp}^{\text{cHL}}$ is equivalent to $(\mathbf{A}'_v; \mathbf{B}'_v, j'_v)_{v \in \Gamma_k} \in \text{Supp}^{\text{cB}}$ (the latter as in Lemma 3.5). Further, the conditional probability that $L_k^{\text{cHL},(2)}(\cdot) = L'(\cdot)$, for any fixed (i.e., deterministic) selection of the righthand side, is proportional to $\prod_{v \in \Gamma_k} \mathbf{L}_{z,v}(\mathbf{A}'_v, i'_v; \mathbf{B}'_v, j'_v) \mathbb{1}_{(\mathbf{A}'_v; \mathbf{B}'_v, j'_v)_{v \in \Gamma_k} \in \text{Supp}^{\text{cB}}}$.

Proof. The lemma follows from Lemma 3.5 and Definition 3.7 relating the color Hall-Littlewood line ensemble and the arrow configurations of the colored q -Boson model; note that (i) and (ii) in the hypotheses of Lemma 3.13 correspond to (i) and (ii) in Lemma 3.5 (for (i), using that $L_k^{\text{cHL},(1)}(\cdot) - L_k^{\text{cHL},(2)}(\cdot)$ decreases by 1 from x to $x+1$ exactly at those x such that an arrow of color 1 exits horizontally from $(-k, x)$, by Lemma 3.9 (iii)). \square

There is also a Gibbs property for the uncolored Hall-Littlewood line ensemble, i.e., $\mathbf{L}^{\text{cHL},(1)}$, obtained by translating Lemma 3.4. We will discuss this in more detail in Section 3.3 next.

3.3. Convergence of line ensembles. In this section we discuss convergence results for a class of discrete line ensembles possessing a certain Gibbs property (that of the uncolored Hall-Littlewood line ensemble). The statement we give for the limit of line ensembles is under a general framework which we introduce now. Because of the general setup, these line ensembles are not necessarily related to the q -Boson vertex model; having said that, as mentioned, the example the framework will be applied to in this paper is the uncolored Hall-Littlewood line ensemble $\mathbf{L}^{\text{cHL},(1)}$.

3.3.1. Hall-Littlewood Gibbs property. The line ensembles we consider will possess the *Hall-Littlewood Gibbs property*, which describes the interactions that curves in the ensemble have with each other. We start by precisely specifying the data we condition on in the Gibbs property.

Definition 3.14. Let $\mathbf{L} : \mathbb{N} \times \Lambda \rightarrow \mathbb{Z}$ be a discrete line ensemble (recall Definition 3.6). Let $\llbracket j, k \rrbracket \subset \mathbb{N}$ and $\llbracket a, b \rrbracket \subset \Lambda$ be intervals. We define $\mathcal{F}_{\text{ext}}(\llbracket j, k \rrbracket, \llbracket a, b \rrbracket, \mathbf{L})$ to be the σ -algebra generated by the collection of random variables $\{L_i(x) : (i, x) \in \mathbb{N} \times \Lambda \setminus (\llbracket j, k \rrbracket \times \llbracket a+1, b-1 \rrbracket)\}$.

When the line ensemble under discussion is clear, we will drop \mathbf{L} from the notation. Similarly when $j = 1$, we will replace $\llbracket 1, k \rrbracket$ by simply k . Thus $\mathcal{F}_{\text{ext}}(k, \llbracket a, b \rrbracket)$ would denote $\mathcal{F}_{\text{ext}}(\llbracket 1, k \rrbracket, \llbracket a, b \rrbracket, \mathbf{L})$.

Next, recall the definition of a Bernoulli path from Definition 2.9. For $a, b, x, y \in \mathbb{Z}$ with $a < b$, $y \leq x \leq y + b - a$, we define a *Bernoulli random walk bridge* $B : \llbracket a, b \rrbracket \rightarrow \mathbb{Z}$ from (a, x) to (b, y) to be a uniformly selected random path from the set of all Bernoulli paths $\gamma : \llbracket a, b \rrbracket \rightarrow \mathbb{Z}$ with $\gamma(a) = x$ and $\gamma(b) = y$ (assuming this set is non-empty).

Definition 3.15 (Weight factor). Let $\llbracket a, b \rrbracket \subseteq \mathbb{Z}$ and fix $q \in [0, 1)$. Let $\gamma = (\gamma_1, \dots, \gamma_k)$, f , and g be a collection of Bernoulli paths (f and g should be thought of as upper and lower boundary curves respectively), all defined on $\llbracket a, b \rrbracket$, with $\gamma_i(x) \geq \gamma_{i+1}(x)$ for $i \in \llbracket 1, k-1 \rrbracket$, $\gamma_1(x) \leq f(x)$, and $\gamma_k(x) \geq g(x)$ for all $x \in \llbracket a, b \rrbracket$. We define the weight factor $W(\gamma, f, g, \llbracket a, b \rrbracket)$ by

$$W(\gamma, f, g, \llbracket a, b \rrbracket) := \prod_{i=0}^k \prod_{x=a+1}^b \left(1 - q^{\Delta_i(x-1)} \mathbb{1}_{\Delta_i(x) = \Delta_i(x-1)-1} \right), \quad (3.9)$$

where $\Delta_i(x) = \gamma_i(x) - \gamma_{i+1}(x)$ and $\gamma_0 = f$ and $\gamma_{k+1} = g$ by convention. For curves which do not satisfy the ordering conditions mentioned above, we define $W(\gamma, f, g, \llbracket a, b \rrbracket) = 0$; observe that (3.9) equals 0 if at any location the separation between consecutive curves drops from 0 to -1 . See also Figure 12. When the interval under consideration is obvious from the context we will drop $\llbracket a, b \rrbracket$

from the notation. Moreover, if $f = \infty$, we drop it from the notation; if in addition $g = -\infty$, then we drop it from the notation as well.

Sometimes, to emphasize whether we are focusing on interaction with the upper curve f , between the curves of γ , or with the lower curve g , we will write

$$W(\gamma, f, g) = W_{\text{up}}(\gamma_1, f) \cdot W_{\text{int}}(\gamma) \cdot W_{\text{low}}(\gamma_k, g),$$

where, in (3.9), $W_{\text{up}}(\gamma_1, f)$ is the factor corresponding to $i = 0$, $W_{\text{int}}(\gamma)$ is the product corresponding to $i = 1, \dots, k-1$, and $W_{\text{low}}(\gamma_k, g)$ to the factor with $i = k$.

The following is the Gibbs property that the line ensembles in the general framework we are setting up will possess; it originally appeared and was studied in [CD18].

Definition 3.16. (Hall-Littlewood Gibbs property) We say a discrete line ensemble \mathbf{L} satisfies the (uncolored) *Hall-Littlewood Gibbs property* (with parameter $q \in [0, 1)$) if the following holds for any $\llbracket j, k \rrbracket \subset \mathbb{N}$ and $\llbracket a, b \rrbracket \subset \Lambda$. Conditionally on $\mathcal{F} = \mathcal{F}_{\text{ext}}(\llbracket j, k \rrbracket, \llbracket a, b \rrbracket, \mathbf{L})$, the distribution of $\mathbf{L}|_{\llbracket j, k \rrbracket \times \llbracket a, b \rrbracket}$ is given by a collection of $k - j + 1$ Bernoulli random walk bridges $\mathbf{B} = (B_j, \dots, B_k)$, where $B_i(a) = L_i(a)$ and $B_i(b) = L_i(b)$ for each $i \in \llbracket j, k \rrbracket$, reweighted by the Radon-Nikodym derivative $W(\mathbf{B}, L_{j-1}, L_{k+1}) / \mathbb{E}_{\mathcal{F}}[W(\mathbf{B}, L_{j-1}, L_{k+1})]$, where $L_0 \equiv \infty$ by convention.

Equivalently, for any bounded function $F : \mathbb{R}^{\llbracket j, k \rrbracket \times \llbracket a, b \rrbracket} \rightarrow \mathbb{R}$,

$$\mathbb{E}_{\mathcal{F}}[F(L_j, \dots, L_k)] = \frac{\mathbb{E}_{\mathcal{F}}[F(B_j, \dots, B_k)W(\mathbf{B}, L_{j-1}, L_{k+1})]}{\mathbb{E}_{\mathcal{F}}[W(\mathbf{B}, L_{j-1}, L_{k+1})]}$$

(here $\mathbb{E}_{\mathcal{F}}[\cdot]$ is shorthand for $\mathbb{E}[\cdot | \mathcal{F}]$, and we will also use analogous notation $\mathbb{P}_{\mathcal{F}}(\cdot)$ for $\mathbb{P}(\cdot | \mathcal{F})$). We will sometimes write $Z = \mathbb{E}_{\mathcal{F}}[W(\mathbf{B}, L_{j-1}, L_{k+1})]$, but this will always be made explicit.

As above, we will usually refer to this property as the Hall-Littlewood Gibbs property (dropping the ‘‘uncolored’’ adjective); this will not cause confusion as we will always explicitly say ‘‘colored’’ when referring to its colored analog.

This Gibbs property is satisfied by $\mathbf{L}^{\text{cHL},(1)}$, but not in general by $\mathbf{L}^{\text{cHL},(j)}$ for $j \geq 2$.

Proposition 3.17. $\mathbf{L}^{\text{cHL},(1)} = (L_1^{\text{cHL},(1)}, L_2^{\text{cHL},(1)}, \dots)$ has the Hall-Littlewood Gibbs property for any boundary condition $\sigma : \llbracket 1, N \rrbracket \rightarrow \llbracket 1, N \rrbracket$.

Proof. This is a direct consequence of Lemma 3.4 after translating to the line ensemble notation from Definition 3.7, using also from Lemma 3.10 that $\mathbf{L}^{\text{cHL},(1)}$ is in distribution the line ensemble associated to the uncolored q -Boson model. \square

A derivation of Proposition 3.17 is also contained in [AB24, Proposition 5.1], and an alternate derivation is present in [CD18, Proposition 3.9] after matching $\mathbf{L}^{\text{cHL},(1)}$ with the (uncolored) Hall-Littlewood process.

3.3.2. Heuristic behavior of the Gibbs property. For intuition, the Gibbs property should be thought of as a resampling property, as in Figure 15 ahead: it says that the following resampling procedure leaves the distribution of the line ensemble unchanged. First, with $\llbracket j, k \rrbracket \subseteq \mathbb{N}$ and $\llbracket a, b \rrbracket \subseteq \Lambda$ fixed, we erase \mathbf{L} on $\llbracket j, k \rrbracket \times \llbracket a+1, b-1 \rrbracket$ while retaining the information of its values on $\mathbb{N} \times \Lambda \setminus (\llbracket j, k \rrbracket \times \llbracket a+1, b-1 \rrbracket)$. Then we attempt to replace L_j, \dots, L_k on $\llbracket a, b \rrbracket$ with a tuple \mathbf{B} of $k - j + 1$ independent Bernoulli random walk bridges with endpoints of B_i equaling $L_i(a)$ and $L_i(b)$ at a and b , respectively: the attempt succeeds with probability $W(\mathbf{B}, L_{j-1}, L_{k+1})$ as given in Definition 3.15, independent of everything else; note that if any individual curve of \mathbf{B} crosses L_{j-1}, L_{k+1} , or any other curve of \mathbf{B} , then $W(\mathbf{B}, L_{j-1}, L_{k+1}) = 0$ and the attempt certainly fails. On the event of \mathbf{B} successfully replacing L_j, \dots, L_k on $\llbracket a, b \rrbracket$, the former’s law is exactly that of k independent Bernoulli random walk bridges under the reweighting by the Radon-Nikodym derivative $W(\mathbf{B}, L_{j-1}, L_{k+1}) / \mathbb{E}_{\mathcal{F}}[W(\mathbf{B}, L_{j-1}, L_{k+1})]$.

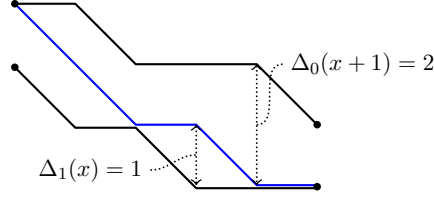


FIGURE 12. An example of the Hall-Littlewood weight factor with a single curve γ . The top and bottom curves (in black) are f and g , respectively, and are fixed, and the blue curve is γ . In calculating the weight factor W , the separation of γ from f and g as captured by $\Delta_i(\cdot)$ is used. In this example, $W(\gamma, f, g) = (1 - q^2) \cdot (1 - q)^2$: the separation $\Delta_0(\cdot)$ between f and γ reduces only at the penultimate step, from 2 to 1, and the separation $\Delta_1(\cdot)$ between γ and g reduces twice, each time from 1 to 0.

The basic idea underlying many of our arguments is that behavior which is unlikely for such reweighted Bernoulli random walk bridges must also be unlikely for the original line ensemble.

The above is really a perspective on Gibbs properties of line ensembles in general, and now we discuss the particular features of the Hall-Littlewood Gibbs property that constitute a major challenge and necessitate the development of new techniques, compared to previous studies of line ensembles with different Gibbs properties. In our setup, we will consider sequences of line ensembles indexed by a parameter N (which should not be confused with the N parameter of the colored S6V model or the colored q -Boson model in Section 3.1). Our goal in Section 3.3 is to give a result of convergence of these line ensembles, rescaled by the KPZ exponents, to the parabolic Airy line ensemble. This means that we scale the spatial argument of the line ensemble by $N^{2/3}$ and the value of the lines by $N^{1/3}$ (both up to constants) in order to obtain a tight, or unit-order, sequence.

At short range, the resampling property penalizes curves coming closer together, as encoded by the indicator function in (3.9). This is a somewhat complicated interaction as it is not always active, and, more importantly, does not satisfy a certain convenient stochastic monotonicity property. Before discussing these aspects, let us first consider how the interaction behaves on the larger scale on which our limits will be taken. This means evaluating the weight function (3.9) when $\llbracket a, b \rrbracket$ is an interval of size of order $N^{2/3}$ and $\Delta_i(x)$ is of order $N^{1/3}$: then W is $(1 - q^{O(N^{1/3})})^{O(kN^{2/3})}$, i.e., essentially 1 when $q \in [0, 1)$ is fixed. This assumes the separation between consecutive curves is of order $N^{1/3}$ throughout the interval; if instead at some location consecutive curves cross, the weight factor becomes zero as before. Thus at large N the weight factor is expected to behave like the indicator function of the curves not intersecting, mimicking the Brownian Gibbs property (see Definition 6.4) for the parabolic Airy line ensemble (the putative limit of our discrete one).

3.3.3. Lack of stochastic monotonicity. Actually establishing this separation (that the above heuristic relies on) is non-trivial and will constitute the bulk of the proof of our convergence results. Some challenges are exactly the earlier mentioned complicated nature of the interaction at short range, from which we must argue we can escape to a larger scale, and that the Hall-Littlewood Gibbs property does not possess a stochastic monotonicity property present in other Gibbs properties previously studied. Stochastic monotonicity means that if one considers the law of the curves of the line ensemble inside $\llbracket j, k \rrbracket \times \llbracket a, b \rrbracket$ conditional on the boundary data, and then considers the same law with the boundary points increased and/or the upper and lower curves increased, the second law is stochastically larger than the first (i.e., there is a coupling of the two laws under which each curve in the second collection, with higher boundary data, is pointwise larger than the corresponding curve in the first collection). The Hall-Littlewood Gibbs property fails to satisfy this because W from (3.9) is a monotone function of the discrete derivative of the distance between consecutive curves and not of the distance itself. See Figure 13 for an example demonstrating the

lack of stochastic monotonicity. The violations of stochastic monotonicity can be fairly severe and it is also possible to find counterexamples to versions of stochastic monotonicity with more conditions imposed, e.g., comparing only boundary conditions which share the same endpoints.

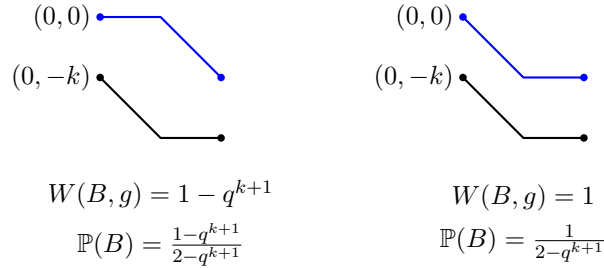


FIGURE 13. An example of the failure of stochastic monotonicity for the Hall-Littlewood Gibbs property. Here g is the lower boundary curve drawn in black (indexed by its starting location $(0, -k)$) and B is the random curve drawn in blue (whose endpoints are fixed). We see that the probability of the higher possibility for B equals $\frac{1 - q^{k+1}}{2 - q^{k+1}}$, which is increasing in k , while stochastic monotonicity requires it to be non-increasing.

The approach to line ensemble tightness we develop relies instead on a form of weak monotonicity for a single curve (a minor refinement of a notion introduced in [CD18]); see Section 8. By this we mean a comparison of partition functions (up to a, possibly large, constant) of certain pairs of laws corresponding to a single curve under different boundary conditions, which translates to a comparison (up to the same constant) of one-point probabilities for a single curve. In particular, it does not hold for collections of more than one curve, and does not imply the existence of a coupling of the two laws such that all points on the pair of curves are ordered. Using this weak monotonicity, we iteratively establish uniform separation of order $N^{1/3}$ between curves further and further down in the line ensemble, simultaneously establishing control on how far down such curves can be. We will discuss and develop this more later (see Section 9); here we next introduce the general framework under which our arguments operate.

3.3.4. Assumptions on line ensembles and their tightness. In this section we formulate some assumptions on general line ensembles under which we will prove tightness. Before stating them, we specify the space we will work on and some conventions about the objects.

Our sequence of discrete line ensembles will be denoted by $\mathbf{L}^N = (L_1^N, L_2^N, \dots)$. Here N is an indexing parameter which has no relation to the parameter in the colored S6V or colored q -Boson models. Though discrete valued, we will regard \mathbf{L}^N as an element of $\mathcal{C}(\mathbb{N} \times \mathbb{R}, \mathbb{R})$, by linearly interpolating $L_i^N(x)$ for $x \in [j, j + 1]$ for each $i \in \mathbb{N}$ and $j \in \mathbb{Z}$; here $\mathbb{N} \times \mathbb{R}$ is given the product topology of the discrete topology on \mathbb{N} and the usual Euclidean topology on \mathbb{R} . We endow the space $\mathcal{C}(\mathbb{N} \times \mathbb{R}, \mathbb{R})$ with the topology of uniform convergence on compact sets, i.e., $\mathbf{f}^{(n)}, \mathbf{f} \in \mathcal{C}(\mathbb{N} \times \mathbb{R}, \mathbb{R})$ satisfy $\mathbf{f}^{(n)} \rightarrow \mathbf{f}$ if for any compact set $K \subseteq \mathbb{R}$ and $i \in \mathbb{N}$ fixed, $f_i^{(n)}(x) \rightarrow f_i(x)$ uniformly over $x \in K$.

Further, we allow a sequence g_N going to ∞ with $N \rightarrow \infty$ such that the values of $L_i^N(x)$ are not specified for $|x| \geq g_N N^{2/3}$, as these values do not affect the existence or value of the limits we consider (which are determined by uniform convergence on compact sets on the $N^{2/3}$ spatial scale); in particular, $L_i^N(x)$ may be defined for such values in any way such that \mathbf{L}^N is an element of $\mathcal{C}(\mathbb{N} \times \mathbb{R}, \mathbb{R})$, without regard for satisfying the assumptions below.

Now we may turn to the precise assumptions we assume on our line ensembles $\mathbf{L}^N = (L_1^N, L_2^N, \dots)$.

Assumption 1 (Hall-Littlewood Gibbs property). \mathbf{L}^N has the Hall-Littlewood Gibbs property with parameter $q \in [0, 1)$ fixed (Definition 3.16).

Assumption 2 (One-point tightness of top curve around parabola). There exist $p \in (-1, 0)$ and $\lambda > 0$ such that, for any $\delta > 0$ there exists $M = M(\delta)$ such that

$$\sup_{x \in \mathbb{R}} \limsup_{N \rightarrow \infty} \mathbb{P} \left(|L_1^N(xN^{2/3}) - pxN^{2/3} + \lambda x^2 N^{1/3}| > MN^{1/3} \right) \leq \delta.$$

Equivalently, for any $\delta > 0$ there exists M such that for all $x \in \mathbb{R}$ there exists N_0 such that, for $N > N_0$,

$$\mathbb{P} \left(|L_1^N(xN^{2/3}) - pxN^{2/3} + \lambda x^2 N^{1/3}| > MN^{1/3} \right) \leq \delta. \quad (3.10)$$

By our convention on the definition of $L_i^N(x)$ for $|x| \geq g_N N^{2/3}$, Assumption 1 is only needed for $L^N|_{\mathbb{N} \times [-g_N N^{2/3}, g_N N^{2/3}]}$. We will not explicitly mention this point or the general point about the definition of $L_i^N(x)$ for $|x| \geq g_N N^{2/3}$ further.

We note that Assumption 2 is satisfied if it is known that the union over $x \in \mathbb{R}$ of the set of subsequential weak limits of $\{N^{-1/3}(L_1^N(xN^{2/3}) - pxN^{2/3} + \lambda x^2 N^{1/3})\}_{N=1}^\infty$ is a tight collection (for instance, as will be the case for our models of interest, if it is a single distribution, e.g., a constant multiple of the GUE Tracy-Widom distribution).

We will need to rescale our line ensembles to state our results. For $p \in (-1, 0)$, $\lambda > 0$, and $N \in \mathbb{N}$, we introduce a scaling operator $T_{p,\lambda,N} : \mathcal{C}(\mathbb{N} \times \mathbb{R}, \mathbb{R}) \rightarrow \mathcal{C}(\mathbb{N} \times \mathbb{R}, \mathbb{R})$ defined by the following for $\mathbf{f} \in \mathcal{C}(\mathbb{N} \times \mathbb{R}, \mathbb{R})$, $i \in \mathbb{N}$, and $x \in \mathbb{R}$:

$$(T_{p,\lambda,N}(\mathbf{f}))_i(x) := \sigma^{-1} N^{-1/3} \left(f_i(\beta x N^{2/3}) - p \beta x N^{2/3} \right) \quad (3.11)$$

where β and σ are such that

$$\sigma^{-1} \beta^2 \lambda = 1 \quad \text{and} \quad \sigma^{-2} \beta p (1 - p) = 2. \quad (3.12)$$

For L^N satisfying Assumption 2, and with p and λ as there, define $\mathfrak{L}^N : \mathbb{N} \times \mathbb{R} \rightarrow \mathbb{R}$ by

$$\mathfrak{L}^N := T_{p,\lambda,N}(L^N). \quad (3.13)$$

The equations (3.12) are the analogs of the conditions (2.9). The first condition will ensure that $\mathfrak{L}_1^N(x)$ decays like $-x^2$; the second will ensure that the large N limit of \mathfrak{L}^N has the Brownian Gibbs property (Definition 6.4) with the correct diffusion coefficient of 2.

Now we may state the tightness result we prove, which is a key result needed to establish our main results, Theorems 2.8 and 2.18; the proof will be given in Section 6.4.

Theorem 3.18 (Tightness of line ensembles). *Let $L^N : \mathbb{N} \times \mathbb{R} \rightarrow \mathbb{R}$ be a line ensemble satisfying Assumptions 1 and 2. Then $\{\mathfrak{L}^N\}_{N=1}^\infty$ is tight in the space $\mathcal{C}(\mathbb{N} \times \mathbb{R}, \mathbb{R})$, under the topology of uniform convergence on compact sets.*

The following is a third assumption which will be needed to ensure that there is a unique limiting line ensemble, and that it is the parabolic Airy line ensemble \mathcal{P} from Definition 2.1.

Assumption 3 (GUE Tracy-Widom convergence). There exists $x \in \mathbb{R}$ such that $\mathfrak{L}_1^N(x) + x^2 \xrightarrow{d}$ GUE-TW (the GUE Tracy-Widom distribution, as defined at the end of Definition 2.1) as $N \rightarrow \infty$.

The following gives the convergence to \mathcal{P} of the rescaled line ensemble \mathfrak{L}^N . It will be proved in Section 6 as a quick consequence of the tightness from Theorem 3.18, together with the recent characterization result for Brownian Gibbsian line ensembles from [AH23b].

Theorem 3.19. *Suppose L^N satisfies Assumptions 1 and 2. Then any subsequential limit of $\{\mathfrak{L}^N\}_{N=1}^\infty$ is $\mathcal{P} + \mathbf{c}$, where $\mathbf{c} \in \mathbb{R}$ is a random variable independent of \mathcal{P} (but which may depend on the subsequence taken), under the topology of uniform convergence on compact sets. If additionally Assumption 3 is satisfied, then $\mathbf{c} = 0$, i.e., $\mathfrak{L}^N \xrightarrow{d} \mathcal{P}$.*

3.4. Last passage percolation in the colored Hall-Littlewood line ensemble. We now turn to stating our results on the relation between $\mathbf{L}^{\text{cHL},(1)}$ and $(\mathbf{L}^{\text{cHL},(2)}, \mathbf{L}^{\text{cHL},(3)}, \dots)$ (under general boundary condition σ) as defined in (3.6). In particular, we give a precise statement of the approximate representation of $L_1^{\text{cHL},(j)}$ as a last passage percolation (LPP) problem in $\mathbf{L}^{\text{cHL},(1)}$, which in fact holds exactly when $q = 0$.

Recall the definition of $\mathbf{L}^{\text{cHL},(j)}$ from (3.6) and the notation for LPP problems from (2.2); this notation is for an LPP problem in an environment given by a family of continuous functions, and for this purpose as well as in the next result, we regard $\mathbf{L}^{\text{cHL},(1)}$ as a collection of continuous functions on the real interval $[0, N + M]$ by linear interpolation, as in the setup introduced in Section 3.3.4. We prove the next result in Section 4.

Theorem 3.20. *Fix $N, M \in \mathbb{N}$, any boundary condition $\sigma : \llbracket 1, N \rrbracket \rightarrow \llbracket 1, N \rrbracket$ and $q \in [0, 1)$. Let $(\mathbf{L}^{\text{cHL},(1)}, \dots, \mathbf{L}^{\text{cHL},(N)})$ be the associated colored Hall-Littlewood line ensemble as given by Definition 3.7. There exist positive constants c (absolute), and $K = K(q)$ such that for any $j, k \geq 1$ and $m \geq K \log N$,*

$$\mathbb{P} \left(\sup_{y \in [0, N+M]} \left| L_1^{\text{cHL},(j)}(y) - \sup_{z \leq y} \left(L_{k+1}^{\text{cHL},(j)}(z) + \mathbf{L}^{\text{cHL},(1)}[(z, k) \rightarrow (y, 1)] \right) \right| \geq km \right) \leq kq^{cm^2}. \quad (3.14)$$

When $q = 0$, $L_1^{\text{cHL},(j)}(y) = \sup_{z \leq y} (L_{k+1}^{\text{cHL},(j)}(z) + \mathbf{L}^{\text{cHL},(1)}[(z, k) \rightarrow (y, 1)])$ for all $y \in [0, N + M]$, $j \in \llbracket 1, N \rrbracket$, and $k \in \mathbb{N}$.

Recall the definition of the Airy sheet from Definition 2.3, the definition of $\mathcal{S}^{\text{S6V}, \varepsilon}$ from (2.15), and the relation of $L_1^{\text{cHL},(j)}$ to the S6V height function h^{S6V} from Proposition 3.12. At this point in our discussion, it should not be hard to believe that, given the representation of $L_1^{\text{cHL},(j)}$ in Theorem 3.20 and the convergence of $\mathbf{L}^{\text{cHL},(1)}$ to \mathcal{P} from Theorem 3.19, the convergence of $\mathcal{S}^{\text{S6V}, \varepsilon}$ to \mathcal{S} will follow (and similarly the convergence of $\mathcal{S}^{\text{ASEP}, \varepsilon}$ which, as mentioned in the beginning of Section 3, will be proved by a limit to ASEP from S6V). Indeed, given the results we have stated in this section, the argument to establish this is at this point well-known, following presentations in [DOV22] and [DV21b]; as a result we give the proof of Theorems 2.18 and 2.8 in Section 7.1 after relegating some of the standard details to Appendix C.

4. APPROXIMATE LPP REPRESENTATION

In this section we prove Theorem 3.20. Recall that we allow a general boundary condition encoded by a function $\sigma : \llbracket 1, N \rrbracket \rightarrow \llbracket 1, N \rrbracket$, where $\sigma(k)$ is the color of the arrow horizontally entering the domain $\mathbb{Z}_{\leq 0} \times \llbracket 1, N + M \rrbracket$ of the colored q -Boson model at $(1, k)$.

4.1. Pitman transform and the $q = 0$ case. For two functions $f, g : \mathbb{Z}_{\geq 0} \rightarrow \mathbb{R}$, we define the *Pitman transform* $\text{PT}(f, g) : \mathbb{Z}_{\geq 0} \rightarrow \mathbb{R}$ by

$$\text{PT}(f, g)(y) := f(y) + \max_{0 \leq y' \leq y} (g(y') - f(y')). \quad (4.1)$$

The Pitman transform should be thought of as an LPP problem across two curves, with the bottom one equal to g and the top equal to f (this interpretation assumes $g(0) = 0$, as will be the case in our context). Indeed, we will ultimately access the LPP value across k lines by iterated applications of PT.

We start by stating and proving a statement in the case of $q = 0$, in order to make the source of the Pitman transform in the colored Hall-Littlewood line ensemble more transparent; we will subsequently turn to obtaining a similar statement in the case of general $q \in [0, 1)$ in Section 4.2.

In this section we will mainly restrict to the case where $\sigma : \llbracket 1, N \rrbracket \rightarrow \llbracket 1, 2 \rrbracket$, i.e., arrows in the colored q -Boson model are only of color 1 or 2, as this will suffice for the proof of Theorem 3.20 (see the end of this section) by color merging. We drop the superscript of ‘‘cHL’’ when writing the colored

Hall-Littlewood line ensemble; for instance we will write $L_i^{(j)}$ for $L_i^{\text{cHL},(j)}$. We will also refer to arrows of color 2 as 2-arrows, and analogously 1-arrows for arrows of color 1. In particular, recalling the relation of the colored Hall-Littlewood line ensemble and the colored q -Boson model from Definition 3.7, $L_k^{(2)}$ corresponds to counts of 2-arrows in the k^{th} column (i.e., $\{-k\} \times \llbracket 1, N + M \rrbracket$) of the colored q -Boson model, while $L_k^{(1)}$ corresponds to combined arrow counts of 1- and 2-arrows in the same column.

Lemma 4.1. *Let $q = 0$. For any boundary condition $\sigma : \llbracket 1, N \rrbracket \rightarrow \llbracket 1, 2 \rrbracket$ and any $k \in \mathbb{N}$,*

$$L_k^{(2)} = \text{PT} \left(L_k^{(1)}, L_{k+1}^{(2)} \right).$$

It turns out that a lower bound actually holds deterministically for all $q \in [0, 1)$. We state and prove it first before giving the proof of Lemma 4.1 that equality holds when $q = 0$.

Lemma 4.2. *For any $q \in [0, 1)$, boundary condition $\sigma : \llbracket 1, N \rrbracket \rightarrow \llbracket 1, 2 \rrbracket$, and $k \in \mathbb{N}$,*

$$L_k^{(2)} \geq \text{PT} \left(L_k^{(1)}, L_{k+1}^{(2)} \right).$$

Proof. Fix y . Recalling the definition (4.1) of the Pitman transform, we must show that

$$L_k^{(2)}(y) \geq L_k^{(1)}(y) + \max_{y' \leq y} \left(L_{k+1}^{(2)}(y') - L_k^{(1)}(y') \right).$$

Let us write $O_k(y) = L_k^{(1)}(y) - L_k^{(2)}(y)$, so that $O_k(y)$ is the number of 1-arrows exiting the k^{th} column in the colored q -Boson model at row strictly higher than y . Then, from the previous display, what we have to show is equivalent to

$$\min_{y' \leq y} \left(O_k(y') + L_k^{(2)}(y') - L_{k+1}^{(2)}(y') \right) \geq O_k(y). \quad (4.2)$$

Now, recall from (3.7) that $L_k^{(2)}(y') \geq L_{k+1}^{(2)}(y')$ for all y' and observe that $O_k(y)$ is non-increasing in y by its definition as the count of 1-arrows (analogous to the fact that $L_k^{(j)}(y+1) \leq L_k^{(j)}(y)$ noted in the third part of (3.7)). This yields that the lefthand side of the previous display is at least the righthand side. \square

Proof of Lemma 4.1. We continue with the notation $O_k(y) = L_k^{(1)}(y) - L_k^{(2)}(y)$ from the previous proof for the count of 1-arrows exiting the k^{th} column at row strictly higher than y . By Lemma 4.2, we must show (4.2) holds with equality, i.e., for some $y' \leq y$,

$$O_k(y') + L_k^{(2)}(y') - L_{k+1}^{(2)}(y') = O_k(y). \quad (4.3)$$

First suppose that $O_k(y') = O_k(y)$ for all $0 \leq y' \leq y$, which is the case that no 1-arrows exit horizontally from any such vertex $(-k, y')$. We observe that $L_k^{(2)}(0) = L_{k+1}^{(2)}(0)$, since both quantities are simply the total number of 2-arrows in the system, and we have established (4.3) at $y' = 0$.

Next we assume that there exists at least one vertex $(-k, y')$ with $y' \leq y$ from which a 1-arrow exits horizontally. Let y_0 be the largest such y' ; equivalently, y_0 is the largest $y' \leq y$ such that $O_k(y') = O_k(y' - 1) - 1$. Observe that then $O_k(y_0) = O_k(y)$ since O_k is non-increasing for each k .

We claim that then $L_k^{(2)}(y_0) = L_{k+1}^{(2)}(y_0)$, which would establish (4.3). Indeed, we know from the weights in the $q = 0$ case from Figure 10 that since a 1-arrow exits horizontally from $(-k, y_0)$, there is no 2-arrow entering that vertex from the left or bottom. The arrows vertically entering $(-k, y_0)$ are precisely the arrows that have exited $(-(k+1), y')$ horizontally for some $y' < y_0$ and which have not exited the k^{th} column strictly below y_0 . Thus all 2-arrows in the $(k+1)^{\text{st}}$ column that have horizontally exited that column strictly below row y_0 have also exited the k^{th} column strictly below row y_0 , and, as we already noted, a 2-arrow does not exit horizontally from $(-k, y_0)$ or $(-(k+1), y_0)$. In other words, $L_k^{(2)}(0) - L_k^{(2)}(y_0) = L_{k+1}^{(2)}(0) - L_{k+1}^{(2)}(y_0)$, which implies our claim, since $L_k^{(2)}(0) = L_{k+1}^{(2)}(0)$. \square

As we saw in Lemma 4.2, $L_k^{(2)}(y) \geq \text{PT}(L_k^{(1)}, L_{k+1}^{(2)})(y)$ deterministically. The next statement gives a bound on how much the deviation can be in the case of general $q \in [0, 1)$ and is the basic ingredient of the proof of Theorem 3.20.

Proposition 4.3. *There exist positive constants c and $K = K(q)$ such that, for any $N \in \mathbb{N}$, boundary condition $\sigma : \llbracket 1, N \rrbracket \rightarrow \llbracket 1, 2 \rrbracket$, $k \in \mathbb{N}$, $q \in [0, 1)$, and $m \geq K \log N$,*

$$\mathbb{P} \left(\max_{y \in \llbracket 0, N+M \rrbracket} \left(L_k^{(2)}(y) - \text{PT}(L_k^{(1)}, L_{k+1}^{(2)})(y) \right) \geq m \right) \leq q^{cm^2}.$$

Before turning to the proof of this statement in Section 4.2, we use it to establish Theorem 3.20.

Proof of Theorem 3.20. Recall that we have dropped the superscript cHL from the notation of the colored line ensembles. Next, it suffices to specialize to the case of $j = 2$. Indeed, the original statement will follow from this special case by Lemma 3.10 (color merging), i.e., the fact that the joint distribution of $(\mathbf{L}^{(1)}, \mathbf{L}^{(j)})$ associated to boundary condition σ is the same as that of $(\mathbf{L}^{(1)}, \mathbf{L}^{(2)})$ associated to boundary condition $\tau \circ \sigma$, where $\tau(i) = 1$ if $i \in \llbracket 1, j-1 \rrbracket$ and $\tau(i) = 2$ if $i \in \llbracket j, N \rrbracket$. In other words, we merge the colors in $\llbracket 1, j-1 \rrbracket$ to be 1 and those in $\llbracket j, N \rrbracket$ to be 2.

Inductively define $\text{PT}^{(1)} = \text{PT}$ and for $k \geq 2$

$$\text{PT}^{(k)} \left((L_i^{(1)})_{i=1}^k, L_{k+1}^{(2)} \right) := \text{PT}^{(k-1)} \left((L_i^{(1)})_{i=1}^{k-1}, \text{PT} \left(L_k^{(1)}, L_{k+1}^{(2)} \right) \right); \quad (4.4)$$

It is easy to show that

$$\text{PT}^{(k)} \left((L_i^{(1)})_{i=1}^k, L_{k+1}^{(2)} \right) = \max_{z \leq y} \left(L_{k+1}^{(2)}(z) + \mathbf{L}^{(1)}[(z, k) \rightarrow (y, 1)] \right). \quad (4.5)$$

With this we see that

$$\begin{aligned} & \mathbb{P} \left(\max_{y \in \llbracket 0, N+M \rrbracket} \left| L_1^{(2)}(y) - \max_{z \leq y} \left(L_{k+1}^{(2)}(z) + \mathbf{L}^{(1)}[(z, k) \rightarrow (y, 1)] \right) \right| \geq km \right) \\ & \leq \mathbb{P} \left(\max_{y \in \llbracket 0, N+M \rrbracket} \left| L_1^{(2)}(y) - \text{PT}(L_1^{(1)}, L_2^{(2)})(y) \right| \geq m \right) \\ & \quad + \sum_{j=1}^{k-1} \mathbb{P} \left(\max_{y \in \llbracket 0, N+M \rrbracket} \left| \text{PT}^{(j)} \left((L_i^{(1)})_{i=1}^j, L_{j+1}^{(2)} \right) (y) - \text{PT}^{(j+1)} \left((L_i^{(1)})_{i=1}^{j+1}, L_{j+2}^{(2)} \right) (y) \right| \geq m \right). \end{aligned} \quad (4.6)$$

In the $q = 0$ case, Lemma 4.1 says that the previous display is 0 for any $m > 0$. For the case of $q \in (0, 1)$, we observe that if h is a function with $\max |h| \leq \varepsilon$ for some $\varepsilon > 0$, then it follows from the representation (4.5) of $\text{PT}^{(k)}$ and the triangle inequality that, for any f_1, \dots, f_k and g ,

$$|\text{PT}^{(k)}((f_i)_{i=1}^k, g) - \text{PT}^{(k)}((f_i)_{i=1}^k, g + h)| \leq 2\varepsilon. \quad (4.7)$$

From Lemma 4.2 and Proposition 4.3 it holds that, for any $j \geq 0$ and $m \geq K \log N$,

$$\mathbb{P} \left(\max_{y \in \llbracket 0, N+M \rrbracket} \left| L_{j+1}^{(2)}(y) - \text{PT}(L_{j+1}^{(1)}, L_{j+2}^{(2)})(y) \right| \geq \frac{1}{2}m \right) \leq q^{cm^2}.$$

Combining this with (4.7) and the definition (4.4) of $\text{PT}^{(j)}$ yields that the j^{th} summand in (4.6) is upper bounded by q^{cm^2} which, on tracing back, completes the proof. \square

The rest of the section is devoted to proving Proposition 4.3.

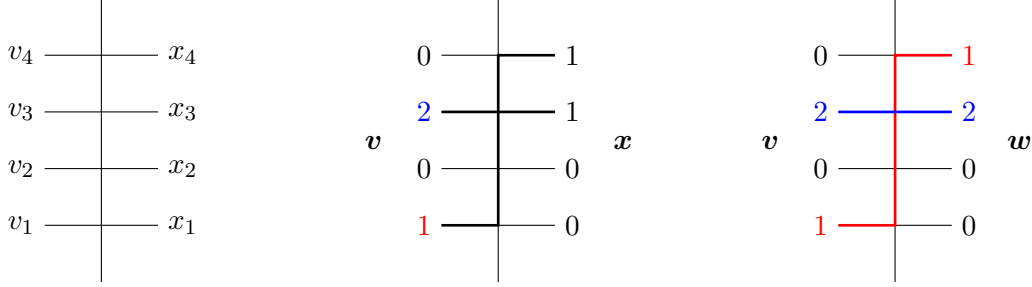


FIGURE 14. A depiction of $\mathbf{v} \in \{0, 1, 2\}^U$, $\mathbf{x} \in \{0, 1\}^U$ (left panel), an example where they are compatible (middle panel), and an example of a $\mathbf{w} \in \text{Val}(\mathbf{v}, \mathbf{x})$ (right panel). Here the 1 and 0 in black on the right side of the middle panel respectively indicate the presence or absence of an arrow of any color, while the colored numbers on the left side of the middle panel and both sides of the right panel indicate the color of the arrow.

4.2. The case of general q . As we saw in the proof of Lemma 4.1, the Pitman transform representation was essentially a consequence of the fact that, when $q = 0$, the colored q -Boson vertex weights force 2-arrows to exit horizontally before 1-arrows. In $q > 0$, 1-arrows can exit before 2-arrows, but will be penalized in weight by a factor of q^m , where m is the number of 2-arrows vertically entering at the vertex where the 1-arrow is exiting (see Figure 10). At a high level, the heuristic behind the proof of Proposition 4.3 is as follows: on the event that the deviation of the height function in the $q > 0$ case from the Pitman transform expression (as it would be in the $q = 0$ case) is m , we can find order m many different locations where a 1-arrow horizontally exits before a 2-arrow, and where there are order m many 2-arrows “in queue”, i.e., vertically entering; this will lead to the q^{cm^2} probability bound for this event.

The precise proof of Proposition 4.3 requires introducing some notation. Let $U = N + M$ (the number of rows in the colored q -Boson model). Fix $\mathbf{v} = (v_1, \dots, v_U) \in \{0, 1, 2\}^U$ and $\mathbf{x} = (x_1, \dots, x_U) \in \{0, 1\}^U$. Here v_y represents the color of the arrow horizontally entering at the y^{th} row and x_y represents the number (of non-zero color) arrows horizontally exiting at the y^{th} row, both counted from the bottom (see Figure 14).

For a $\mathbf{v} \in \{0, 1, 2\}^U$, $j \in \{1, 2\}$ and $y \in \llbracket 1, U \rrbracket$, let the height function (which we call Ht for short) of the j^{th} color be defined by

$$\text{Ht}_j(\mathbf{v}, y) := \#\{y' > y : v_{y'} = j\} = \sum_{y'=y+1}^U \mathbb{1}_{v_{y'}=j},$$

i.e., the number of arrows of color j strictly above row y in \mathbf{v} .

We say that \mathbf{v} and \mathbf{x} are *compatible* if they can arise as the incoming color counts and outgoing total arrow counts at a column, respectively, while satisfying arrow conservation; more precisely, if and only if $\sum_{j=1}^2 (\text{Ht}_j(\mathbf{v}, 0) - \text{Ht}_j(\mathbf{v}, y)) \geq \sum_{y'=1}^y x_{y'}$ for each y and equality holds at $y = U$.

For given $\mathbf{v} \in \{0, 1, 2\}^U$ and $\mathbf{x} \in \{0, 1\}^U$ which are compatible, define $\text{Val}(\mathbf{v}, \mathbf{x})$ (short for “valid”)

$$\text{Val}(\mathbf{v}, \mathbf{x}) := \left\{ \mathbf{w} \in \{0, 1, 2\}^U : \begin{array}{l} w_y = 0 \iff x_y = 0, \text{Ht}_j(\mathbf{w}, 0) = \text{Ht}_j(\mathbf{v}, 0), \\ \text{Ht}_j(\mathbf{w}, y) \geq \text{Ht}_j(\mathbf{v}, y) \text{ for } j = 1, 2, y \in \llbracket 0, U - 1 \rrbracket \end{array} \right\},$$

to be the set of valid assignments of outgoing colors at a column with incoming color counts given by \mathbf{v} and outgoing arrow counts given by \mathbf{x} (see Figure 14); here, valid informally means that colored arrow conservation holds.

For $\mathbf{v} \in \{0, 1, 2\}^U$ and $\mathbf{w} \in \text{Val}(\mathbf{v}, \mathbf{x})$, define VertCt_j (short for “vertical count”) by

$$\begin{aligned} \text{VertCt}_j(\mathbf{v}, \mathbf{w}, y) &:= (\text{Ht}_j(\mathbf{v}, 0) - \text{Ht}_j(\mathbf{v}, y)) - (\text{Ht}_j(\mathbf{w}, 0) - \text{Ht}_j(\mathbf{w}, y)) \\ &= \text{Ht}_j(\mathbf{w}, y) - \text{Ht}_j(\mathbf{v}, y) = \sum_{y'=1}^y \mathbb{1}_{v_{y'}=j} - \mathbb{1}_{w_{y'}=j} \end{aligned} \quad (4.8)$$

be the number of arrows of color j vertically exiting the vertex at height y ; the second equality is since $\text{Ht}_j(\mathbf{v}, 0) = \text{Ht}_j(\mathbf{w}, 0)$ is the total number of j -arrows in the system (equal since $\mathbf{w} \in \text{Val}(\mathbf{v}, \mathbf{x})$). Note that $\text{VertCt}_j(\mathbf{v}, \mathbf{w}, y)$ is a function only of v_1, \dots, v_y and w_1, \dots, w_y .

We next define a specific assignment $\mathbf{w}^* \in \text{Val}(\mathbf{v}, \mathbf{x})$ for any given compatible pair (\mathbf{v}, \mathbf{x}) , which is the deterministic (and unique) assignment of colors to the outgoing arrows that would occur in the $q = 0$ colored q -Boson model. It is defined as follows: we specify w_y^* iteratively starting with $y = 1$ and continuing in increasing order by:

- $w_y^* = 2$ if $\mathbb{1}_{v_y=2} + \text{VertCt}_2(\mathbf{v}, \mathbf{w}^*, y-1) \geq 1$ (i.e., if there is at least one 2-arrow that can exit the vertex at height y) and $x_y = 1$; note that the condition is well-defined since $\text{VertCt}_2(\mathbf{v}, \mathbf{w}^*, y-1)$ does not depend on $w_{y'}^*$ for any $y' \geq y$;
- $w_y^* = 1$ if $\mathbb{1}_{v_y=2} + \text{VertCt}_2(\mathbf{v}, \mathbf{w}^*, y-1) = 0$ and $\mathbb{1}_{v_y=1} + \text{VertCt}_1(\mathbf{v}, \mathbf{w}^*, y-1) \geq 1$ (i.e., if there are no 2-arrows and at least one 1-arrow that can exit the vertex at height y) and $x_y = 1$;
- $w_y^* = 0$ if $x_y = 0$.

The fact that (\mathbf{v}, \mathbf{x}) are compatible ensures that exactly one of the above three conditions holds for each y .

Fix $\mathbf{v} \in \{0, 1, 2\}^U$ and $\mathbf{x} \in \{0, 1\}^U$ which are compatible, let $\mathbf{w} \in \text{Val}(\mathbf{v}, \mathbf{x})$, and let \mathbf{w}^* be as defined above. We define the Pitman error $\text{PE}(\mathbf{w})$ of \mathbf{w} by

$$\text{PE}(\mathbf{w}) := \max_{y \leq U} (\text{Ht}_2(\mathbf{w}, y) - \text{Ht}_2(\mathbf{w}^*, y)),$$

i.e., it is the maximal height difference of 2-arrows between \mathbf{w} and \mathbf{w}^* over all rows. Observe that $\text{Ht}_2(\mathbf{w}, y) \geq \text{Ht}_2(\mathbf{w}^*, y)$ for each $y \leq U$. Indeed, as we said, it is easy to show that \mathbf{w}^* is the configuration that would arise in the $q = 0$ setting, so by Lemma 4.1, $\text{Ht}_2(\mathbf{w}^*, \cdot)$ may be regarded as the Pitman transform of the incoming color counts \mathbf{v} and the outgoing arrow counts \mathbf{x} ; then Lemma 4.2 implies that $\text{Ht}_2(\mathbf{w}, y) \geq \text{Ht}_2(\mathbf{w}^*, y)$. Alternatively, since \mathbf{w}^* always releases 2-arrows as soon as it is possible, $\text{Ht}_2(\mathbf{w}^*, y)$ is minimal over all $\mathbf{w} \in \text{Val}(\mathbf{v}, \mathbf{x})$ for any y , which again verifies that $\text{Ht}_2(\mathbf{w}, y) \geq \text{Ht}_2(\mathbf{w}^*, y)$.

We need some notation for the weight of configurations. For a compatible pair (\mathbf{v}, \mathbf{x}) and $\mathbf{w} \in \text{Val}(\mathbf{v}, \mathbf{x})$, let $\mathbf{VertCt}(\mathbf{v}, \mathbf{w}, y) = (\text{VertCt}_1(\mathbf{v}, \mathbf{w}, y), \text{VertCt}_2(\mathbf{v}, \mathbf{w}, y))$. Further let $\mathbf{L}_{z,y} = \mathbf{L}_1$ if $y \in \llbracket 1, N \rrbracket$ and $\mathbf{L}_{z,y} = \mathbf{L}_z$ (recall that $z \in (0, 1)$ is the fixed spectral parameter) if $y \in \llbracket N+1, N+M \rrbracket$, where \mathbf{L}_u is read from Figure 10. Now define

$$\text{Wgt}_y(\mathbf{v}, \mathbf{w}) := \mathbf{L}_{z,y}(v_y, \mathbf{VertCt}(\mathbf{v}, \mathbf{w}, y-1); w_y, \mathbf{VertCt}(\mathbf{v}, \mathbf{w}, y)) \quad (4.9)$$

to be the vertex weight at y , with incoming and outgoing horizontal arrows of v_y and w_y , respectively, and incoming and outgoing vertical arrows of $\mathbf{VertCt}(\mathbf{v}, \mathbf{w}, y-1)$ and $\mathbf{VertCt}(\mathbf{v}, \mathbf{w}, y)$, respectively. Next, define the weight of the configuration determined by \mathbf{v} and \mathbf{w} by

$$\text{Wgt}(\mathbf{v}, \mathbf{w}) := \prod_{y=1}^U \text{Wgt}_y(\mathbf{v}, \mathbf{w}). \quad (4.10)$$

The next lemma is a deterministic statement about the weights of configurations w with high values of $\text{PE}(\mathbf{w})$.

Lemma 4.4. Fix $N, M \in \mathbb{N}$. There exist positive absolute constants c and C and $K = K(q)$, such that the following holds for any spectral parameter $z \in (0, 1)$ (which may depend on N, M). Fix a compatible pair $(\mathbf{v}, \mathbf{x}) \in \{0, 1, 2\}^U \times \{0, 1\}^U$. There exists a mapping $f : \text{Val}(\mathbf{v}, \mathbf{x}) \rightarrow \text{Val}(\mathbf{v}, \mathbf{x})$ such that, if $\mathbf{w} \in \text{Val}(\mathbf{v}, \mathbf{x})$ with $m := \text{PE}(\mathbf{w})$ and $\text{Wgt}(\mathbf{v}, \mathbf{w}) > 0$, then $\text{Wgt}(\mathbf{v}, \mathbf{w})/\text{Wgt}(\mathbf{v}, f(\mathbf{w})) \leq Cq^{cm^2}$ whenever $m > K \log N$. Further, for any $\mathbf{w} \in \text{Val}(\mathbf{v}, \mathbf{x})$ with $m := \text{PE}(\mathbf{w})$ and $m \geq K \log N$, $\#f^{-1}(\{\mathbf{w}\}) \leq N^{2m}$.

This statement should be interpreted as giving a bound on the conditional probability of a given configuration exhibiting $\max_y L_k^{(2)}(y) - \text{PT}(L_k^{(1)}, L_{k+1}^{(2)})(y) \geq m$ given $L_k^{(1)}$ and $L_{k+1}^{(2)}$ (which will determine \mathbf{v} and \mathbf{x}). Then Proposition 4.3 will follow by averaging over the conditioned data; we give this proof now before proving Lemma 4.4 in Section 4.3.

Proof of Proposition 4.3. Recall from (3.8) that $\mathcal{F}_k^{\text{cHL}}$ is the σ -algebra generated by $L^{(1)}, L_{k+1}^{(2)}, L_{k+2}^{(2)}, \dots$. We condition on $\mathcal{F}_k^{\text{cHL}}$ and use the tower property of conditional expectations to write

$$\begin{aligned} & \mathbb{P} \left(\max_{y \in [0, N+M]} L_k^{(2)}(y) - \text{PT}(L_k^{(1)}, L_{k+1}^{(2)})(y) \geq m \right) \\ &= \mathbb{E} \left[\mathbb{P} \left(\max_{y \in [0, N+M]} L_k^{(2)}(y) - \text{PT}(L_k^{(1)}, L_{k+1}^{(2)})(y) \geq m \mid \mathcal{F}_k^{\text{cHL}} \right) \right]. \end{aligned}$$

Let $\mathbf{v} \in \{0, 1, 2\}^U$ and $\mathbf{x} \in \{0, 1\}^U$ be given by

$$v_y = \left(L_{k+1}^{(2)}(y-1) - L_{k+1}^{(2)}(y) \right) + \left(L_{k+1}^{(1)}(y-1) - L_{k+1}^{(1)}(y) \right) \quad \text{and} \quad x_y = L_k^{(1)}(y-1) - L_k^{(1)}(y);$$

in words, they are the horizontally incoming colors and the horizontally outgoing arrow counts at column k . They are compatible. Let $A(\mathbf{v}, \mathbf{x}, m')$ be the set of $\mathbf{w} \in \text{Val}(\mathbf{v}, \mathbf{x})$ such that $\text{PE}(\mathbf{w}) = m'$ and $\text{Wgt}(\mathbf{v}, \mathbf{w}) > 0$. Now, it is immediate from the Gibbs property of the colored Hall-Littlewood line ensemble, Lemma 3.13 (and can also be seen directly from the Gibbs property of the colored q -Boson model, Lemma 3.5), that

$$\begin{aligned} & \mathbb{P} \left(\max_{y \in [0, N+M]} L_k^{(2)}(y) - \text{PT}(L_k^{(1)}, L_{k+1}^{(2)})(y) \geq m \mid \mathcal{F}_k^{\text{cHL}} \right) \\ &= \frac{\sum_{m'=m}^{\infty} \sum_{\mathbf{w} \in A(\mathbf{v}, \mathbf{x}, m')} \text{Wgt}(\mathbf{v}, \mathbf{w})}{\sum_{\mathbf{w} \in \text{Val}(\mathbf{v}, \mathbf{x})} \text{Wgt}(\mathbf{v}, \mathbf{w})}. \end{aligned} \tag{4.11}$$

For each $\mathbf{w} \in A(\mathbf{v}, \mathbf{x}, m')$, let $f(\mathbf{w}) \in \text{Val}(\mathbf{v}, \mathbf{x})$ be the configuration obtained from Lemma 4.4, and recall $\#f^{-1}(\mathbf{w}) \leq N^{2m'}$. Since $m' \geq m \geq K \log N$, we know that $\text{Wgt}(\mathbf{v}, \mathbf{w})/\text{Wgt}(\mathbf{v}, f(\mathbf{w}))$ is upper bounded by $Cq^{c(m')^2}$. So we see that, since $\#f^{-1}(\{\mathbf{w}\}) \leq N^{2m'}$ for $\mathbf{w} \in A(\mathbf{v}, \mathbf{x}, m')$,

$$\sum_{\mathbf{w} \in A(\mathbf{v}, \mathbf{x}, m')} \text{Wgt}(\mathbf{v}, \mathbf{w}) \leq Cq^{c(m')^2} \sum_{\mathbf{w} \in A(\mathbf{v}, \mathbf{x}, m')} \text{Wgt}(\mathbf{v}, f(\mathbf{w})) \leq CN^{2m'} q^{c(m')^2} \sum_{\mathbf{w} \in \text{Val}(\mathbf{v}, \mathbf{x})} \text{Wgt}(\mathbf{v}, \mathbf{w}).$$

Substituting this into (4.11), and using that $q^{\frac{1}{2}c(m')^2} \leq C^{-1}N^{-2m'}$ by raising K if necessary (and recalling $m' \geq m \geq K \log N$), yields that the righthand side of that equation is upper bounded by $q^{c'm^2}$ for some absolute constant $c > 0$. This completes the proof. \square

4.3. Construction of the alternate configuration.

Proof of Lemma 4.4. First, to ensure that the f we need to produce is defined for all inputs, for any $\mathbf{w} \in \text{Val}(\mathbf{v}, \mathbf{x})$ such that $\text{PE}(\mathbf{w}) < K \log N$ (for a $K = K(q)$ to be set later) or $\text{Wgt}(\mathbf{v}, \mathbf{w}) = 0$, we define $f(\mathbf{w}) = \mathbf{w}$. So in the remainder of the proof, we may assume that \mathbf{w} is such that

$\text{PE}(\mathbf{w}) > K \log N$ and $\text{Wgt}(\mathbf{v}, \mathbf{w}) > 0$. It will be useful to keep track of a running Pitman error by row y , for which we define

$$\text{PE}(\mathbf{w}, y) := \max_{y' \leq y} (\text{Ht}_2(\mathbf{w}, y') - \text{Ht}_2(\mathbf{w}^*, y')).$$

Let $m' \in \llbracket 1, m \rrbracket$. We fix $y = y(m')$ to be the smallest such that $\text{PE}(\mathbf{w}, y) = m'$; since $\text{PE}(\mathbf{w}, 0) = 0$, \mathbf{w} is such that $\text{PE}(\mathbf{w}, U) = \text{PE}(\mathbf{w}) = m$, and $\text{PE}(\mathbf{w}, y')$ increases by at most 1 when y' increases by 1, such a y exists.

We claim that $w_y = 1$ and $w_y^* = 2$. We first observe that since $\text{PE}(\mathbf{w}, y) > \text{PE}(\mathbf{w}, y - 1)$ and $\text{Ht}_2(\mathbf{w}, \cdot)$, $\text{Ht}_2(\mathbf{w}^*, \cdot)$ are non-increasing and have increments in $\{-1, 0\}$, it must hold that $\text{Ht}_2(\mathbf{w}, y) = \text{Ht}_2(\mathbf{w}, y - 1)$ and $\text{Ht}_2(\mathbf{w}^*, y) = \text{Ht}_2(\mathbf{w}^*, y - 1) - 1$. This means that $w_y^* = 2$, which implies $w_y = 1$ since $w_y \in \{1, 2\}$ (both \mathbf{w} and \mathbf{w}^* have the same outgoing arrow counts) and $\text{Ht}_2(\mathbf{w}, y) = \text{Ht}_2(\mathbf{w}, y - 1)$.

Next we claim that $\text{VertCt}_2(\mathbf{v}, \mathbf{w}, y - 1) \geq m'$. To see this we first write, using the definition (4.8) of $\text{VertCt}_2(\mathbf{v}, \mathbf{w}, y - 1)$ and noting that, by definition of y , $\text{Ht}_2(\mathbf{w}, y - 1) - \text{Ht}_2(\mathbf{w}^*, y - 1) = m' - 1$,

$$\begin{aligned} \text{VertCt}_2(\mathbf{v}, \mathbf{w}, y - 1) &= \text{Ht}_2(\mathbf{w}, y - 1) - \text{Ht}_2(\mathbf{v}, y - 1) \\ &= \text{VertCt}_2(\mathbf{v}, \mathbf{w}^*, y - 1) + \text{Ht}_2(\mathbf{w}, y - 1) - \text{Ht}_2(\mathbf{w}^*, y - 1) \\ &= \text{VertCt}_2(\mathbf{v}, \mathbf{w}^*, y - 1) + m' - 1. \end{aligned} \quad (4.12)$$

Now it suffices to show that $\text{VertCt}_2(\mathbf{v}, \mathbf{w}^*, y - 1) \geq 1$. We know that $w_y^* = 2$, so $v_y = 2$ or $\text{VertCt}_2(\mathbf{v}, \mathbf{w}^*, y - 1) \geq 1$ (or both). But $w_y = 1$ and the weight of the vertex with a horizontally incoming 2-arrow and an outgoing 1-arrow is zero, by Figure 10. So we have that $v_y \neq 2$ (since we have assumed $\text{Wgt}(\mathbf{v}, \mathbf{w}) > 0$), which implies that $\text{VertCt}_2(\mathbf{v}, \mathbf{w}^*, y - 1) \geq 1$. Returning to (4.12), we have shown that $\text{VertCt}_2(\mathbf{v}, \mathbf{w}, y - 1) \geq m'$. Thus we have now established that with y defined as above, it holds that

$$w_y = 1, w_y^* = 2, \text{VertCt}_2(\mathbf{v}, \mathbf{w}, y - 1) \geq m', \text{ and } \text{VertCt}_2(\mathbf{v}, \mathbf{w}^*, y - 1) \geq 1. \quad (4.13)$$

With these preliminaries in place, we turn to exhibiting a particular configuration $f(\mathbf{w})$ such that $\text{Wgt}(\mathbf{w})/\text{Wgt}(f(\mathbf{w})) \leq Cq^{cm^2}$. We let $K_0 := 2(\log q^{-1})^{-1}$ and $K := 2K_0$. For $m \geq K \log N$, we will define a sequence of configurations $\mathbf{w}^{(0)}, \mathbf{w}^{(1)}, \dots, \mathbf{w}^{(R)} \in \text{Val}(\mathbf{v}, \mathbf{x})$ where $\mathbf{w}^{(0)} := \mathbf{w}$ and $R := m - K_0 \log N$ such that $\mathbf{w}^{(i)}$ has $\text{PE}(\mathbf{w}^{(i)}) \geq m - i$ and

$$\frac{\text{Wgt}(\mathbf{v}, \mathbf{w}^{(i-1)})}{\text{Wgt}(\mathbf{v}, \mathbf{w}^{(i)})} \leq q^{m-i-K_0 \log N-1} (1 + q^{K_0 \log N-1})^N. \quad (4.14)$$

We define $f(\mathbf{w})$ to be $\mathbf{w}^{(R)}$. Clearly this will suffice to establish $\text{Wgt}(\mathbf{w})/\text{Wgt}(f(\mathbf{w})) \leq Cq^{cm^2}$ as then by multiplying together the inequalities we would obtain that, for absolute constants c and C ,

$$\frac{\text{Wgt}(\mathbf{v}, \mathbf{w})}{\text{Wgt}(\mathbf{v}, \mathbf{w}^{(R)})} \leq q^{mR - \sum_{i=1}^R i - RK_0 \log N - R} (1 + q^{K_0 \log N-1})^{RN} \leq Cq^{cm^2}, \quad (4.15)$$

the final inequality for $m \geq K \log N$. So now we must show (4.14); we will establish that $\#f^{-1}(\{\tilde{\mathbf{w}}\}) \leq N^{2m}$ for any $\tilde{\mathbf{w}}$ with $\text{PE}(\tilde{\mathbf{w}}) = m \geq K \log N$ and $\text{Wgt}(\mathbf{v}, \mathbf{w}) > 0$ after specifying the sequence of configurations.

Reindexing, to establish (4.14), we must show that if we have a configuration \mathbf{w} with $\text{PE}(\mathbf{w}) \geq m' \geq K \log N$, then we can produce a configuration \mathbf{w}' with $\text{PE}(\mathbf{w}') \geq m' - 1$ and

$$\frac{\text{Wgt}(\mathbf{v}, \mathbf{w})}{\text{Wgt}(\mathbf{v}, \mathbf{w}')} \leq q^{m' - K_0 \log N - 1} (1 + q^{K_0 \log N - 1})^N. \quad (4.16)$$

Now, by (4.13), since $\text{PE}(\mathbf{w}) = m$, for any $m' \in \llbracket K \log N, m \rrbracket$ there exists a first vertex (whose row height we labeled y), where a 1-arrow exits horizontally and there are at least m' 2-arrows entering vertically, i.e., $w_y = 1$ and $\text{VertCt}_2(\mathbf{v}, \mathbf{w}, y - 1) \geq m'$. Since we have assumed $m' \geq K \log N$

and all 2-arrows eventually exit, there exists a value $y' > y$ which is the smallest one greater than y such that $v_{y'} \neq 2$, $w_{y'} = 2$, and $\text{VertCt}_2(\mathbf{w}, y' - 1) = \lceil \frac{1}{2}K \log N \rceil = \lceil K_0 \log N \rceil$. In particular, for all $u \in \llbracket y, y' - 1 \rrbracket$,

$$\text{VertCt}_2(\mathbf{v}, \mathbf{w}, u) \geq \frac{1}{2}K \log N = K_0 \log N. \quad (4.17)$$

We define \mathbf{w}' by swapping the exiting arrows at y and y' , i.e., by $w'_u = w_u$ for all $u \notin \{y, y'\}$, $w'_{y'} = w_y = 1$, and $w'_y = w_{y'} = 2$. Observe that since there are at most N possible locations for such a swap, and $f(\mathbf{w})$ is defined by a sequence of $R = m - K_0 \log N < m$ such swaps, it follows that $\#f^{-1}(\{\tilde{\mathbf{w}}\}) \leq \binom{N}{2}^m < N^{2m}$ for any $\tilde{\mathbf{w}} \in \text{Val}(\mathbf{v}, \mathbf{x})$ with $\text{PE}(\tilde{\mathbf{w}}) = m$. Next observe that, for $u \in \llbracket y, y' - 1 \rrbracket$,

$$\begin{aligned} \text{VertCt}_1(\mathbf{v}, \mathbf{w}', u) &= \text{VertCt}_1(\mathbf{v}, \mathbf{w}, u) + 1 \quad \text{and} \\ \text{VertCt}_2(\mathbf{v}, \mathbf{w}', u) &= \text{VertCt}_2(\mathbf{v}, \mathbf{w}, u) - 1. \end{aligned} \quad (4.18)$$

It is immediate that $\text{PE}(\mathbf{w}') \geq m' - 1$. To upper bound $\text{Wgt}(\mathbf{v}, \mathbf{w})/\text{Wgt}(\mathbf{v}, \mathbf{w}')$, we note that the vertex configurations at u are identical in \mathbf{w} and \mathbf{w}' for $u \notin \llbracket y, y' \rrbracket$, so the ratio is the ratio of the product of the vertex weights for vertices at u with $u \in \llbracket y, y' \rrbracket$, i.e., (recall the definition of Wgt_u and Wgt from (4.9) and (4.10) respectively)

$$\frac{\text{Wgt}(\mathbf{v}, \mathbf{w})}{\text{Wgt}(\mathbf{v}, \mathbf{w}')} = \prod_{u=y}^{y'} \frac{\text{Wgt}_u(\mathbf{v}, \mathbf{w})}{\text{Wgt}_u(\mathbf{v}, \mathbf{w}')}.$$

To estimate this, we first note that $w_u = w'_u$ for $u \in \llbracket y + 1, y' - 1 \rrbracket$ and recall that (4.18) holds for $u \in \llbracket y, y' - 1 \rrbracket$.

Recall the spectral parameter $z \in (0, 1)$. For a vertex height $u \in \llbracket 1, U \rrbracket$, let

$$\tilde{z}(u) := z \text{ if } u \in \llbracket N + 1, N + M \rrbracket \text{ and } \tilde{z}(u) := 1 \text{ if } u \in \llbracket 1, N \rrbracket, \quad (4.19)$$

and, for $j \in \{1, 2\}$,

$$A_j(u) := \text{VertCt}_j(\mathbf{v}, \mathbf{w}, u - 1). \quad (4.20)$$

In the following, we will be reading vertex weights from Figure 10. Now, since $w_y = 1$, $\text{Wgt}_y(\mathbf{v}, \mathbf{w}) = \tilde{z}(y)q^{A_2(y)}$ or $\tilde{z}(y)(1 - q^{A_1(y)})q^{A_2(y)}$, depending on whether $v_y = 1$ or 0 respectively. Since $A_2(y) \geq m$ as shown in (4.13), both possibilities for the weight are upper bounded by $\tilde{z}(y)q^m$. Similarly since $w'_{y'} = 2$ and $\text{VertCt}_2(\mathbf{v}, \mathbf{w}', y - 1) = \text{VertCt}_2(\mathbf{v}, \mathbf{w}, y - 1) = A_2(y)$, $\text{Wgt}_{y'}(\mathbf{v}, \mathbf{w}') = \tilde{z}(y)(1 - q^{A_2(y)}) \geq \tilde{z}(y)(1 - q^m)$. Thus

$$\frac{\text{Wgt}_y(\mathbf{v}, \mathbf{w})}{\text{Wgt}_{y'}(\mathbf{v}, \mathbf{w}')} \leq \frac{\tilde{z}(y)q^m}{\tilde{z}(y)(1 - q^m)} = \frac{q^m}{1 - q^m}.$$

Next we turn to the y' vertex. Here, $w_{y'} = 2$ and $A_2(y') = \lceil K_0 \log N \rceil$ (see before (4.17)), so $\text{Wgt}_{y'}(\mathbf{v}, \mathbf{w}) = \tilde{z}(y')(1 - q^{\lceil K_0 \log N \rceil})$ independently of $v_{y'} \in \{0, 1\}$, while $\text{Wgt}_{y'}(\mathbf{v}, \mathbf{w}') = \tilde{z}(y')q^{\lceil K_0 \log N \rceil - 1}$ or $\tilde{z}(y')(1 - q^{\text{VertCt}_1(\mathbf{v}, \mathbf{w}', y' - 1)})q^{\lceil K_0 \log N \rceil - 1}$ (depending on $v_{y'} = 1$ or 0 respectively, since $v_{y'} \neq 2$), which is lower bounded by $\tilde{z}(y')(1 - q)^{\lceil K_0 \log N \rceil - 1}$, since, as noted in (4.18), $\text{VertCt}_2(\mathbf{v}, \mathbf{w}', y' - 1) = \text{VertCt}_2(\mathbf{v}, \mathbf{w}, y' - 1) - 1 = \lceil K_0 \log N \rceil - 1$. So

$$\frac{\text{Wgt}_{y'}(\mathbf{v}, \mathbf{w})}{\text{Wgt}_{y'}(\mathbf{v}, \mathbf{w}')} \leq \frac{\tilde{z}(y')(1 - q^{\lceil K_0 \log N \rceil})}{\tilde{z}(y')(1 - q)^{\lceil K_0 \log N \rceil - 1}} = \frac{1 - q^{\lceil K_0 \log N \rceil}}{(1 - q)^{\lceil K_0 \log N \rceil - 1}}.$$

Finally we turn to looking at the weight of vertex u for $u \in \llbracket y + 1, y' - 1 \rrbracket$. Recall that $w_u = w'_u$ for this range of u . If $w_u = 0$, the vertex weights are 1 for both \mathbf{w} and \mathbf{w}' . If $w_u = 1$, then, using

(4.18), and with $\tilde{z}(u)$ as in (4.19) and $A_j(u)$ as in (4.20),

$$\frac{\text{Wgt}_u(\mathbf{v}, \mathbf{w})}{\text{Wgt}_u(\mathbf{v}, \mathbf{w}')} = \begin{cases} \frac{\tilde{z}(u)(1 - q^{A_1(u)})q^{A_2(u)}}{\tilde{z}(u)(1 - q^{A_1(u)+1})q^{A_2(u)-1}} & v_u = 0 \\ \frac{\tilde{z}(u)q^{A_2(u)}}{\tilde{z}(u)q^{A_2(u)-1}} & v_u = 1, \end{cases}$$

which is at most 1. Finally, we consider the case $w_u = 2$. Recall that $A_2(u) \geq \lceil K_0 \log N \rceil$ by (4.17). If $v_u = 2$, $\text{Wgt}_u(\mathbf{v}, \mathbf{w})/\text{Wgt}_u(\mathbf{v}, \mathbf{w}') = 1$, while if $v_u = 0$ or 1,

$$\frac{\text{Wgt}_u(\mathbf{v}, \mathbf{w})}{\text{Wgt}_u(\mathbf{v}, \mathbf{w}')} = \frac{\tilde{z}(u)(1 - q^{A_2(u)})}{\tilde{z}(u)(1 - q^{A_2(u)-1})} = 1 + q^{A_2(u)-1} \cdot \frac{1 - q}{1 - q^{A_2(u)-1}} \leq 1 + q^{\lceil K_0 \log N \rceil - 1}.$$

Combining the above inequalities, and using that the number of locations u where $w_u \neq 0$ is N (and that if $w_u = 0$ the ratio is 1), we obtain that

$$\begin{aligned} \frac{\text{Wgt}(\mathbf{v}, \mathbf{w})}{\text{Wgt}(\mathbf{v}, \mathbf{w}')} &= \prod_{u=y}^{y'} \frac{\text{Wgt}_u(\mathbf{v}, \mathbf{w})}{\text{Wgt}_u(\mathbf{v}, \mathbf{w}')} \leq \frac{q^m}{1 - q^m} \cdot \frac{1 - q^{\lceil K_0 \log N \rceil}}{q^{\lceil K_0 \log N \rceil - 1}} \left(1 + q^{K_0 \log N - 1}\right)^N \\ &\leq q^{m - \lceil K_0 \log N \rceil} \left(1 + q^{\lceil K_0 \log N \rceil - 1}\right)^N. \end{aligned}$$

This implies (4.16), completing the proof. \square

5. PROPERTIES OF ASEP AND S6V

In this section we collect some properties of the colored S6V model and ASEP that will be useful in future sections, in particular, a form of stationarity and one-point tightness.

5.1. Colored stochastic six-vertex model. We work with packed boundary condition for the colored S6V model; recall the definition from Section 2.3. In particular, we have arrows entering horizontally at every site along $\{1\} \times \llbracket -N, N \rrbracket$, with the color of the arrow entering $(1, k)$ being k . Also recall that the color of the arrow exiting horizontally from (t, k) is $j_{(t,k)}$ and from (2.12) that

$$h^{\text{S6V}}(x, 0; y, t) = \# \{k > y : j_{(t,k)} \geq x\}$$

for $x \in \llbracket -N, N \rrbracket$ and $y \in \llbracket -N, \infty \rrbracket$. It is easy to check from this description that, for any $k \in \llbracket -N, N \rrbracket$ fixed,

$$h^{\text{S6V}}(x, 0; y, t) \stackrel{d}{=} h^{\text{S6V}}(x + k, 0; y + k, t) + k \tag{5.1}$$

as processes in (x, y, t) on the domain $\llbracket \max(-N - k, -N), \min(N - k, N) \rrbracket \times \llbracket \max(-N - k, -N), \infty \rrbracket \times \mathbb{N}$; this uses that, when $y \geq x$, $h^{\text{S6V}}(x, 0; y, t) - (N - y)$ is the number of arrows starting at a site $(1, i)$ for some $i \in \llbracket x, y \rrbracket$ which horizontally exit a vertex (t, i) for some $i \in \llbracket y + 1, \infty \rrbracket$, which is a quantity whose distribution is invariant on shifting x and y by the same constant.

The following records a one-point convergence result on the limiting one-point fluctuations of h^{S6V} in its rescaled form $\mathcal{S}^{\text{S6V}, \varepsilon}$ as defined in (2.15) (which recall involves a parameter α controlling the location in the rarefaction fan where the height function is evaluated). It was originally essentially shown in [BCG16], but proved in the slightly improved form we require in [CD18].

Proposition 5.1 (One-point distributional limit of S6V). *Let $q \in [0, 1)$, $z \in (0, 1)$, and $\alpha \in (z, z^{-1})$. Fix $x, y \in \mathbb{R}$. Then, as $\varepsilon \rightarrow 0$, $\mathcal{S}^{\text{S6V}, \varepsilon}(x; y) + (x - y)^2 \xrightarrow{d} \text{GUE-TW}$, the GUE Tracy-Widom distribution (see end of Definition 2.1).*

Proof. By (5.1) and the expression defining $\mathcal{S}^{\text{S6V},\varepsilon}$ in Definition 2.17, it follows that $\mathcal{S}^{\text{S6V},\varepsilon}(x; y) \stackrel{d}{=} \mathcal{S}^{\text{S6V},\varepsilon}(0; y - x)$, so it suffices to prove the case $x = 0$. When $q \in (0, 1)$, this case is an immediate consequence of combining [CD18, Theorems 2.3 and 2.5] and translating the notation. When $q = 0$, we first note that by Proposition 3.12, $\mathcal{S}^{\text{S6V},\varepsilon}(0; \cdot)$ is a rescaled version of the top line of the uncolored Hall-Littlewood line ensemble $\mathbf{L}^{\text{cHL},(1)}(\cdot)$ from Section 3.2, which consists of non-intersecting Bernoulli paths. The scaling limit of the latter is proven in [DFF⁺21, Corollary 1.3] as well as in [DNV23, Theorem 1.5] to be \mathcal{P} , from which the one-point statement we claim follows immediately. \square

5.2. Colored ASEP and relation to colored S6V. Next we recall the model of colored ASEP from Section 2.2. Because the approximate LPP representation of Theorem 3.20 is in terms of the colored Hall-Littlewood line ensemble associated to the colored q -Boson model which has a direct distributional equivalence only with colored S6V, we need to relate colored ASEP to colored S6V.

Consider the colored S6V model under packed boundary condition with

$$N = \lfloor \delta^{-1}t \rfloor \tag{5.2}$$

for $\delta, t > 0$ with $q \in [0, 1)$ and $z = \frac{1-\delta}{1-\delta q}$ (from Figure 8, this means that the probability of the higher color arrow moving straight through a vertex vertically is $q\delta$ and horizontally is δ). We will evaluate the colored height function on the vertical line $\{M\} \times \llbracket -N, \infty \rrbracket$ with $M = \lfloor \delta^{-1}t \rfloor$. Consider colored ASEP with the usual jump rates of 1 to the right and q to the left. It is known from [BCG16, Agg17] that by evaluating the height function of the S6V model near $(M, N) = (\lfloor \delta^{-1}t \rfloor, \lfloor \delta^{-1}t \rfloor)$ one obtains the ASEP height function in the distributional limit as $\delta \rightarrow 0$.

Unfortunately, this description poses issues to use directly, namely, in the $\delta \rightarrow 0$ limit the domain becomes infinite even for fixed t . This means that estimates we wish to apply in the ASEP setting like Theorem 3.20 (probability bound on the deviation m from the approximate LPP representation), which only apply for $m \geq K(q) \log N$, would not hold.

5.2.1. Effective coupling. We instead make use of an effective coupling proven in [AB24] of colored S6V with $N = \lfloor \delta^{-1}t \rfloor$ as in (5.2) and colored ASEP at time t which allows to take $\delta \rightarrow 0$ at a particular rate with $t \rightarrow \infty$. We will take $\delta = t^{-\theta}$ for some $\theta > 0$ large enough. We define

$$h^{\text{ASEP},\theta}(x, 0; y, t) := \lfloor t^{1+\theta} \rfloor + x + 1 - h^{\text{S6V}}(-x, 0; \lfloor t^{1+\theta} \rfloor - y - 1, \lfloor t^{1+\theta} \rfloor); \tag{5.3}$$

the first argument of h^{S6V} is $-x$ because $h^{\text{ASEP}}(x, 0; \cdot, t)$ involves counts of particles of color greater than or equal to $-x$ and not x (recall (2.5)). As we will see, the presence of negative signs in going between $h^{\text{ASEP},\theta}$ and h^{S6V} arises from the fact that the ASEP particle configuration can be read off (under a coupling that we will introduce shortly) of a horizontal line in the S6V model, but the S6V height function considers arrow counts on a vertical line.

We note that (5.1) implies that

$$h^{\text{ASEP},\theta}(\cdot, 0; \cdot, t) \stackrel{d}{=} h^{\text{ASEP},\theta}(\cdot + k, 0; \cdot + k, t) \tag{5.4}$$

for any $k \in \mathbb{Z}$ fixed, matching the relation satisfied by h^{ASEP} (it is easily seen from the latter's definition (2.5) that (5.4) holds with h^{ASEP} in place of $h^{\text{ASEP},\theta}$).

The properties of the coupling between $h^{\text{ASEP},\theta}$ and h^{ASEP} that we need is as follows.

Lemma 5.2 (Effective coupling of ASEP with S6V). *There exists $C > 0$ such that, for any $\theta > 0$ and $t \geq 1$, there is a coupling such that $h^{\text{ASEP},\theta}(x, 0; y, t) = h^{\text{ASEP}}(x, 0; y, t)$ for all $|x|, |y| \leq 2t$ with probability at least $1 - Ct^{3-\theta/8}$.*

In the remainder of the paper we will assume θ is a large fixed constant such as 40 so that, by the Borel-Cantelli lemma, Lemma 5.2 implies that with probability one $h^{\text{ASEP},\theta}(x, 0; y, t) = h^{\text{ASEP}}(x, 0; y, t)$ for all $|x|, |y| \leq 2t$ and for all t large enough. To prove Lemma 5.2, we will need the following statements for colored ASEP and colored S6V, which are essentially implications of the

finite speed of propagation in the models. As their proofs are straightforward, we defer them to Appendix B. Define

$$\tilde{h}^{\text{ASEP}}(x, 0; y, t) := \#\{z \in \llbracket y + 1, \lfloor 4t \rfloor \rrbracket : \eta_t(z) \geq -x\}, \quad (5.5)$$

where recall $(\eta_t(k))_{k \in \mathbb{Z}}$ records the state of the colored ASEP at time t . In words, \tilde{h}^{ASEP} is a variant of the colored ASEP height function (2.5) where particles beyond location $\lfloor 4t \rfloor$ are not counted.

Lemma 5.3. *There exist $C, c > 0$ such that, for all $t > 0$, with probability at least $1 - C \exp(-ct)$,*

$$(h^{\text{ASEP}}(x, 0; y, t))_{|x|, |y| \leq 2t} = (\tilde{h}^{\text{ASEP}}(x, 0; y, t))_{|x|, |y| \leq 2t}, \quad (5.6)$$

Lemma 5.4. *Let $\delta, t > 0$, $N = \lfloor \delta^{-1}t \rfloor$, and $z = \frac{1-\delta}{1-\delta q}$. There exist absolute constants $C, c > 0$ such that, with probability at least $C \exp(-ct)$, it holds that, for all $|x| \leq 2t$ and $z \geq \lfloor 4t \rfloor$,*

$$h^{\text{S6V}}(x, 0; \lfloor \delta^{-1}t \rfloor - z, \lfloor \delta^{-1}t \rfloor) = \lfloor \delta^{-1}t \rfloor - x + 1,$$

where note the righthand side is the total number of arrows of color at least x in the system.

Proof of Lemma 5.2. Let $\delta > 0$. Recall $h^{\text{S6V}}(-x, 0; \lfloor \delta^{-1}t \rfloor - y - 1, \lfloor \delta^{-1}t \rfloor)$ is the number of arrows of color greater than or equal to $-x$ passing strictly above $(\lfloor \delta^{-1}t \rfloor, \lfloor \delta^{-1}t \rfloor - y - 1)$, and let \tilde{h}^{ASEP} be as in (5.5). Also recall the packed boundary and initial conditions for colored S6V and colored ASEP, respectively. We note that in both colored S6V and colored ASEP, color merging (Remarks 2.6 and 2.16) implies that the distribution of $(\tilde{h}^{\text{ASEP}}(x, 0; y, t))_{|x|, |y| \leq 2t}$ and $(h^{\text{S6V}}(x, 0; y, t))_{|x|, |y| \leq 2t}$ are unchanged by merging all particles/arrows of color strictly greater than $\lfloor 2t \rfloor$ to have color $\lfloor 2t \rfloor + 1$, and merging all particles/arrows of color strictly smaller than $-\lfloor 2t \rfloor$ to have color $-\lfloor 2t \rfloor - 1$. We work with these color merged versions of the packed initial conditions (this is required as the result we invoke from [AB24] states that only finitely many colors exist in the systems).

We work with the coupling whose existence is asserted in [AB24, Proposition B.2]. Then we know that, on an event \mathbf{E}_1 with probability at least $1 - C\delta^{1/8}t^3$ (and we work on this event in the remainder of the proof), for all $|x| \leq 2t$, $|y| \leq 4t$, there is an arrow of color x exiting vertically from $(\lfloor \delta^{-1}t \rfloor + y, \lfloor \delta^{-1}t \rfloor)$ (i.e., along the horizontal line at height $\lfloor \delta^{-1}t \rfloor$) if and only if there is a particle of color x at location y in colored ASEP at time t . However, the S6V height function we defined in (2.12) is in terms of arrow counts on a vertical and not horizontal line.

To handle this, we claim that, with probability at least $1 - 32\delta t^2$, the color of the arrow exiting horizontally from $(\lfloor \delta^{-1}t \rfloor, \lfloor \delta^{-1}t \rfloor - y)$ is the same as that of the arrow exiting vertically from $(\lfloor \delta^{-1}t \rfloor + y, \lfloor \delta^{-1}t \rfloor)$ for all $y \in \llbracket -\lfloor 4t \rfloor, \lfloor 4t \rfloor \rrbracket$; call the event that this occurs for a given y by $\mathbf{E}_2(y)$ and define $\mathbf{E}_2 = \bigcap_{y \in \llbracket -\lfloor 4t \rfloor, \lfloor 4t \rfloor \rrbracket} \mathbf{E}_2(y)$. Let $\mathbf{v}_t = (\lfloor \delta^{-1}t \rfloor, \lfloor \delta^{-1}t \rfloor)$ and $\ell_t = \lfloor 4t \rfloor$, and define the squares S_1 and S_2 with corners given by $\{\mathbf{v}_t, \mathbf{v}_t + (-\ell_t, 0), \mathbf{v}_t + (0, \ell_t), \mathbf{v}_t + (-\ell_t, \ell_t)\}$ and $\{\mathbf{v}_t, \mathbf{v}_t + (\ell_t, 0), \mathbf{v}_t + (0, -\ell_t), \mathbf{v}_t + (\ell_t, -\ell_t)\}$, respectively. To see that our claim holds, note first that for $\mathbf{E}_2(y)$ to not hold for some $y \in \llbracket -\lfloor 4t \rfloor, \lfloor 4t \rfloor \rrbracket$, it must be the case that at least one vertex in the squares S_1 and S_2 (for the cases of $y \leq 0$ and $y > 0$ respectively) allows at least one arrow to pass straight through vertically or horizontally; the probability of this happening at any given vertex is at most δ . A union bound over the $32t^2$ vertices in the two squares proves the claim that $\mathbb{P}(\mathbf{E}_2^c) \leq 32\delta t^2$.

Let \mathbf{E}_3 and \mathbf{E}_4 be the events that $\tilde{h}^{\text{ASEP}}(x, 0; y, t) = h^{\text{ASEP}}(x, 0; y, t)$ and $h^{\text{S6V}}(x, 0; \lfloor \delta^{-1}t \rfloor - \lfloor 4t \rfloor, \lfloor \delta^{-1}t \rfloor) = \lfloor \delta^{-1}t \rfloor - x + 1$ hold for all $|x|, |y| \leq 2t$. By Lemmas 5.3 and 5.4, $\mathbb{P}((\mathbf{E}_3 \cup \mathbf{E}_4)^c) \leq C \exp(-ct)$ for some $C, c > 0$.

Set $\delta = t^{-\theta}$. Under the coupling above and on $\mathbf{E} := \mathbf{E}_1 \cap \mathbf{E}_2 \cap \mathbf{E}_3 \cap \mathbf{E}_4$, we will show that $h^{\text{ASEP}, \theta}(x, 0; y, t) = h^{\text{ASEP}}(x, 0; y, t)$ for all $|x|, |y| \leq 2t$. First, by the definition of \tilde{h}^{ASEP} , on $\mathbf{E}_1 \cap \mathbf{E}_2$ and for $|x|, |y| \leq 2t$,

$$\tilde{h}^{\text{ASEP}}(x, 0; y, t) = \#\{k \in \llbracket y + 1, \lfloor 4t \rfloor \rrbracket : j_{(\lfloor \delta^{-1}t \rfloor, \lfloor \delta^{-1}t \rfloor - k)} \geq -x\}$$

$$\begin{aligned}
&= h^{\text{S6V}}(-x, 0; \lfloor \delta^{-1}t \rfloor - \lfloor 4t \rfloor - 1, \lfloor \delta^{-1}t \rfloor) - h^{\text{S6V}}(-x, 0; \lfloor \delta^{-1}t \rfloor - y - 1, \lfloor \delta^{-1}t \rfloor) \\
&= \lfloor \delta^{-1}t \rfloor + x + 1 - h^{\text{S6V}}(-x, 0; \lfloor \delta^{-1}t \rfloor - y - 1, \lfloor \delta^{-1}t \rfloor) = h^{\text{ASEP}, \theta}(x, 0; y, t),
\end{aligned}$$

the penultimate equality on \mathbf{E}_3 . The proof is completed by the fact that $\tilde{h}^{\text{ASEP}}(x, 0; y, t) = h^{\text{ASEP}}(x, 0; y, t)$ on \mathbf{E}_4 and noting that it holds for all large enough C and all $t \geq 1$ that $\mathbb{P}(\mathbf{E}^c) \leq C(\exp(-ct) + \delta t^2 + \delta^{1/8}t^3) \leq C\delta^{1/8}t^3$ (since $\delta = t^{-\theta}$). \square

5.2.2. One-point tightness. The one-point tightness for $h^{\text{ASEP}, \theta}$ that we require follows from Lemma 5.2 and the following one-point convergence result for h^{ASEP} . Recall the ASEP sheet $\mathcal{S}^{\text{ASEP}, \varepsilon}$ from (2.8) and the parameter α controlling the macroscopic location around which the height function h^{ASEP} is evaluated.

Proposition 5.5. *Let $q \in [0, 1)$ and $\alpha \in (-1, 1)$. Fix $x, y \in \mathbb{R}$. Then, as $\varepsilon \rightarrow 0$, $\mathcal{S}^{\text{ASEP}, \varepsilon}(x; y) + (x - y)^2 \xrightarrow{d} \text{GUE-TW}$, the GUE Tracy-Widom distribution.*

Proof. Again by stationarity of h^{ASEP} (as noted after (5.4)) it suffices to prove the case $x = 0$. This follows from [TW09, Theorem 3], and is also stated in a form closer to ours in [BO17, Theorem 11.3]. \square

We can combine this result with the coupling in Lemma 5.2 to obtain a one-point tightness statement for $h^{\text{ASEP}, \theta}$. The rescaled version $\mathcal{S}^{\text{ASEP}, \theta, \varepsilon}$ we work with is defined by (2.8) with $h^{\text{ASEP}, \theta}$ in place of h^{ASEP} with $\theta = 40$, i.e., for $\alpha \in (-1, 1)$ fixed and recalling $\mu(\alpha)$, $\sigma(\alpha)$, and $\beta(\alpha)$ from (2.6) and (2.7),

$$\begin{aligned}
\mathcal{S}^{\text{ASEP}, \theta, \varepsilon}(x; y) &:= \sigma(\alpha)^{-1} \varepsilon^{1/3} \left(\mu(\alpha) 2\varepsilon^{-1} + \mu'(\alpha) \beta(\alpha) (y - x) \varepsilon^{-2/3} \right. \\
&\quad \left. - h^{\text{ASEP}, \theta}(\beta(\alpha) x \varepsilon^{-2/3}, 0; 2\alpha \varepsilon^{-1} + \beta(\alpha) y \varepsilon^{-2/3}, 2\gamma^{-1} \varepsilon^{-1}) \right). \tag{5.7}
\end{aligned}$$

Corollary 5.6. *Fix $\theta = 40$. Let $q \in [0, 1)$, $\alpha \in (-1, 1)$ and $x, y \in \mathbb{R}$. Then, as $\varepsilon \rightarrow 0$, $\mathcal{S}^{\text{ASEP}, \theta, \varepsilon}(x; y) + (x - y)^2 \xrightarrow{d} \text{GUE-TW}$, the GUE Tracy-Widom distribution.*

Proof. This follows immediately from Lemma 5.2 and Proposition 5.5. \square

6. PRELIMINARIES FOR LINE ENSEMBLE TIGHTNESS

In this section we start by introducing some line ensemble notions that will be necessary in the proof of Theorem 3.18 on tightness of line ensembles. Then in Section 6.2 we introduce the Brownian Gibbs property and give the proof of Theorem 3.19 (on the convergence of line ensembles to the parabolic Airy line ensemble), assuming Theorem 3.18 and that all subsequential limits possess the Brownian Gibbs property, which will be proven in later sections. In Section 6.3 we will relate the colored Hall-Littlewood line ensemble, with appropriate centerings, to colored ASEP (in the approximate form (7.7)) and colored S6V such that the former's top curves are the height functions of the respective models, in such a way that the corresponding uncolored line ensembles satisfy the assumptions introduced in Section 3.3.4. Finally in Section 6.4 we collect some ingredient statements needed to prove Theorem 3.18 and give the latter's proof assuming them; the ingredient statements will be proved in later sections.

6.1. The Strong Gibbs property. We will need at one or two places a stronger version of the Gibbs property which allows us to resample on certain random domains known as stopping domains, analogous to the strong Markov property and stopping times.

Definition 6.1 (Stopping domain). Fix $k \in \mathbb{N}$ and let \mathbf{L} be a discrete line ensemble (Definition 3.6). A pair of random variables $\mathfrak{l}, \mathfrak{r} \in \mathbb{Z}$ forms a stopping domain $\llbracket \mathfrak{l}, \mathfrak{r} \rrbracket$ with respect to (L_1, \dots, L_k) if, for all $\ell, r \in \mathbb{Z}$ with $\ell < r$,

$$\{\mathfrak{l} \leq \ell, \mathfrak{r} \geq r\} \in \mathcal{F}_{\text{ext}}(k, \llbracket \ell, r \rrbracket, \mathbf{L}).$$

We define the σ -algebra $\mathcal{F}_{\text{ext}}(k, \llbracket \mathfrak{l}, \mathfrak{r} \rrbracket, \mathbf{L})$ to be the collection of all events A such that $A \cap \{\mathfrak{l} \leq \ell, \mathfrak{r} \geq r\} \in \mathcal{F}_{\text{ext}}(k, \llbracket \ell, r \rrbracket, \mathbf{L})$ (as in Definition 3.14) for all $\ell < r$.

Proposition 6.2 (Strong Gibbs property). *Let $k \in \mathbb{N}$ and let $\llbracket \mathfrak{l}, \mathfrak{r} \rrbracket$ be a stopping domain. Let $F : \{(\ell, r, f_1, \dots, f_k) : \ell < r \text{ and } (f_1, \dots, f_k) \in \mathbb{R}^{\llbracket 1, k \rrbracket \times \llbracket \ell, r \rrbracket}\} \rightarrow \mathbb{R}$ be bounded. If \mathbf{L} is a discrete line ensemble that has the Hall-Littlewood Gibbs property, it holds that, almost surely,*

$$\mathbb{E}[F(\mathfrak{l}, \mathfrak{r}, L_1, \dots, L_k) \mid \mathcal{F}_{\text{ext}}(k, \llbracket \mathfrak{l}, \mathfrak{r} \rrbracket, \mathbf{L})] = \frac{\mathbb{E}[F(\mathfrak{l}, \mathfrak{r}, B_1, \dots, B_k)W(\mathbf{B}, L_{k+1}) \mid \mathcal{F}_{\text{ext}}(k, \llbracket \mathfrak{l}, \mathfrak{r} \rrbracket, \mathbf{L})]}{\mathbb{E}[W(\mathbf{B}, L_{k+1}) \mid \mathcal{F}_{\text{ext}}(k, \llbracket \mathfrak{l}, \mathfrak{r} \rrbracket, \mathbf{L})]},$$

where $\mathbf{B} = (B_1, \dots, B_k)$ is a collection of k independent Bernoulli random walk bridges with $B_i(x) = L_i(x)$ for $x \in \{\mathfrak{l}, \mathfrak{r}\}$ and $i = 1, \dots, k$.

Similar statements have been proven for continuous line ensembles, e.g., [CH14, Lemma 2.5]. The proof amounts to decomposing based on the exact value of \mathfrak{l} and \mathfrak{r} (which is straightforward here as everything is discrete) and using the Hall-Littlewood Gibbs property on each of the resulting events; we do not record the details here.

6.2. The Brownian Gibbs property. To introduce the Brownian Gibbs property, we will need notation for the σ -algebra we condition on for continuous line ensembles. We first precisely define the meaning of a continuous line ensemble.

Definition 6.3 (Continuous line ensemble). Fix a (possibly infinite) interval $\Lambda \subseteq \mathbb{R}$. A Λ -indexed continuous line ensemble $\mathfrak{L} = (\mathfrak{L}_1, \mathfrak{L}_2, \dots)$ is a random variable defined on a probability space $(\Omega, \mathcal{F}, \mathbb{P})$, taking values in $\mathcal{C}(\mathbb{N} \times \Lambda, \mathbb{R})$, such that (again writing the first argument of \mathfrak{L} as a subscript, i.e., $\mathfrak{L}_i(\cdot) := \mathfrak{L}(i, \cdot)$) $\mathfrak{L}_i(y) \geq \mathfrak{L}_{i+1}(y)$ for any $y \in \Lambda$ and $i \in \mathbb{N}$. Here $\mathbb{N} \times \Lambda$ is given the product topology of the discrete topology and the Euclidean topology, and $\mathcal{C}(\mathbb{N} \times \Lambda, \mathbb{R})$ has the topology of uniform convergence on compact sets.

Recall again the σ -algebra \mathcal{F}_{ext} in the case of discrete line ensembles from Definition 3.14. In the case of a continuous line ensemble $\mathfrak{L} : \mathbb{N} \times \mathbb{R} \rightarrow \mathbb{R}$, we will write, for $a, b \in \mathbb{R}$ and $j, k \in \mathbb{N}$ with $a < b$ and $j < k$, $\mathcal{F}_{\text{ext}}(\llbracket j, k \rrbracket, [a, b], \mathfrak{L})$ to be the σ -algebra generated by the collection of random variables

$$\{\mathfrak{L}_i(x) : (i, x) \in \mathbb{N} \times \mathbb{R} \setminus (\llbracket j, k \rrbracket \times [a, b])\}.$$

(Compared to Definition 3.14, we have replaced $\llbracket a+1, b-1 \rrbracket$ with $[a, b]$ in the second bullet point, so that $\mathfrak{L}_i(a)$ and $\mathfrak{L}_i(b)$ are still conditioned on, for each $i \in \llbracket j, k \rrbracket$). We will again often adopt the shorthand $\mathcal{F}_{\text{ext}}(k, [a, b], \mathbf{L}) = \mathcal{F}_{\text{ext}}(\llbracket 1, k \rrbracket, [a, b], \mathbf{L})$.

Definition 6.4 (Brownian Gibbs property). A line ensemble $\mathfrak{L} = (\mathfrak{L}_1, \mathfrak{L}_2, \dots) : \mathbb{N} \times \mathbb{R} \rightarrow \mathbb{R}$ is said to satisfy the Brownian Gibbs property if the following holds for any $\llbracket j, k \rrbracket \subseteq \mathbb{N}$ and $[a, b] \subseteq \mathbb{R}$. Conditional on $\mathcal{F}_{\text{ext}}(\llbracket j, k \rrbracket, [a, b], \mathfrak{L})$, the distribution of $\mathfrak{L}_{\llbracket j, k \rrbracket \times [a, b]}$ is that of $k - j + 1$ independent rate two Brownian bridges $B_j^{\text{Br}}, \dots, B_k^{\text{Br}}$, with $B_i^{\text{Br}}(x) = \mathfrak{L}_i(x)$ for each $x \in \{a, b\}$ and $i \in \llbracket j, k \rrbracket$, conditioned on $\mathfrak{L}_{j-1}(x) > B_j^{\text{Br}}(x) > \dots > B_k^{\text{Br}}(x) > \mathfrak{L}_{k+1}(x)$ for all $x \in [a, b]$ (with $\mathfrak{L}_0 \equiv \infty$ by convention).

Recall now the framework for line ensemble convergence in Section 3.3.4. In particular, Theorem 3.18 asserts that for any sequence of discrete line ensembles \mathbf{L}^N satisfying Assumptions 1 and 2, the rescaled line ensembles \mathfrak{L}^N defined in (3.13) forms a tight sequence, and Theorem 3.19

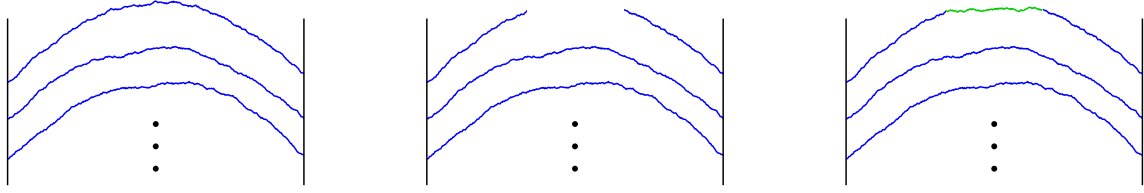


FIGURE 15. A depiction of a special case, with $k = 1$, of the Brownian Gibbs property: in the left panel is the original line ensemble \mathfrak{L} , in the middle panel we condition on the data which is depicted, essentially forgetting what has been erased, and in the right panel we resample the forgotten data, which is conditionally distributed as a rate two Brownian bridge between the endpoints, conditioned to avoid the second curve \mathfrak{L}_2 .

characterizes the subsequential limits and says that, under the additional Assumption 3, the original sequence converges to \mathcal{P} .

Theorem 3.19 is an immediate consequence of knowing that all subsequential limit points of \mathfrak{L}^N satisfy the Brownian Gibbs property, on combining with a recent characterization result for \mathcal{P} [AH23b]. These two statements are given precisely next. Proposition 6.5 is proved in Section 12.

Proposition 6.5. *Let \mathfrak{L}^N satisfy Assumptions 1 and 2, let \mathfrak{L}^N be defined as in (3.13), and let \mathfrak{L} be any subsequential weak limit of \mathfrak{L}^N as $N \rightarrow \infty$. Then \mathfrak{L} has the Brownian Gibbs property.*

Proposition 6.6 ([AH23b, Corollary 2.11 (2)]). *Suppose \mathfrak{L} is a line ensemble with the Brownian Gibbs property such that, for any $\varepsilon > 0$, there exists a constant $C = C(\varepsilon) > 0$ such that*

$$\mathbb{P}(|\mathfrak{L}_1(x) + x^2| > \varepsilon|x| + C) \leq \varepsilon$$

for all $x \in \mathbb{R}$. Then there exists a parabolic Airy line ensemble \mathcal{P} and an independent random variable \mathfrak{c} such that $\mathfrak{L}_i(x) = \mathcal{P}_i(x) + \mathfrak{c}$ for all $i \in \mathbb{N}$ and $x \in \mathbb{R}$.

We give the proof of Theorem 3.19 given these two statements and Theorem 3.18 now.

Proof of Theorem 3.19. By Theorem 3.18 and Proposition 6.5, we know that $\{\mathfrak{L}^N\}_{N=1}^\infty$ is tight and that all subsequential limits have the Brownian Gibbs property. Let \mathfrak{L} be such a subsequential limit. By the characterization theorem (Proposition 6.6), it follows that \mathfrak{L} equals the parabolic Airy line ensemble up to an independent random constant shift. Then Assumption 3 guarantees that the constant shift is zero, completing the proof. \square

Remark 6.7. In Section 7, we will apply the strong characterization Proposition 6.6 of [AH23b] (indirectly, through Theorem 3.19) to the line ensembles coming from S6V and ASEP. In the case of ASEP for $\alpha = 0$, we can circumvent Proposition 6.6. Indeed, in Appendix B.3, we will give an alternate proof of that case using [QS22, Theorem 2.2] (along with Lemma 5.2) to infer that \mathfrak{L}_1^N converges to the parabolic Airy₂ process and the characterization theorem from [DM21] (which asserts that if two Brownian Gibbsian line ensembles have the same top curve, in law, then the entire line ensembles are equal in law) to conclude that that limiting line ensemble is the parabolic Airy line ensemble.

In the next section we will define centered versions of the colored Hall-Littlewood line ensembles which are associated to S6V and ASEP, and verify that they satisfy the assumptions from Section 3.3.4.

6.3. Verifying the assumptions for colored S6V and colored ASEP.

6.3.1. *S6V*. Recall that we work in the domain $\mathbb{Z}_{\geq 1} \times \llbracket -N, \infty \rrbracket$ and that we evaluate the colored height function on the vertical line $x = \lfloor \varepsilon^{-1} \rfloor$. Fix $q \in [0, 1)$, $z \in (0, 1)$, and $\alpha \in (z, z^{-1})$ and recall $\mu(\alpha)$ from (2.13) and $L_i^{\text{cHL},(j)}$ from (3.6) with parameters q, z, N , and $M = \lfloor \varepsilon^{-1} \rfloor$. Define $\mathbf{L}^{\text{S6V},(j),\varepsilon}$ for $j \in \llbracket 1, N \rrbracket$ by, for $y \in \llbracket -\lfloor \alpha \varepsilon^{-1} \rfloor, N + M - \lfloor \alpha \varepsilon^{-1} \rfloor \rrbracket$,

$$L_i^{\text{S6V},(j),\varepsilon}(y) := L_i^{\text{cHL},(j)}(\lfloor \alpha \varepsilon^{-1} \rfloor + y) + j - N - \lfloor \mu(\alpha) \varepsilon^{-1} \rfloor. \quad (6.1)$$

Observe that, since $h^{\text{S6V}}(j, 0; \cdot, \lfloor \varepsilon^{-1} \rfloor) \stackrel{d}{=} L_1^{\text{cHL},(j)}(\cdot)$ as functions on $\llbracket 1, N - 1 \rrbracket$ from Proposition 3.12, it follows that, as functions on $\llbracket -\lfloor \alpha \varepsilon^{-1} \rfloor + 1, N - 1 - \lfloor \alpha \varepsilon^{-1} \rfloor \rrbracket$ and jointly over $j \in \llbracket 1, N \rrbracket$,

$$L_1^{\text{S6V},(j),\varepsilon}(\cdot) \stackrel{d}{=} h^{\text{S6V}}(j, 0; \lfloor \alpha \varepsilon^{-1} \rfloor + \cdot, \lfloor \varepsilon^{-1} \rfloor) + j - N - \lfloor \mu(\alpha) \varepsilon^{-1} \rfloor. \quad (6.2)$$

Lemma 6.8. $\mathbf{L}^{\text{S6V},(1),\varepsilon}$ satisfies Assumptions 1, 2, and 3 with $p = \mu'(x)$ and $\lambda = \frac{1}{2}\mu''(x)$ (as defined in (2.13)) and with ε^{-1} in place of N .

Proof. Since $\mathbf{L}^{\text{cHL},(1)}$ marginally has the Hall-Littlewood Gibbs property (Proposition 3.17), and since the Gibbs property is not changed by deterministic constant shifts of the curves, it follows that $\mathbf{L}^{\text{S6V},(1),\varepsilon}$ has the Hall-Littlewood Gibbs property. That Assumptions 2 and 3 hold follows immediately from combining Propositions 3.12 and 5.1 with (6.2). \square

6.3.2. *ASEP*. Fix $q \in [0, 1)$, $\alpha \in (-1, 1)$ and define $\gamma = 1 - q$. Let $\theta = 40$ and

$$K_{\varepsilon,\theta} = \lfloor (2\gamma^{-1}\varepsilon^{-1})^{1+\theta} \rfloor - \lfloor 2\alpha\varepsilon^{-1} \rfloor - 1.$$

Next we define line ensembles $\mathbf{L}^{\text{ASEP},(j),\theta,\varepsilon}$ for $j \in \llbracket 1, \lfloor (2\gamma^{-1}\varepsilon^{-1})^{1+\theta} \rfloor \rrbracket$. Recall $\mu(\alpha) = \frac{1}{4}(1 - \alpha)^2$ from (2.6). They are specified by setting, for $y \in \llbracket 1 - K_{\varepsilon,\theta}, N + M - K_{\varepsilon,\theta} \rrbracket$, and where the parameters for the righthand side are $z = \frac{1-\varepsilon}{1-\varepsilon q}$ and $M = N = \lfloor (2\gamma^{-1}\varepsilon^{-1})^{1+\theta} \rfloor$,

$$L_i^{\text{ASEP},(j),\theta,\varepsilon}(y) := L_i^{\text{cHL},(j)}(K_{\varepsilon,\theta} + y) - \lfloor (2\gamma^{-1}\varepsilon^{-1})^{1+\theta} \rfloor + j - 1 + \lfloor \frac{1}{2}(1 - \alpha)^2\varepsilon^{-1} \rfloor. \quad (6.3)$$

The relation between $L_1^{\text{ASEP},(j),\theta,\varepsilon}$ and $h^{\text{ASEP},\theta}$ (recall (5.3) and $h^{\text{S6V}}(j, 0; \cdot, \lfloor (2\gamma^{-1}\varepsilon^{-1})^{1+\theta} \rfloor) \stackrel{d}{=} L_1^{\text{cHL},(j)}(\cdot)$) is

$$L_1^{\text{ASEP},(j),\theta,\varepsilon}(\cdot) \stackrel{d}{=} -h^{\text{ASEP},\theta}(-j, 0; \lfloor 2\alpha\varepsilon^{-1} \rfloor - \cdot, \lfloor 2\gamma^{-1}\varepsilon^{-1} \rfloor) + \lfloor \frac{1}{2}(1 - \alpha)^2\varepsilon^{-1} \rfloor. \quad (6.4)$$

Lemma 6.9. $\mathbf{L}^{\text{ASEP},(1),\theta,\varepsilon}$ satisfies Assumptions 1, 2, and 3 with $p = -\frac{1}{2}(1 - \alpha)$ and $\lambda = \frac{1}{8}$ and with ε^{-1} in place of N .

Proof. As in the case of $\mathbf{L}^{\text{S6V},(1),\varepsilon}$, it is immediate from Proposition 3.17 that $\mathbf{L}^{\text{ASEP},(1),\theta,\varepsilon}$ has the Hall-Littlewood Gibbs property. It follows from Corollary 5.6 that Assumptions 2 and 3 hold. \square

Next, we set up some of the ingredients for the proof of Theorem 3.18, which will also be useful in Section 7 on the tightness and limit of $\mathcal{S}^{\text{S6V},\varepsilon}$ and $\mathcal{S}^{\text{ASEP},\varepsilon}$. In particular, we are working in the setup of Theorem 3.18, i.e., we have a sequence of discrete line ensembles \mathbf{L}^N indexed by N and defined on $\mathbb{N} \times \mathbb{Z}$ that satisfy Assumptions 1 and 2.

6.4. Ingredients for proof of tightness. Proving tightness of the path measures requires us to establish one-point tightness, as well as control on the modulus of continuity, for all curves. We state the estimates we need and then use them to give the proof of Theorem 3.18.

6.4.1. *One-point tightness of all curves.* Note that from Assumption 2 we have one-point tightness for L_1^N and, since line ensembles which satisfy the Hall-Littlewood Gibbs property must by definition be ordered, we therefore have control on the upper tail of L_k^N for every k . The lower tail for the k^{th} curve for $k \geq 2$ is more delicate, however, and we record a statement for it now.

Theorem 6.10. *Fix $k \in \mathbb{N}$, $T > 0$, and $\varepsilon > 0$. Then there exist $N_0 = N_0(k, T, \varepsilon)$ and $R = R(k, T, \varepsilon) > 0$ such that, for $N \geq N_0$,*

$$\mathbb{P} \left(\inf_{sN^{-2/3} \in [-T, T]} (L_k^N(s) - ps + \lambda s^2 N^{-1}) \leq -RN^{1/3} \right) < \varepsilon.$$

We will prove Theorem 6.10 in Sections 9 and 10. As mentioned in Sections 1.3.3 and 3.3.3, the proof inductively interweaves uniform lower tail control of the k^{th} curve over an interval with control over uniform separation between the $(k-1)^{\text{st}}$ and k^{th} curves, both on the fluctuation scale $N^{1/3}$. Obtaining control on these two quantities forms the bulk of the technical work of the proof of Theorem 3.18.

6.4.2. *Modulus of continuity.* To prove tightness of path measures, we also need control on the modulus of continuity of L_k^N . As in earlier works establishing tightness for line ensembles with Gibbs properties, this comes down to controlling the partition function of the Gibbs property, in order to transfer modulus of continuity estimates from the base path measure (in this case, Bernoulli random walk bridges) to the line ensemble. For an interval $[-TN^{2/3}, TN^{2/3}]$, recall from Definition 3.16 that the partition function of the top k curves is

$$Z_N^{k, [-T, T], \mathbf{L}^N(-TN^{2/3}), \mathbf{L}^N(TN^{2/3}), L_{k+1}^N} := \mathbb{E}_{\mathcal{F}}[W(B_1, \dots, B_k, L_{k+1}^N)], \quad (6.5)$$

where $\mathcal{F} = \mathcal{F}_{\text{ext}}(k, \llbracket -TN^{2/3}, TN^{2/3} \rrbracket, \mathbf{L}^N)$ and (B_1, \dots, B_k) is a collection of k independent Bernoulli random walk bridges with B_i from $(-TN^{2/3}, L_i^N(-TN^{2/3}))$ to $(TN^{2/3}, L_i^N(TN^{2/3}))$.

Remark 6.11. Note here that we have written certain quantities, such as $\pm TN^{2/3}$, without floors, though they are meant to be integers to be completely precise. Here as in the rest of the paper we will often drop the requisite floor symbols to ease the notation, since this will not affect our arguments.

The control we need on the partition function is the following. It is proved in Section 11.

Proposition 6.12. *Let $T \geq 2$ and $k \in \mathbb{N}$. Then for any $\varepsilon > 0$ there exist $\delta = \delta(k, T, \varepsilon) > 0$ and $N_0 = N_0(k, T, \varepsilon)$ such that, for $N \geq N_0$,*

$$\mathbb{P} \left(Z_N^{k, [-T, T], \mathbf{L}^N(-TN^{2/3}), \mathbf{L}^N(TN^{2/3}), L_{k+1}^N} > \delta \right) \geq 1 - \varepsilon.$$

The control we need on the base path measure of Bernoulli random walk bridges is as follows. As its proof is quite standard, we defer it to Appendix B.

Lemma 6.13. *There exist C and $c > 0$ such that, for $n \in \mathbb{N}$, $p \in (-1, 0)$, B a Bernoulli random walk bridge from $(0, 0)$ to (n, pn) , all $0 \leq y < z \leq n$, and $M > 0$,*

$$\mathbb{P} \left(\sup_{x \in [y, z]} |B(x) - B(y) - p(x - y)| > M|z - y|^{1/2} \right) \leq C \exp(-cM^2).$$

At several locations, we will also need to use normal or Brownian bridge approximations for Bernoulli random walk bridges. We will require the Brownian bridges to have an explicit variance coming from the increment of the Bernoulli random walk bridge being approximated. For this we make use of the following Komlós-Major-Tusnády (KMT) coupling result for Bernoulli random walk bridges, which is obtained by combining [CD18, Theorem 4.5] with the exponential Markov inequality.

Lemma 6.14 (KMT coupling, [CD18, Theorem 4.5]). *Let $p \in (-1, 0)$ and $\{z_N\}_{N \in \mathbb{N}} \subseteq \mathbb{R}$. For each N , let B^N be a Bernoulli random walk bridge from $(0, 0)$ to (N, z_N) . There exist positive constants $C, c < \infty$ (depending on p) such that there is a coupling between B^N and a Brownian bridge B^{Br} with variance $p(1-p)$ from $(0, 0)$ to (N, z_N) with*

$$\mathbb{P} \left(\sup_{0 \leq t \leq N} |B^{\text{Br}}(t) - B^N(t)| > R \right) \leq C \exp \left(-cR + C(\log N)^2 + N^{-1}|z_N - pN|^2 \right).$$

Note that the variance of the Brownian bridge being $p(1-p)$ can be understood by the fact that the Bernoulli random walk bridge, if it has the endpoint $(N, z_N) \approx (N, pN)$, will behave like a Bernoulli random walk with parameter p , whose increments indeed have variance $p(1-p)$.

Assuming Proposition 6.12, we can give the following corollary on the modulus of continuity of L_k^N . Recall from Section 3.3.4 that we view L_k^N as a \mathbb{R} -valued function via linear interpolation.

Corollary 6.15. *Let $T \geq 2$ and $k \in \mathbb{N}$. For any $\varepsilon > 0$ and $\rho > 0$, there exist $\delta = \delta(k, T, \varepsilon, \rho) > 0$ and $N_0 = N_0(k, T, \varepsilon, \rho)$ such that, for $N \geq N_0$,*

$$\mathbb{P} \left(\sup_{|x|, |y| \leq TN^{2/3}, |x-y| \leq \delta N^{2/3}} |L_k^N(x) - L_k^N(y) - p(x-y)| \geq \rho N^{1/3} \right) \leq \varepsilon.$$

Remark 6.16. Before giving the proof of Corollary 6.15, we point out a notational practice that will be used many times throughout the rest of the paper: we will often introduce events (e.g., $\mathbf{A}(X)$) whose definition involves an abstract \mathbb{R} -valued process X and then in the course of the proof write different processes (e.g., L_k^N) in place of X to mean the event whose definition is that of $\mathbf{A}(X)$ with the process in question in place of X . In spite of a random process being part of the notation for the event, the event itself is fixed, i.e., does not depend on the instantiation of the process. This convention will be convenient because when applying the Hall-Littlewood Gibbs property we will often be working with events whose only difference is that a collection of Bernoulli random walk bridges is in place of a collection of curves of the line ensemble \mathbf{L}^N .

Proof of Corollary 6.15. For a random process $X : [-TN^{2/3}, TN^{2/3}] \rightarrow \mathbb{R}$, define

$$\text{ModCon}_N(\delta, \rho, X) := \left\{ \sup_{|x|, |y| \leq TN^{2/3}, |x-y| \leq \delta N^{2/3}} |X(x) - X(y) - p(x-y)| \geq \rho N^{1/3} \right\}.$$

So $\text{ModCon}_N(\delta, \rho, L_k^N)$ is the event whose probability we are trying to upper bound. Let $\mathcal{F} = \mathcal{F}_{\text{ext}}(k, [-TN^{2/3}, TN^{2/3}], \mathbf{L}^N)$,

$$Z_N := Z_N^{k, [-T, T], \mathbf{L}^N(-TN^{2/3}), \mathbf{L}^N(TN^{2/3}), L_{k+1}^N},$$

and $\text{Fav}(\delta', M)$ be the event defined by

$$\text{Fav}(\delta', M) := \{Z_N > \delta'\} \cap \left\{ |L_1^N(\pm TN^{2/3})|, |L_k^N(\pm TN^{2/3})| \leq M \right\};$$

we pick δ' and M such that $\mathbb{P}(\text{Fav}(\delta', M)) \geq 1 - \varepsilon$, which is possible by Proposition 6.12, one-point tightness of L_1^N from Assumption 2, and Theorem 6.10. Note that this event is \mathcal{F} -measurable.

Now by using this bound on $\mathbb{P}(\text{Fav}(\delta', M))$, the Hall-Littlewood Gibbs property, and the fact that $W \leq 1$ (W being from Definition 3.15), the probability we are bounding equals

$$\begin{aligned} \mathbb{E} \left[\mathbb{P}_{\mathcal{F}} \left(\text{ModCon}_N(\delta, \rho, L_k^N) \right) \right] &\leq \mathbb{E} \left[\mathbb{P}_{\mathcal{F}} \left(\text{ModCon}_N(\delta, \rho, L_k^N) \right) \mathbb{1}_{\text{Fav}(\delta', M)} \right] + \varepsilon \\ &= \mathbb{E} \left[Z_N^{-1} \mathbb{E}_{\mathcal{F}} \left[\mathbb{1}_{\text{ModCon}_N(\delta, \rho, L_k^N)} W(\mathbf{B}, L_{k+1}^N) \right] \mathbb{1}_{\text{Fav}(\delta', M)} \right] + \varepsilon \\ &\leq \mathbb{E} \left[Z_N^{-1} \mathbb{P}_{\mathcal{F}} \left(\text{ModCon}_N(\delta, \rho, B_k) \right) \mathbb{1}_{\text{Fav}(\delta', M)} \right] + \varepsilon, \end{aligned}$$

where $\mathbf{B} = (B_1, \dots, B_k)$ is a collection of k independent Bernoulli random walk bridges with B_i 's endpoints given by $L_i^N(-TN^{2/3})$ and $L_i^N(TN^{2/3})$. Since we have a lower bound of δ' on Z_N on the event $\text{Fav}(\delta', M)$, we obtain that the righthand side of the previous display is upper bounded by

$$(\delta')^{-1} \cdot \mathbb{E} \left[\mathbb{P}_{\mathcal{F}} (\text{ModCon}_N(\delta, \rho, B_k)) \mathbb{1}_{\text{Fav}(\delta', M)} \right] + \varepsilon.$$

By the modulus of continuity estimates for Bernoulli random walks from Lemma 6.13, the probability inside the expectation in the previous line can be made smaller than $\delta'\varepsilon$ for an appropriately small choice of δ . Relabeling ε completes the proof. \square

Assuming Theorem 6.10 on the lower tail and Proposition 6.12 (therefore Corollary 6.15), we may quickly give the proof of tightness.

Proof of Theorem 3.18. Recall that \mathfrak{L}^N is defined by (3.13). By an easy extension of [Bil13, Theorem 7.3] (see also [DFF⁺21, Lemma 2.4]), to show tightness of \mathfrak{L}^N it suffices to show, for every $k \in \mathbb{N}$:

- (1) $\lim_{R \rightarrow \infty} \lim_{N \rightarrow \infty} \mathbb{P} (|\mathfrak{L}_k^N(0)| \geq R) = 0$ and
- (2) For all $\varepsilon > 0$ and $M \in \mathbb{N}$,

$$\lim_{\delta \rightarrow 0} \lim_{N \rightarrow \infty} \mathbb{P} \left(\sup_{|x|, |y| \leq M, |x-y| \leq \delta} |\mathfrak{L}_k^N(x) - \mathfrak{L}_k^N(y)| \geq \varepsilon \right) = 0.$$

The first item is immediate from Theorem 6.10 and Assumption 2, using the ordering of the curves, while (2) follows from Corollary 6.15. \square

7. AIRY SHEET AND TIGHTNESS OF S6V SHEET

In this section we address tightness and convergence to the Airy sheet of the colored height functions of our models. As in Section 5, we restrict to packed boundary or initial conditions.

7.1. Convergence to the Airy sheet. We will give a single proof of Theorems 2.8 and 2.18 using a unified notation for the objects arising from both S6V and ASEP, as follows. We will use $\mathbf{L}^{(j),N}$ for line ensembles corresponding to different colors in the two models. The S6V case will correspond to identifying $\mathbf{L}^{(j),N}$ with $\mathbf{L}^{\text{S6V},(j),\varepsilon}$, and the ASEP case to identifying the same with $\mathbf{L}^{\text{ASEP},(j),\theta,\varepsilon}$, as defined in (6.1) and (6.3), and in both cases under the identification of N with ε^{-1} . Next recall the scaling operator $T_{p,\lambda,N}$ from (3.11). For a sequence (indexed by N) of collections of line ensembles $\{\mathbf{L}^{(j),N}\}_j$ such that $\mathbf{L}^{(1),N}$ satisfies Assumptions 1, 2 (with parameters $p \in (-1, 0)$ and $\lambda > 0$), and 3, we define the rescaled line ensemble $\mathfrak{L}^{(j),N}$ by

$$\mathfrak{L}^{(j),N} = T_{p,\lambda,N}(\mathbf{L}^{(j),N});$$

we will use this definition and assume that $\mathbf{L}^{(1)}$ satisfies Assumptions 1, 2, and 3 throughout this section without further comment. Note that Theorem 3.19 implies $\mathfrak{L}^{(1),N} \xrightarrow{d} \mathcal{P}$, the parabolic Airy line ensemble (Definition 2.1).

Recall that the top lines of the line ensembles $\mathbf{L}^{\text{S6V},(j),\varepsilon}$ and $\mathbf{L}^{\text{ASEP},(j),\theta,\varepsilon}$ correspond to the height functions of arrows or particles of color above a threshold determined by j (the threshold being j for S6V and $-j$ for ASEP), and that varying j under the colored coupling of the underlying models corresponds to varying the location of the start of the step initial condition. To encode the line ensembles corresponding to the step initial condition started, in rescaled coordinates, at x in a notationally unified way, we define the following. Recalling β from (3.12), let

$$\mathfrak{L}_k^N(x; y) := \mathfrak{L}_k^{(\lfloor \beta x N^{2/3} \rfloor), N}(y). \quad (7.1)$$

Next we define $\mathcal{S}^N : \mathbb{R}^2 \rightarrow \mathbb{R}$ by

$$\mathcal{S}^N(x; y) := \mathfrak{L}_1^N(x; y) \quad (7.2)$$

for $(x, y) \in [-N^{1/6}, N^{1/6}]^2$ and in an arbitrary way such that the resulting function is continuous for all $(x, y) \notin [-N^{1/6}, N^{1/6}]^2$; the latter will not affect our limit statements since we work in the topology of uniform convergence on compact sets. This definition encompasses the S6V and ASEP cases by taking $(x, y) \mapsto \mathcal{S}^N(x; y)$ to equal $\mathcal{S}^{\text{S6V}, \varepsilon}$ and $(x, y) \mapsto \mathcal{S}^{\text{ASEP}, \theta, \varepsilon}(-x; -y)$ respectively (as defined in (2.15) and (2.8)), with $N = \lfloor \varepsilon^{-1} \rfloor$. That this is consistent with the definitions of $\mathcal{S}^{\text{S6V}, \varepsilon}$ and $\mathbf{L}^{\text{S6V}, (j), \varepsilon}$ (and the analogs for ASEP) follows from the definitions (6.1) for S6V and (6.3) for ASEP, along with Proposition 3.12 (relating the colored Hall-Littlewood line ensemble and the S6V height functions).

We also assume the following stationarity property for all z fixed, where $g_N \leq N$ is a fixed sequence with $g_N \rightarrow \infty$ as $N \rightarrow \infty$: as processes in x, y over the domain defined by $x, y, x+z, y+z \in [-g_N, g_N]$,

$$\mathcal{S}^N(x; y) \stackrel{d}{=} \mathcal{S}^N(x+z; y+z); \quad (7.3)$$

that this property holds for the S6V and ASEP cases follows for S6V from (5.1) (and the presence of the $+j$ term in the definition (6.1)) along with (6.2), and for ASEP from (5.4) and (6.4).

We will soon need to invoke Theorem 3.20 on the approximate representation of $\mathbf{L}^{\text{cHL}(j)}$ in terms of a last passage percolation problem in $\mathbf{L}^{\text{cHL}, (1)}$. To avoid a notational clash with the symbol N indexing the sequence of line ensembles \mathbf{L}^N , in this section we will use \mathbb{N} for the parameter implicit in $\mathbf{L}^{\text{cHL}, (j)}$ from Definition 3.7 (and thus also the parameter defining the domain of the colored S6V model from Section 2.3). We will also make the assumption that there exists $D > 0$ such that

$$\mathbb{N} \leq N^D, \quad (7.4)$$

which we will later verify holds in our cases of interest.

The following is a convergence statement for \mathcal{S}^N (i.e., S6V and ASEP simultaneously); it will be proved in Section 7.2.

Theorem 7.1. *Assume that $\mathbf{L}^{(1), N}$ satisfies Assumptions 1 and 2, and is such that $\mathfrak{L}^{(1), N} \xrightarrow{d} \mathcal{P}$ as $N \rightarrow \infty$, in the topology of uniform convergence on compact sets of $\mathcal{C}(\mathbb{N} \times \mathbb{R}, \mathbb{R})$, and that (7.3) and (7.4) hold. Further assume (3.14) holds with $\mathbf{L}^{(1), N}, \mathbf{L}^{(j), N}$ in place of $\mathbf{L}^{\text{cHL}, (1)}, \mathbf{L}^{\text{cHL}, (j)}$, respectively. Then $\mathcal{S}^N \xrightarrow{d} \mathcal{S}$ in $\mathcal{C}(\mathbb{R}^2, \mathbb{R})$ in the topology of uniform convergence on compact sets as $N \rightarrow \infty$.*

We now prove Theorems 2.8 and 2.18.

Proof of Theorem 2.8. We take $\mathcal{S}^N(x; y) = \mathcal{S}^{\text{ASEP}, \theta, \varepsilon}(-x; -y)$ as processes in (x, y) with $N = \varepsilon^{-1}$, and note from (5.2) that \mathbb{N} in this case equals $\lfloor (2\gamma^{-1})^{1+\theta} \varepsilon^{-(1+\theta)} \rfloor = \lfloor (2\gamma^{-1} \varepsilon^{-1})^{41} \rfloor$; so (7.4) holds. Analogously we take $\mathbf{L}^{(j), N} = \mathbf{L}^{\text{ASEP}, (j), \theta, \varepsilon}$. Now, $\mathbf{L}^{(1), N}$ satisfies Assumptions 1, 2, and 3 by Lemma 6.9, so, by Theorem 3.19, $\mathfrak{L}^{(1), N} \xrightarrow{d} \mathcal{P}$. Next, (7.3) holds due to (5.4), and (3.14) holds due to Theorem 3.20 along with (6.3). Thus Theorem 7.1 yields that $\mathcal{S}^{\text{ASEP}, \theta, \varepsilon}(x; y) \rightarrow \mathcal{S}(-x; -y)$ in distribution as continuous processes on \mathbb{R}^2 as $\varepsilon \rightarrow 0$. By Lemma 5.2, we then obtain that $\mathcal{S}^{\text{ASEP}, \varepsilon}(x; y) \rightarrow \mathcal{S}(-x; -y)$ in the same topology as $\varepsilon \rightarrow 0$ as well. That $\mathcal{S}(-x; -y) \stackrel{d}{=} \mathcal{S}(x; y)$ by [DV21b, Proposition 1.23] as processes completes the proof of Theorem 2.8. \square

Proof of Theorem 2.18. Recall that $\mathcal{S}^{\text{S6V}, \varepsilon}$ is defined in terms of a colored S6V model defined on $\mathbb{Z}_{\geq 1} \times \llbracket -\mathbb{N}, \infty \rrbracket$. Let $\tilde{\mathcal{S}}^{\text{S6V}, \varepsilon}$ be the same with $\mathbb{N} = \varepsilon^{-2}$ if the original $\mathbb{N} > \varepsilon^{-2}$, and let $\tilde{\mathcal{S}}^{\text{S6V}, \varepsilon} = \mathcal{S}^{\text{S6V}, \varepsilon}$ otherwise; let $\tilde{\mathbf{L}}^{\text{S6V}, (j), \varepsilon}$ be the associated colored line ensemble from (6.1). We claim that there is a coupling of $\mathcal{S}^{\text{S6V}, \varepsilon}$ and $\tilde{\mathcal{S}}^{\text{S6V}, \varepsilon}$ such that the two agree on $[-\varepsilon^{-1/6}, \varepsilon^{-1/6}]^2$ with probability $1 - o(1)$ as $\varepsilon \rightarrow 0$. Assuming this claim, it is sufficient to prove that $\tilde{\mathcal{S}}^{\text{S6V}, \varepsilon} \xrightarrow{d} \mathcal{S}$ as $\varepsilon \rightarrow 0$, and this will follow from Theorem 7.1 with $N = \varepsilon^{-1}$, $\mathcal{S}^N = \tilde{\mathcal{S}}^{\text{S6V}, \varepsilon}$, and $\mathbf{L}^{(j), N} = \tilde{\mathbf{L}}^{\text{S6V}, (j), \varepsilon}$ once its assumptions are verified. Now, $\mathbf{L}^{(1), N}$ satisfies Assumption 1, 2, and 3 by Lemma 6.8, so, by Theorem 3.19, $\mathfrak{L}^{(1), N} \xrightarrow{d} \mathcal{P}$. The remaining assumptions of Theorem 7.1 are verified since the conditions (7.3), (7.4), and (3.14) are satisfied by (5.1), by (6.2), and by combining Theorem 3.20 with (6.1), respectively.

The claim we made on the coupling between $\mathcal{S}^{\text{S6V},\varepsilon}$ and $\tilde{\mathcal{S}}^{\text{S6V},\varepsilon}$ follows immediately from [AB24, Lemma B.3], which is a finite speed of propagation estimate: roughly speaking, it says that two colored S6V models which have boundary conditions agreeing on a large interval have a coupling such that the arrow configurations agree in a large region. In our case, the boundary conditions of the two systems agree on $\llbracket -\lfloor \varepsilon^{-2} \rfloor, \lfloor \varepsilon^{-2} \rfloor \rrbracket$ and we require the arrow configurations to agree on $\{\lfloor \varepsilon^{-1} \rfloor\} \times \llbracket \lfloor \alpha \varepsilon^{-1} - 2\varepsilon^{-5/6} \rfloor, \lfloor \alpha \varepsilon^{-1} + 2\varepsilon^{-5/6} \rfloor \rrbracket$. [AB24, Lemma B.3] yields that there is a coupling such that this holds with probability at least $1 - \exp(-c\varepsilon^{-2})$ for some $c > 0$ (take U, V, T, K there to respectively be $-\lfloor \frac{1}{2}\varepsilon^{-2} \rfloor, \lfloor \frac{1}{2}\varepsilon^{-2} \rfloor, \lfloor R\varepsilon^{-1} \rfloor$, and $\lfloor \delta R^{-1}\varepsilon^{-1} \rfloor$ for some large constant R and small constant $\delta > 0$). This completes the proof of Theorem 2.18. \square

In the next section we begin setting up some statements needed for the proof of Theorem 7.1 before giving the proof at the end of the section.

7.2. Setup for Airy sheet convergence. For a sequence of random variables $\{X_{N,k}\}_{N,k=1}^\infty$ defined on a common probability space, we adopt the notation

$$X_{N,k} = \mathfrak{o}(r_{N,k}) \quad \text{if} \quad \sum_{k=1}^{\infty} \limsup_{N \rightarrow \infty} \mathbb{P}(|X_{N,k}| \geq \varepsilon r_{N,k}) < \infty \quad (7.5)$$

for every $\varepsilon > 0$, i.e., $\lim_{k \rightarrow \infty} \lim_{N \rightarrow \infty} X_{N,k}/r_{N,k} = 0$, where the inner limit should be understood as any weak limit of $\{X_{N,k}/r_{N,k}\}_N$ and the outer limit as an almost sure one, by the Borel-Cantelli lemma. The notation also makes sense if $X_{N,k} = X_N$ and $r_{N,k} = r_N$ for all k for some sequences X_N, r_N such that $X_N/r_N \rightarrow 0$ almost surely as $N \rightarrow \infty$. Also, $X_{N,k} \geq \mathfrak{o}(r_{N,k})$ means that $X_{N,k} \mathbb{1}_{X_{N,k} \leq 0} = \mathfrak{o}(r_{N,k})$, and $X_{N,k} \leq \mathfrak{o}(r_{N,k})$ means $X_{N,k} \mathbb{1}_{X_{N,k} \geq 0} = \mathfrak{o}(r_{N,k})$.

Next recall the notation (2.2) for last passage percolation (LPP) values. In the notation (7.1) and for $\delta > 0$, consider (3.14) of Theorem 3.20, as assumed in Theorem 7.1, with k set to $N^{1/6}$ and $m = \sigma \delta N^{1/3}$ with σ as in (3.12). A union bound over x implies that, for $\delta > K(q)N^{-1/3} \log N$ (which, under (7.4), holds if $\delta > DK(q)N^{-1/3} \log N$),

$$\mathbb{P} \left(\sup_{x, |y| \in (0, g_N]} \left| \mathcal{S}^N(x; y) - \max_{w \leq y} \left(\mathfrak{L}_{N^{1/6}}^N(x; w) + \mathfrak{L}^{(1),N}[(w, N^{1/6} - 1) \rightarrow (y, 1)] \right) \right| \geq \delta N^{1/6} \right) \leq CN^{\frac{7}{6}} q^{c\sigma^2 \delta^2 N^{2/3}}. \quad (7.6)$$

Now set $\delta = N^{-1/4}$ and note that $N^{-1/11} \gg \delta N^{1/6} = N^{-1/12}$. For fixed $q \in [0, 1)$ and $k \in \mathbb{N}$, (7.6) implies that for all $x, |y| \in (0, g_N]$ and $N \geq N_0$, with $\mathfrak{o}(N^{-1/11})$ a random quantity satisfying (7.5) whose distribution does not depend on x or y ,

$$\begin{aligned} \mathcal{S}^N(x; y) &= \max_{w \leq y} \left(\mathfrak{L}_{N^{1/6}}^N(x; w) + \mathfrak{L}^{(1),N}[(w, N^{1/6} - 1) \rightarrow (y, 1)] \right) + \mathfrak{o}(N^{-1/11}), \\ &= \max_{w \leq z \leq y} \left(\mathfrak{L}_{N^{1/6}}^N(x; w) + \mathfrak{L}^{(1),N}[(w, N^{1/6} - 1) \rightarrow (z, k)] + \mathfrak{L}^{(1),N}[(z, k) \rightarrow (y, 1)] \right) \\ &\quad + \mathfrak{o}(N^{-1/11}), \end{aligned} \quad (7.7)$$

where in the second line we used the fact that the LPP problem is a variational problem to split it up at line k (see for example [DOV22, Lemma 3.2]).

Let $Z_k^N(x, y)$ be the maximizer (of the maximum over z) in (7.7) (the largest one in the event that there are multiple). The following records control on the location of Z_k^N which will be necessary for the proofs of Theorem 2.8 and 2.18. Because its proof is similar to [DOV22, Lemma 7.1], we defer it to Appendix C.

Proposition 7.2. *Under the hypotheses of Theorem 7.1, it holds that, for any $x > 0$ and $y \in \mathbb{R}$,*

$$Z_k^N(x, y) = -\sqrt{\frac{k}{2x}} + \mathfrak{o}(k^{1/2}).$$

Moreover, $\{Z_k^N(x, y)\}_{N \in \mathbb{N}}$ is tight for each fixed $k \in \mathbb{N}$, $x > 0$, and $y \in \mathbb{R}$.

To prove Theorem 7.1, we also need to know that \mathcal{S}^N forms a tight sequence in $\mathcal{C}(\mathbb{R}^2, \mathbb{R})$, recorded in the following proposition. It will be proved in Section 7.3, where we will establish the necessary modulus of continuity estimates.

Proposition 7.3. *Under the hypotheses of Theorem 7.1, $\{\mathcal{S}^N\}_{N=1}^\infty$ is tight in $\mathcal{C}(\mathbb{R}^2, \mathbb{R})$ under the topology of uniform convergence on compact sets.*

The following monotonicity statement on differences of LPP values will be useful in the proof of Theorem 7.1 and has been proved many times in the literature; see for example [DOV22, Proposition 3.8], [GH23, Lemma 2.10], or [BBS20, Lemma B.2].

Lemma 7.4 (Crossing lemma, [DOV22, GH23, BBS20]). *Let $\mathbf{f} = (f_1, \dots, f_k)$ be a sequence of continuous functions with $f_i : \mathbb{R} \rightarrow \mathbb{R}$. Then, for any $y_1 < y_2$*

$$z \mapsto f[(z, k) \rightarrow (y_1, 1)] - f[(z, k) \rightarrow (y_2, 1)]$$

is non-increasing.

Now we may give the proof of Theorem 7.1; given all the machinery developed by now, its proof is quite similar to that of [DV21b, Theorem 4.4].

Proof of Theorem 7.1. We know from Proposition 7.3 that \mathcal{S}^N is tight as a law on $\mathcal{C}(\mathbb{R}^2, \mathbb{R})$ with the topology of uniform convergence on compact sets. So we only need to show that all subsequential limits equal \mathcal{S} , equivalently, that they satisfy (i) and (ii) in Definition 2.3.

That (i) holds follows from (7.3). We will next show that (ii) holds for any subsequential limit of \mathcal{S}^N . Recall from (7.7) that, for all $x \in [0, g_N]$, $y_i \in [-g_N, g_N]$ simultaneously, with $i \in \{1, 2\}$,

$$\begin{aligned} \mathcal{S}^N(x; y_i) &= \sup_{w \leq z \leq y_i} \left(\mathfrak{L}_{N^{1/6}}^N(x; w) + \mathfrak{L}^{(1), N}[(w, N^{1/6} - 1) \rightarrow (z, k)] + \mathfrak{L}^{(1), N}[(z, k) \rightarrow (y_i, 1)] \right) \\ &\quad + \mathfrak{o}(N^{-1/11}) \end{aligned} \tag{7.8}$$

holds. We assume in what follows that $y_1 < y_2$, without loss of generality.

From Proposition 7.2, for every $k \in \mathbb{N}$, $x > 0$ and $y_1, y_2 \in \mathbb{R}$, there exists $Z_k^N(x, y_1)$ and $Z_k^N(x, y_2)$ which are tight sequences in N (for each fixed k , x , and y) such that the above supremum in z is attained at $Z_k^N(x, y_i)$.

Consider the tight collection of random objects

$$\{\mathcal{S}^N\}_{N=1}^\infty, \{\mathfrak{L}^{(1), N}\}_{N=1}^\infty, \{Z_k^N(x, y) : k \in \mathbb{N}, x \in \mathbb{Q}_{>0}, y \in \mathbb{Q}\}_{N=1}^\infty; \tag{7.9}$$

for the first collection, each member is an element of $\mathcal{C}(\mathbb{R}^2, \mathbb{R})$ endowed with the topology of uniform convergence on compact sets; for the second collection, each member is an element of $\mathcal{C}(\mathbb{R} \times \mathbb{N}, \mathbb{R})$ again endowed with the topology of uniform convergence on compact sets; and for the third collection, each member is a function $\mathbb{N} \times \mathbb{Q}_{>0} \times \mathbb{Q} \rightarrow \mathbb{R}$, i.e., an element of $\mathbb{R}^{\mathbb{N} \times \mathbb{Q}_{>0} \times \mathbb{Q}}$. For this last space we have the usual topology generated by cylinders, which corresponds to convergence of all finite collections.

As we noted above, tightness for \mathcal{S}^N is a consequence of Proposition 7.3. We have assumed tightness for $\mathfrak{L}^{(1), N}$ and that it weakly converges to \mathcal{P} , the parabolic Airy line ensemble. Finally, tightness of the final collection in the previous display follows from the tightness of $Z_k^N(x, y)$ for fixed k , x , and y from Proposition 7.2 (since the topology is characterized by convergence of finite collections).

As a result, we have tightness of all the collections in (7.9) jointly, which means we can extract a subsequence along which all four collections converge. We assume for notational convenience that the subsequence is the whole sequence, i.e., we will continue labeling the sequence by N . We denote the limiting objects by

$$\tilde{\mathcal{S}}, \mathcal{P}, \{Z_k(x, y) : k \in \mathbb{N}, x \in \mathbb{Q}_{>0}, y \in \mathbb{Q}\},$$

where \mathcal{P} is the parabolic Airy line ensemble, as noted above. That $\tilde{\mathcal{S}}(0; \cdot) = \mathcal{P}_1(\cdot)$ follows immediately from the definition (7.2) of $\mathcal{S}^N(0; \cdot)$, so the first part of (ii) of Definition 2.3 is verified. Next recall from Proposition 7.2 that, almost surely,

$$\lim_{k \rightarrow \infty} \frac{Z_k(x, y_i)}{\sqrt{k}} = -\frac{1}{\sqrt{2x}}. \quad (7.10)$$

Returning to (7.8) and by the definition of $Z_k^N(x, y_2)$, we see that, for every $k \in \mathbb{N}$,

$$\begin{aligned} \mathcal{S}^N(x; y_2) &= \sup_{w \leq Z_k^N(x, y_2)} \left(\mathfrak{L}_{N^{1/6}}^N(x; w) + \mathfrak{L}^{(1), N}[(w, N^{1/6} - 1) \rightarrow (Z_k^N(x, y_2), k)] \right) \\ &\quad + \mathfrak{L}^{(1), N}[(Z_k^N(x, y_2), k) \rightarrow (y_2, 1)] + \mathfrak{o}(1) \\ \mathcal{S}^N(x; y_1) &\geq \sup_{w \leq Z_k^N(x, y_2)} \left(\mathfrak{L}_{N^{1/6}}^N(x; w) + \mathfrak{L}^{(1), N}[(w, N^{1/6} - 1) \rightarrow (Z_k^N(x, y_2), k)] \right) \\ &\quad + \mathfrak{L}^{(1), N}[(Z_k^N(x, y_2), k) \rightarrow (y_1, 1)] + \mathfrak{o}(1). \end{aligned} \quad (7.11)$$

Subtracting the first from the second then yields that

$$\begin{aligned} \mathcal{S}^N(x; y_1) - \mathcal{S}^N(x; y_2) &\geq \mathfrak{L}^{(1), N}[(Z_k^N(x, y_2), k) \rightarrow (y_1, 1)] - \mathfrak{L}^{(1), N}[(Z_k^N(x, y_2), k) \rightarrow (y_2, 1)] \\ &\quad + \mathfrak{o}(1). \end{aligned} \quad (7.12)$$

By the convergence of $Z_k^N(x, y_2)$ to $Z_k(x, y_2)$ and the uniform convergence on compact sets of $\mathfrak{L}^{(1), N}$ to \mathcal{P} , taking $N \rightarrow \infty$ yields

$$\tilde{\mathcal{S}}(x; y_1) - \tilde{\mathcal{S}}(x; y_2) \geq \mathcal{P}[(Z_k(x, y_2), k) \rightarrow (y_1, 1)] - \mathcal{P}[(Z_k(x, y_2), k) \rightarrow (y_2, 1)].$$

Now, we know from the crossing lemma (Lemma 7.4) and since $y_1 < y_2$ that the righthand side is non-increasing in the argument which equals $Z_k(x, y_2)$; we will use this to replace $Z_k(x, y_2)$ by approximately $-\sqrt{k/(2x)}$. In more detail, fix $\varepsilon > 0$. We know from (7.10) that for all large enough k (depending on ε),

$$Z_k(x, y_2) \leq -\sqrt{\frac{k}{2(x + \varepsilon)}}. \quad (7.13)$$

Thus it follows that for all such k ,

$$\tilde{\mathcal{S}}(x; y_1) - \tilde{\mathcal{S}}(x; y_2) \geq \mathcal{P}\left[\left(\sqrt{k/(2(x + \varepsilon))}, k\right) \rightarrow (y_1, 1)\right] - \mathcal{P}\left[\left(\sqrt{k/(2(x + \varepsilon))}, k\right) \rightarrow (y_2, 1)\right]. \quad (7.14)$$

Now taking $k \rightarrow \infty$ in the righthand side and recalling the definition (2.3) of \mathcal{S} increments yields that, for every $\varepsilon > 0$,

$$\tilde{\mathcal{S}}(x; y_1) - \tilde{\mathcal{S}}(x; y_2) \geq \mathcal{S}(x + \varepsilon, y_1) - \mathcal{S}(x + \varepsilon, y_2).$$

Taking $\varepsilon \rightarrow 0$ and invoking the continuity of \mathcal{S} yields $\tilde{\mathcal{S}}(x; y_1) - \tilde{\mathcal{S}}(x; y_2) \geq \mathcal{S}(x; y_1) - \mathcal{S}(x; y_2)$. (Note that it is only in this step that we crucially rely on the fact that \mathcal{S} exists, has the coupling with \mathcal{P} , and is continuous; without these facts, it would not be possible to take $\varepsilon \rightarrow 0$ in (7.14) directly to obtain the same with $\varepsilon = 0$, as one first has to take $k \rightarrow \infty$, at which point continuity is not *a priori* available.)

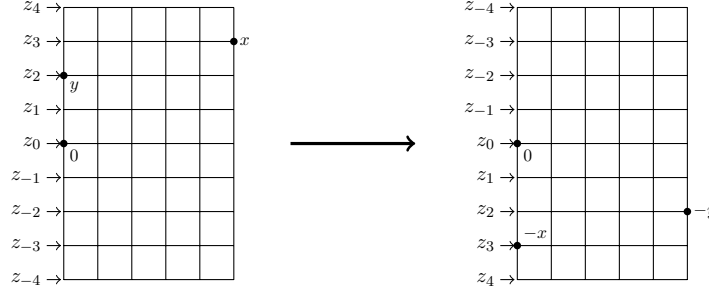


FIGURE 16. A depiction of the transformation of the domain of the colored S6V model used in the proof of Lemma 7.5. The z_i labels at the left side indicate the spectral parameter for the colored S6V weights on the corresponding row.

An analogous argument using $Z_k^N(x, y_1)$ in place of $Z_k^N(x, y_2)$ will give (7.11) with an equality for $\mathcal{S}^N(x; y_1)$ and a lower bound for $\mathcal{S}^N(x; y_2)$ (with $Z_k^N(x, y_1)$ on the righthand side for both); then we obtain a lower bound for $\mathcal{S}^N(x; y_2) - \mathcal{S}^N(x; y_1)$ analogous to (7.12). Since $y_1 < y_2$, a lower bound on $Z_k(x, y_1)$ in place of (7.13), again invoking Lemma 7.4, and taking the limit $N \rightarrow \infty$ and then $\varepsilon \rightarrow 0$ as above yields $\tilde{\mathcal{S}}(x; y_1) - \tilde{\mathcal{S}}(x; y_2) \leq \mathcal{S}(x; y_1) - \mathcal{S}(x; y_2)$. This completes the proof after noting \mathcal{S} itself enjoys the desired coupling with \mathcal{P} , which yields it for $\tilde{\mathcal{S}}$ as well. \square

7.3. Tightness of \mathcal{S}^N . In this section we show tightness of \mathcal{S}^N in $\mathcal{C}(\mathbb{R}^2, \mathbb{R})$, i.e., prove Proposition 7.3; recall that $\mathcal{S}^N(x; y)$ is just shorthand for the objects $\mathcal{S}^{\text{S6V}, \varepsilon}(x; y)$ and $\mathcal{S}^{\text{ASEP}, \theta, \varepsilon}(-x; -y)$, as processes. To prove tightness of the process, it is sufficient to prove one-point tightness and uniform-in- N modulus of continuity estimates. The basic idea is to reduce the modulus of continuity estimates for \mathcal{S}^N into the same where one argument of \mathcal{S}^N is fixed; then, we can make use of modulus of continuity estimates for line ensembles.

The first ingredient for this is the following symmetrization lemma, which follows as a consequence of general shift-invariance results for colored vertex models [BGW22, Gal21].

Lemma 7.5. *It holds that $\mathcal{S}^N(y; x) \stackrel{d}{=} \mathcal{S}^N(-x; -y)$ as processes in (x, y) .*

Proof. Recall that N is the parameter controlling the dimension of the domain of the colored S6V model. To establish the lemma, it suffices to show, for fixed $K \in \llbracket -N, N \rrbracket$ and $t \in \mathbb{N}$, that

$$h^{\text{S6V}}(y, 0; K + x, t) + y \stackrel{d}{=} h^{\text{S6V}}(-x, 0; K - y, t) - x \quad (7.15)$$

jointly across all x, y such that $K + x, K - y \in \llbracket -N, N \rrbracket$, as $\mathcal{S}^N(y; x)$ and $\mathcal{S}^N(-x; -y)$ are scaled and shifted versions of the lefthand and righthand sides, respectively, in both the cases of ASEP and S6V (recall (7.2), (2.15), (5.7)). It further suffices to establish the case of $K = 0$; for combining the $(K, x, y) \mapsto (0, K + x, y)$ case of (7.15) with (5.1) yields

$$h^{\text{S6V}}(y, 0; K + x, t) + y \stackrel{d}{=} h^{\text{S6V}}(-K - x, 0; -y, t) - K - x \stackrel{d}{=} h^{\text{S6V}}(-x, 0; K - y, t) - x.$$

We show the $K = 0$ case of (7.15) now. First, in the case of $x < y$, the height functions are trivially equal: $h^{\text{S6V}}(y, 0; x, t) = N - y + 1$ and $h^{\text{S6V}}(-x, 0; -y, t) = N + x + 1$, since in both cases the lefthand sides are just the total number of arrows of the corresponding colors in the system.

So we may assume $x \geq y$. We now invoke [Gal21, Theorem 1.6]; let us explain the special case of its content that we need briefly now. Consider two colored S6V models on $\llbracket 1, t \rrbracket \times \llbracket -N, N \rrbracket$, with spectral parameters z_i at row i in the first and $z_{\tau(i)}$ at row i in the second, where $\tau : \llbracket -N, N \rrbracket \rightarrow \llbracket -N, N \rrbracket$ is a permutation; see Figure 16. In more detail, the measure is defined by setting the vertex weights (as in Figure 8) of vertices in row i with spectral parameter z_i (or $z_{\tau(i)}$ in place of z , and the probability of a particular arrow configuration is the product of the vertex weights.

Then [Gal21, Theorem 1.6] yields the following distributional equality. Let $k \in \mathbb{N}$ and $x_i, x'_i, y_i, y'_i \in \llbracket -\mathbb{N}, \mathbb{N} \rrbracket$ for $i = 1, \dots, k$ with $x_i \geq y_i$ and $x'_i \geq y'_i$, and under the additional condition that $\{z_j : y_i \leq j \leq x_i\} = \{z_{\tau(j)} : y'_i \leq j \leq x'_i\}$ (as multisets) for each i . Then,

$$\begin{aligned} & (h_1^{\text{S6V}}(y_1, 0; x_1, t) + y_1, \dots, h_1^{\text{S6V}}(y_k, 0; x_k, t) + y_k) \\ & \stackrel{d}{=} (h_2^{\text{S6V}}(y'_1, 0; x'_1, t) + y'_1, \dots, h_2^{\text{S6V}}(y'_k, 0; x'_k, t) + y'_k), \end{aligned} \quad (7.16)$$

where the subscript corresponds to whether the statistic is in the first or second colored S6V model (that is, left or right in Figure 16) just described. (in the notation of [Gal21], Theorem 1.6 there does not include the $+y_i$ or $+y'_i$ terms above; this is because the height function considered in [Gal21] counts the number of colored arrows below a given height and not above as in our setting. Translating from one to the other introduces the mentioned terms.)

For our situation, let $\tau(i) = -i$, i.e., we reverse the order of the formal spectral parameters, and for any choice of $x_i \geq y_i$, define $x'_i = -y_i$ and $y'_i = -x_i$. Then $x'_i \geq y'_i$ and clearly it holds that $\{z_{\tau(j)} : y'_i \leq j \leq x'_i\} = \{z_j : y_i \leq j \leq x_i\}$. Applying the distributional equality of (7.16) and specializing to the case that all spectral parameters are equal yields that

$$(h^{\text{S6V}}(y, 0; x, t) + y)_{x, y \in \llbracket -\mathbb{N}, \mathbb{N} \rrbracket, x \geq y} \stackrel{d}{=} (h^{\text{S6V}}(-x, 0; -y, t) - x)_{x, y \in \llbracket -\mathbb{N}, \mathbb{N} \rrbracket, x \geq y},$$

which yields the $K = 0$ case of (7.15) and completes the proof. \square

A second ingredient to prove the modulus of continuity estimates is the following monotonicity statement, sometimes called a quadrangle inequality, which will allow us to reduce the supremum over two arguments present in the modulus of continuity to a supremum over a single one; it is the analog of the crossing lemma (Lemma 7.4) for S6V and ASEP. In the context of last passage percolation models, such quadrangle inequalities have previously been used in similar ways (e.g., [DV21b]) as well as for other purposes (e.g., [BGH21, BBS20, BSS24, GH23, GHZ23]).

Lemma 7.6 (Quadrangle inequality). *For any $x_1 \leq x_2$ and $y_1 \leq y_2$,*

$$\mathcal{S}^N(x_1; y_1) + \mathcal{S}^N(x_2; y_2) \geq \mathcal{S}^N(x_1; y_2) + \mathcal{S}^N(x_2; y_1).$$

Proof. Recall from (2.12) the definition $h^{\text{S6V}}(x, 0; y, t) = \#\{k > y : j_{(t,k)} \geq x\}$. It suffices from the definition of \mathcal{S}^N in the cases of ASEP (5.7) and S6V (2.15) in terms of h^{S6V} to prove that $h^{\text{S6V}}(x_1, 0; y_1, t) + h^{\text{S6V}}(x_2, 0; y_2, t) \geq h^{\text{S6V}}(x_1, 0; y_2, t) + h^{\text{S6V}}(x_2, 0; y_1, t)$ for any $x_1 \leq x_2$, $y_1 \leq y_2$, $t \in \mathbb{N}$. To that end, observe that for any $x \in \mathbb{Z}$ and $y_1 \leq y_2$,

$$h^{\text{S6V}}(x, 0; y_1, t) - h^{\text{S6V}}(x, 0; y_2, t) = \#\{k \in \llbracket y_1 + 1, y_2 \rrbracket : j_{(t,k)} \geq x\},$$

which is clearly non-increasing in x , as was to be shown. \square

With these ingredients we give the proof of Proposition 7.3.

Proof of Proposition 7.3. We need to prove one-point tightness of \mathcal{S}^N as well as establish uniform-in- N modulus of continuity estimates. The tightness of $\{\mathcal{S}^N(x; y)\}_{N=1}^\infty$ for fixed x, y follows immediately from the stationarity of \mathcal{S}^N (recall (7.3)) and Assumption 2. For uniform-in- N modulus of continuity, we first observe that, from Lemma 7.6, for any $x, y \in [-K, K]$ and $x_1 \leq x_2$ and $y_1 \leq y_2$,

$$\begin{aligned} \mathcal{S}^N(K; y_1) - \mathcal{S}^N(K; y_2) & \leq \mathcal{S}^N(x; y_1) - \mathcal{S}^N(x; y_2) \leq \mathcal{S}^N(-K; y_1) - \mathcal{S}^N(-K; y_2) \\ \mathcal{S}^N(x_1; K) - \mathcal{S}^N(x_2; K) & \leq \mathcal{S}^N(x_1; y) - \mathcal{S}^N(x_2; y) \leq \mathcal{S}^N(x_1; -K) - \mathcal{S}^N(x_2; -K). \end{aligned}$$

In particular, we see that, for any $x_1, x_2, y_1, y_2 \in [-K, K]$,

$$\begin{aligned} & |\mathcal{S}^N(x_1; y_1) - \mathcal{S}^N(x_2; y_2)| \\ & \leq |\mathcal{S}^N(x_1; y_1) - \mathcal{S}^N(x_1; y_2)| + |\mathcal{S}^N(x_1; y_2) - \mathcal{S}^N(x_2; y_2)| \end{aligned}$$

$$\leq \max_{z \in \{+K, -K\}} |\mathcal{S}^N(z; y_1) - \mathcal{S}^N(z; y_2)| + \max_{z \in \{+K, -K\}} |\mathcal{S}^N(x_1; z) - \mathcal{S}^N(x_2; z)|.$$

By Lemma 7.5 the marginal distribution of the second term is the same as that of the first with x_i in place of y_i . Finally, the modulus of continuity over a single argument, i.e., of $y \mapsto \mathcal{S}^N(x; y)$ for x fixed, is the same as that of the top line of a rescaled line ensemble (see (7.2)) and therefore follows from Corollary 6.15. So by Corollary 6.15 and a union bound, for any $\rho > 0$ and $\varepsilon > 0$ there exists $\delta > 0$ such that, with probability at least $1 - \varepsilon$, whenever $|y_1 - y_2| \leq \delta$ and $|x_1 - x_2| \leq \delta$, the previous display is upper bounded by ρ . This completes the proof. \square

8. WEAK MONOTONICITY STATEMENTS FOR ONE PATH

As indicated in Section 3.3.3, a technical challenge in proving tightness for Hall-Littlewood Gibbs line ensembles is that the Gibbs property does not enjoy a form of stochastic monotonicity that previous proofs of tightness of prelimiting line ensembles have relied heavily upon.

This was a difficulty faced in [CD18] as well, and is one of the reasons the analysis there is restricted to the top curve. To get around the lack of monotonicity, they found a weaker form of monotonicity for a single curve with a lower boundary condition that does hold, in terms of a comparison of partition functions up to a constant multiplicative factor. Our analysis will rely on a similar weak monotonicity statement, but with the observation that it holds under slightly more general conditions (Corollary 8.5), namely in the presence of fixed upper and lower curves that the random curve must avoid, in addition to a possibly different lower boundary curve it interacts with via the weight factor W from Definition 3.15.

In the next section, we introduce some monotonicity statements for basic objects such as non-intersecting Bernoulli random walk bridges. In Section 8.2 we give the weak monotonicity statements.

8.1. Monotonicity statements for random walks and Gaussian objects. Here we collect some well-known statements of forms of monotonicity enjoyed by objects underlying the Gibbs properties, such as non-intersecting random walks and Gaussian random variables.

The following is a straightforward computation using the form of the density of the normal distribution, and we point the reader to its proof in [CHH23]. Recall the notation $\mathcal{N}(m, \sigma^2)$ for the normal distribution with mean m and variance σ^2 .

Lemma 8.1 ([CHH23, Lemma 5.15]). *Fix $r > 0$, $m \in \mathbb{R}$, and $\sigma^2 > 0$. Let X be distributed as $\mathcal{N}(m, \sigma^2)$. Then the quantity $\mathbb{P}(X \geq s + r \mid X \geq s)$ is a strictly decreasing function of $s \in \mathbb{R}$.*

The next lemma quotes a form of stochastic monotonicity in the boundary data of non-intersecting Bernoulli random walk bridges. The result has appeared in the literature a number of times, e.g., [CEP00, Lemma 18] or, in notation closer to ours, [DFF⁺21, Lemma 7.3]. Recall the definition of a Bernoulli path from Definition 2.9 and that of a Bernoulli random walk bridge from before Definition 3.15.

Lemma 8.2 ([CEP00, DFF⁺21]). *Fix an interval $\llbracket a, b \rrbracket \subseteq \mathbb{Z}$. Let $\vec{x}^*, \vec{y}^* \in \mathbb{Z}^k$ be such that $x_1^* \geq \dots \geq x_k^*$ and $y_1^* \geq \dots \geq y_k^*$ for $* \in \{\uparrow, \downarrow\}$. Let $f^*, g^* : \llbracket a, b \rrbracket \rightarrow \mathbb{Z}$ be Bernoulli paths such that $f^*(a) \geq x_1^*$, $f^*(b) \geq y_1^*$, $g^*(a) \leq x_k^*$, $g^*(b) \leq y_k^*$ for $* \in \{\uparrow, \downarrow\}$. Suppose $f^\uparrow(x) \geq f^\downarrow(x)$, $g^\uparrow(x) \geq g^\downarrow(x)$ for all $x \in \llbracket a, b \rrbracket$ and $x_i^\uparrow \geq x_i^\downarrow$, $y_i^\uparrow \geq y_i^\downarrow$ for all $i = 1, \dots, k$.*

Let $\mathbf{B}^ = (B_1^*, \dots, B_k^*)$ be a collection of independent Bernoulli random walk bridges, with B_i^* from (a, x_i^*) to (b, y_i^*) , conditioned on $g^*(x) \leq B_k^*(x) \leq \dots \leq B_1^*(x) \leq f^*(x)$ for all $x \in \llbracket a, b \rrbracket$ and for $* \in \{\uparrow, \downarrow\}$. Then there is a coupling between \mathbf{B}^\uparrow and \mathbf{B}^\downarrow such that*

$$B_i^\uparrow(x) \geq B_i^\downarrow(x)$$

for all $x \in \llbracket a, b \rrbracket$ and $i = 1, \dots, k$.

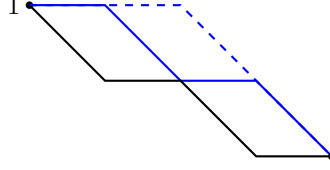


FIGURE 17. The solid blue path is pointwise (weakly) larger than the black path, but the two paths do not satisfy the hypotheses of Lemma 8.3; to go from black to blue, one needs to switch the black path’s down-steps at positions 1 and 3 to flat-steps, and its flat-steps at positions 2 and 4 to down-steps. The dashed blue path is the changed portion of the solid blue path obtained after flipping the first down-step (at position 2) to a flat-step and the second flat-step (at position 3) to a down-step.

8.2. Weak monotonicity. We start with a deterministic lemma about the weight of certain pairs of ordered paths with the same endpoints constrained to lie above a curve ℓ_{bot} . Define

$$c(q) := \prod_{i=1}^{\infty} (1 - q^i) > 0.$$

In the following, we call a down-step an increment of -1 in a Bernoulli path and a flat step an increment of 0 . Flipping a down-step to a flat-step (or vice versa) means keeping the left endpoint the same and changing the increment from -1 to 0 (or from 0 to -1) and keeping all other increments the same. We also recall the definition of the weight factor W and the notational device W_{low} from (3.9).

Lemma 8.3. *Let $\llbracket a, b \rrbracket \subseteq \mathbb{Z}$ be a fixed interval and $\ell_{\text{bot}} : \llbracket a, b \rrbracket \rightarrow \mathbb{Z}$ be a Bernoulli path. Let $\ell_{\downarrow}, \ell_{\uparrow} : \llbracket a, b \rrbracket \rightarrow \mathbb{Z}$ be Bernoulli paths with the same endpoints satisfying the property that there exist $t \in \llbracket a, b \rrbracket$ and $k \leq \min(t - a, b - t)$ such that flipping k down-steps in $\llbracket a, t \rrbracket$ in ℓ_{\downarrow} to flat-steps and k flat-steps in $\llbracket t, b \rrbracket$ in ℓ_{\downarrow} to down-steps yields ℓ_{\uparrow} . Then*

$$W_{\text{low}}(\ell_{\downarrow}, \ell_{\text{bot}}) \leq c(q)^{-1} \cdot W_{\text{low}}(\ell_{\uparrow}, \ell_{\text{bot}}).$$

While the hypotheses on ℓ_{\downarrow} and ℓ_{\uparrow} imply that $\ell_{\downarrow} \leq \ell_{\uparrow}$ pointwise, the two are not equivalent. This is because we require all the flat-to-up switches and all the up-to-flat switches to occur on either side of a given location t , which is a stronger condition; an example of a pair of paths which are pointwise ordered but do not satisfy this stronger condition is given in Figure 17.

We also point out the important detail that Lemma 8.3 requires the interaction through W to be only of a single path ℓ_{\downarrow} or ℓ_{\uparrow} , and with only a lower boundary curve; in particular, the comparison of partition functions is not claimed in the presence of an upper boundary.

Lemma 8.3 was originally proved in the course of the proof of [CD18, Lemma 4.1]; we reproduce the proof here.

Proof of Lemma 8.3. We assume that $\ell_{\downarrow}(i) \geq \ell_{\text{bot}}(i)$ for all $i \in \llbracket a, b \rrbracket$ as otherwise the lefthand side of the inequality to be shown is zero and we are done. Let $x_1 < \dots < x_k \leq t$ and $t \leq y_k < \dots < y_1$ be respectively the coordinates of the left endpoints of the down-steps that are flipped to flat-steps and of the flat-steps that are flipped to down-steps in going from ℓ_{\downarrow} to ℓ_{\uparrow} . Define $\ell_{\downarrow} = \ell_0, \ell_1, \dots, \ell_k = \ell_{\uparrow}$ by letting ℓ_j be obtained from ℓ_{\downarrow} after performing the flips at x_1, \dots, x_j and y_1, \dots, y_j only.

Now, ℓ_j differs from ℓ_{j-1} only on $\llbracket x_j + 1, y_j \rrbracket$, where the former is raised by 1 compared to the latter. Recall that $W_{\text{low}}(\ell_i, \ell_{\text{bot}}) = \prod_{x=a+1}^b (1 - \mathbb{1}_{\Delta_i(x-1) - \Delta_i(x) = 1} q^{\Delta_i(x-1)})$, where $\Delta_i(x) = \ell_i(x) - \ell_{\text{bot}}(x)$. By examining how each factor of the product changes on going from $W_{\text{low}}(\ell_{j-1}, \ell_{\text{bot}})$ to $W_{\text{low}}(\ell_j, \ell_{\text{bot}})$, it follows that:

- the factor corresponding to $x = x_j + 1$ changes from $1 - \mathbb{1}_{\Delta_{j-1}(x_j) - \Delta_{j-1}(x_j+1) = 1} q^{\Delta_{j-1}(x_j)}$ to 1, i.e., it (weakly) increases;

- the factors corresponding to $x \in \llbracket x_j + 2, y_j \rrbracket$ change from $1 - \mathbb{1}_{\Delta_{j-1}(x-1) - \Delta_{j-1}(x)=1} q^{\Delta_{j-1}(x-1)}$ to $1 - \mathbb{1}_{\Delta_j(x-1) - \Delta_j(x)=1} q^{\Delta_j(x-1)} = 1 - \mathbb{1}_{\Delta_{j-1}(x-1) - \Delta_{j-1}(x)=1} q^{\Delta_{j-1}(x-1)+1}$, i.e., they (weakly) increase;
- the factor corresponding to $x = y_j + 1$ changes from $1 - \mathbb{1}_{\Delta_{j-1}(y_j) - \Delta_{j-1}(y_j+1)=1} q^{\Delta_{j-1}(y_j)}$ to $1 - \mathbb{1}_{\Delta_j(y_j) - \Delta_j(y_j+1)=1} q^{\Delta_j(y_j)} = 1 - \mathbb{1}_{\Delta_{j-1}(y_j) - \Delta_{j-1}(y_j+1)=0} q^{\Delta_{j-1}(y_j)+1}$.

The last change can be a decrease depending on the indicator function, but the decrease is by at most a factor of $1 - q^{m_j}$, where $m_j = 1 + \min_{x \in \llbracket x_j+1, y_j \rrbracket} (\ell_{j-1}(x) - \ell_{\text{bot}}(x))$. Thus we have shown that

$$W_{\text{low}}(\ell_{j-1}, \ell_{\text{bot}}) \leq (1 - q^{m_j})^{-1} W_{\text{low}}(\ell_j, \ell_{\text{bot}}).$$

Since ℓ_j differs from ℓ_{j-1} by increasing the path by 1 on $\llbracket x_j + 1, y_j \rrbracket$, we obtain $m_j \geq m_{j-1} + 1$. This implies the claim. \square

Corollary 8.4. *Let $\llbracket a, b \rrbracket \subseteq \mathbb{Z}$ be a fixed interval and $\ell_{\text{bot}} : \llbracket a, b \rrbracket \rightarrow \mathbb{Z}$ be a Bernoulli path. Suppose B^\downarrow and B^\uparrow are random Bernoulli paths with respective laws \mathbb{P}_1 and \mathbb{P}_2 which can be coupled such that they almost surely satisfy the hypothesis of Lemma 8.3 (in particular t and k there may be random). Then*

$$\mathbb{E}_1 \left[W_{\text{low}}(B^\downarrow, \ell_{\text{bot}}) \right] \leq c(q)^{-1} \mathbb{E}_2 \left[W_{\text{low}}(B^\uparrow, \ell_{\text{bot}}) \right].$$

Proof. This follows by taking expectations in the inequality of Lemma 8.3. \square

The following shows that we have the comparison of partition functions in the case of paths which interact with a lower boundary via the Hall-Littlewood Gibbs weight and additionally avoid some upper and lower curves (the latter may differ from the lower boundary curve). We will use this fact heavily in our arguments as a replacement for the full monotonicity property enjoyed by line ensembles and Gibbs properties previously studied.

Corollary 8.5. *Let $\llbracket a, b \rrbracket \subseteq \mathbb{Z}$ be a fixed interval and $\ell_{\text{bot}} : \llbracket a, b \rrbracket \rightarrow \mathbb{Z}$ be a Bernoulli path. Let $f, g : \llbracket a, b \rrbracket \rightarrow \mathbb{Z}$ be Bernoulli paths with $g(i) \leq f(i)$ for all $i \in \llbracket a, b \rrbracket$. Let $t \in \llbracket a, b \rrbracket$, $z \in \mathbb{Z}$, $x \in \llbracket g(a), f(a) \rrbracket$, and $y \in \llbracket g(b), f(b) \rrbracket$ be such that, with B a Bernoulli random walk bridge from (a, x) to (b, y) (we assume there exists at least one Bernoulli path connecting those two points),*

$$\mathbb{P} \left(g(i) \leq B(i) \leq f(i) \text{ for all } i \in \llbracket a, b \rrbracket, \ell(t) \leq z \right) > 0.$$

Let B^\downarrow and B^\uparrow be distributed as Bernoulli random walk bridges from (a, x) to (b, y) conditioned to satisfy $g(x) \leq B^\downarrow(x) \leq f(x)$ and $g(x) \leq B^\uparrow(x) \leq f(x)$ for all $x \in \llbracket a, b \rrbracket$, with B^\downarrow additionally conditioned on $B^\downarrow(t) \leq z$. Let \mathbb{E}_1 and \mathbb{E}_2 be the expectation operators associated with their respective laws. Then it holds that

$$\mathbb{E}_1 \left[W_{\text{low}}(B^\downarrow, \ell_{\text{bot}}) \right] \leq c(q)^{-1} \mathbb{E}_2 \left[W_{\text{low}}(B^\uparrow, \ell_{\text{bot}}) \right].$$

Before proving Corollary 8.5, let us give an example showing how it will be used to obtain a comparison of one-point probabilities. Let ℓ_{bot} , f , and g be as in the corollary and fix t . Let B be a Bernoulli random walk bridge from (a, x) to (b, y) , conditioned to avoid f and g , and let L be the same but reweighted by the Radon-Nikodym derivative $W_{\text{low}}(L, \ell_{\text{bot}}) / \mathbb{E}[W_{\text{low}}(L, \ell_{\text{bot}})]$. Then we see that

$$\begin{aligned} \mathbb{P}(L(t) \leq z) &= \frac{\mathbb{E}[\mathbb{1}_{B(t) \leq z} W_{\text{low}}(B, \ell_{\text{bot}})]}{\mathbb{E}[W_{\text{low}}(B, \ell_{\text{bot}})]} = \frac{\mathbb{E}[W_{\text{low}}(B, \ell_{\text{bot}}) \mid B(t) \leq z]}{\mathbb{E}[W_{\text{low}}(B, \ell_{\text{bot}})]} \cdot \mathbb{P}(B(t) \leq z) \\ &\leq c(q)^{-1} \mathbb{P}(B(t) \leq z), \end{aligned}$$

the last inequality by Corollary 8.5. The final probability is simply a non-intersecting Bernoulli random walk bridge, for which tools like monotonicity (Lemma 8.2) and two-point estimates for the underlying unconditioned Bernoulli random walk bridge (Lemma 6.13) are available. We emphasize again, however, that while Corollary 8.5 allows the interaction via W_{low} to be with a lower curve ℓ_{bot} , it required that there be no upper curve for that interaction (unlike the case with the full weight factor W); in applications, when we will have to work with the full factor W , we will need to make other context-specific arguments to remove the upper boundary interaction before performing the above argument to get a probability comparison. We also note that the comparison is only of one-point probabilities and is thus not simply the same up to a multiplicative constant as the form of stochastic monotonicity available for non-intersecting Bernoulli random walk bridges (Lemma 8.2).

Now we turn to the proof of Corollary 8.5. We will need the following quantitative form of monotonicity for a single Bernoulli random walk bridge conditioned on avoiding an upper and lower boundary curve. A similar statement appeared for (multiple) non-intersecting Brownian bridges in [AH23a, Lemma 2.4]. Its proof consists of a construction of a Markov chain on pairs of paths (respectively with the two boundary conditions) whose dynamics preserve the quantitative ordering and whose stationary distribution has the desired marginals. Similar ideas have appeared many times, e.g., [CH14, DFF⁺21, AH23a], and thus we defer the proof to Appendix B.

Lemma 8.6. *Let $\llbracket a, b \rrbracket \subseteq \mathbb{Z}$ be a fixed interval and $f, g : \llbracket a, b \rrbracket \rightarrow \mathbb{Z}$ be Bernoulli paths with $g(i) \leq f(i)$ for all $i \in \llbracket a, b \rrbracket$. Let $x^\uparrow, x^\downarrow, y^\uparrow, y^\downarrow \in \mathbb{Z}$ be such that $g(a) \leq x^\downarrow \leq x^\uparrow \leq f(a)$ and $g(b) \leq y^\downarrow \leq y^\uparrow \leq f(b)$. Let $M = \max(x^\uparrow - x^\downarrow, y^\uparrow - y^\downarrow)$. Let B^* be a Bernoulli random walk bridge from (a, x^*) to (b, y^*) conditioned on $g(x) \leq B^*(x) \leq f(x)$ for $x \in \llbracket a, b \rrbracket$, for $*$ $\in \{\uparrow, \downarrow\}$. There exists a coupling of B^\uparrow and B^\downarrow such that, almost surely for all $x \in \llbracket a, b \rrbracket$,*

$$B^\downarrow(x) \leq B^\uparrow(x) \leq B^\downarrow(x) + M.$$

Proof of Corollary 8.5. We may assume that $z < f(t)$ as otherwise B^\uparrow and B^\downarrow have the same distribution and the claim is trivial. Next we observe that $B^\uparrow(t)$ stochastically dominates $B^\downarrow(t)$, using Lemma 8.2.

As a consequence, it is sufficient to show that a coupling meeting the hypothesis of Lemma 8.3 exists between two Bernoulli random walk bridges B^\uparrow and B^\downarrow from (a, x) to (b, y) conditioned on avoiding both f and g with B^* additionally conditioned on $B^*(t) = z^*$ for $*$ $\in \{\downarrow, \uparrow\}$, where $z^\uparrow \geq z^\downarrow$. Indeed, with the latter statement in hand, one can obtain the desired coupling between the original B^\downarrow and B^\uparrow by first coupling $B^\uparrow(t)$ and $B^\downarrow(t)$ via the stochastic domination, and then making use of the previous statement which is conditioned on the value of $B^*(t)$.

To show the statement we have reduced to, it is sufficient to prove the case where $z^\uparrow = z^\downarrow + 1$, as then the full statement follows by iteration. By the Gibbs property for non-intersecting Bernoulli random walk bridges, it is further sufficient to show that there exists a coupling between B^\uparrow and B^\downarrow where the former is now a Bernoulli random walk bridge from (a, x) to (t, z) and the latter is one from (a, x) to $(t, z - 1)$, both conditioned on avoiding f and g on $\llbracket a, t \rrbracket$, with the property that B^\uparrow is obtained from B^\downarrow by flipping one down-step of the latter to a flat-step; a similar proof will then show the analogous statement on $\llbracket t, b \rrbracket$, and one obtains the desired coupling by concatenating the couplings on either side of t (which yields the correct marginal distributions by the Gibbs property for non-intersecting Bernoulli random walk bridges).

Finally, we prove the last statement we have reduced to by induction on the interval length $k = t - a$. More explicitly, we establish by induction on k that there exists a coupling between two Bernoulli random walk bridges B^\uparrow and B^\downarrow , the first from (a, x) to (t, z) and the second from (a, x) to $(t, z - 1)$, each conditioned on avoiding both f and g , such that B^\uparrow is obtained from B^\downarrow by flipping a single down-step to a flat-step. Here z is assumed to be such that such paths exist.

In the case that $k = 1$ the claim is trivial, as B^\uparrow must consist of a single flat-step and B^\downarrow a single down-step. Assuming the statement holds for k , we now show it for $k + 1$. Using Lemma 8.6 (as

the right endpoint of B^\uparrow is higher by 1 than B^\downarrow , we first couple $B^\uparrow(t-1)$ and $B^\downarrow(t-1)$ so that $B^\downarrow(t-1) \leq B^\uparrow(t-1) \leq B^\downarrow(t-1) + 1$. Note that there are three possibilities for the individual values of $B^\uparrow(t-1)$, and $B^\downarrow(t-1)$ and we give the coupling of the whole paths depending on the case:

- (1) $B^\uparrow(t-1) = z + 1$, $B^\downarrow(t-1) = z$: in this case both paths must follow down steps in the last slot, and we couple $B^\uparrow|_{\llbracket a, t-1 \rrbracket}$ and $B^\downarrow|_{\llbracket a, t-1 \rrbracket}$ using the induction hypothesis.
- (2) $B^\uparrow(t-1) = z$, $B^\downarrow(t-1) = z$: in this case B^\uparrow must have a flat-step in the last slot and B^\downarrow must have a down-step, and we couple $B^\uparrow|_{\llbracket a, t-1 \rrbracket}$ and $B^\downarrow|_{\llbracket a, t-1 \rrbracket}$ to be equal.
- (3) $B^\uparrow(t-1) = z$, $B^\downarrow(t-1) = z - 1$: in this case B^\uparrow and B^\downarrow must both have a flat-step in the last slot, and we couple $B^\uparrow|_{\llbracket a, t-1 \rrbracket}$ and $B^\downarrow|_{\llbracket a, t-1 \rrbracket}$ using the induction hypothesis.

(Note that the case of $B^\uparrow(t-1) = z + 1$, $B^\downarrow(t-1) = z - 1$ is excluded by the coupling at $t - 1$.) It is immediate that the above coupling satisfies the hypothesis of Lemma 8.3 and has the correct marginals. This completes the induction step and hence the proof. \square

9. LOWER TAIL ESTIMATES

In this section we start developing the proof of Theorem 6.10 on the lower tail of the k^{th} curve of L^N (recall the definitions and hypotheses from Section 6). In particular, in this section, as well as Sections 10, 11, and 12, L^N will be assumed to satisfy Assumptions 1 and 2 without explicit mention.

9.1. The pieces for the lower tail. Theorem 6.10 is proved by an induction argument. The induction hypothesis will combine the lower tail estimate for a given curve with a statement that curves remain uniformly separated; the ultimate result of uniform separation will also be useful at several other locations (in particular, in the proof of Proposition 6.5, that weak limits have the Brownian Gibbs property) and we record it as a separate theorem.

In what follows, for a (measurable) set $A \subseteq \mathbb{R}$, an integer $k \in \mathbb{N}$, a (possibly infinite) interval $\Lambda \subseteq \mathbb{N}$ with $\llbracket 1, k + 1 \rrbracket \subseteq \Lambda$, a stochastic process $\mathbf{X} : \Lambda \times \mathbb{R} \rightarrow \mathbb{R}$, and $\delta > 0$, we define the event

$$\text{Sep}_k^N(\delta, A, \mathbf{X}) = \left\{ \min_{i=1, \dots, k} \inf_{x \in N^{-2/3} \in A} (X_i(x) - X_{i+1}(x)) \geq \delta N^{1/3} \right\}. \quad (9.1)$$

We will sometimes drop some of the parameters from the notation, depending on the context, when it is obvious what they are. We also recall the convention for the notation for event names mentioned in Remark 6.16. The use of the event Sep_k^N (and similar ones) is that, on it, the weight factor W (3.9) is very close to 1 for all large enough N , as stated next.

Lemma 9.1. *Fix an interval $[a, b]$, $k \in \mathbb{N}$, $q \in [0, 1)$, $\varepsilon > 0$, and $\delta > 0$. Let $\mathbf{X} : \llbracket 1, k \rrbracket \times \llbracket aN^{2/3}, bN^{2/3} \rrbracket$ be a collection of Bernoulli paths. There exists $N_0 = N_0(q, \varepsilon, \delta, b - a, k)$ such that, if $X_i(x) > X_{i+1}(x) + \delta N^{1/3}$ for all $x \in \llbracket aN^{2/3}, bN^{2/3} \rrbracket$ and $i \in \llbracket 1, k - 1 \rrbracket$, then, for $N > N_0$, $W(\mathbf{X}, \llbracket aN^{2/3}, bN^{2/3} \rrbracket) > 1 - \varepsilon$.*

Proof. Under the conditions assumed, $W(\mathbf{X}, \llbracket aN^{2/3}, bN^{2/3} \rrbracket) > (1 - q^{\delta N^{1/3}})^{k(b-a)N^{2/3}}$, from which the claim follows. \square

Next we state the result on uniform separation. It will be proved later in this section.

Theorem 9.2 (Uniform separation). *Fix $k \in \mathbb{N}$, $T > 2$, and $\varepsilon > 0$. There exist $\delta = \delta(k, T, \varepsilon) > 0$ and $N_0 = N_0(k, T, \varepsilon)$ such that, for $N \geq N_0$,*

$$\mathbb{P}(\text{Sep}_k^N(\delta, [-T, T], L^N)) \geq 1 - \varepsilon.$$

We also adopt the following convenient notational convention in the following sections: \bar{L}_k^N will denote L_k^N with the linear growth removed, i.e., with p as in Assumption 2

$$\bar{L}_k^N(x) = L_k^N(x) - px.$$

An important part of the induction step proving Theorems 6.10 and 9.2 is captured in the next proposition.

Proposition 9.3 (Lower tail inductive step). *Fix $k \in \mathbb{N}$. Suppose for any $T \geq 2$ and $\varepsilon > 0$, there exist $M = M(k, T, \varepsilon)$ and $\delta = \delta(k, T, \varepsilon) > 0$ such that*

$$\mathbb{P} \left(\inf_{sN^{-2/3} \in [-T, T]} \bar{L}_{k-1}^N(s) < -MN^{1/3} \right) \leq \varepsilon \quad \text{and} \quad \mathbb{P}(\text{Sep}_{k-2}^N(\delta, [-T, T], \mathbf{L}^N)^c) \leq \varepsilon. \quad (9.2)$$

Then for any $T \geq 2$ and $\varepsilon > 0$, there exist $R = R(k, T, \varepsilon)$ and $N_0 = N_0(k, T, \varepsilon)$ such that, for $N \geq N_0$,

$$\mathbb{P} \left(\inf_{sN^{-2/3} \in [-T, T]} \bar{L}_k^N(s) < -RN^{1/3} \right) \leq \varepsilon.$$

We will prove this statement in Section 9.2. To complete the induction step we also need a bound on the separation between the k and $(k+1)$ th curves. This is the next proposition.

Proposition 9.4 (Uniform separation inductive step). *Let $k \in \mathbb{N}$ and, for any $j \in \mathbb{N}$, let Sep_j^N be as in (9.1). Suppose for any $\varepsilon > 0$ and $T \geq 2$ there exist $\eta = \eta(k, T, \varepsilon) > 0$, $M = M(k, T, \varepsilon)$, and $N_0 = N_0(k, T, \varepsilon)$ such that, for $N \geq N_0$,*

$$\mathbb{P}(\text{Sep}_{k-2}^N(\eta, [-T, T], \mathbf{L}^N)^c) < \varepsilon \quad \text{and} \quad \mathbb{P} \left(\inf_{xN^{-2/3} \in [-T, T]} \bar{L}_k^N(x) < -MN^{1/3} \right) \leq \varepsilon. \quad (9.3)$$

Then for any $\varepsilon > 0$ and $T \geq 2$, there exist $\delta = \delta(k, T, \varepsilon) > 0$ and $N_0 = N_0(k, T, \varepsilon)$ such that, for $N \geq N_0$

$$\mathbb{P}(\text{Sep}_{k-1}^N(\delta, [-T, T], \mathbf{L}^N)) \geq 1 - \varepsilon.$$

We will prove Proposition 9.4 in Section 10. Next we will prove Theorems 6.10 and 9.2 together using Propositions 9.3 and 9.4.

Proof of Theorems 6.10 and 9.2. We prove the following statement by induction, which implies both theorems: for any $\varepsilon > 0$ there exists $M = M(\varepsilon, k, T)$ and $\delta = \delta(\varepsilon, k, T)$ such that

$$\mathbb{P} \left(\inf_{xN^{-2/3} \in [-T, T]} \bar{L}_k^N(x) \geq -MN^{1/3} \right) \geq 1 - \varepsilon \quad \text{and} \quad \mathbb{P}(\text{Sep}_{k-1}^N(\delta, [-T, T], \mathbf{L}^N)) \geq 1 - \varepsilon. \quad (9.4)$$

By convention, $L_0^N \equiv \infty$ so the $k = 0$ case is trivially true. We now show the induction statement that if the displayed statement holds for $k-1$, it also holds for k .

Indeed, the induction hypothesis says that the hypotheses (9.2) of Proposition 9.3 hold, which yields that for any $\varepsilon > 0$ and $T \geq 2$, there exists M such that the first inequality in (9.4) holds. Now the first hypothesis in (9.3) of Proposition 9.4 holds by the induction hypothesis, and the second hypothesis in (9.3) holds by the deduction just made. Thus we obtain the second inequality in (9.4) from Proposition 9.4, completing the induction step and thus the proof. \square

9.2. Setting up the proof of Proposition 9.3. We start by stating that the k^{th} curve cannot be uniformly low on a large interval. This is the first step in the proof of Proposition 9.3, and will be proved in Section 9.3. For an interval $I \subseteq \mathbb{R}$ and $R > 0$, we define the event

$$\text{Low}_k^I(R) := \left\{ \sup_{sN^{-2/3} \in I} \bar{L}_k^N(s) \leq -RN^{1/3} \right\}. \quad (9.5)$$

Lemma 9.5. *Let $k \in \mathbb{N}$ and let $\text{Sep}_{k-2}^N(\delta, \{T, U\}, \mathbf{L}^N)$ be as in (9.1). Suppose for any $\varepsilon > 0$, T , and U there exist $\delta = \delta(\varepsilon, k, T, U) > 0$, $M = M(\varepsilon, k, U)$, and $N_0 = N_0(k, T, \varepsilon)$ such that, for $N \geq N_0$,*

$$\mathbb{P} \left(\inf_{sN^{-2/3} \in [-U, U]} \bar{L}_{k-1}^N(s) < -MN^{1/3} \right) \leq \varepsilon \quad \text{and} \quad \mathbb{P}(\text{Sep}_{k-2}^N(\delta, \{T, U\}, \mathbf{L}^N)^c) \leq \varepsilon.$$

Then for any $\varepsilon > 0$ and $t > 0$, there exist $U = U(\varepsilon, T)$, $R_{\text{low}} = R_{\text{low}}(T, U, \varepsilon, k)$, and $N_0 = N_0(k, U, \varepsilon)$ such that, for $N \geq N_0$,

$$\mathbb{P} \left(\text{Low}_k^{[T, U]}(R_{\text{low}}) \right) \leq \varepsilon.$$

Next we state a lower tail bound for the k^{th} curve at a single point on the event that there exist points on either side which are not too low, and conditioned on the $(k-1)^{\text{st}}$ curve not being too low. This is the second step in the proof of Proposition 9.3; it will be proved in Section 9.4.

Lemma 9.6. *Let $[a, b]$ be an interval, $k \in \mathbb{N}$, and $\delta > 0$. Then there exist $N_0 = N_0(\delta, b-a)$, $C = C(b-a) > 0$, and $c = c(k) > 0$ such that, for any $t \in [a, b]$, $R > 0$, $K \geq 1$, and $N > N_0$,*

$$\mathbb{P} \left(\begin{array}{l} \bar{L}_k^N(tN^{2/3}) < -(R+K)N^{1/3}, \\ \sup_{xN^{-2/3} \in [a, t]} \bar{L}_k^N(x) \wedge \sup_{xN^{-2/3} \in [t, b]} \bar{L}_k^N(x) \geq -RN^{1/3} \mid \inf_{xN^{-2/3} \in [a, b]} \bar{L}_{k-1}^N(x) > -(R-\delta)N^{1/3} \end{array} \right) \leq C \exp(-cK^2/(b-a)).$$

Further, C can be taken to be increasing in $b-a$, and N_0 can be taken to be increasing in $b-a$ and decreasing in δ .

Assuming these two lemmas, getting the uniform bound Proposition 9.3 is a fairly standard chaining argument; we give it now before returning to the proofs of Lemmas 9.5 and 9.6 in Sections 9.3 and 9.4, respectively.

Proof of Proposition 9.3. We start by proving a lower tail bound for L_k^N at the boundaries and midpoint of $[-TN^{2/3}, TN^{2/3}]$, and then we will turn to setting up a chaining argument to extend to the infimum over the whole interval.

For $U > T$ and $R > 0$, let $\text{Low}_k^{[-U, -T]}(\frac{1}{4}R)$ and $\text{Low}_k^{[T, U]}(\frac{1}{4}R)$ be as in (9.5). Using Lemma 9.5 (whose hypothesis is assumed in (9.2)), and the same after reflecting in the line $\{x=0\}$, we obtain $U > T$ and R such that

$$\mathbb{P} \left(\text{Low}_k^{[-U, -T]}(\frac{1}{4}R) \cup \text{Low}_k^{[T, U]}(\frac{1}{4}R) \right) \leq \frac{1}{3}\varepsilon; \quad (9.6)$$

we may raise R if necessary so that $\exp(-cR^2/(2U)) < \frac{1}{3}\varepsilon$, where c is as in Lemma 9.6 (which is possible by the monotonicity of the above probability in R). Next, using (9.2), we may raise R further if necessary so that

$$\mathbb{P} \left(\inf_{sN^{-2/3} \in [-U, U]} \bar{L}_{k-1}^N(s) \leq -\frac{1}{8}RN^{1/3} \right) \leq \frac{1}{3}\varepsilon. \quad (9.7)$$

Let $\text{NotLow}_k = (\text{Low}_k^{[-U,-T]}(\frac{1}{4}R) \cup \text{Low}_k^{[T,U]}(\frac{1}{4}R))^c$. Then we see that

$$\begin{aligned} & \mathbb{P} \left(\bar{L}_k^N(-TN^{2/3}) < -\frac{1}{2}RN^{1/3} \mid \inf_{xN^{-2/3} \in [-U,U]} \bar{L}_{k-1}^N(x) > -\frac{1}{8}RN^{1/3} \right) \\ & \leq \mathbb{P} \left(\bar{L}_k^N(-TN^{2/3}) < -\frac{1}{2}RN^{1/3}, \text{NotLow}_k \mid \inf_{xN^{-2/3} \in [-U,U]} \bar{L}_{k-1}^N(x) > -\frac{1}{8}RN^{1/3} \right) \\ & \quad + \mathbb{P} \left(\text{Low}_k^{[-U,-T]}(\frac{1}{4}R) \cup \text{Low}_k^{[T,U]}(\frac{1}{4}R) \mid \inf_{xN^{-2/3} \in [-U,U]} \bar{L}_{k-1}^N(x) > -\frac{1}{8}RN^{1/3} \right) \\ & \leq \exp(-cR^2/(2U)) + \frac{1}{2}\varepsilon \leq \varepsilon, \end{aligned}$$

the penultimate inequality using Lemma 9.6, (9.6), and (9.7). A similar argument, along with a union bound and a relabeling of ε , yields

$$\mathbb{P} \left(\min_{xN^{-2/3} \in \{-T,0,T\}} \bar{L}_k^N(x) < -\frac{1}{2}RN^{1/3} \mid \inf_{xN^{-2/3} \in [-U,U]} \bar{L}_{k-1}^N(x) > -\frac{1}{8}RN^{1/3} \right) < \varepsilon. \quad (9.8)$$

Now we set up the chaining argument to obtain a bound on the lower tail of the infimum of \bar{L}_k^N . For any integer $\ell \geq 0$, let $S_\ell := \{ \lfloor T(-1 + i2^{-\ell})N^{2/3} \rfloor : i = 0, 1, \dots, 2^{\ell+1} \}$ (we will omit the floors in the notation for convenience in the rest of the proof) and define

$$\mathbf{E}_\ell := \left\{ \inf_{x \in S_\ell} \bar{L}_k^N(x) > -\alpha_\ell RN^{1/3} \right\},$$

where

$$\alpha_\ell := \frac{1}{2} + \delta \sum_{j=1}^{\ell} 2^{-j/4},$$

with $\delta = \frac{1}{4}(\sum_{j=1}^{\infty} 2^{-j/4})^{-1} > 0$, so that $\frac{1}{2} < \alpha_\ell < \frac{3}{4}$ for all $\ell \geq 0$. It is easy to see that

$$\left\{ \inf_{xN^{-2/3} \in [-T,T]} \bar{L}_k^N(x) < -RN^{1/3} \right\} \subseteq \bigcup_{\ell=0}^{\lceil \frac{1}{2} \log_2 N \rceil} (\mathbf{E}_\ell)^c.$$

Indeed, at $\ell = \frac{1}{2} \log_2 N$, the spacing between consecutive points in S_ℓ becomes equal to $TN^{2/3-1/2} = TN^{1/6}$. Since \bar{L}_k^N is a Bernoulli path and since $\alpha_\ell \leq \frac{3}{4}$, this implies that, on the complement of the righthand side of the previous display, for R and N sufficiently large we have

$$\inf_{xN^{-2/3} \in [-T,T]} \bar{L}_k^N(x) \geq \inf_{x \in \bigcup_{\ell=0}^{2^{-1} \log_2 N} S_\ell} \bar{L}_k^N(x) - TN^{1/6} > -\frac{3}{4}RN^{1/3} - TN^{1/6} > -RN^{1/3}.$$

Further, it holds that (for convenience defining $\mathbf{E}_{-1} = \Omega$, i.e., the entire space)

$$\bigcup_{\ell=0}^{\lceil \frac{1}{2} \log_2 N \rceil} \mathbf{E}_\ell^c = \bigcup_{\ell=0}^{\lceil \frac{1}{2} \log_2 N \rceil} (\mathbf{E}_{\ell-1} \cap \mathbf{E}_\ell^c).$$

Thus, since we have

$$\begin{aligned} & \mathbb{P} \left(\inf_{xN^{-2/3} \in [-T,T]} \bar{L}_k^N(x) < -RN^{1/3} \right) \\ & \leq \mathbb{P} \left(\inf_{xN^{-2/3} \in [-T,T]} \bar{L}_k^N(x) < -RN^{1/3} \mid \inf_{sN^{-2/3} \in [-U,U]} \bar{L}_{k-1}^N(s) > -\frac{1}{8}RN^{1/3} \right) \\ & \quad + \mathbb{P} \left(\inf_{sN^{-2/3} \in [-U,U]} \bar{L}_{k-1}^N(s) \leq -\frac{1}{8}RN^{1/3} \right) \end{aligned}$$

and the second term is bounded by $\frac{1}{3}\varepsilon$ by (9.7), it is enough to bound

$$\sum_{\ell=0}^{\frac{1}{2} \log_2 N} \mathbb{P} \left(\mathbf{E}_{\ell-1} \cap \mathbf{E}_{\ell}^c \mid \inf_{xN^{-2/3} \in [-U, U]} \bar{L}_{k-1}^N(x) > -\frac{1}{8}RN^{1/3} \right).$$

We have bounded $\mathbb{P}(\mathbf{E}_0^c \mid \inf_{xN^{-2/3} \in [-U, U]} \bar{L}_{k-1}^N(x) > -\frac{1}{8}RN^{1/3})$ by ε above in (9.8). For the $\ell \geq 1$ terms, we observe that Lemma 9.6 (with R there equal to $\alpha_{\ell-1}R$, $K = (\alpha_{\ell} - \alpha_{\ell-1})R$, and $\delta = \alpha_{\ell-1} - \frac{1}{8} > 0$ uniformly over ℓ) implies that there exists N_0 independent of ℓ such that, for $N > N_0$, the ℓ^{th} term is upper bounded (using a union bound over the $2^{\ell+1}$ points in S_{ℓ} and noting that $\alpha_{\ell} - \alpha_{\ell-1} = \delta 2^{-\ell/4}$ and the separation between points in S_{ℓ} is $2^{-\ell}$) by

$$2^{\ell+1} \cdot C \exp \left(-c(\delta 2^{-\ell/4} R)^2 / 2^{-\ell} \right) = 2^{\ell+1} \cdot C \exp(-c\delta^2 2^{\ell/2} R^2).$$

Summing this from $\ell = 1$ to ∞ yields a bound of $C \exp(-c\delta^2 R^2)$, which can be made smaller than ε by raising R further if required. Relabeling ε completes the proof. \square

9.3. The k^{th} curve cannot be uniformly too low on an interval.

Proof of Lemma 9.5. The idea of the proof is the following. Under the event $\text{Low}_k^{[T, U]}(R_{\text{low}})$ for a large enough interval $[T, U]$, it will be likely that the top $k-1$ curves fall, as the k^{th} curve that typically ‘‘supports’’ them is too far down. In particular, under this conditioning, the 1st curve will with reasonable probability be at a low position around say the midpoint of $[T, U]$. This event’s (unconditional) probability is known to be small using lower tail control from Assumption 2. Since the event we conditioned on turned an unlikely event into a likely one, it must have a low probability. The basic proof idea originates in [CH14], but is made more complicated here by the lack of stochastic monotonicity of the Hall-Littlewood Gibbs property. Now we give the details.

For R_1 a constant to be chosen next, let

$$\text{NotHigh}_1(x, R_1) := \left\{ \bar{L}_1^N(xN^{2/3}) + \lambda x^2 N^{1/3} \leq R_1 N^{1/3} \right\},$$

and define, for R_{low} to be set,

$$A_k^{[T, U]}(R_1) := \text{NotHigh}_1(T, R_1) \cap \text{NotHigh}_1(U, R_1) \cap \text{Low}_k^{[T, U]}(R_{\text{low}}). \quad (9.9)$$

Now by Assumption 2, there exist $R_1 = R_1(\varepsilon)$ and $N_0 = N_0(T, U, \varepsilon)$ large enough such that, for all U and for $N \geq N_0$,

$$\mathbb{P} \left(\text{NotHigh}_1(T, R_1)^c \cup \text{NotHigh}_1(U, R_1)^c \right) \leq \frac{1}{2}\varepsilon; \quad (9.10)$$

note that R_1 can be set independently of U . We set R_1 to be such a value for the remainder of the proof.

Next let $\mathbf{B} = (B_1, \dots, B_{k-1})$ be a collection of $k-1$ independent Bernoulli random walk bridges, the i^{th} one having endpoints

$$u_i = (TN^{2/3}, L_i^N(TN^{2/3})) \quad \text{and} \quad v_i = (UN^{2/3}, L_i^N(UN^{2/3})). \quad (9.11)$$

Note that these points are all upper bounded by $pTN^{2/3} - \lambda T^2 N^{1/3} + R_1 N^{1/3}$ and $pUN^{2/3} - \lambda U^2 N^{1/3} + R_1 N^{1/3}$, respectively, on $\text{NotHigh}_1(T, R_1) \cap \text{NotHigh}_1(U, R_1)$.

Let $\text{Sep}_{k-2}^N(\delta, \{T, U\}, \mathbf{L}^N)$ be as in (9.1). By hypothesis we know there exists $\delta = \delta(T, U, \varepsilon, k)$ such that

$$\mathbb{P} \left(\text{Sep}_{k-2}^N(\delta, \{T, U\}, \mathbf{L}^N)^c \right) \leq \frac{1}{2}\varepsilon. \quad (9.12)$$

Also let $R_{k-1} = R_{k-1}(T, U, \varepsilon, k)$ be such that, with

$$\text{BdyCtrl}_{k-1}(R_{k-1}) := \left\{ \min_{xN^{-2/3} \in \{T, U\}} \bar{L}_{k-1}^N(x) \geq -R_{k-1}N^{1/3} \right\},$$

it holds that

$$\mathbb{P}(\text{BdyCtrl}_{k-1}(R_{k-1})^c) \leq \frac{1}{2}\varepsilon, \quad (9.13)$$

which is possible by the hypothesis of Lemma 9.5 that we are working under.

We now set $R_{\text{low}} = R_{k-1} + U$ in the definition (9.9) of $\mathbf{A}_k^{[T, U]}(R_1)$. Also let $C_N(T, U)$ be the midpoint of the line joining the upper bounds on u_1 and v_1 mentioned above; more precisely, it is given by

$$\begin{aligned} C_N(T, U) &:= p \cdot \frac{1}{2}(T + U)N^{2/3} - \frac{1}{2}\lambda(T^2 + U^2)N^{1/3} + R_1N^{1/3} \\ &= p \cdot \frac{1}{2}(T + U)N^{2/3} - \frac{1}{4}\lambda(T + U)^2N^{1/3} - \frac{1}{4}\lambda(U - T)^2N^{1/3} + R_1N^{1/3}. \end{aligned} \quad (9.14)$$

Let $\mathcal{F} = \mathcal{F}_{\text{ext}}(k-1, \llbracket TN^{2/3}, UN^{2/3} \rrbracket, \mathbf{L}^N)$ be as in Definition 3.14, i.e., the σ -algebra generated by $\{L_i^N(x) : (i, x) \notin \llbracket 1, k-1 \rrbracket \times \llbracket TN^{2/3} + 1, UN^{2/3} - 1 \rrbracket\}$. Note that $\mathbf{A}_k^{[T, U]}(R_1)$, $\text{BdyCtrl}_{k-1}(R_{k-1})$, and $\text{Sep}_{k-2}^N(\delta) := \text{Sep}_{k-2}^N(\delta, \{T, U\}, \mathbf{L}^N)$ are \mathcal{F} -measurable. For a process $X : \mathbb{R} \rightarrow \mathbb{R}$, define the event $\text{UpTail}(U, X)$ by

$$\text{UpTail}(U, X) := \left\{ X\left(\frac{1}{2}(T + U)N^{2/3}\right) \geq C_N(T, U) + \frac{1}{8}\lambda(U - T)^2N^{1/3} \right\}, \quad (9.15)$$

and recall the notational convention from Remark 6.16. Then, by the previous bounds (9.12) and (9.13) on $\mathbb{P}(\text{Sep}_{k-2}^N(\delta)^c)$ and $\mathbb{P}(\text{BdyCtrl}_{k-1}(R_{k-1})^c)$, respectively, and the Hall-Littlewood Gibbs property,

$$\begin{aligned} &\mathbb{P}\left(\text{UpTail}(U, L_1^N) \mid \mathbf{A}_k^{[T, U]}(R_1)\right) \\ &\leq \mathbb{P}\left(\text{UpTail}(U, L_1^N), \text{Sep}_{k-2}^N(\delta), \text{BdyCtrl}_{k-1}(R_{k-1}) \mid \mathbf{A}_k^{[T, U]}(R_1)\right) \\ &\quad + \frac{\varepsilon}{\mathbb{P}(\mathbf{A}_k^{[T, U]}(R_1))} \\ &\leq \mathbb{E}\left[\mathbb{E}_{\mathcal{F}}\left[\mathbb{1}_{\text{UpTail}(U, B_1)}W(\mathbf{B}, L_k^N) \mid \frac{\mathbb{1}_{\text{Sep}_{k-2}^N(\delta), \text{BdyCtrl}_{k-1}(R_{k-1})}}{\mathbb{E}_{\mathcal{F}}[W(\mathbf{B}, L_k^N)]} \mid \mathbf{A}_k^{[T, U]}(R_1)\right]\right] \\ &\quad + \frac{\varepsilon}{\mathbb{P}(\mathbf{A}_k^{[T, U]}(R_1))}, \end{aligned} \quad (9.16)$$

where recall from (9.11) that $\mathbf{B} = (B_1, \dots, B_{k-1})$ is a family of Bernoulli random walk bridges on $\llbracket TN^{2/3}, UN^{2/3} \rrbracket$, with B_i starting and ending at $L_i^N(TN^{2/3})$ and $L_i^N(UN^{2/3})$, respectively, for $i \in \llbracket 1, k-1 \rrbracket$, and W is as in Definition 3.16.

For an interval I , define the event

$$\text{NonInt}_{k-2}(I, \mathbf{B}) := \left\{ B_i(x) \geq B_{i+1}(x) \text{ for all } i \in \llbracket 1, k-2 \rrbracket, x \in I \right\}. \quad (9.17)$$

In the rest of the proof we adopt the shorthand $\text{NonInt}_{k-2}(\mathbf{B}) = \text{NonInt}_{k-2}(\llbracket TN^{2/3}, UN^{2/3} \rrbracket, \mathbf{B})$. Since $W(\mathbf{B}) = 0$ on $\text{NonInt}_{k-2}(\mathbf{B})^c$, it follows that the ratio of \mathcal{F} -conditional probabilities in (9.16) equals

$$\frac{\mathbb{E}_{\mathcal{F}}\left[\mathbb{1}_{\text{UpTail}(U, B_1)}W(\mathbf{B}) \mid \text{NonInt}_{k-2}(\mathbf{B})\right]}{\mathbb{E}_{\mathcal{F}}\left[W(\mathbf{B}) \mid \text{NonInt}_{k-2}(\mathbf{B})\right]}. \quad (9.18)$$

Controlling the denominator. Next, we lower bound the denominator of (9.18) on the event $\text{Sep}_{k-2}^N(\delta) \cap \text{BdyCtrl}_{k-1}(R_{k-1})$ and conditionally on $\mathbf{A}_k^{[T,U]}(R_1)$. We claim that there exists $\rho = \rho(\delta, T, U, k) > 0$ such that, on $\text{Sep}_{k-2}^N(\delta)$,

$$\mathbb{P}_{\mathcal{F}} \left(\min_{i=1, \dots, k-2} \inf_{xN^{-2/3} \in [T, U]} (B_i(x) - B_{i+1}(x)) \geq \rho N^{1/3} \mid \text{NonInt}_{k-2}(\mathbf{B}) \right) \geq \frac{1}{2}. \quad (9.19)$$

To see this, we first let $\alpha = \alpha(T, U, \delta, k) > 0$ be such that $\mathbb{P}_{\mathcal{F}}(\text{NonInt}_{k-2}(\mathbf{B})) \geq \alpha$ on $\text{Sep}_{k-2}^N(\delta)$; the existence of α uses that the separation of B_i from B_{i+1} at the endpoints of $TN^{2/3}$ and $UN^{2/3}$ is at least $\delta N^{1/3}$ on $\text{Sep}_{k-2}^N(\delta)$, and that $\text{NonInt}_{k-2}(\mathbf{B})$ holds if the fluctuation of each bridge is at most $\frac{1}{4}\delta N^{1/3}$ on the interval of size $(U - T)N^{2/3}$, which has positive probability, e.g., by convergence of (rescaled) \mathbf{B} to independent Brownian bridges with endpoint separation at least δ (see e.g., [DM21, Lemma 5.2]). Then, by a union bound and the independence of B_i we obtain

$$\begin{aligned} \mathbb{P}_{\mathcal{F}} \left(\min_{i=1, \dots, k-2} \inf_{xN^{-2/3} \in [T, U]} (B_i(x) - B_{i+1}(x)) < \rho N^{1/3} \mid \text{NonInt}_{k-2}(\mathbf{B}) \right) \\ \leq \sum_{i=1}^{k-2} \mathbb{P}_{\mathcal{F}} \left(\inf_{xN^{-2/3} \in [T, U]} (B_i(x) - B_{i+1}(x)) < \rho N^{1/3} \mid \text{NonInt}_{k-2}(\mathbf{B}) \right) \\ \leq \alpha^{-1} \sum_{i=1}^{k-2} \mathbb{P}_{\mathcal{F}} \left(0 \leq \inf_{xN^{-2/3} \in [T, U]} (B_i(x) - B_{i+1}(x)) < \rho N^{1/3} \right). \end{aligned}$$

This can be made smaller than $\frac{1}{2}$ for all large enough N by setting $\rho > 0$ small enough, depending on δ, T, U , and k (note that α depends on the same parameters); this can again be seen by the convergence of a rescaled version of \mathbf{B} to a collection of independent Brownian bridges with endpoint separation at least δ , and noting that the corresponding Brownian bridge probability can be made arbitrarily small by setting ρ correspondingly. Thus (9.19) has been proved.

Recall from Definition 3.16 the decomposition $W = W_{\text{int}} \cdot W_{\text{low}}$ with $W_{\text{low}} = W_{\text{low}}(B_{k-1}, L_k^N)$ being the weight associated to the lower boundary condition L_k^N and $W_{\text{int}} = W_{\text{int}}(\mathbf{B})$ being the weight associated to the interior interactions between the B_i . By Lemma 9.1, on the event in (9.19), and conditionally on $\text{NonInt}_{k-2}(\mathbf{B})$ (and so with conditional probability at least $\frac{1}{2}$),

$$W_{\text{int}}(\mathbf{B}) \geq (1 - q^{\rho N^{1/3}})^{(U-T)N^{2/3} \cdot (k-1)} \geq \frac{1}{2}$$

for large enough N (depending on $\rho, T - U$, and k , therefore on T, U, ε , and k). Further observe that, on $\mathbf{A}_k^{[T,U]}(R_1) \cap \text{BdyCtrl}_{k-1}(R_{k-1})$, and with $\bar{B}_{k-1}(x) = B_{k-1}(x) - px$,

$$\min \left(\bar{B}_{k-1}(TN^{2/3}), \bar{B}_{k-1}(UN^{2/3}) \right) - \sup_{xN^{-2/3} \in [T, U]} \bar{L}_k^N = (-R_{k-1} + R_{\text{low}})N^{1/3} \geq UN^{1/3},$$

where recall R_{k-1} depends on U and $R_{\text{low}} = R_{k-1} + U$ was set earlier.

So it follows that B_{k-1} , with conditional probability (given $\text{NonInt}_{k-2}(\mathbf{B})$) at least $\frac{3}{4}$, for all U large enough, stays $\frac{1}{2}UN^{1/3}$ above L_k^N throughout the interval $[TN^{2/3}, UN^{2/3}]$ (e.g., again by using weak convergence to non-intersecting Brownian bridges and since $\frac{1}{2}U \gg U^{1/2}$ for such U), and, on that event, by Lemma 9.1,

$$W_{\text{low}}(B_{k-1}, L_k^N) \geq (1 - q^{\frac{1}{2}UN^{1/3}})^{(U-T)N^{2/3}} \geq \frac{1}{2}$$

for large enough N (depending on U).

Thus we have that both $W_{\text{int}}(\mathbf{B}) \geq \frac{1}{2}$ and $W_{\text{low}}(B_{k-1}, L_k^N) \geq \frac{1}{2}$ on an event of conditional probability (given $\text{NonInt}_{k-2}(\mathbf{B})$) at least $\frac{1}{4}$. So, on $\text{Sep}_{k-2}^N(\delta) \cap \text{BdyCtrl}_{k-1}(R_{k-1})$ and conditionally on $\mathbf{A}_k^{[T,U]}(R_1)$, we may lower bound $\mathbb{E}_{\mathcal{F}}[W(\mathbf{B}, L_k^N) \mid \text{NonInt}_{k-2}(\mathbf{B})]$ by $\frac{1}{2} \cdot \frac{1}{2} \cdot \frac{1}{4} = \frac{1}{16}$.

Bounding the conditional random walk bridge probability. Thus, and also using $W(\mathbf{B}, L_k^N) \leq 1$, we see that the first term in (9.16) is upper bounded by

$$16 \cdot \mathbb{E} \left[\mathbb{P}_{\mathcal{F}}(\text{UpTail}(U, B_1) \mid \text{NonInt}_{k-2}(\mathbf{B})) \mid \mathbf{A}_k^{[T,U]}(R_1) \right]. \quad (9.20)$$

Recall from (9.11) that B_i is a Bernoulli random walk bridge from $(TN^{2/3}, L_i^N(TN^{2/3}))$ to $(UN^{2/3}, L_i^N(UN^{2/3}))$ and that, on $\mathbf{A}_k^{[T,U]}(R_1)$, $\bar{L}_1^N(TN^{2/3}) \leq (-\lambda T^2 + R_1)N^{1/3}$ and $\bar{L}_1^N(UN^{2/3}) \leq (-\lambda U^2 + R_1)N^{1/3}$. Let $\tilde{\mathbf{B}} = (\tilde{B}_1, \dots, \tilde{B}_{k-1})$ be a collection of $k-1$ Bernoulli random walk bridges with \tilde{B}_i from

$$\begin{aligned} & (TN^{2/3}, pTN^{2/3} + (-\lambda T^2 + R_1 + (k-i)U^{1/2})N^{1/3}) \quad \text{to} \\ & (UN^{2/3}, pUN^{2/3} + (-\lambda U^2 + R_1 + (k-i)U^{1/2})N^{1/3}). \end{aligned}$$

Since these endpoints are higher than the corresponding endpoints of \mathbf{B} , it holds that the law of $\tilde{\mathbf{B}}$ conditionally on $\text{NonInt}_{k-2}(\tilde{\mathbf{B}})$ stochastically dominates that of \mathbf{B} conditional on $\text{NonInt}_{k-2}(\mathbf{B})$ by Lemma 8.2. Thus it follows that (9.20) is upper bounded by (dropping the \mathcal{F} and the outer expectation since $\tilde{\mathbf{B}}$ does not have any dependence on data from \mathcal{F})

$$16 \cdot \mathbb{P} \left(\text{UpTail}(U, \tilde{B}_1) \mid \text{NonInt}_{k-2}(\tilde{\mathbf{B}}) \right).$$

Observe that there is an absolute constant $c > 0$ such that $\mathbb{P}(\text{NonInt}_{k-2}(\tilde{\mathbf{B}})) > c$ for all large enough U , since \tilde{B}_i are separated by order $U^{1/2}$ at their endpoints and the non-intersection is imposed on an interval of length $U - T$. Thus the previous display is upper bounded by

$$16c^{-1} \cdot \mathbb{P} \left(\text{UpTail}(U, \tilde{B}_1) \right). \quad (9.21)$$

Now we recall the definitions (9.14) of $C_N(T, U)$ as the midpoint of the line joining the points $(TN^{2/3}, pTN^{2/3} - \lambda T^2 N^{1/3} + R_1 N^{1/3})$ and $(UN^{2/3}, pUN^{2/3} - \lambda U^2 N^{1/3} + R_1 N^{1/3})$. It follows that

$$\mathbb{E} \left[\tilde{B}_1 \left(\frac{1}{2}(T+U)N^{2/3} \right) \right] \leq C_N(T, U) + (k-1)U^{1/2}N^{1/3}.$$

Thus, recalling the definition (9.15) of UpTail , the quantity (9.21) is upper bounded by

$$16c^{-1} \cdot \mathbb{P} \left(\tilde{B}_1 \left(\frac{1}{2}(T+U)N^{2/3} \right) \geq \mathbb{E} \left[\tilde{B}_1 \left(\frac{1}{2}(T+U)N^{2/3} \right) \right] - kU^{1/2}N^{1/3} + \frac{1}{8}(U-T)^2 N^{1/3} \right) \leq \varepsilon$$

for large enough U , the inequality using upper bounds on Bernoulli random walk bridge one-point tails (Lemma 6.13).

Returning to L_1^N . Overall, returning to (9.16) and (9.18), we have shown that

$$\mathbb{P} \left(\text{UpTail}(U, L_1^N) \mid \mathbf{A}_k^{[T,U]}(R_1) \right) \leq \varepsilon + \frac{\varepsilon}{\mathbb{P} \left(\mathbf{A}_k^{[T,U]}(R_1) \right)}.$$

We claim that $\mathbb{P}(\mathbf{A}_k^{[T,U]}(R_1)) < 3\varepsilon$. Otherwise, we would have that $\mathbb{P}(\mathbf{A}_k^{[T,U]}(R_1)) \geq 3\varepsilon$, which would imply that $\mathbb{P}(\text{UpTail}(U, L_1^N) \mid \mathbf{A}_k^{[T,U]}(R_1)) \leq \varepsilon + \frac{1}{3} \leq \frac{1}{2}$ for large enough U . This would further imply (recalling the definition (9.15) of UpTail) that

$$\begin{aligned} & \mathbb{P} \left(\mathbf{A}_k^{[T,U]}(R_1) \right) \\ & \leq \left(\mathbb{P} \left(\text{UpTail}(U, L_1^N)^c \mid \mathbf{A}_k^{[T,U]}(R_1) \right) \right)^{-1} \cdot \mathbb{P} \left(\text{UpTail}(U, L_1^N)^c \right) \\ & \leq \left(1 - \frac{1}{2} \right)^{-1} \mathbb{P} \left(\text{UpTail}(U, L_1^N)^c \right) \\ & = 2 \cdot \mathbb{P} \left(L_1^N \left(\frac{1}{2}(T+U)N^{2/3} \right) - \frac{1}{2}p(T+U)N^{2/3} < \left(-\frac{1}{4}\lambda(T+U)^2 - \frac{1}{8}\lambda(U-T)^2 + R_1 \right) N^{1/3} \right). \end{aligned}$$

By the one-point tightness of L_1^N (Assumption 2), for large enough U (depending on R_1 and T) and all $N > N_0$ (for a N_0 depending on U), this is upper bounded by ε , which is a contradiction; recall here the important observation made after (9.10) that R_1 was chosen independently of U . This establishes that $\mathbb{P}(\mathbf{A}_k^{[T,U]}(R_1)) < 3\varepsilon$.

With these choices of R_1 , R_{low} , U , and N_0 , and recalling the definition (9.9) of $\mathbf{A}_k^{[T,U]}(R_1)$ and the bound (9.10) on the probability of NotHigh_1^c , we see that, for $N \geq N_0$,

$$\mathbb{P}\left(\text{Low}_k^{[T,U]}(R_{\text{low}})\right) \leq \mathbb{P}\left(\mathbf{A}_k^{[T,U]}(R_1)\right) + \mathbb{P}\left(\text{NotHigh}_1(T, R_1)^c \cup \text{NotHigh}(U, R_1)^c\right) \leq 4\varepsilon.$$

Relabeling ε completes the proof. \square

9.4. The k^{th} curve cannot be too low at a given point. Here we prove Lemma 9.6. We will need a version of the Hall-Littlewood Gibbs property on a random interval. As we have seen, random intervals defined by information outside the interval satisfy a strong Gibbs property (Definition 6.1 and Proposition 6.2), analogous to a strong Markov property, in which case the behavior inside the interval under the resampling is the same. Here, however, we will need to resample on a random interval defined in a way that is dependent on the behavior of the process inside, and the description of the resampling is recorded here.

Let $a, b \in \mathbb{Z}$ be integers, let $k \in \mathbb{N}$ be a natural number, let $\Lambda \subseteq \mathbb{Z}$ be an interval containing $\llbracket a, b \rrbracket$, and let $\mathbf{L} : \mathbb{N} \times \Lambda \rightarrow \mathbb{Z}$ be a discrete line ensemble (Definition 3.6) with the Hall-Littlewood Gibbs property (Assumption 1). Let $p \in (-1, 0)$ and recall the notation $\bar{L}_k(x) = L_k(x) - px$ (note that we do not assume \mathbf{L} satisfies Assumption 2, so p need not be as in that assumption). Let $m \in \mathbb{R}$ and $t \in \llbracket a, b \rrbracket$, and define

$$a' := \max\{x \in \llbracket a, t \rrbracket : \bar{L}_k(x) \geq m\} \quad \text{and} \quad b' := \min\{x \in \llbracket t, b \rrbracket : \bar{L}_k(x) \geq m\}. \quad (9.22)$$

Next define the σ -algebra

$$\mathcal{F}_{\text{ext}}(\{k\}, \llbracket a', b' \rrbracket, \mathbf{L}) := \left\{ A \cap \{a' = x, b' = y\} : A \in \mathcal{F}_{\text{ext}}(\{k\}, \llbracket x, y \rrbracket, \mathbf{L}), x \in \llbracket a, t \rrbracket, y \in \llbracket t, b \rrbracket \right\}.$$

For any c, d , let $\mathbb{E}^{x,y,\llbracket c,d \rrbracket}$ be the expectation operator associated to a probability measure $\mathbb{P}^{x,y,\llbracket c,d \rrbracket}$ under which B is distributed as a Bernoulli random walk bridge from (c, x) to (d, y) , and let $\bar{B}(x) := B(x) - px$. Finally, let $\Omega = \{(\ell, c, d) : c \in \llbracket a, t \rrbracket, b \in \llbracket t, d \rrbracket, \ell \in \Omega_{\llbracket c,d \rrbracket}\}$, where $\Omega_{\llbracket c,d \rrbracket} := \{f : \llbracket c, d \rrbracket \rightarrow \mathbb{Z}, f \text{ a Bernoulli path}\}$ is the space of Bernoulli paths (Definition 2.9) on $\llbracket c, d \rrbracket$. We will give the proof of the following lemma in Appendix B.

Lemma 9.7. *Let $k \in \mathbb{N}$, let $\Lambda \subseteq \mathbb{Z}$ be an interval, and let $\mathbf{L} : \mathbb{N} \times \Lambda \rightarrow \mathbb{Z}$ be a discrete line ensemble satisfying Assumption 1, and let $p \in (-1, 0)$. Let $m \in \mathbb{R}$, $\llbracket a, b \rrbracket \subseteq \mathbb{Z}$, and $t \in \llbracket a, b \rrbracket$, and let a' and b' be as in (9.22). Let $\mathcal{F} = \mathcal{F}_{\text{ext}}(\{k\}, \llbracket a', b' \rrbracket, \mathbf{L})$. For any measurable function $F : \Omega \rightarrow \mathbb{R}$, it holds that*

$$\begin{aligned} & \mathbb{E}_{\mathcal{F}} [F(L_k|_{\llbracket a', b' \rrbracket}, a', b')] \\ &= Z^{-1} \cdot \mathbb{E}^{z_1, z_2, \llbracket a', b' \rrbracket} [F(B, a', b') W(B, L_{k-1}, L_{k+1}, \llbracket a', b' \rrbracket) \mid \bar{B}(s) < m \forall s \in \llbracket a' + 1, b' - 1 \rrbracket], \end{aligned}$$

where $z_1 = L_k(a')$, $z_2 = L_k(b')$, and $Z = \mathbb{E}^{z_1, z_2, \llbracket a', b' \rrbracket} [W(B, L_{k-1}, L_{k+1}, \llbracket a', b' \rrbracket) \mid \bar{B}(s) < m \forall s \in \llbracket a' + 1, b' - 1 \rrbracket]$.

Proof of Lemma 9.6. For notational convenience, we prove the statement with $2K$ in place of K . On the event

$$\mathbb{E}(t, a, b) := \left\{ \left(\bar{L}_k^N(tN^{2/3}) \leq -(R + 2K)N^{1/3}, \right. \right. \\ \left. \left. \left(\sup_{xN^{-2/3} \in \llbracket a, t \rrbracket} \bar{L}_k^N(x) \right) \wedge \left(\sup_{xN^{-2/3} \in \llbracket t, b \rrbracket} \bar{L}_k^N(x) \right) \geq -RN^{1/3} \right\},$$

define the random times a' and b' by

$$\begin{aligned} a' &:= N^{-2/3} \cdot \max \left\{ x \in \llbracket aN^{2/3}, tN^{2/3} \rrbracket : \bar{L}_k^N(x) \geq -(R+K)N^{1/3} \right\} \quad \text{and} \\ b' &:= N^{-2/3} \cdot \min \left\{ x \in \llbracket tN^{2/3}, bN^{2/3} \rrbracket : \bar{L}_k^N(x) \geq -(R+K)N^{1/3} \right\}. \end{aligned}$$

Since L_k^N is a Bernoulli path, it follows that $\bar{L}_k^N(a'N^{2/3}), \bar{L}_k^N(b'N^{2/3}) = \lceil -(R+K)N^{1/3} \rceil$ on $\mathbf{E}(t, a, b)$; in the remainder of the proof, we ignore the ceiling and assume that $\bar{L}_k^N(a'N^{2/3}) = \bar{L}_k^N(b'N^{2/3}) = -(R+K)N^{1/3}$.

Let B be a Bernoulli random walk bridge from

$$(a'N^{2/3}, pa'N^{2/3} - (R+K)N^{1/3}) \quad \text{to} \quad (b'N^{2/3}, pb'N^{2/3} - (R+K)N^{1/3})$$

conditioned to remain strictly below the line $px - (R+K)N^{1/3}$ on $[a'N^{2/3}+1, b'N^{2/3}-1]$. Let $\bar{B}(x) := B(x) - px$. By Lemma 9.7, conditional on the σ -algebra $\mathcal{F} := \mathcal{F}_{\text{ext}}(\{k\}, \llbracket a'N^{2/3}, b'N^{2/3} \rrbracket, \mathbf{L}^N)$, the law of $L_k^N|_{[a'N^{2/3}, b'N^{2/3}]}$ is that of B reweighted by the Radon-Nikodym derivative proportional to $W(B, L_{k-1}^N, L_{k+1}^N) = W_{\text{up}}(B, L_{k-1}^N)W_{\text{low}}(B, L_{k+1}^N)$ (recall from Definition 3.15), where we drop the interval $\llbracket a'N^{2/3}, b'N^{2/3} \rrbracket$ on which W is evaluated from the notation. Then, by the Hall-Littlewood Gibbs property, the definitions of a' and b' , and since $W_{\text{up}}(B, L_{k-1}^N) \leq 1$, with $Z = \mathbb{E}_{\mathcal{F}}[W(B, L_{k-1}^N, L_{k+1}^N)]$,

$$\begin{aligned} &\mathbb{P} \left(\mathbf{E}(t, a, b) \mid \inf_{xN^{-2/3} \in [a, b]} \bar{L}_{k-1}^N(x) > -(R-\delta)N^{1/3} \right) \\ &= \mathbb{E} \left[\mathbb{E}_{\mathcal{F}} \left[\mathbb{1}_{\bar{B}(tN^{2/3}) \leq -(R+2K)N^{1/3}} W(B, L_{k-1}^N, L_{k+1}^N) Z^{-1} \right] \mid \inf_{xN^{-2/3} \in [a, b]} \bar{L}_{k-1}^N(x) > -(R-\delta)N^{1/3} \right] \\ &\leq \mathbb{E} \left[\mathbb{E}_{\mathcal{F}} \left[\mathbb{1}_{\bar{B}(tN^{2/3}) \leq -(R+2K)N^{1/3}} W_{\text{low}}(B, L_{k+1}^N) Z^{-1} \right] \mid \inf_{xN^{-2/3} \in [a, b]} \bar{L}_{k-1}^N(x) > -(R-\delta)N^{1/3} \right]. \end{aligned}$$

Since $\bar{L}_{k-1}^N \geq -(R-\delta)N^{1/3}$ throughout the interval $[a'N^{2/3}, b'N^{2/3}]$ and $\bar{B} \leq -(R+K)N^{1/3}$ on the interval $[a'N^{2/3}, b'N^{2/3}]$, it follows that $W_{\text{up}}(B, L_{k-1}^N) \geq (1 - q^{(\delta+K)N^{1/3}})^{(b-a)N^{2/3}} \geq \frac{1}{2}$ for all $N > N_0$, for an N_0 which can be taken to be increasing in $b-a$, decreasing in δ , and independent of K as well as k . Thus $Z \geq \frac{1}{2} \mathbb{E}_{\mathcal{F}}[W_{\text{low}}(B, L_{k+1}^N)]$, which implies that the previous display is upper bounded by

$$\begin{aligned} &2 \cdot \mathbb{E} \left[\frac{\mathbb{E}_{\mathcal{F}} \left[\mathbb{1}_{\bar{B}(tN^{2/3}) \leq -(R+2K)N^{1/3}} W_{\text{low}}(B, L_{k+1}^N) \right]}{\mathbb{E}_{\mathcal{F}} [W_{\text{low}}(B, L_{k+1}^N)]} \mid \inf_{xN^{-2/3} \in [a, b]} \bar{L}_{k-1}^N(x) > -(R-\delta)N^{1/3} \right] \\ &= 2 \cdot \mathbb{E} \left[\frac{\mathbb{E}_{\mathcal{F}} [W_{\text{low}}(B, L_{k+1}^N) \mid \bar{B}(tN^{2/3}) \leq -(R+2K)N^{1/3}]}{\mathbb{E}_{\mathcal{F}} [W_{\text{low}}(B, L_{k+1}^N)]} \right. \\ &\quad \left. \times \mathbb{P}_{\mathcal{F}} \left(\bar{B}(tN^{2/3}) \leq -(R+2K)N^{1/3} \right) \mid \inf_{xN^{-2/3} \in [a, b]} \bar{L}_{k-1}^N(x) > -(R-\delta)N^{1/3} \right]. \end{aligned}$$

By weak monotonicity (Corollary 8.5) and noting that the conditional probability factor is deterministic, the previous display is upper bounded by

$$2c(q)^{-1} \cdot \mathbb{P} \left(\bar{B}(tN^{2/3}) \leq -(R+2K)N^{1/3} \right).$$

This probability is in turn upper bounded by $C \exp(-cK^2/(b'-a')) \leq C \exp(-cK^2/(b-a))$. This follows by stochastic monotonicity of Bernoulli random walk bridges (Lemma 8.2): $B(tN^{2/3}) \geq B'(tN^{2/3})$ where B' is a Bernoulli random walk bridge from $(a'N^{2/3}, pa'N^{2/3} - (R + \frac{3}{2}K)N^{1/3})$ to

$(b'N^{2/3}, pb'N^{2/3} - (R + \frac{3}{2}K)N^{1/3})$ (i.e., lowered endpoints) conditioned on staying below $px - (R + K)N^{1/3}$, so we only need to bound

$$\mathbb{P} \left(\tilde{B}(tN^{2/3}) \leq -(R + 2K)N^{1/3} \mid \sup_{xN^{-2/3} \in [a', b']} \tilde{B}(x) - px \leq -(R + K)N^{1/3} \right),$$

where \tilde{B} is a Bernoulli random walk bridge with the same endpoints as B' . There exists $\eta = \eta(b - a) > 0$ such that the probability of the event being conditioned on is at least η , and η is decreasing in $b - a$ (the fact that η can be taken independent of K uses that $K \geq 1$); in particular, the bound is uniform in N . The probability of $\tilde{B}(tN^{2/3}) \leq -(R + 2K)N^{1/3}$ is at most $\tilde{C} \exp(-cK^2/(b - a))$ by Lemma 6.13. This completes the proof with $C = \tilde{C}\eta^{-1}$. \square

10. UNIFORM SEPARATION OF CURVES

In this section we prove Proposition 9.4 which, recall, assumes control on the lower tail of the k^{th} curve and on separation between the first $k - 1$ curves and obtains control on the separation between the first k curves. In this section we again assume \mathbf{L}^N satisfies Assumptions 1 and 2 without further explicit mention.

10.1. Control on the lower curve. We will need some control over the k^{th} curve, in particular that it does not increase too quickly, at least at some random location. For this we prove the following deterministic statement about continuous functions whose range is controlled.

Lemma 10.1. *Let $T > 0$, $\delta \in (0, \frac{1}{30}T)$, and $f : [0, T] \rightarrow \mathbb{R}$ be continuous. Suppose $M > 0$ is such that $\sup_{x, y \in [0, T]} |f(x) - f(y)| \leq M$. Then, with $P = 3MT^{-1}$, there exists $U \in [0, \frac{1}{2}T]$ such that*

$$f(x) \leq f(U) + P(x - U) \text{ for } x \in [U, U + \delta].$$

Proof. Let $f^-(x) = f(x) - Px$. Next for $i = 0, 1, \dots$, let $I_i = [i \cdot 2\delta, (i + 1)2\delta]$, $J_i = I_i + \delta = [(i + \frac{1}{2})2\delta, (i + \frac{3}{2})2\delta]$, $x_i^I = \operatorname{argmax}_{I_i} f^-$ and $x_i^J = \operatorname{argmax}_{J_i} f^-$ (taking the smallest in the case of multiple maximizers).

We claim that there is an i such that $I_i \subseteq [0, \frac{1}{2}T]$, $J_i \subseteq [0, \frac{1}{2}T]$, and at least one of $x_i^I \in [\inf I_i, \inf I_i + \delta]$ or $x_i^J \in [\inf J_i, \inf J_i + \delta]$ holds, i.e., the maximizer lies in the left half of the interval. Observe that this would complete the proof, since the length of the second half of I_i or J_i is δ , and for such an i , by taking $U = x_i^I$ (if it is the I_i case), it holds for $x \in [U, \sup I_i]$ that $f(x) - Px \leq f(x_i^I) - P(x_i^I)$, and similarly for the J_i case.

Suppose our claim does not hold. Let i_{\max} be the largest i such that $J_i \subseteq [0, \frac{1}{2}T]$. Under our contrapositive hypothesis, $x_i^J \in [(i + 1)2\delta, (i + \frac{3}{2})2\delta]$ and $x_i^I \in [(i + \frac{1}{2})2\delta, (i + 1)2\delta]$ for each $i \in [0, i_{\max}]$. This implies that $x_i^I \in J_i$ and $x_i^J \in I_{i+1}$ for each i , so for each i ,

$$f^-(x_i^J) \geq f^-(x_i^I) \geq f^-(x_{i-1}^J).$$

Iterating, this gives that

$$f^-(x_{i_{\max}}^J) \geq f^-(x_0^J) \implies f(x_{i_{\max}}^J) \geq f(x_0^J) + P(x_{i_{\max}}^J - x_0^J).$$

This contradicts the fact that $\sup_{x, y \in [0, T]} |f(x) - f(y)| \leq M$ since $x_{i_{\max}}^J \geq \frac{1}{2}T - 2\delta$, $x_0^J \leq 3\delta$, and $P = 3M/T$ (we implicitly use that $5\delta \leq \frac{1}{6}T$). This completes the proof. \square

To have control on the range of L_k^N as needed to apply Lemma 10.1, we need control on the upper tail of L_k^N over an interval in addition to the lower tail control we have assumed. This uniform upper tail control is provided by the following bound due to [CD18] on the upper tail of L_1^N , and the fact that the curves in \mathbf{L}^N are ordered. Recall the notation $\bar{L}_j^N(x) = L_j^N(x) - px$.

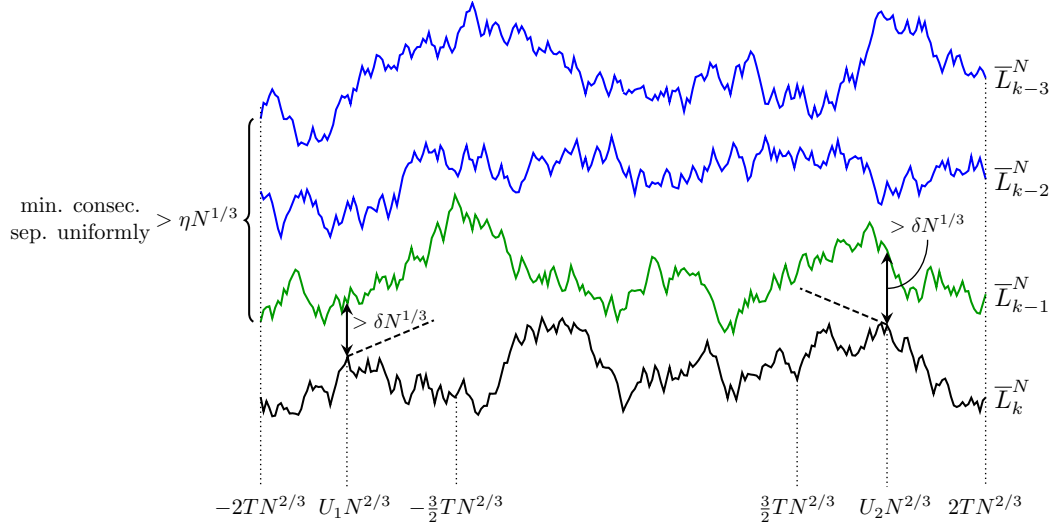


FIGURE 18. A depiction of the setup for Lemma 10.3. The dashed slanted lines represent the lines of slope $\pm PN^{-1/3}$ upper bounding \bar{L}_k^N on two intervals of size $N^{2/3}$. Uniform separation between the blue curves holds with high probability by assumption, and the lemma yields random points U_1 and U_2 where separation between \bar{L}_{k-1}^N and \bar{L}_k^N holds.

Proposition 10.2 ([CD18, Lemma 5.2]). *Let $\varepsilon > 0$ and $T > 0$. There exist $N_0 = N_0(\varepsilon, T)$ and $M = M(\varepsilon, T)$ such that, for $N \geq N_0$,*

$$\mathbb{P} \left(\sup_{sN^{-2/3} \in [-T, T]} \bar{L}_1^N(s) \geq MN^{1/3} \right) \leq \varepsilon.$$

The following statement uses Lemma 10.1 to obtain separation between L_{k-1}^N and L_k^N at a single random point; see Figure 18. It will be proved in Section 10.2.

Lemma 10.3 (One-point separation). *Fix $k \in \mathbb{N}$ and $T \geq 2$, and let $\text{Sep}_{k-2}^N(\eta, [-3T, -T]) := \text{Sep}_{k-2}^N(\eta, [-3T, -T], \mathbf{L}^N)$ be as in (9.1) and similarly for $\text{Sep}_{k-2}^N(\eta, [T, 3T])$. Suppose for any $\varepsilon > 0$ there exist $M = M(T, k, \varepsilon)$ and $N_0 = N_0(k, T, \varepsilon)$ such that, for $N \geq N_0$,*

$$\mathbb{P} \left(\inf_{xN^{-2/3} \in [-2T, 2T]} \bar{L}_k^N(x) \geq -MN^{1/3} \right) \geq 1 - \varepsilon \quad (10.1)$$

and there exists $\eta = \eta(T, k, \varepsilon) > 0$ such that, for $N \geq N_0$,

$$\min \left\{ \mathbb{P} \left(\text{Sep}_{k-2}^N(\eta, [-3T, -T]) \right), \mathbb{P} \left(\text{Sep}_{k-2}^N(\eta, [T, 3T]) \right) \right\} \geq 1 - \varepsilon. \quad (10.2)$$

Now fix any $\varepsilon > 0$. There exists $P = P(k, T, \varepsilon)$, $\delta = \delta(k, T, \varepsilon) > 0$, and $N_0 = N_0(k, T, \varepsilon)$ such that the following holds for $N > N_0$. With probability at least $1 - \varepsilon$, there exist random L_k^N -measurable points $U_1 \in [-2T, -\frac{3}{2}T]$ and $U_2 \in [\frac{3}{2}T, 2T]$ such that $L_{k-1}^N(U_i N^{2/3}) > L_k^N(U_i N^{2/3}) + \delta N^{1/3}$ for $i = 1, 2$, and

$$\begin{aligned} \bar{L}_k^N(x) &\leq \bar{L}_k^N(U_1 N^{2/3}) + (x - U_1 N^{2/3})PN^{-1/3} && \text{for } xN^{-2/3} \in [U_1, U_1 + 1], \\ \bar{L}_k^N(x) &\leq \bar{L}_k^N(U_2 N^{2/3}) + (U_2 N^{2/3} - x)PN^{-1/3} && \text{for } xN^{-2/3} \in [U_2 - 1, U_2]. \end{aligned}$$

Note that the range of L_k^N is of order $N^{1/3}$ and the interval size is of order $N^{2/3}$, so that the quantity $3MT^{-1}$ in Lemma 10.1 is of order $N^{-1/3}$; this is the source of the $N^{-1/3}$ factors in the previous display.

Lemma 10.3 is the main step in the proof of Proposition 9.4 on uniform separation between these curves. A second technical ingredient that will be needed is an estimate about uniform separation for a Bernoulli random walk bridge, which we state next. As its proof is fairly straightforward, it will be proved in Appendix B.

Lemma 10.4 (Random walk uniform separation). *Fix M, p , and $T \geq 2$. Let $U_1 \in [-2T, -\frac{3}{2}T]$ and $U_2 \in [\frac{3}{2}T, 2T]$. Let B^{RW} be a Bernoulli random walk bridge from $(U_1 N^{2/3}, z_1)$ to $(U_2 N^{2/3}, z_2)$, for some $z_i \in \mathbb{Z}$ such that $z_i - pU_i N^{2/3} \in [-MN^{1/3}, MN^{1/3}]$ for $i \in \{1, 2\}$; B^{Br} be a Brownian bridge of variance $p(1-p)$ with the same endpoints; and $f : [U_1 N^{2/3}, U_2 N^{2/3}] \rightarrow \mathbb{R}$ be a function with $f(U_i N^{2/3}) \leq z_i$ for $i \in \{1, 2\}$. Let $\{B^{\text{Br}} \geq f\}$ denote $\{B^{\text{Br}}(x) \geq f(x) \forall x \in [U_1 N^{2/3}, U_2 N^{2/3}]\}$ (and analogously for $\{B^{\text{RW}} \geq f\}$) and suppose, for some $\omega, \rho > 0$, that*

$$\mathbb{P}\left(B^{\text{Br}} \geq f + \omega N^{1/3}\right) \geq \rho.$$

Then for any $\varepsilon > 0$ there exists $\delta = \delta(\varepsilon, \rho, M, p, \omega, T) > 0$ such that

$$\mathbb{P}\left(\inf_{x \in [-TN^{2/3}, TN^{2/3}]} (B^{\text{RW}}(x) - f(x)) \leq \delta N^{1/3} \mid B^{\text{RW}} \geq f\right) \leq \varepsilon.$$

We give the proof of Proposition 9.4 assuming the previous two statements now. The proof will involve an event Fav consisting of favorable conditions on \mathbf{L}^N . We point out that a different event with the same name was used in the proof of Corollary 6.15, and in fact we will use the same name for a number of different events in upcoming proofs. The name will refer to a single event locally within each proof, however, and so should not cause confusion.

Proof of Proposition 9.4. By Lemma 10.3, using (9.3), there exists $P = P(\varepsilon, T, k)$ and $\eta = \eta(\varepsilon, T, k) > 0$ such that with probability at least $1 - \varepsilon$ there exist random L_k^N -measurable $U_1 \in [-2T, -\frac{3}{2}T]$ and $U_2 \in [\frac{3}{2}T, 2T]$ such that $L_{k-1}^N(U_i N^{2/3}) > L_k^N(U_i N^{2/3}) + \eta N^{1/3}$ for $i = 1, 2$ and

$$\begin{aligned} \bar{L}_k^N(x) &\leq \bar{L}_k^N(U_1 N^{2/3}) + (x - U_1 N^{2/3})PN^{-1/3} \quad \text{for } xN^{-2/3} \in [U_1, U_1 + 1], \quad \text{and} \\ \bar{L}_k^N(x) &\leq \bar{L}_k^N(U_2 N^{2/3}) + (U_2 N^{2/3} - x)PN^{-1/3} \quad \text{for } xN^{-2/3} \in [U_2 - 1, U_2]. \end{aligned} \quad (10.3)$$

By (9.3), after decreasing $\eta > 0$ if necessary (and dropping \mathbf{L}^N from the notation of Sep_{k-2}^N), we have that

$$\mathbb{P}(\text{Sep}_{k-2}^N(\eta, [-2T, 2T])^c) \leq \varepsilon. \quad (10.4)$$

Let $\delta \in (0, \eta)$ be a real number, to be set precisely later, but for now we will use that $\delta < \eta$. It clearly holds using (10.4) that, since $\delta < \eta$,

$$\mathbb{P}(\text{Sep}_{k-1}^N(\delta, [-T, T])^c) \leq \mathbb{P}\left(\inf_{xN^{-2/3} \in [-T, T]} (L_{k-1}^N(x) - L_k^N(x)) \leq \delta N^{1/3}\right) + \varepsilon. \quad (10.5)$$

Let $\mathcal{F} = \mathcal{F}_{\text{ext}}(k-1, \llbracket U_1 N^{2/3}, U_2 N^{2/3} \rrbracket)$ be as in Definition 3.14, i.e., the σ -algebra generated by $\{L_i^N(x) : (i, x) \notin \llbracket 1, k-1 \rrbracket \times \llbracket U_1 N^{2/3} + 1, U_2 N^{2/3} - 1 \rrbracket\}$. Recall that U_i are L_k^N -measurable. Define the \mathcal{F} -measurable favourable event Fav by

$$\begin{aligned} \text{Fav} := &\left\{ \min_{i=1, \dots, k-1} \min_{xN^{-2/3} \in \{U_1, U_2\}} (L_i^N(x) - L_{i+1}^N(x)) > \eta N^{1/3} \right\} \\ &\cap \left\{ \sup_{xN^{-2/3} \in [-2T, 2T]} |\bar{L}_k^N(x)| \leq MN^{1/3} \right\}. \end{aligned}$$

By the definition of U_1 and U_2 and (10.4), the upper bound on the supremum (Proposition 10.2), and the upper bound on the lower tail (9.3), there exists $M = M(\varepsilon, k, T)$ such that $\mathbb{P}(\text{Fav}^c) \leq 3\varepsilon$. Let $\mathbf{B} = (B_1, \dots, B_{k-1})$ be a $(k-1)$ -tuple of independent Bernoulli random walk bridges, with B_i from

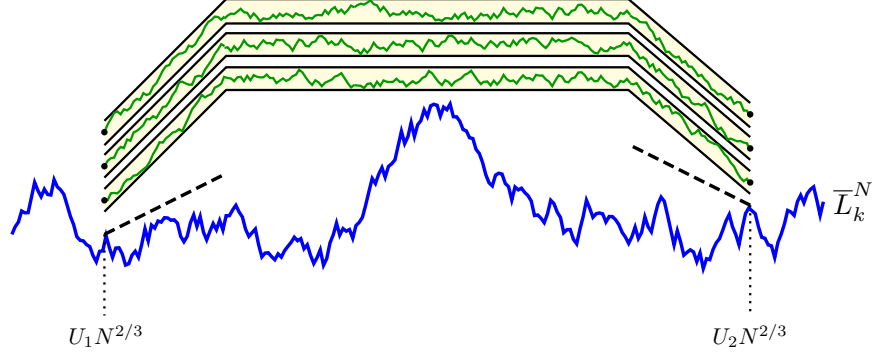


FIGURE 19. The event we consider (after subtracting off the affine shift of slope p) to obtain a lower bound on the denominator in (10.6). The dashed lines are the lines of slope $\pm PN^{-1/3}$ that upper bound L_k^N on $[U_i N^{1/3}, (U_i + 1)N^{2/3}]$ for $i = 1, 2$ respectively, and the separation between the points in black at $U_i N^{2/3}$ is at least $\eta N^{1/3}$, implying that the separation between the resampled curves is at least $\frac{1}{3}\eta N^{1/3}$ throughout $[U_1 N^{2/3}, U_2 N^{2/3}]$.

$(U_1 N^{2/3}, L_i^N(U_1 N^{2/3}))$ to $(U_2 N^{2/3}, L_i^N(U_2 N^{2/3}))$. Now $[U_1 N^{2/3}, U_2 N^{2/3}]$ forms a stopping domain (Definition 6.1) with respect to $(L_1^N, \dots, L_{k-1}^N)$; by the strong Gibbs property (Proposition 6.2) and the just recorded bound on $\mathbb{P}(\text{Fav}^c)$, the first term on the righthand side of (10.5) is upper bounded by (with W as in (3.9))

$$\begin{aligned} & \mathbb{E} \left[\frac{\mathbb{E}_{\mathcal{F}} \left[\mathbb{1}_{\inf_{xN^{-2/3} \in [-T, T]} (B_{k-1}(x) - L_k^N(x)) \leq \delta N^{1/3}} W(\mathbf{B}, L_k^N) \right]}{\mathbb{E}_{\mathcal{F}}[W(\mathbf{B}, L_k^N)]} \mathbb{1}_{\text{Fav}} \right] + 4\varepsilon \\ & \leq \mathbb{E} \left[\frac{\mathbb{E}_{\mathcal{F}} \left[\mathbb{1}_{\inf_{xN^{-2/3} \in [-T, T]} (B_{k-1}(x) - L_k^N(x)) \leq \delta N^{1/3}} W(\mathbf{B}, L_k^N) \mid B_{k-1} \geq L_k^N \right]}{\mathbb{E}_{\mathcal{F}}[W(\mathbf{B}, L_k^N)]} \mathbb{1}_{\text{Fav}} \right] + 4\varepsilon, \quad (10.6) \end{aligned}$$

where $B_{k-1} \geq L_k^N$ is shorthand for $B_{k-1}(x) \geq L_k^N(x)$ for all $xN^{-2/3} \in [U_1, U_2]$ and the inequality uses that $W(\mathbf{B}, L_k^N) = 0$ if $B_{k-1}(x) < L_k^N(x)$ for any $xN^{-2/3} \in [U_1, U_2]$.

We first lower bound the denominator of the first term of (10.6). We construct deterministic disjoint channels of width $\frac{2}{3}\eta N^{1/3}$ which are separated by $\frac{1}{3}\eta N^{1/3}$ for the paths to stay inside; see Figure 19. Let $Y = \max(MN^{1/3}, \bar{L}_k^N(U_1 N^{2/3}) + PN^{1/3}, \bar{L}_k^N(U_2 N^{2/3}) + PN^{1/3})$. Let $\ell_i^L : [U_1 N^{2/3}, (U_1 + 1)N^{2/3}]$ be the line joining

$$\left(U_1 N^{2/3}, \bar{L}_i^N(U_1 N^{2/3}) - \frac{1}{3}\eta N^{1/3} \right) \quad \text{and} \quad \left((U_1 + 1)N^{2/3}, Y + (k - i)\eta N^{1/3} \right).$$

Similarly let $\ell_i^R : [(U_2 - 1)N^{2/3}, U_2 N^{2/3}]$ be the line joining

$$\left(U_2 N^{2/3}, \bar{L}_i^N(U_2 N^{2/3}) - \frac{1}{3}\eta N^{1/3} \right) \quad \text{and} \quad \left((U_2 - 1)N^{2/3}, Y + (k - i)\eta N^{1/3} \right).$$

Note that, on Fav, it holds that

$$\ell_i^*(x) - \ell_{i+1}^*(x) \geq \eta N^{1/3} \quad (10.7)$$

for each $* \in \{L, R\}$ and $xN^{-2/3} \in [U_1, U_1 + 1]$ and $[U_2 - 1, U_2]$ respectively, by the fact that $L_i^N(U_j N^{2/3}) - L_{i+1}^N(U_j N^{2/3}) \geq \eta N^{1/3}$ for each $j \in \{1, 2\}$ on Fav. For $xN^{-2/3} \in [U_1, U_2]$ and

$i \in \llbracket 1, k-1 \rrbracket$, define the set $\text{Chan}_i(x) \subseteq \mathbb{R}$ (short for channels) by

$$\begin{cases} [(Y + (k-i)\eta)N^{1/3}, (Y + (k-i + \frac{2}{3})\eta)N^{1/3}], & \text{if } xN^{-2/3} \in [U_1 + 1, U_2 - 1] \\ [\ell_i^L(x), \ell_i^L(x) + \frac{2}{3}\eta N^{1/3}], & \text{if } xN^{-2/3} \in [U_1, U_1 + 1] \\ [\ell_i^R(x), \ell_i^R(x) + \frac{2}{3}\eta N^{1/3}], & \text{if } xN^{-2/3} \in [U_2 - 1, U_2]. \end{cases}$$

Note, by (10.7) and the first line of the above definition of $\text{Chan}_i(x)$, that for each $xN^{-2/3} \in [U_1, U_2]$ and $i \in \llbracket 1, k-1 \rrbracket$, $\text{Chan}_i(x)$ is an interval of size $\frac{2}{3}\eta N^{1/3}$ and

$$\inf \text{Chan}_i(x) \geq \sup \text{Chan}_{i+1}(x) + \frac{1}{3}\eta N^{1/3}$$

(the infimum and supremum being of the set for fixed x). Also observe that $\inf \text{Chan}_{k-1}(x) \geq \bar{L}_k^N(U_1 N^{2/3}) + PN^{-1/3}(x - U_1 N^{2/3}) + \frac{1}{3}\eta N^{1/3}$ for all $x \in [U_1 N^{2/3}, (U_1 + 1)N^{2/3}]$ and $\inf \text{Chan}_{k-1}(x) \geq \bar{L}_k^N(U_2 N^{2/3}) + PN^{-1/3}(U_2 N^{2/3} - x) + \frac{1}{3}\eta N^{1/3}$ for all $x \in [(U_2 - 1)N^{2/3}, U_2 N^{2/3}]$.

Let $\bar{B}_i(x) = B_i(x) - px$ and define the event Chan of staying in the channels by

$$\text{Chan} := \left\{ \bar{B}_i(x) \in \text{Chan}_i(x) \text{ for all } x \in [U_1 N^{2/3}, U_2 N^{2/3}], i \in \llbracket 1, k-1 \rrbracket \right\}.$$

Then observe $\mathbb{P}(\text{Chan})$ is lower bounded by some $\alpha = \alpha(\eta, k, T) = \alpha(\varepsilon, k, T) > 0$ (as can be seen using the weak convergence of $\bar{\mathbf{B}}$ to independent Brownian bridges whose endpoints are separated by at least η , after rescaling); this also uses that $\min_{i \in \llbracket 1, k-1 \rrbracket, x \in \{U_1, U_2\}} \bar{L}_i^N(xN^{2/3}) \geq -MN^{1/3}$ holds on Fav (since L_i^N are ordered). Since $\bar{L}_k^N(x) \leq MN^{1/3}$ for $xN^{-2/3} \in [-2T, 2T]$ on Fav and the channels are separated from each other and from \bar{L}_k^N by at least $\frac{1}{3}\eta N^{1/3}$, it follows that, on Chan , by Lemma 9.1,

$$W(\mathbf{B}, L_k^N) \geq (1 - q^{\frac{1}{3}\eta N^{1/3}})^{4kTN^{2/3}} \geq \frac{1}{2}$$

for all large enough N . Thus we obtain that, on Fav ,

$$\mathbb{E}_{\mathcal{F}}[W(\mathbf{B}, L_k^N)] \geq \mathbb{E}_{\mathcal{F}}[W(\mathbf{B}, L_k^N) \mid \text{Chan}] \cdot \mathbb{P}_{\mathcal{F}}(\text{Chan}) \geq \frac{1}{2}\alpha.$$

Putting this back into (10.6) and using $W(\mathbf{B}, L_k^N) \leq 1$ yields that

$$\begin{aligned} & \mathbb{P} \left(\inf_{xN^{-2/3} \in [-T, T]} (L_{k-1}^N(x) - L_k^N(x)) \leq \delta N^{1/3} \right) \\ & \leq 2\alpha^{-1} \mathbb{E} \left[\mathbb{P}_{\mathcal{F}} \left(\inf_{xN^{-2/3} \in [-T, T]} (B_{k-1}(x) - L_k^N(x)) \leq \delta N^{1/3} \mid B_{k-1} \geq L_k^N \right) \mathbb{1}_{\text{Fav}} \right] + 4\varepsilon. \end{aligned}$$

By Lemma 10.4, there exists $\delta = \delta(M, T, \varepsilon, k, \alpha) = \delta(T, \varepsilon, k) > 0$ such that the conditional probability in the previous display is upper bounded by $\alpha\varepsilon$; the hypothesis on the lower bound on the probability of $\{B^{\text{Br}}(x) \geq L_k^N(x) + \omega N^{1/3} \forall x \in [U_1, U_2]\}$ for some $\omega > 0$ and with B^{Br} a Brownian bridge is guaranteed, using the separation of $\eta N^{1/3}$ at U_1, U_2 guaranteed on Fav and the control from (10.3) on L_k^N in the immediate neighborhoods of U_1, U_2 included in their definition, by a construction similar to the one used to lower bound $\mathbb{E}_{\mathcal{F}}[W(\mathbf{B}, L_k^N)]$ just above, but with $k = 1$; such an ω and the lower bound on the resulting probability depend on only T, P , and η , thus on ε, T , and k . Combining with (10.5), this completes the proof after relabeling ε . \square

10.2. Proof of one-point separation. In this section we start the proof of Lemma 10.3. In its proof, we will need to know that the $(k-1)^{\text{st}}$ curve cannot drop too quickly. This is recorded in the next statement and will be proved in Section 10.3.

Lemma 10.5 (No quick drops). *Fix $k \in \mathbb{N}$. Suppose for any $T \geq 2$ and $\varepsilon > 0$ there exist $\eta = \eta(\varepsilon, k, T) > 0$, $M = M(\varepsilon, k, T)$, and $N_0 = N_0(\varepsilon, k, T)$ such that, for any $j \in \llbracket 1, k \rrbracket$ (recalling the definition of Sep_{j-2}^N from (9.1)) and $N \geq N_0$,*

$$\mathbb{P} \left(\inf_{xN^{-2/3} \in [-T, T]} \bar{L}_{j-1}^N(x) \geq -MN^{1/3} \right) \geq 1 - \varepsilon \quad \text{and} \quad \mathbb{P}(\text{Sep}_{j-2}^N(\eta, [-T, T], \mathbf{L}^N)) > 1 - \varepsilon.$$

Now fix $T \geq 2$, $\eta > 0$ and $\varepsilon > 0$. There exist $\delta = \delta(k, T, \eta, \varepsilon) > 0$ and $N_0 = N_0(k, T, \varepsilon, \eta)$ such that, for any random real number $a \in [-T, T]$ that is measurable with respect to $\mathcal{F}_{\text{ext}}(k-1, \mathbb{Z}, \mathbf{L}^N)$ (recall Definition 3.14), i.e., with respect to $(L_k^N, L_{k+1}^N, \dots)$, it holds for $N \geq N_0$ that

$$\mathbb{P} \left(\inf_{xN^{-2/3} \in [-\delta, \delta]} \bar{L}_{k-1}^N(aN^{2/3} + x) < \bar{L}_{k-1}^N(aN^{2/3}) - \eta N^{1/3} \right) \leq \varepsilon.$$

Proof of Lemma 10.3. We prove the existence of such a U_1 , as the proof for U_2 follows from reflection into the line $\{x = 0\}$ and the whole statement then follows from a union bound.

Preliminaries. Let $\text{RangeCtrl}_k(M) = \{\sup_{xN^{-2/3} \in [-2T, 2T]} |\bar{L}_k^N(x)| \leq MN^{1/3}\}$. By hypothesis (10.1) and Proposition 10.2 there exists $M = M(T, k, \varepsilon)$ such that $\mathbb{P}(\text{RangeCtrl}_k(M)) \geq 1 - \varepsilon$. For a P to be set, let SlopeCtrl_k be the event that there exists random $U_1 \in [-2T, -\frac{3}{2}T]$ with

$$\bar{L}_k^N(x) \leq \bar{L}_k^N(U_1N^{2/3}) + (x - U_1N^{2/3})PN^{-1/3} \quad \text{for } xN^{-2/3} \in [U_1, U_1 + 1].$$

We define U_1 by taking it to be the minimum point satisfying the above if there are multiple. By Lemma 10.1, there exists a deterministic $P = P(M) = P(k, T, \varepsilon)$ such that $\text{RangeCtrl}_k(M) \subseteq \text{SlopeCtrl}_k$ and we work on the former event for the remainder of the proof.

Next define (where the below name is short for “single curve separation”), for $k \in \mathbb{N}$, an interval I , and a process $X : I \rightarrow \mathbb{R}$,

$$\text{SingSep}_{k-2}^N(\eta, I, X) := \left\{ \inf_{xN^{-2/3} \in I} (L_{k-2}^N(x) - X(x)) > \eta N^{1/3} \right\}. \quad (10.8)$$

We adopt the shorthand $\text{SingSep}_{k-2}^N(\eta, L_{k-1}^N) = \text{SingSep}_{k-2}^N(\eta, [-3T, -T], L_{k-1}^N)$ in the rest of this proof. By hypothesis (10.2), we can find $\eta = \eta(T, k, \varepsilon) > 0$ such that $\mathbb{P}(\text{SingSep}_{k-2}^N(2\eta, L_{k-1}^N)^c) < \frac{1}{6}\varepsilon$ (though ahead we will actually work on the event $\text{SingSep}_{k-2}^N(\eta, L_{k-1}^N)$). Next let

$$\text{OnePtSep}_k^N(\delta, L_{k-1}^N) = \left\{ L_{k-1}^N(U_1N^{2/3}) > L_k^N(U_1N^{2/3}) + \delta N^{1/3} \right\}; \quad (10.9)$$

We wish to bound the probability $\mathbb{P}(\text{OnePtSep}_k^N(\delta, L_{k-1}^N)^c)$. Let $\mathcal{F} = \mathcal{F}_{\text{ext}}(\{k-1\}, \llbracket [-3TN^{2/3}], [-TN^{2/3}] \rrbracket)$ be the σ -algebra generated by $\{L_i^N(x) : (i, x) \notin \{k-1\} \times \llbracket [-3TN^{2/3}] + 1, [-TN^{2/3}] - 1 \rrbracket\}$. Notice that U_1 and $L_{k+1}^N(U_1N^{2/3})$ are \mathcal{F} -measurable. For $\rho > 0$ to be specified, define the \mathcal{F} -measurable event Fav by

$$\begin{aligned} \text{Fav} := & \left\{ \sup_{xN^{-2/3} \in [-3T, -T]} \bar{L}_k^N(x) \leq MN^{1/3}, \min_{xN^{-2/3} \in \{-3T, -T\}} \left(\bar{L}_{k-2}^N(x) - \bar{L}_{k-1}^N(x) \right) > 2\eta N^{1/3} \right\} \\ & \cap \left\{ \min_{xN^{-2/3} \in \{-3T, -T\}} \bar{L}_{k-1}^N(x) \geq -MN^{1/3} \right\} \\ & \cap \left\{ \min_{zN^{-2/3} \in \{-3T, U_1\}} \inf_{xN^{-2/3} \in [0, \rho]} \left(\bar{L}_{k-2}^N(z+x) - \bar{L}_{k-2}^N(z) \right) > -\frac{1}{2}\eta N^{1/3} \right\} \\ & \cap \left\{ \min_{zN^{-2/3} \in \{U_1, -T\}} \inf_{xN^{-2/3} \in [0, \rho]} \left(\bar{L}_{k-2}^N(z-x) - \bar{L}_{k-2}^N(z) \right) > -\frac{1}{2}\eta N^{1/3} \right\} \\ & \cap \left\{ \bar{L}_{k-2}^N(U_1N^{2/3}) > \bar{L}_k^N(U_1N^{2/3}) + 2\eta N^{1/3} \right\}. \end{aligned} \quad (10.10)$$

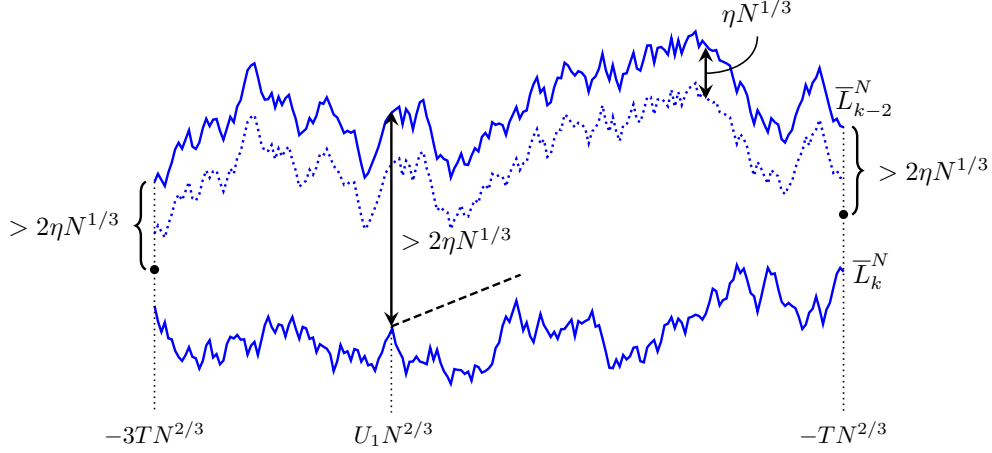


FIGURE 20. A depiction of the properties assumed under Fav . The dotted blue curve is \bar{L}_{k-2}^N brought down by $\eta N^{1/3}$, which is what the Bernoulli random walk bridge between the endpoints of L_{k-1}^N (black dots) that have been conditioned on must avoid under SingSep_{k-2} . This occurs with positive probability because we can find a corridor of width $\eta N^{1/3}$ around the starting black points and avoiding \bar{L}_k^N and \bar{L}_{k-2}^N because of the other conditions included in Fav .

Note that the parameter in the first line of Fav is 2η and not η as in $\text{SingSep}_{k-2}^N(\eta, L_{k-1}^N)$ that we work on; this will be needed later to guarantee a little extra space.

By Proposition 10.2 (upper bound on $\sup L_1^N$), the assumed lower tail bound (10.1), and the above bound on $\mathbb{P}(\text{SingSep}_{k-2}^N(2\eta, L_k^N)^c)$, we can find M such that the probability of the complement of the events in the first two lines is at most $\varepsilon/3$. By Lemma 10.5 we can find $\rho > 0$ such that the probability of the complement of the events in the third and fourth line is also at most $\varepsilon/3$; finally, the above bound on $\mathbb{P}(\text{SingSep}_{k-2}^N(2\eta, L_k^N)^c)$ along with the fact that $L_{k-1}^N \geq L_k^N$ guarantees that the fifth line's event's complement's probability is at most $\frac{1}{3}\varepsilon$ for the same choice of η as above. Thus overall we have $\mathbb{P}(\text{Fav}^c) \leq \varepsilon$.

Now we bound $\mathbb{P}(\text{OnePtSep}_k^N(\delta, L_{k-1}^N)^c)$ by

$$\mathbb{P}(\text{OnePtSep}_k^N(\delta, L_{k-1}^N)^c, \text{SingSep}_{k-2}^N(\eta, L_{k-1}^N), \text{Fav}) + 2\varepsilon. \quad (10.11)$$

Using the Gibbs property and weak monotonicity. Applying the Gibbs property and letting B be a Bernoulli random walk bridge with endpoints $(-3TN^{2/3}, L_{k-1}^N(-3TN^{2/3}))$ and $(-TN^{2/3}, L_{k-1}^N(-TN^{2/3}))$, the first term in (10.11) is equal to (and recalling the definition of W from (3.9))

$$\begin{aligned} & \mathbb{E} \left[\frac{\mathbb{E}_{\mathcal{F}} [\mathbb{1}_{\text{OnePtSep}_k^N(\delta, B)^c, \text{SingSep}_{k-2}^N(\eta, B)} W(B, L_{k-2}^N, L_k^N)]}{\mathbb{E}_{\mathcal{F}} [W(B, L_{k-2}^N, L_k^N)]} \mathbb{1}_{\text{Fav}} \right] \\ & \leq \mathbb{E} \left[\frac{\mathbb{E}_{\mathcal{F}} [\mathbb{1}_{\text{OnePtSep}_k^N(\delta, B)^c} W(B, L_{k-2}^N, L_k^N) \mid \text{SingSep}_{k-2}^N(\eta, B)]}{\mathbb{E}_{\mathcal{F}} [W(B, L_{k-2}^N, L_k^N) \mid \text{SingSep}_{k-2}^N(\eta, B)]} \mathbb{1}_{\text{Fav}} \right]. \end{aligned} \quad (10.12)$$

We wish to use weak monotonicity (Corollary 8.5) to control this expression. This requires us to remove the interaction via W with the upper boundary condition L_{k-2}^N , but we may include a non-intersection interaction with an upper curve. The following argument first aims to use the upper non-intersection freedom to remove the upper W -interaction.

Write $W(B, L_{k-2}^N, L_k^N) = W_{\text{up}}(B, L_{k-2}^N) \cdot W_{\text{low}}(B, L_k^N)$ (as in Definition 3.15). Then we see by Lemma 9.1 that, when B satisfies $\text{SingSep}_{k-2}^N(\eta, B)$,

$$W_{\text{up}}(B, L_{k-2}^N) \geq (1 - q^{\eta N^{1/3}})^{2TN^{2/3}} \geq \frac{1}{2}$$

almost surely for all large enough N . Thus

$$\mathbb{E}_{\mathcal{F}} [W(B, L_{k-2}^N, L_k^N) \mid \text{SingSep}_{k-2}^N(\eta, B)] \geq \frac{1}{2} \mathbb{E} [W_{\text{low}}(B, L_k^N) \mid \text{SingSep}_{k-2}^N(\eta, B)].$$

Let $B \geq L_k^N$ be shorthand for the event $B(x) \geq L_k^N(x)$ for all $xN^{-2/3} \in [-3T, -T]$. By using the previous display and that $W_{\text{up}}(B, L_{k-2}^N) \leq 1$, we see that (10.12) is upper bounded by

$$\begin{aligned} & 2 \cdot \mathbb{E} \left[\frac{\mathbb{E}_{\mathcal{F}} [\mathbb{1}_{\text{OnePtSep}_k^N(\delta, B)^c} W_{\text{low}}(B, L_k^N) \mid \text{SingSep}_{k-2}^N(\eta, B)]}{\mathbb{E}_{\mathcal{F}} [W_{\text{low}}(B, L_k^N) \mid \text{SingSep}_{k-2}^N(\eta, B)]} \mathbb{1}_{\text{Fav}} \right] \\ &= 2 \cdot \mathbb{E} \left[\frac{\mathbb{E}_{\mathcal{F}} [\mathbb{1}_{\text{OnePtSep}_k^N(\delta, B)^c} W_{\text{low}}(B, L_k^N) \mid B \geq L_k^N, \text{SingSep}_{k-2}^N(\eta, B)]}{\mathbb{E}_{\mathcal{F}} [W_{\text{low}}(B, L_k^N) \mid B \geq L_k^N, \text{SingSep}_{k-2}^N(\eta, B)]} \mathbb{1}_{\text{Fav}} \right], \end{aligned} \quad (10.13)$$

the equality due to the fact that $W_{\text{low}}(B, L_k^N) = 0$ if $B(x) < L_k^N(x)$ for any $xN^{-2/3} \in [-3T, -T]$ and since $B \geq L_k^N$ has positive (though *a priori* possibly tending to 0 with $N \rightarrow \infty$) probability. We put $B \geq L_k^N$ in the conditioning because we need it to ensure that $B(U_1 N^{2/3})$ does not come too close to $L_k^N(U_1 N^{2/3})$ (the other interaction of B with L_k^N via W will next be removed by weak monotonicity).

The display (10.13) now equals

$$\begin{aligned} & 2 \cdot \mathbb{E} \left[\frac{\mathbb{E}_{\mathcal{F}} [W_{\text{low}}(B, L_k^N) \mid B \geq L_k^N, \text{SingSep}_{k-2}^N(\eta, B), \text{OnePtSep}_k^N(\delta, B)^c]}{\mathbb{E}_{\mathcal{F}} [W_{\text{low}}(B, L_k^N) \mid B \geq L_k^N, \text{SingSep}_{k-2}^N(\eta, B)]} \right. \\ & \quad \left. \times \mathbb{P}_{\mathcal{F}} \left(\text{OnePtSep}_k^N(\delta, B)^c \mid B \geq L_k^N, \text{SingSep}_{k-2}^N(\eta, B) \right) \mathbb{1}_{\text{Fav}} \right]. \end{aligned}$$

Note that $\text{SingSep}_{k-2}^N(\eta, B)$ is simply an upper non-intersection boundary condition for B and $\text{OnePtSep}_k^N(\delta, B)^c$ is a one-point lower tail event at a deterministic location when conditioned on \mathcal{F} . Thus by the weak monotonicity statement Corollary 8.5, the first ratio in the previous display is upper bounded by $c(q)^{-1}$. Also invoking monotonicity of non-intersecting Bernoulli random walk bridges (Lemma 8.2), the previous display is upper bounded by

$$2c(q)^{-1} \cdot \mathbb{E} \left[\mathbb{P}_{\mathcal{F}} \left(\text{OnePtSep}_k^N(\delta, B)^c \mid B(U_1 N^{2/3}) \geq L_k^N(U_1 N^{2/3}), \text{SingSep}_{k-2}^N(\eta, B) \right) \mathbb{1}_{\text{Fav}} \right]. \quad (10.14)$$

Simplifying the conditioning. We claim, on Fav , that $\mathbb{P}_{\mathcal{F}}(\text{SingSep}_{k-2}^N(\eta, B) \mid B(U_1 N^{2/3}) \geq L_k^N(U_1 N^{2/3})) \geq \alpha$ for some $\alpha = \alpha(\varepsilon, k, T) > 0$. First, it is sufficient to lower bound

$$\mathbb{P}_{\mathcal{F}} \left(\text{SingSep}_{k-2}^N(\eta, B), B(U_1 N^{2/3}) \geq L_k^N(U_1 N^{2/3}) \right). \quad (10.15)$$

See Figure 21. Recall the definition (10.10) of Fav , and that B is a Bernoulli random walk bridge between $(-3TN^{2/3}, L_{k-1}^N(-3TN^{2/3}))$ and $(-TN^{2/3}, L_{k-1}^N(-TN^{2/3}))$. On Fav , the separation of B from L_{k-2}^N is at least $2\eta N^{1/3}$ at $-3TN^{2/3}$ and $-TN^{2/3}$; \bar{L}_{k-2}^N falls from its values at $-3TN^{2/3}$, $-TN^{2/3}$, and $U_1 N^{2/3}$ by at most $\frac{1}{2}\eta N^{1/3}$ in an interval of size $\rho N^{2/3}$ on either side of those values (if that interval lies inside $[-3T, -T]$); the separation of L_{k-2}^N from L_k^N at $U_1 N^{2/3}$ is at least $2\eta N^{1/3}$; and $\bar{L}_{k-2}^N \geq -MN^{1/3}$.

Let $\bar{B}(x) = B(x) - px$. By the above, the event $\{\text{SingSep}_{k-2}^N(\eta, B), B(U_1 N^{2/3}) \geq L_k^N(U_1 N^{2/3})\}$ occurs if, (i) \bar{B} falls from $\bar{B}(-3TN^{2/3})$ at $-3TN^{2/3}$ to $-(M + 4\eta)N^{1/3}$ at $(-3T + \rho)N^{2/3}$ while not

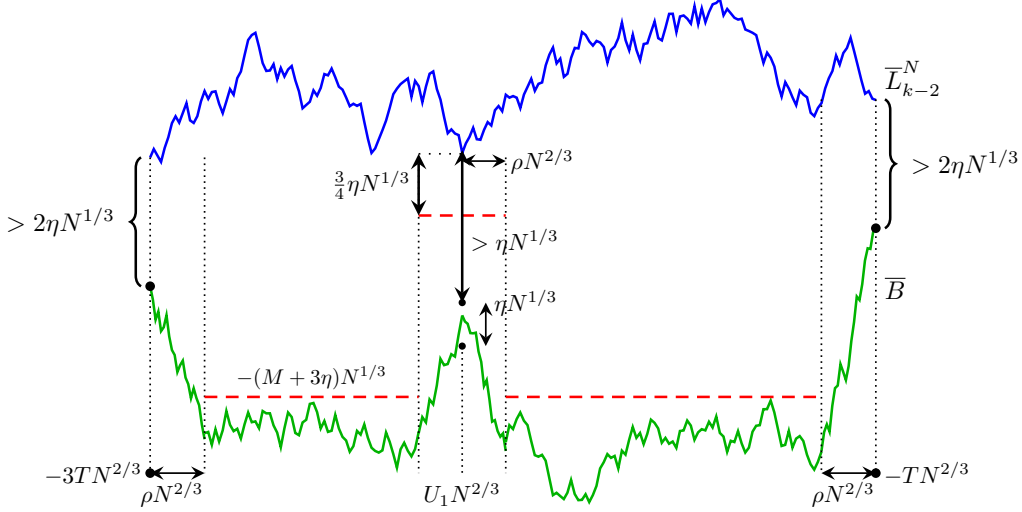


FIGURE 21. A depiction of the argument lower bounding (10.15). The green curve is the Bernoulli random walk bridge B , and the dashed red lines are curves which it must avoid. In each of the intervals of size $\rho N^{2/3}$ (one to the right of $-3TN^{2/3}$, one on either side of $U_1N^{2/3}$, and one to the left of $-TN^{2/3}$), \bar{L}_{k-2}^N falls from the relevant boundary point by at most $\frac{1}{2}\eta N^{1/3}$. The bottom black dot at location $U_1N^{2/3}$ is the value of $\bar{L}_k^N(U_1N^{2/3})$.

going above $\bar{L}_{k-2}^N(-3TN^{2/3}) - \frac{3}{4}\eta N^{1/3}$ in $[-3TN^{2/3}, (-3T+\rho)N^{2/3}]$; (ii) stays below $-(M+3\eta)N^{1/3}$ on $[(-3T+\rho)N^{2/3}, (U_1-\rho)N^{2/3}]$; (iii) jumps up to lie in $[\bar{L}_k^N(U_1N^{2/3}), \bar{L}_k^N(U_1N^{2/3}) + \eta N^{1/3}]$ at $U_1N^{2/3}$ while not exceeding $\bar{L}_{k-2}^N(U_1N^{2/3}) - \frac{3}{4}\eta N^{1/3}$ on $[(U_1-\rho)N^{2/3}, U_1N^{2/3}]$; and repeating similar properties in reverse on $[U_1N^{2/3}, -TN^{2/3}]$. Since on Fav it holds that $\bar{L}_k^N(U_1N^{2/3}) \leq MN^{1/3}$ and $\inf_{xN^{2/3} \in \{-3T, -T\}N^{2/3}} \bar{L}_{k-1}^N(x) \geq -MN^{1/3}$, it follows that the probability of this event is indeed lower bounded by a positive constant $\alpha = \alpha(M, \eta, T, \rho) = \alpha(\varepsilon, k, T)$.

Thus (10.14) is upper bounded by

$$\begin{aligned} & 2c(q)^{-1} \cdot \mathbb{E} \left[\frac{\mathbb{P}_{\mathcal{F}}(\text{OnePtSep}_k^N(\delta, B)^c \mid B(U_1N^{2/3}) \geq L_k^N(U_1N^{2/3}))}{\mathbb{P}_{\mathcal{F}}(\text{SingSep}_{k-2}^N(\eta, B) \mid B(U_1N^{2/3}) \geq L_k^N(U_1N^{2/3}))} \mathbb{1}_{\text{Fav}} \right] \\ & \leq 2c(q)^{-1} \alpha^{-1} \cdot \mathbb{E} \left[\mathbb{P}_{\mathcal{F}}(\text{OnePtSep}_k^N(\delta, B)^c \mid B(U_1N^{2/3}) \geq L_k^N(U_1N^{2/3})) \mathbb{1}_{\text{Fav}} \right]. \end{aligned}$$

Invoking a Gaussian comparison. It is not hard to see that for small enough δ , the previous display is smaller than ε . Indeed, recalling the definition (10.9) of OnePtSep_k^N and letting $X \sim \mathcal{N}(0, 1)$, by a normal approximation Bernoulli random walk bridges (Lemma 6.14), for large enough N (depending on δ), the previous display is upper bounded by

$$2c(q)^{-1} \alpha^{-1} \mathbb{E} \left[\mathbb{P}_{\mathcal{F}} \left(\sigma X + \mu \leq \delta N^{1/3} \mid \sigma X + \mu > 0 \right) \mathbb{1}_{\text{Fav}} \right] + \frac{1}{2}\varepsilon, \quad (10.16)$$

where

$$\begin{aligned} \mu & := \frac{U_1 + 3T}{2T} \bar{L}_{k-1}^N(-TN^{2/3}) - \frac{T + U_1}{2T} \bar{L}_{k-1}^N(-3TN^{2/3}) - \bar{L}_k^N(U_1N^{2/3}) \quad \text{and} \\ \sigma^2 & := p(1-p) \cdot \frac{(U_1 + 3T)(-T - U_1)N^{2/3}}{2T}; \end{aligned}$$

the factor of $p(1-p)$ in σ^2 arises, as explained after Lemma 6.14, since B is a Bernoulli random walk bridge with slope p , making its increments have variance approximately $p(1-p)$. Since

$\bar{L}_{k-1}^N(-3TN^{2/3}), \bar{L}_{k-1}^N(-TN^{2/3}) > -MN^{1/3}$ and $\bar{L}_k^N(U_1N^{2/3}) \leq MN^{1/3}$ on Fav, it follows that, again on Fav,

$$\mu \geq -2MN^{1/3}.$$

Since $U_1 \in [-2T, -\frac{3}{2}T]$, it follows that

$$\sigma^2 \geq \frac{3}{8}p(1-p)TN^{2/3}.$$

Let $K = \frac{3}{8}p(1-p)T$. Recall from Lemma 8.1 that $\mathbb{P}_{\mathcal{F}}(X < r + \delta N^{1/3} \mid X > r)$ is increasing as a function of r for any fixed $\delta > 0$ and N . Since $-\sigma^{-1}\mu \leq (\frac{8}{3}(p(1-p)T)^{-1})^{1/2}2M = 2K^{-1/2}M$, (10.16) is upper bounded by

$$\begin{aligned} & 2c(q)^{-1}\alpha^{-1}\mathbb{E}\left[\mathbb{P}_{\mathcal{F}}\left(X \leq -\sigma^{-1}\mu + \sigma^{-1}\delta N^{1/3} \mid X > -\sigma^{-1}\mu\right) \mathbb{1}_{\text{Fav}}\right] + \frac{1}{2}\varepsilon, \\ & \leq 2c(q)^{-1}\alpha^{-1}\mathbb{E}\left[\mathbb{P}_{\mathcal{F}}\left(X \leq -\sigma^{-1}\mu + K^{-1/2}\delta \mid X > -\sigma^{-1}\mu\right) \mathbb{1}_{\text{Fav}}\right] + \frac{1}{2}\varepsilon \\ & \leq 2c(q)^{-1}\alpha^{-1}\mathbb{P}\left(X \leq 2K^{-1/2}M + K^{-1/2}\delta \mid X > 2K^{-1/2}M\right) + \frac{1}{2}\varepsilon. \end{aligned}$$

It is now a simple computation using standard normal bounds that the first term is upper bounded by $\frac{1}{2}\varepsilon$ if δ is made small enough (independent of N). Returning to (10.11), we see that we have bounded $\mathbb{P}(\text{OnePtSep}_k^N(\delta, L_{k-1}^N)^c)$ by 3ε . This completes the proof after relabeling ε . \square

10.3. No quick drops. In this section we prove Lemma 10.5. We first establish a one-point version of this statement, which will then be upgraded via a chaining argument. To state this one-point version we introduce notation for two events. First, we use the shorthand $\text{SingSep}_{k-2}^N(\eta, L_{k-1}^N) := \text{SingSep}_{k-2}^N(\eta, [-2T, 2T], L_{k-1}^N)$ with the latter as defined in (10.8). Second, for any real numbers $M, \eta_0, \delta_0 > 0$, let $\text{Fav} = \text{Fav}(M, \eta_0, \delta_0)$ be defined by

$$\begin{aligned} \text{Fav} & := \left\{ \min_{xN^{-2/3} \in \{a, 2T\}} \bar{L}_{k-1}^N(x) > -MN^{1/3}, \inf_{xN^{-2/3} \in [-2T, 2T]} \bar{L}_{k-2}^N(x) \geq -MN^{1/3} \right\} \\ & \cap \left\{ \min_{xN^{-2/3} \in \{a, 2T\}} \left(\bar{L}_{k-2}^N(x) - \bar{L}_{k-1}^N(x) \right) \geq 4\eta_0 N^{1/3} \right\} \\ & \cap \left\{ \inf_{xN^{-2/3} \in [0, \delta_0]} \bar{L}_{k-2}^N(aN^{2/3} + x) > \bar{L}_{k-2}^N(aN^{2/3}) - \frac{1}{2}\eta_0 N^{1/3} \right\} \\ & \cap \left\{ \inf_{xN^{-2/3} \in [0, \delta_0]} \bar{L}_{k-2}^N(2TN^{2/3} - x) > \bar{L}_{k-2}^N(2TN^{2/3}) - \frac{1}{2}\eta_0 N^{1/3} \right\}. \end{aligned} \tag{10.17}$$

Lemma 10.6. *Fix $M, T \geq 2, \delta_0 > 0$ and $0 < \eta < \frac{1}{2}\eta_0$. There exist $c = c(M, T) > 0$ and $C = C(M, T, \eta_0, \delta_0)$ such that, for any random real number $a \in [-T, T]$ that is measurable with respect to $(L_k^N, L_{k+1}^N, \dots)$ and any $\delta > 0$ and $N \geq 1$,*

$$\begin{aligned} & \mathbb{P}\left(\bar{L}_{k-1}^N((a + \delta)N^{2/3}) < \bar{L}_{k-1}^N(aN^{2/3}) - \eta N^{1/3}, \text{Fav}(M, \eta_0, \delta_0), \text{SingSep}_{k-2}^N(2\eta_0, L_{k-1}^N)\right) \\ & \leq C \exp\left(-c \frac{\eta^2}{|\delta|}\right). \end{aligned}$$

Proof of Lemma 10.5. Recall that we must bound $\mathbb{P}(\inf_{xN^{-2/3} \in [-\delta, \delta]} L_{k-1}^N(aN^{2/3} + x) < L_{k-1}^N(x))$. We will replace the interval $[-\delta, \delta]$ by $[0, \delta]$ in the following argument; the case of $[-\delta, 0]$ follows by reflection in the line $\{x = 0\}$, and the case of $[-\delta, \delta]$ then follows by a union bound.

Fix $\eta > 0$. For any $j \in \mathbb{N}$, $\delta > 0$, and random real number a which is measurable with respect to $(L_{j+1}^N, L_{j+2}^N, \dots)$, let the event $\text{Drop}_j^N(a, \delta, \eta)$ be defined by

$$\text{Drop}_j^N(a, \delta, \eta) = \left\{ \inf_{xN^{-2/3} \in [0, \delta]} \bar{L}_j^N(aN^{2/3} + x) < \bar{L}_j^N(aN^{2/3}) - \eta N^{1/3} \right\}.$$

We prove the lemma by induction on $j \in \llbracket 1, k-1 \rrbracket$. So we may assume that for any $T \geq 2$, $\varepsilon > 0$, and $\eta > 0$ there exists δ_0 such that, for any $a \in [-2T, 2T]$ that is measurable with respect to $(L_j^N, L_{j+1}^N, \dots)$,

$$\mathbb{P}(\text{Drop}_{j-1}^N(a, \delta_0, \eta)) \leq \varepsilon. \quad (10.18)$$

Then we must show that, for any fixed $T \geq 2$, $\eta > 0$ and $\varepsilon > 0$, there exists $\delta > 0$ such that, for any $a \in [-T, T]$ that is measurable with respect to $(L_{j+1}^N, L_{j+2}^N, \dots)$,

$$\mathbb{P}(\text{Drop}_j^N(a, \delta, \eta)) \leq \varepsilon.$$

Note that it is sufficient to prove this for a smaller η if needed since $\mathbb{P}(\text{Drop}_j^N(a, \delta, \eta))$ is decreasing in η .

We prove the base case $j = 1$ and the induction step simultaneously (in the case of $j = 1$ the induction hypothesis (10.18) holds trivially). Our argument is by a chaining argument to upgrade the one-point bound from Lemma 10.6 to a uniform bound. Let $x_{i,\ell} = a + i2^{-\ell}\delta$ for $i = 0, 1, \dots, 2^\ell$ and define

$$\mathbf{E}_\ell := \bigcap_{i=1}^{2^\ell} \left\{ \bar{L}_j^N(x_{i,\ell}N^{2/3}) > \bar{L}_j^N(x_{\lfloor i/2 \rfloor, \ell-1}N^{2/3}) - \alpha_\ell \eta N^{1/3} \right\},$$

where $\alpha_\ell := \rho 2^{-\ell/4}$ with $\rho := \frac{1}{4}(\sum_{j=1}^\infty 2^{-j/4})^{-1}$ (which is clearly positive), so that $\sum_{\ell=0}^\infty \alpha_\ell < \frac{1}{4}$. We claim that, with $\ell_{\max} = \lceil \frac{1}{2} \log_2 N \rceil$,

$$\text{Drop}_j^N(a, \delta, \eta) \subseteq \bigcup_{\ell=0}^{\ell_{\max}} (\mathbf{E}_\ell)^c. \quad (10.19)$$

Indeed, it holds that $(x_{i+1, \ell_{\max}} - x_{i, \ell_{\max}})N^{2/3} = \delta N^{2/3-1/2} = \delta N^{1/6}$; since L_j^N is a Bernoulli path, this implies that, on the complement of the righthand side of the previous display, i.e., on $\cap_{\ell=0}^{\ell_{\max}} \mathbf{E}_\ell$, and for all large enough N (depending on η, δ),

$$\begin{aligned} \inf_{xN^{-2/3} \in [0, \delta]} \bar{L}_j^N(aN^{2/3} + x) &\geq \inf_{\substack{i=1, \dots, 2^\ell \\ \ell=0, \dots, \ell_{\max}}} \bar{L}_j^N(x_{i,\ell}N^{2/3}) - \delta N^{1/6} \\ &> \inf_{\substack{i=1, \dots, 2^\ell \\ \ell=0, \dots, \ell_{\max}}} \bar{L}_j^N(x_{i,\ell}N^{2/3}) - \frac{1}{2}\eta N^{1/3}. \end{aligned}$$

For any i and ℓ , setting $i_{m+1} := \lfloor i_m/2 \rfloor$ for $m \geq 1$ and $i_0 = i$, again on $\cap_{\ell=0}^{\ell_{\max}} \mathbf{E}_\ell$,

$$\begin{aligned} \bar{L}_j^N(x_{i,\ell}N^{2/3}) &= \sum_{m=0}^{\ell} \bar{L}_j^N(x_{i_m, \ell-m}N^{2/3}) - \bar{L}_j^N(x_{i_{m+1}, \ell-m-1}N^{2/3}) + \bar{L}_j^N(aN^{2/3}) \\ &\geq \bar{L}_j^N(aN^{2/3}) - \sum_{m=0}^{\ell} \alpha_{\ell-m} \eta N^{1/3} \geq \bar{L}_j^N(aN^{2/3}) - \frac{1}{4}\eta N^{1/3} \end{aligned}$$

by the definition of α_ℓ . So, on $\cap_{\ell=0}^{\ell_{\max}} \mathbf{E}_\ell$, it indeed holds that $\inf_{xN^{-2/3} \in [0, \delta]} \bar{L}_j^N(aN^{2/3} + x) > \bar{L}_j^N(aN^{2/3}) - \eta N^{1/3}$, i.e., (10.19) holds.

Let $\text{SingSep}_{j-1}^N(2\eta_0) = \text{SingSep}_{j-1}^N(2\eta_0, [-2T, 2T], L_j^N)$ be as defined in (10.8). Let $\eta_0 > 0$ be such that $\mathbb{P}(\text{SingSep}_{j-1}^N(2\eta_0))$, as well as the probability of the second event in (10.17), is at least $1 - \frac{1}{8}\varepsilon$, which is possible by the assumptions in Lemma 10.5. By (10.18), let $\delta_0 > 0$ be such that

$$\mathbb{P}(\text{Drop}_{j-1}^N(a, \delta_0, \frac{1}{2}\eta_0) \cup \text{Drop}_{j-1}^N(2T, \delta_0, \frac{1}{2}\eta_0)) \leq \frac{1}{8}\varepsilon.$$

Let $\text{Fav}(M, \eta_0, \delta_0)$ be as in Lemma 10.6, i.e., (10.17). Now, by the assumptions in Lemma 10.5 and these choices, performing a union bound shows that we may choose M such that $\mathbb{P}(\text{Fav}(M, \eta_0, \delta_0)^c \cup \text{SingSep}_{j-1}^N(2\eta_0)^c) \leq \frac{1}{2}\varepsilon$. Reduce η if necessary so that it is less than $\frac{1}{2}\eta_0$. Then, by (10.19),

$$\begin{aligned} \mathbb{P}(\text{Drop}_j^N(a, \delta, \eta)) &\leq \mathbb{P}(\text{Drop}_j^N(a, \delta, \eta), \text{Fav}(M, \eta_0, \delta_0), \text{SingSep}_{j-1}^N(2\eta_0)) + \frac{1}{2}\varepsilon \\ &\leq \sum_{\ell=0}^{\ell_{\max}} \mathbb{P}(\mathbf{E}_\ell^c, \text{Fav}(M, \eta_0, \delta_0), \text{SingSep}_{j-1}^N(2\eta_0)) + \frac{1}{2}\varepsilon. \end{aligned}$$

By Lemma 10.6 and a union bound over the 2^ℓ events in \mathbf{E}_ℓ^c , we know that the sum in the previous display is upper bounded, for $\delta > 0$, by

$$\sum_{\ell=0}^{\infty} 2^\ell C \exp\left(-c\alpha_\ell^2 \eta^2 / (2^{-\ell}\delta)\right) = \sum_{\ell=0}^{\infty} 2^\ell C \exp\left(-c\delta^{-1}\rho^2 2^{-\ell/2+\ell}\eta^2\right).$$

This is upper bounded by $C \exp(-c\delta^{-1}\eta^2)$. Setting $\delta > 0$ small enough such that this is upper bounded by $\frac{1}{2}\varepsilon$ completes the proof. \square

Next we turn to establishing the one-point statement of there being no quick drops (Lemma 10.6).

Proof of Lemma 10.6. Note that a is measurable with respect to $(L_k^N, L_{k+1}^N, \dots)$ by hypothesis, so $[aN^{2/3}, 2TN^{2/3}]$ forms a stopping domain (Definition 6.1) with respect to $(L_1^N, \dots, L_{k-1}^N)$. Let $\mathcal{F} = \mathcal{F}_{\text{ext}}(\{k-1\}, \llbracket aN^{2/3}, 2TN^{2/3} \rrbracket, \mathbf{L}^N)$ be as in that definition, i.e., it is the σ -algebra generated by $\{L_i^N(x) : (i, x) \notin \{k-1\} \times \llbracket aN^{2/3} + 1, TN^{2/3} - 1 \rrbracket\}$. Note also that Fav (10.17) is \mathcal{F} -measurable, and recall SingSep_{k-2}^N from (10.8). Let B be a Bernoulli random walk bridge from $(aN^{2/3}, L_{k-1}^N(aN^{2/3}))$ to $(2TN^{2/3}, L_{k-1}^N(2TN^{2/3}))$ and $\bar{B}(x) = B(x) - px$. By the strong Hall-Littlewood Gibbs property (Proposition 6.2), the probability in the statement of the lemma equals

$$\begin{aligned} &\mathbb{E} \left[\frac{\mathbb{E}_{\mathcal{F}} \left[\mathbb{1}_{\bar{B}((a+\delta)N^{2/3}) < \bar{L}_{k-1}^N(aN^{2/3}) - \eta N^{1/3}, \text{SingSep}_{k-2}^N(2\eta_0, B)} W(B, L_{k-2}^N, L_k^N) \right]}{\mathbb{E}_{\mathcal{F}}[W(B, L_{k-2}^N, L_k^N)]} \mathbb{1}_{\text{Fav}} \right] \\ &\leq \mathbb{E} \left[\frac{\mathbb{E}_{\mathcal{F}} \left[\mathbb{1}_{\bar{B}((a+\delta)N^{2/3}) < \bar{L}_{k-1}^N(aN^{2/3}) - \eta N^{1/3}, W(B, L_{k-2}^N, L_k^N) \mid \text{SingSep}_{k-2}^N(2\eta_0, B)} \right]}{\mathbb{E}_{\mathcal{F}}[W(B, L_{k-2}^N, L_k^N) \mid \text{SingSep}_{k-2}^N(2\eta_0, B)]} \mathbb{1}_{\text{Fav}} \right] \\ &= \mathbb{E} \left[\frac{\mathbb{E}_{\mathcal{F}}[W(B, L_{k-2}^N, L_k^N) \mid \text{SingSep}_{k-2}^N(2\eta_0, B), \bar{B}((a+\delta)N^{2/3}) < \bar{L}_{k-1}^N(aN^{2/3}) - \eta N^{1/3}]}{\mathbb{E}_{\mathcal{F}}[W(B, L_{k-2}^N, L_k^N) \mid \text{SingSep}_{k-2}^N(2\eta_0, B)]} \right. \\ &\quad \left. \times \mathbb{P}_{\mathcal{F}} \left(\bar{B}((a+\delta)N^{2/3}) < \bar{L}_{k-1}^N(aN^{2/3}) - \eta N^{1/3} \mid \text{SingSep}_{k-2}^N(2\eta_0, B) \right) \mathbb{1}_{\text{Fav}} \right]. \end{aligned}$$

Now, on $\text{SingSep}_{k-2}^N(2\eta_0, B)$, it holds by Lemma 9.1 that $W_{\text{up}}(B, L_{k-2}^N) \geq \frac{1}{2}$ (recall from Definition 3.15) for all large enough N , and $W_{\text{up}}(B, L_{k-2}^N) \leq 1$ trivially. Thus the previous display is upper bounded by

$$2 \cdot \mathbb{E} \left[\frac{\mathbb{E}_{\mathcal{F}}[W(B, L_k^N) \mid \text{SingSep}_{k-2}^N(2\eta_0, B), \bar{B}((a+\delta)N^{2/3}) < \bar{L}_{k-1}^N(aN^{2/3}) - \eta N^{1/3}]}{\mathbb{E}_{\mathcal{F}}[W(B, L_k^N) \mid \text{SingSep}_{k-2}^N(2\eta_0, B)]} \right]$$

$$\times \mathbb{P}_{\mathcal{F}} \left(\overline{B}((a + \delta)N^{2/3}) < \overline{L}_{k-1}^N(aN^{2/3}) - \eta N^{1/3} \mid \text{SingSep}_{k-2}^N(2\eta_0, B) \right) \mathbb{1}_{\text{Fav}} \Big].$$

By Corollary 8.5, the first factor in the previous line is upper bounded by $c(q)^{-1}$, yielding that the previous display is upper bounded by

$$2c(q)^{-1} \mathbb{E} \left[\mathbb{P}_{\mathcal{F}} \left(\overline{B}((a + \delta)N^{2/3}) < \overline{L}_{k-1}^N(aN^{2/3}) - \eta N^{1/3} \mid \text{SingSep}_{k-2}^N(2\eta_0, B) \right) \mathbb{1}_{\text{Fav}} \right].$$

We wish to remove the conditioning event, for which we first lower bound its probability, on Fav. Now, on Fav, the separation between \overline{B} and \overline{L}_{k-2}^N at $aN^{2/3}$ and $2TN^{2/3}$ is at least $4\eta_0 N^{1/3}$. Further, \overline{L}_{k-2}^N drops by at most $\frac{1}{2}\eta_0 N^{1/3}$ in $[aN^{2/3}, (a + \delta_0)N^{2/3}]$ and $[(2T - \delta_0)N^{2/3}, 2TN^{2/3}]$ and remains above $-MN^{1/3}$ on all of $[-2TN^{2/3}, 2TN^{2/3}]$. Thus for \overline{B} to maintain a separation of $2\eta_0 N^{1/3}$ with \overline{L}_{k-2}^N on $[-2TN^{2/3}, 2TN^{2/3}]$, it is sufficient if it does the following (similar to Figure 21 in the proof of Lemma 10.3): drops to or below $-(M + 4\eta_0)N^{1/3}$ in $[aN^{2/3}, (a + \delta_0)N^{2/3}]$ and never goes above $\overline{L}_{k-1}^N(aN^{2/3}) + \frac{1}{2}\eta_0 N^{1/3}$ in the same interval, stays below $-(M + 3\eta_0)N^{1/3}$ on $[(a + \delta_0)N^{2/3}, (2T - \delta_0)N^{2/3}]$, and jumps up to $\overline{L}_{k-1}^N(2TN^{2/3})$ at $2TN^{2/3}$ while staying below $\overline{L}_{k-1}^N(2TN^{2/3}) + \frac{1}{2}\eta_0 N^{1/3}$ on $[(2T - \delta_0)N^{2/3}, 2TN^{2/3}]$. The probability that \overline{B} satisfies these conditions is lower bounded by some deterministic $\alpha = \alpha(T, \delta_0, M, \eta_0) > 0$ (since the same is true for the Brownian bridge weak limit of the rescaled \overline{B}), using also that $\overline{L}_{k-1}^N(aN^{2/3}), \overline{L}_{k-1}^N(2TN^{2/3}) \in [-MN^{1/3}, MN^{1/3}]$ on Fav. This yields that the previous display is upper bounded by

$$2\alpha^{-1}c(q)^{-1} \mathbb{E} \left[\mathbb{P}_{\mathcal{F}} \left(\overline{B}((a + \delta)N^{2/3}) < \overline{L}_{k-1}^N(aN^{2/3}) - \eta N^{1/3} \right) \mathbb{1}_{\text{Fav}} \right].$$

Since $\overline{B}(2TN^{2/3}), \overline{B}(aN^{2/3}) \in [-MN^{1/3}, MN^{1/3}]$ (so that the endpoints of B define a line of slope $p + O(1)MN^{-1/3}$), it follows by one-point bounds on Bernoulli random walk bridges (Lemma 6.13) that, for all $\delta > 0$, the previous display is upper bounded by

$$C\alpha^{-1}c(q)^{-1} \exp(-c\delta^{-1}\eta^2).$$

This completes the proof. \square

11. PARTITION FUNCTION AND NON-INTERSECTION PROBABILITY ESTIMATES

In this section we prove Proposition 6.12. The argument is fairly standard given what we have already done; it first appeared in [CH14], and has been used in a number of subsequent works [CH16, CD18, DFF⁺21, DFF⁺21, BCD23]. It relies on sampling from a measure on paths on a larger interval where the interaction between paths is turned off in the interval of interest and considering the Radon-Nikodym derivative of this measure with the original one; if one has a probability lower bound on the partition function of the new measure, it can be made into a high probability lower bound on the partition function of the original measure, by an argument that can be understood as a form of “size-biased” sampling.

However, our arguments are slightly more complicated than in earlier works as the larger interval we work on is $[U_1, U_2]$ (defined as in Lemma 10.3 such that there is control on the growth of the lower curve near U_i) and so is random. This is because we need some such control on the lower curve at the boundaries of the interval to obtain a lower bound on the partition function for the new measure mentioned above. In the earlier works, this lower bound was achieved on a deterministic interval, using the stochastic monotonicity and other features of the Gibbs property that were available in those models.

As in the last two sections, we assume here that L_k^N satisfies Assumptions 1 and 2 without explicitly mentioning it in the statements.

11.1. Lower bounding the partition function. Fix $T \geq 2$. Let $U_1 \in [-2T, -\frac{3}{2}T]$ be the largest point and $U_2 \in [\frac{3}{2}T, 2T]$ be the smallest point such that

$$\begin{aligned}\bar{L}_{k+1}^N(x) &\leq \bar{L}_{k+1}^N(U_1 N^{2/3}) + (x - U_1 N^{2/3})PN^{-1/3} && \text{for } xN^{-2/3} \in [U_1, U_1 + 1] \\ \bar{L}_{k+1}^N(x) &\leq \bar{L}_{k+1}^N(U_2 N^{2/3}) + (U_2 N^{2/3} - x)PN^{-1/3} && \text{for } xN^{-2/3} \in [U_2 - 1, U_2],\end{aligned}\tag{11.1}$$

for a P to be specified later. In the event that such a U_1 does not exist, we set it to $-2T$, and in the event that such a U_2 does not exist, we set it to $2T$.

Fix an interval $[-\frac{3}{2}T, \frac{3}{2}T] \subseteq [a, b] \subseteq [-2T, 2T]$ and $\mathbf{x}, \mathbf{y} \in \{\mathbf{z} \in \mathbb{R}^k : z_1 > \dots > z_k\}$. We define a discrete line ensemble (Definition 3.6) $\tilde{\mathbf{L}}^N = (\tilde{L}_1^N, \dots, \tilde{L}_k^N)$, where each $\tilde{L}_i^N : \llbracket aN^{2/3}, bN^{2/3} \rrbracket \rightarrow \mathbb{R}$ with $\tilde{L}_i^N(aN^{2/3}) = x_i$ and $\tilde{L}_i^N(bN^{2/3}) = y_i$, as follows. The law $\tilde{\mathbb{P}}_N^{[a,b],\mathbf{x},\mathbf{y}}$ of $\tilde{\mathbf{L}}^N$ is specified via its Radon-Nikodym derivative with respect to the law $\mathbb{P}_{\text{free},N}^{k,[a,b],\mathbf{x},\mathbf{y}}$ of k independent Bernoulli random walk bridges on $\llbracket aN^{2/3}, bN^{2/3} \rrbracket$, the j^{th} from $(aN^{2/3}, x_j)$ to $(bN^{2/3}, y_j)$ for each j : for $\gamma : \llbracket 1, k \rrbracket \times \llbracket aN^{2/3}, bN^{2/3} \rrbracket \rightarrow \mathbb{Z}$ a collection of k Bernoulli paths with endpoints $(aN^{2/3}, x_j)$ and $(bN^{2/3}, y_j)$ for $j = 1, \dots, k$,

$$\frac{d\tilde{\mathbb{P}}_N^{[a,b],\mathbf{x},\mathbf{y}}}{d\mathbb{P}_{\text{free},N}^{k,[a,b],\mathbf{x},\mathbf{y}}}(\gamma) \propto \prod_{i=1}^k \prod_{x \in I_{N,T}} \left(1 - q^{\Delta_i(x)} \mathbb{1}_{\Delta_i(x) = \Delta_i(x-1) - 1}\right)\tag{11.2}$$

where $I_{N,T} = \llbracket U_1 N^{2/3}, U_2 N^{2/3} \rrbracket \setminus \llbracket -TN^{2/3}, TN^{2/3} \rrbracket$ and $\Delta_i(x) = \gamma_i(x) - \gamma_{i+1}(x)$ with $\gamma_{k+1} = L_{k+1}^N$ by convention. In words, $\tilde{\mathbb{P}}_N^{[a,b],\mathbf{x},\mathbf{y}}$ is the usual Hall-Littlewood Gibbs measure but where the interaction is absent on $\llbracket -TN^{2/3}, TN^{2/3} \rrbracket$.

Writing in the just introduced notation, the definition (6.5) reads

$$Z_N^{k,[-T,T],\mathbf{x},\mathbf{y},g} = \mathbb{E}_{\text{free},N}^{k,[-T,T],\mathbf{x},\mathbf{y}}[W(\mathbf{B}, g)]\tag{11.3}$$

(recall W from (3.9)), where, under $\mathbb{E}_{\text{free}}^{k,[-T,T],\mathbf{x},\mathbf{y}}$, $\mathbf{B} = (B_1, \dots, B_k)$ is a collection of k independent Bernoulli random walk bridges, with B_i from $(-TN^{2/3}, x_i)$ to $(TN^{2/3}, y_i)$.

Lemma 11.1. *Suppose $g : [aN^{2/3}, bN^{2/3}] \rightarrow \mathbb{R}$ satisfies (with $\bar{g}(x) := g(x) - px$)*

$$\begin{aligned}\bar{g}(x) &\leq \bar{g}(aN^{2/3}) + (x - aN^{2/3})PN^{-1/3} && \text{for } xN^{-2/3} \in [a, a + 1] \\ \bar{g}(x) &\leq \bar{g}(bN^{2/3}) + (bN^{2/3} - x)PN^{-1/3} && \text{for } xN^{-2/3} \in [b - 1, b],\end{aligned}\tag{11.4}$$

Suppose also that M is such that $\sup_{xN^{-2/3} \in [a,b]} |g(x)| \leq MN^{1/3}$, and that there exists $\eta > 0$ such that $x_i > x_{i+1} + \eta N^{1/3}$ and $y_i > y_{i+1} + \eta N^{1/3}$ for each $i = 1, \dots, k$, with $x_{k+1} = g(aN^{2/3})$ and $y_{k+1} = g(bN^{2/3})$. Then there exist $\delta > 0$, $\varepsilon > 0$, and N_0 , all depending on k, M, T, η , such that, for all $N \geq N_0$,

$$\tilde{\mathbb{P}}_N^{[a,b],\mathbf{x},\mathbf{y}} \left(Z_N^{k,[-T,T],\tilde{\mathbf{L}}^N(-TN^{2/3}),\tilde{\mathbf{L}}^N(TN^{2/3}),g} > \delta \right) > \varepsilon,$$

where $\tilde{\mathbf{L}}^N(TN^{2/3})$ and $\tilde{\mathbf{L}}^N(-TN^{2/3})$ in the superscript respectively indicate $(\tilde{L}_i^N(TN^{2/3}))_{i=1}^k$ and $(\tilde{L}_i^N(-TN^{2/3}))_{i=1}^k$.

Proof. We adopt the shorthand $Z_N^{k,T,g} = Z_N^{k,[-T,T],\tilde{\mathbf{L}}^N(-TN^{2/3}),\tilde{\mathbf{L}}^N(TN^{2/3}),g}$. With some positive probability $2\varepsilon > 0$ (independent of N) it holds that k independent Bernoulli random walk bridges $\mathbf{B} = (B_1, \dots, B_k)$ starting from $(aN^{2/3}, \mathbf{x})$ and going to $(bN^{2/3}, \mathbf{y})$ reach points at $(a+1)N^{2/3}$ and $(b-1)N^{2/3}$ which are all above $2MN^{1/3}$ and are separated by at least $N^{1/3}$; reach points at $\pm TN^{2/3}$ which have the same properties; and do so while staying separated (from each other as well as from g) by at least $\frac{1}{2}\eta N^{1/3}$ on $[aN^{2/3}, -TN^{2/3}]$ and $[TN^{2/3}, bN^{2/3}]$; this uses the condition

(11.4) controlling g and the initial separation of $\eta N^{1/3}$ between the endpoints of \mathbf{B} . Call this event Corr (for corridors).

On Corr , it holds that the righthand side of (11.5) is lower bounded by $\frac{1}{2}$ for all large enough N by lower bounding it as in the proof of Lemma 9.1; and the implicit normalization factor in (11.5) is trivially upper bounded by 1. Thus with $\mathbb{P}_N^{[a,b],\mathbf{x},\mathbf{y}}$ -probability at least ε , we have that the entries of $\tilde{\mathbf{L}}^N(-TN^{2/3})$, $\tilde{\mathbf{L}}^N(TN^{2/3})$ are separated by at least $N^{1/3}$ and are all above $2MN^{1/3}$.

We claim that there exists $\delta > 0$ such that, on the event that the entries of $\tilde{\mathbf{L}}^N(\pm TN^{2/3})$ have the just mentioned properties, $Z_N^{k,T,g} > \delta$. Indeed, with some positive probability 2δ , k independent Bernoulli random walk bridges from $(-TN^{2/3}, \tilde{\mathbf{L}}^N(-TN^{2/3}))$ to $(TN^{2/3}, \tilde{\mathbf{L}}^N(TN^{2/3}))$ will maintain separation at least $\frac{1}{2}N^{1/3}$ throughout $[-TN^{2/3}, TN^{2/3}]$ while staying above $MN^{1/3}$. On this event, the weight function W is again lower bounded by $\frac{1}{2}$ for all large enough N by Lemma 9.1. This completes the proof. \square

Proof of Proposition 6.12. We adopt the shorthand $Z_N^{k,T} = Z_N^{k,[-T,T],\mathbf{L}^N(-TN^{2/3}),\mathbf{L}^N(TN^{2/3}),L_{k+1}^N}$. By Theorem 6.10 (lower tail control) and Proposition 10.2 (upper tail control), there exists $M = M(\varepsilon, k, T)$ such that $\mathbb{P}(\text{RangeCtrl}) \geq 1 - \frac{1}{4}\varepsilon$, where

$$\text{RangeCtrl} = \left\{ \sup_{xN^{-2/3} \in [-2T, 2T]} |L_{k+1}^N(x)| \leq MN^{1/3} \right\}.$$

Let U_1 and U_2 be as in (11.1). On RangeCtrl , by Lemma 10.1, there exists $P = P(\varepsilon, k, T, M) = P(\varepsilon, k, T)$ such that $U_1 \neq -2T$ and $U_2 \neq 2T$, i.e., (11.1) holds. Next, by Theorem 9.2, let $\eta = \eta(\varepsilon, k, T) > 0$ be such that $\mathbb{P}(\text{Sep}_k^N(\eta, \{U_1, U_2\}, \mathbf{L}^N)) > 1 - \frac{1}{4}\varepsilon$. Let $\text{Fav} = \text{RangeCtrl} \cap \text{Sep}_k^N(\eta, \{U_1, U_2\}, \mathbf{L}^N)$, so that $\mathbb{P}(\text{Fav}^c) \leq \frac{1}{2}\varepsilon$.

Let $\mathcal{F} = \mathcal{F}_{\text{ext}}(k, \llbracket U_1 N^{2/3}, U_2 N^{2/3} \rrbracket, \mathbf{L}^N)$, and note that $\llbracket U_1 N^{2/3}, U_2 N^{2/3} \rrbracket$ forms a stopping domain with respect to (L_1^N, \dots, L_k^N) (Definition 6.1), since U_1, U_2 are measurable with respect to L_{k+1}^N . Conditionally on \mathcal{F} , let \mathbb{P}_N be the law of $\mathbf{L}^N|_{\llbracket 1, k \rrbracket \times \llbracket U_1 N^{2/3}, U_2 N^{2/3} \rrbracket}$ and adopt the shorthand $\tilde{\mathbb{P}}_N$ for the law defined by (11.2). Let $\tilde{\mathbf{L}}^N \sim \tilde{\mathbb{P}}_N$. Again conditionally on \mathcal{F} , define $\tilde{\mathbf{L}}^{N,\text{res}}$ and $\mathbf{L}^{N,\text{res}}$ (“res” short for restricted) by

$$\tilde{L}_i^{N,\text{res}} := \tilde{L}_i^N|_{\llbracket U_1 N^{2/3}, U_2 N^{2/3} \rrbracket \setminus \llbracket -TN^{2/3}, TN^{2/3} \rrbracket}$$

and $L_i^{N,\text{res}} := L_i^N|_{\llbracket U_1 N^{2/3}, U_2 N^{2/3} \rrbracket \setminus \llbracket -TN^{2/3}, TN^{2/3} \rrbracket}$ for $i \in \llbracket 1, k \rrbracket$, and let $\tilde{\mathbb{P}}_N^{\text{res}}$ and $\mathbb{P}_N^{\text{res}}$, respectively, be their laws. Note that, for any collection $\gamma : \llbracket 1, k \rrbracket \times \llbracket U_1 N^{2/3}, U_2 N^{2/3} \rrbracket \setminus \llbracket -TN^{2/3}, TN^{2/3} \rrbracket \rightarrow \mathbb{Z}$ of Bernoulli paths,

$$\frac{d\mathbb{P}_N^{\text{res}}}{d\tilde{\mathbb{P}}_N^{\text{res}}}(\gamma) = (\tilde{Z}_N^{k,T})^{-1} Z_N^{k,T}(\gamma), \quad (11.5)$$

where $Z_N^{k,T}(\gamma) := Z_N^{k,[-T,T],\gamma(-TN^{2/3}),\gamma(TN^{2/3}),L_{k+1}^N}$ as in (11.3) and $\tilde{Z}_N^{k,T} := \tilde{\mathbb{E}}_N[Z_N^{k,T}(\gamma)]$. Since $Z_N^{k,T}(\gamma)$ is a function of $\gamma(\pm TN^{2/3})$ (L_{k+1}^N is conditioned on), which have the same joint distribution when γ is distributed as $\tilde{\mathbb{P}}_N^{\text{res}}$ or $\tilde{\mathbb{P}}_N$, it holds that $\tilde{Z}_N^{k,T} = \tilde{\mathbb{E}}_N[Z_N^{k,T}(\gamma)]$. Similarly, $Z_N^{k,T} = Z_N^{k,T}(\mathbf{L}^N)$ has the same distribution under \mathbb{P}_N and $\mathbb{P}_N^{\text{res}}$. Thus, since Fav is \mathcal{F} -measurable,

$$\mathbb{P}\left(Z_N^{k,T} < \delta\right) \leq \mathbb{E}\left[\mathbb{P}_{\mathcal{F}}\left(Z_N^{k,T} < \delta\right) \mathbb{1}_{\text{Fav}}\right] + \mathbb{P}(\text{Fav}^c) = \mathbb{E}\left[\mathbb{P}_N^{\text{res}}\left(Z_N^{k,T} < \delta\right) \mathbb{1}_{\text{Fav}}\right] + \frac{1}{2}\varepsilon.$$

Now by (11.5), the previous display equals

$$\mathbb{E}\left[\left(\tilde{Z}_N^{k,T}\right)^{-1} \tilde{\mathbb{E}}_N^{\text{res}}\left[\mathbb{1}_{Z_N^{k,T} < \delta} Z_N^{k,T}\right] \mathbb{1}_{\text{Fav}}\right] + \frac{1}{2}\varepsilon. \quad (11.6)$$

On Fav, $(L_i^N(\pm TN^{2/3}))_{i=1}^k$ and L_{k+1}^N satisfy the conditions in Lemma 11.1. So we have that, for some $\delta', \varepsilon' > 0$ (the δ, ε provided by Lemma 11.1),

$$\tilde{Z}_N^{k,T} = \tilde{\mathbb{E}}[Z_N^{k,T}] \geq \rho := \delta' \varepsilon',$$

This yields that (11.6) is upper bounded by

$$\rho^{-1} \cdot \mathbb{E} \left[\tilde{\mathbb{E}}_N^{\text{res}} \left[\mathbb{1}_{Z_N^{k,T} < \delta} \right] \right] + \frac{1}{2} \varepsilon \leq \delta \rho^{-1} + \frac{1}{2} \varepsilon.$$

Picking $\delta = \frac{1}{2} \varepsilon \rho$ completes the proof. \square

12. BROWNIAN GIBBS PROPERTY IN THE LIMIT

In this section we prove that all weak limit points of \mathfrak{L}^N as defined in (3.13) possess the Brownian Gibbs property, thus establishing Proposition 6.5. The first step is to compare the partition function associated to the Hall-Littlewood Gibbs property with the probability of separation (its analog for the Brownian Gibbs property); we do this in the next section. Then we will give the proof of Proposition 6.5 in Section 12.2. As in the last few sections, we assume, without explicitly stating it again, that \mathbf{L}^N satisfies Assumptions 1 and 2.

12.1. Comparing the partition function and the separation probability. To emphasize the separation required with the lower boundary condition, in this section we extend the notation (9.1) as follows: for a set $A \subseteq \mathbb{R}$, an integer $k \in \mathbb{N}$, $\Lambda \subseteq \mathbb{N}$ a (possibly infinite) interval with $\llbracket 1, k \rrbracket \subseteq \Lambda$, a process $\mathbf{X} : \Lambda \times \mathbb{R} \rightarrow \mathbb{R}$, a process $Y : \mathbb{R} \rightarrow \mathbb{R}$, and $\delta > 0$, we define the event

$$\text{Sep}_k^N(\delta, A, \mathbf{X}, Y) = \left\{ \min_{i=1, \dots, k-1} \inf_{x \in N^{-2/3} \in A} (X_i(x) - X_{i+1}(x)) \geq \delta N^{1/3} \right\} \cap \left\{ \inf_{x \in N^{-2/3} \in A} (X_k(x) - Y(x)) \geq \delta N^{1/3} \right\}, \quad (12.1)$$

i.e., in the notation (9.1), if we define $\tilde{\mathbf{X}} : \llbracket 1, k+1 \rrbracket \times \mathbb{R} \rightarrow \mathbb{R}$ by $\tilde{X}_i(\cdot) = X_i(\cdot)$ for $i = 1, \dots, k$ and $\tilde{X}_{k+1}(\cdot) = Y(\cdot)$, then $\text{Sep}_k^N(\delta, A, \mathbf{X}, Y) = \text{Sep}_k^N(\delta, A, \tilde{\mathbf{X}})$. At times we will drop the set A from the notation, but this will be explicitly stated.

For the next statement, recall W from Definition 3.15.

Lemma 12.1. *Fix $a > b$ and $k \in \mathbb{N}$. Let $\mathcal{F} = \mathcal{F}_{\text{ext}}(k, \llbracket aN^{2/3}, bN^{2/3} \rrbracket, \mathbf{L}^N)$ and $\mathbf{B} = (B_1, \dots, B_k)$ be a collection of k independent Bernoulli random walk bridges, with B_i from $(aN^{2/3}, L_i^N(aN^{2/3}))$ to $(bN^{2/3}, L_i^N(bN^{2/3}))$. For any $\varepsilon > 0$, there exist $N_0 = N_0(\varepsilon, k, b-a)$ and $\delta = \delta(\varepsilon, k, b-a) > 0$ such that, for all $N \geq N_0$,*

$$\mathbb{P} \left(\frac{\mathbb{E}_{\mathcal{F}}[W(\mathbf{B}, L_{k+1}^N, \llbracket aN^{2/3}, bN^{2/3} \rrbracket)]}{\mathbb{P}_{\mathcal{F}}(\text{Sep}_k^N(\delta, [a, b], \mathbf{B}, L_{k+1}^N))} \in [1 - \varepsilon, 1 + \varepsilon] \right) \geq 1 - \varepsilon.$$

Proof. Adopt the shorthand $\text{Sep}_k^N(\delta, \mathbf{B}, L_{k+1}^N) = \text{Sep}_k^N(\delta, [a, b], \mathbf{B}, L_{k+1}^N)$ and drop the interval $\llbracket aN^{2/3}, bN^{2/3} \rrbracket$ from the W notation. We first pick $\delta > 0$ such that, by Theorem 9.2,

$$\mathbb{P}(\text{Sep}_k^N(\delta, \mathbf{L}^N, L_{k+1}^N)) \geq 1 - \varepsilon^2.$$

Since the lefthand side of this inequality equals $\mathbb{E}[\mathbb{P}_{\mathcal{F}}(\text{Sep}_k^N(\delta, \mathbf{L}^N, L_{k+1}^N))]$, and the conditional probability is a random variable taking values in $[0, 1]$, it follows that, with probability at least $1 - \varepsilon$,

$$\mathbb{P}_{\mathcal{F}}(\text{Sep}_k^N(\delta, \mathbf{L}^N, L_{k+1}^N)) \geq 1 - \varepsilon.$$

We work on the event that the previous inequality holds. We have the following string of inequalities, using $W(\mathbf{B}, L_{k+1}^N) \leq 1$ in the first inequality, the Hall-Littlewood Gibbs property to go from the second to the third line, and the previous display for the inequality in the last line:

$$\begin{aligned} \mathbb{P}_{\mathcal{F}}(\text{Sep}_k^N(\delta, \mathbf{B}, L_{k+1}^N)) &\geq \mathbb{E}_{\mathcal{F}}[\mathbb{1}_{\text{Sep}_k^N(\delta, \mathbf{B}, L_{k+1}^N)} W(\mathbf{B}, L_{k+1}^N)] \\ &= \frac{\mathbb{E}_{\mathcal{F}}[\mathbb{1}_{\text{Sep}_k^N(\delta, \mathbf{B}, L_{k+1}^N)} W(\mathbf{B}, L_{k+1}^N)]}{\mathbb{E}_{\mathcal{F}}[W(\mathbf{B}, L_{k+1}^N)]} \cdot \mathbb{E}_{\mathcal{F}}[W(\mathbf{B}, L_{k+1}^N)] \\ &= \mathbb{P}_{\mathcal{F}}(\text{Sep}_k^N(\delta, \mathbf{L}^N, L_{k+1}^N)) \cdot \mathbb{E}_{\mathcal{F}}[W(\mathbf{B}, L_{k+1}^N)] \geq (1 - \varepsilon) \mathbb{E}_{\mathcal{F}}[W(\mathbf{B}, L_{k+1}^N)]. \end{aligned}$$

It also trivially holds that $\mathbb{E}_{\mathcal{F}}[W(\mathbf{B}, L_{k+1}^N)] \geq \mathbb{E}_{\mathcal{F}}[W(\mathbf{B}, L_{k+1}^N) \mathbb{1}_{\text{Sep}_k^N(\delta, \mathbf{B}, L_{k+1}^N)}]$ and that, on the event $\text{Sep}_k^N(\delta, \mathbf{B}, L_{k+1}^N)$ and by Lemma 9.1, $W(\mathbf{B}, L_{k+1}^N) \geq 1 - \varepsilon$ for all large enough N . This yields that, for such N ,

$$\mathbb{E}_{\mathcal{F}}[W(\mathbf{B}, L_{k+1}^N)] \geq (1 - \varepsilon) \mathbb{P}_{\mathcal{F}}(\text{Sep}_k^N(\delta, \mathbf{B}, L_{k+1}^N)).$$

This completes the proof after relabeling ε . \square

Corollary 12.2. *Fix $\varepsilon \in (0, 1)$, $k \in \mathbb{N}$, $M > 0$, and $a < b$. Let $\mathcal{F} = \mathcal{F}_{\text{ext}}(k, [aN^{2/3}, bN^{2/3}], L^N)$ and $\mathbf{B} = (B_1, \dots, B_k)$ be a collection of k independent Bernoulli random walk bridges with B_i from $(aN^{2/3}, L_i^N(aN^{2/3}))$ to $(bN^{2/3}, L_i^N(bN^{2/3}))$. There exist $N_0 = N_0(\varepsilon, k, b - a, M)$ and $\delta = \delta(\varepsilon, k, b - a, M) > 0$ such that, for any $N \geq N_0$, the following holds with probability at least $1 - \varepsilon$. For any bounded measurable function $F : \mathcal{C}([1, k] \times [aN^{2/3}, bN^{2/3}], \mathbb{R}) \rightarrow \mathbb{R}$ such that $\sup |F| \leq M$,*

$$\left| \frac{\mathbb{E}_{\mathcal{F}} [F(\mathbf{B}) W(\mathbf{B}, L_{k+1}^N, [aN^{2/3}, bN^{2/3}])]}{\mathbb{E}_{\mathcal{F}} [W(\mathbf{B}, L_{k+1}^N, [aN^{2/3}, bN^{2/3}])]} - \mathbb{E}_{\mathcal{F}} [F(\mathbf{B}) \mid \text{Sep}_k^N(\delta, [a, b], \mathbf{B}, L_{k+1}^N)] \right| \leq \varepsilon.$$

Proof. We again adopt the shorthand $\text{Sep}_k^N(\delta, \mathbf{B}, L_{k+1}^N) = \text{Sep}_k^N(\delta, [a, b], \mathbf{B}, L_{k+1}^N)$ and drop the interval $[aN^{2/3}, bN^{2/3}]$ from the W notation. We may assume that $F \geq 0$ as we have assumed F is bounded and adding a constant to F does not change the lefthand side of the inequality we are proving. Let $\varepsilon' = \varepsilon M^{-1}$. Pick $\delta > 0$ from Lemma 12.1 with ε there equal to ε' , and let $N_0 = N_0(\varepsilon, k, b - a, M)$ be such that $W(\mathbf{B}, L_{k+1}^N) \geq 1 - \varepsilon'$ on $\text{Sep}_k^N(\delta, \mathbf{B}, L_{k+1}^N)$ for $N > N_0$ (by Lemma 9.1). Then

$$\begin{aligned} \frac{\mathbb{E}_{\mathcal{F}} [F(\mathbf{B}) W(\mathbf{B}, L_{k+1}^N)]}{\mathbb{E}_{\mathcal{F}} [W(\mathbf{B}, L_{k+1}^N)]} &\geq \frac{\mathbb{E}_{\mathcal{F}} [F(\mathbf{B}) \mathbb{1}_{\text{Sep}_k^N(\delta, \mathbf{B}, L_{k+1}^N)} W(\mathbf{B}, L_{k+1}^N)]}{\mathbb{E}_{\mathcal{F}} [W(\mathbf{B}, L_{k+1}^N)]} \\ &\geq (1 - \varepsilon') \frac{\mathbb{E}_{\mathcal{F}} [F(\mathbf{B}) \mathbb{1}_{\text{Sep}_k^N(\delta, \mathbf{B}, L_{k+1}^N)}]}{\mathbb{E}_{\mathcal{F}} [W(\mathbf{B}, L_{k+1}^N)]}. \end{aligned}$$

Now invoking Lemma 12.1 and our choice of δ , with probability at least $1 - \varepsilon$, the previous display is lower bounded by

$$\frac{1 - \varepsilon'}{1 + \varepsilon'} \cdot \frac{\mathbb{E}_{\mathcal{F}} [F(\mathbf{B}) \mathbb{1}_{\text{Sep}_k^N(\delta, \mathbf{B}, L_{k+1}^N)}]}{\mathbb{P}_{\mathcal{F}}(\text{Sep}_k^N(\delta, \mathbf{B}, L_{k+1}^N))} = \frac{1 - \varepsilon'}{1 + \varepsilon'} \cdot \mathbb{E}_{\mathcal{F}} [F(\mathbf{B}) \mid \text{Sep}_k^N(\delta, \mathbf{B}, L_{k+1}^N)].$$

Rearranging this gives one side of the claimed inequality after relabeling ε , since F is bounded by M , and the other is obtained by replacing F with $M - F$, and rearranging appropriately again. \square

12.2. Brownian Gibbs property in the limit. Throughout this section, we recall the definition of the Brownian Gibbs property from Definition 6.4.

Lemma 12.3. *For each $N \in \mathbb{N}$, let B^N be a Bernoulli random walk bridge from $(0, 0)$ to (N, z_N) , and suppose $z_N/N \rightarrow p \in (-1, 0)$ as $N \rightarrow \infty$. Then*

$$N^{-1/2}(B^N(Nt) - z_N t) \xrightarrow{d} B^{\text{Br}}(t)$$

as $N \rightarrow \infty$ as processes on $\mathcal{C}([0, 1], \mathbb{R})$ with the topology of uniform convergence, where B^{Br} is a Brownian bridge on $[0, 1]$ with zero endpoints and variance $p(1 - p)$.

Proof. This follows from the KMT coupling Lemma 6.14 (with the p there equal to z_N/N here). \square

Proof of Proposition 6.5. It is sufficient to prove the resampling property when resampling the top k curves for any $k \in \mathbb{N}$, i.e., prove Definition 6.4 holds with $j = 1$, as the conditional distribution in the case of $j > 1$ is obtained from the $j = 1$ case along with the fact that non-intersecting Brownian bridges have the Brownian Gibbs property themselves [DM21, Lemma 2.13] (this is stated in the case of no lower boundary condition, but the proof also applies if there is one). More precisely, given an interval $[a, b]$ and knowledge that the Brownian Gibbs property holds for a line ensemble \mathfrak{L} when $j = 1$ (i.e., when conditioned on $\mathcal{F}_{\text{ext}}(k, [a, b], \mathfrak{L})$), to obtain the same for $j > 1$, one further conditions on $\mathcal{F}_{\text{ext}}(\llbracket j, k \rrbracket, [a, b], \mathfrak{L})$ and makes use of [DM21, Lemma 2.13] along with the fact that iterative conditioning is commutative [Kal21, Theorem 8.15].

Now we turn to prove the $j = 1$ case. For $k \in \mathbb{N}$ and $a < b$, let $\mathfrak{B} : \llbracket 1, k \rrbracket \times [a, b] \rightarrow \mathbb{R}$ with $\mathfrak{B} = (\mathfrak{B}_1, \dots, \mathfrak{B}_k)$ be a collection of k rate two independent Brownian bridges, with $\mathfrak{B}_i(x) = \mathfrak{L}_i(x)$ for $i \in \llbracket 1, k \rrbracket$ and $x \in \{a, b\}$. Similar to (12.1), we extend the definition (9.17) to emphasize the lower boundary condition: for an interval I , define

$$\text{NonInt}_k(I, \mathfrak{B}, \mathfrak{L}_{k+1}) := \left\{ \mathfrak{B}_1(x) > \mathfrak{B}_2(x) > \dots > \mathfrak{B}_k(x) > \mathfrak{L}_{k+1}(x) \text{ for all } x \in I \right\}.$$

In the rest of the proof we take $I = [a, b]$ and omit it from the notation. Let $\mathcal{F} = \mathcal{F}_{\text{ext}}(k, [a, b], \mathfrak{L})$. For any $k \in \mathbb{N}$, $a < b$, and $F : \mathcal{C}(\llbracket 1, k \rrbracket \times [a, b], \mathbb{R}) \rightarrow \mathbb{R}$ bounded and continuous, we have to show that

$$\mathbb{E}[F(\mathfrak{L}) \mid \mathcal{F}] = \mathbb{E}_{\mathcal{F}}[F(\mathfrak{B}) \mid \text{NonInt}(\mathfrak{B}, \mathfrak{L}_{k+1})],$$

where $F(\mathbf{X})$ is shorthand for $F(\mathbf{X}|_{\llbracket 1, k \rrbracket \times [a, b]})$.

By the definition of conditional expectations, and a monotone class argument, the previous display will be proven if we show that, for any $j \in \mathbb{N}$, $c < d$, and $G : \mathcal{C}(\llbracket 1, j \rrbracket \times [c, d] \setminus (\llbracket 1, k \rrbracket \times [a, b]), \mathbb{R}) \rightarrow \mathbb{R}$ bounded and continuous (with $G(\mathbf{X})$ shorthand for $G(\mathbf{X}|_{\llbracket 1, j \rrbracket \times [c, d] \setminus (\llbracket 1, k \rrbracket \times [a, b])})$),

$$\mathbb{E}[F(\mathfrak{L}) \cdot G(\mathfrak{L})] = \mathbb{E}[\mathbb{E}_{\mathcal{F}}[F(\mathfrak{B}) \mid \text{NonInt}(\mathfrak{B}, \mathfrak{L}_{k+1})] \cdot G(\mathfrak{L})]. \quad (12.2)$$

By Skorokhod's representation theorem and by the weak convergence of \mathfrak{L}^N to \mathfrak{L} , we may assume that we work on a probability space such that $\mathfrak{L}^N \rightarrow \mathfrak{L}$ uniformly on compact sets almost surely. Then we obtain, with $\mathcal{F}^N := \mathcal{F}_{\text{ext}}^N(k, \llbracket \beta^{-1}aN^{2/3}, \beta^{-1}bN^{2/3} \rrbracket, \mathbf{L}^N)$, by the dominated convergence theorem and the Hall-Littlewood Gibbs property, that

$$\begin{aligned} \mathbb{E}[F(\mathfrak{L}) \cdot G(\mathfrak{L})] &= \lim_{N \rightarrow \infty} \mathbb{E}[F(\mathfrak{L}^N) \cdot G(\mathfrak{L}^N)] \\ &= \lim_{N \rightarrow \infty} \mathbb{E}[\mathbb{E}[F(\mathfrak{L}^N) \mid \mathcal{F}^N] \cdot G(\mathfrak{L}^N)] \\ &= \lim_{N \rightarrow \infty} \mathbb{E}\left[\frac{\mathbb{E}_{\mathcal{F}^N}[F(\mathfrak{B}^N)W(\mathbf{B}^N, L_{k+1}^N)]}{\mathbb{E}_{\mathcal{F}^N}[W(\mathbf{B}^N, L_{k+1}^N)]} \cdot G(\mathfrak{L}^N) \right], \end{aligned} \quad (12.3)$$

the last line using the Hall-Littlewood Gibbs property and with $\mathfrak{B}^N = (B_1^N, \dots, B_k^N) : \llbracket 1, k \rrbracket \times [a, b] \rightarrow \mathbb{R}$ given by (recall p from Assumption 2, β and σ from (3.12), and the definition of \mathfrak{L}^N in terms of \mathbf{L}^N from (3.13)) $\mathfrak{B}^N = T_{p,\lambda,N}(\mathbf{B}^N)$, i.e.,

$$\mathfrak{B}_i^N(x) = \sigma^{-1} N^{-1/3} \left(B_i^N(\beta x N^{2/3}) - p \beta x N^{2/3} \right)$$

with $\mathbf{B}^N = (B_1^N, \dots, B_k^N)$ a family of k independent Bernoulli random walk bridges, with B_i^N from $(\beta^{-1} a N^{2/3}, L_i^N(\beta^{-1} a N^{2/3}))$ to $(\beta^{-1} b N^{2/3}, L_i^N(\beta^{-1} b N^{2/3}))$. Now, by Lemma 12.3, it holds that \mathfrak{B}^N converges weakly as $N \rightarrow \infty$ to $\mathfrak{B} = (\mathfrak{B}_1, \dots, \mathfrak{B}_k)$, as above, a collection of k independent rate two Brownian bridges with \mathfrak{B}_i going from $(a, \mathfrak{L}_i(a))$ to $(b, \mathfrak{L}_i(b))$; the fact that the rate of the Brownian bridges is 2 is a consequence of the relation (3.12) between β and σ in the definitions of \mathfrak{L}^N and thus \mathfrak{B}^N .

Recall the extended definition of Sep from (12.1). Because it requires separation of order $N^{1/3}$, which should not be present for the limiting objects, we define an event ScSep (scaled separation) for an interval $[a, b] \subset \mathbb{R}$, an integer $k \in \mathbb{N}$, a (possibly infinite) interval $\Lambda \subseteq \mathbb{N}$ such that $\llbracket 1, k \rrbracket \subseteq \Lambda$, and processes $\mathbf{X} : \Lambda \times \mathbb{R} \rightarrow \mathbb{R}$ and $Y : \mathbb{R} \rightarrow \mathbb{R}$, by

$$\begin{aligned} \text{ScSep}_k(\delta, [a, b], \mathbf{X}, Y) := & \left\{ \min_{i=1, \dots, k-1} \inf_{x \in [a, b]} (X_i(x) - X_{i+1}(x)) \geq \delta \right\} \\ & \cap \left\{ \inf_{x \in [a, b]} (X_{k+1}(x) - Y(x)) \geq \delta \right\}. \end{aligned}$$

Then observe that, by the definitions of \mathfrak{B}^N and \mathfrak{L}^N , it holds that

$$\text{Sep}_k^N(\delta \sigma, [\beta^{-1} a, \beta^{-1} b], \mathbf{B}^N, L_{k+1}^N) = \text{ScSep}_k(\delta, [a, b], \mathfrak{B}^N, \mathfrak{L}_{k+1}^N).$$

By Corollary 12.2 and the previous display, we obtain that there is a sequence $\varepsilon_{N,\delta} \downarrow \varepsilon_\delta$ as $N \rightarrow \infty$, where ε_δ is a sequence which goes to 0 as $\delta \downarrow 0$, such that (12.3) equals

$$\begin{aligned} & \lim_{N \rightarrow \infty} \mathbb{E} \left[(\mathbb{E}_{\mathcal{F}^N} [F(\mathfrak{B}^N) \mid \text{ScSep}_k(\delta, [a, b], \mathfrak{B}^N, \mathfrak{L}_{k+1}^N)] + \varepsilon_{N,\delta}) \cdot G(\mathfrak{L}^N) \right] \\ &= \mathbb{E} \left[\lim_{N \rightarrow \infty} (\mathbb{E}_{\mathcal{F}^N} [F(\mathbf{B}^N) \mid \text{ScSep}_k(\delta, [a, b], \mathfrak{B}^N, \mathfrak{L}_{k+1}^N)] + \varepsilon_{N,\delta}) \cdot \lim_{N \rightarrow \infty} G(\mathfrak{L}^N) \right] \\ &= \mathbb{E} [(\mathbb{E}_{\mathcal{F}} [F(\mathfrak{B}) \mid \text{ScSep}_k(\delta, [a, b], \mathfrak{B}, \mathfrak{L}_{k+1})] + \varepsilon_\delta) \cdot G(\mathfrak{L})]; \end{aligned}$$

the penultimate equality used the dominated convergence theorem since F and G are bounded and continuous, and the final equality used the Portmanteau theorem along with the fact that $\mathbb{P}(\text{ScSep}_k(\delta, [a, b], \mathfrak{B}, \mathfrak{L}_{k+1})) > 0$ (since \mathfrak{L}_{k+1} is a continuous function and with probability 1 there is strictly positive separation between the endpoints of \mathfrak{B}_i and \mathfrak{B}_{i+1} as well as between those of \mathfrak{B}_k and \mathfrak{B}_{k+1} , as follows from Theorem 9.2) to also take the limit of the conditioning.

Finally taking $\delta \rightarrow 0$ and using that $\mathbb{E}_{\mathcal{F}} [F(\mathfrak{B}) \mid \text{ScSep}_k(\delta, [a, b], \mathfrak{B}, \mathfrak{L}_{k+1})] \rightarrow \mathbb{E}_{\mathcal{F}} [F(\mathfrak{B}) \mid \text{NonInt}(\mathfrak{B}, \mathfrak{L}_{k+1})]$ completes the proof. \square

APPENDIX A. THE YANG-BAXTER EQUATION, S6V, AND THE q -BOSON MODEL

In this section we give a self-contained proof of the partition function expression in (3.1) and of Proposition 3.12 on the distributional relation of the top line of the colored Hall-Littlewood line ensemble and the colored height function of the colored S6V model. First, recall the description of the colored q -Boson model from Section 3.1 and the colored S6V model from Section 2.3, with the domain restriction performed as in Section 3.2.1. In particular, in both models we have a spectral parameter $z \in (0, 1)$ fixed and a boundary condition $\sigma : \llbracket 1, N \rrbracket \rightarrow \llbracket 1, N \rrbracket$ where the arrow horizontally entering $(1, k)$ (for colored S6V) and the arrow horizontally entering $(-K, k)$ for all large enough K (for colored q -Boson) are both of color $\sigma(k)$, for each $k \in \llbracket 1, N \rrbracket$. To explain the relation between the colored q -Boson model and the colored S6V model, we need the Yang-Baxter

relation enjoyed by these models, which we introduce next. Then in Section A.2 we establish the expression for the partition function of the colored q -Boson model and in Section A.3 we give the proof of Proposition 3.12.

A.1. Yang-Baxter equation. The Yang-Baxter equation is an equality of partition functions of configurations consisting of three vertices. In our case, the first vertex has vertex weight given by the weights of the colored S6V model (Figure 8) and the other two vertices have weights given by the L_u weights (Figure 10). Let us write the weights from Figure 8 with spectral parameter $u \in (0, 1)$ as $R_u(a, i; b, j)$ with $a, i, b, j \in \llbracket 0, N \rrbracket$, where recall a, i, b, j respectively represent the colors of the arrows vertically entering, horizontally entering, vertically exiting, and horizontally exiting from the vertex. Unlike the convention in Section 2.3, here we will take 0 to represent the absence of an arrow, so as to match the setup of the colored q -Boson model. In this notation, the Yang-Baxter equation can be written as follows; it was originally due to [KRS81, Baz85, Jim86], but the notation we have adopted is from [BW22] (it can also be verified directly from the formulas for the weights).

Lemma A.1 (Yang-Baxter equation, [BW22, Proposition 2.3.1]). *Fix $a_1, i_1, b_2, j_2 \in \llbracket 0, N \rrbracket$ and $\mathbf{I}, \mathbf{J} \in \mathbb{Z}_{\geq 0}^N$. Let $x, y \in (0, 1)$ and let $z = y/x$. Then it holds that*

$$\begin{aligned} & \sum_{\substack{b_1, j_1 \in \llbracket 0, N \rrbracket, \\ \mathbf{K} \in \mathbb{Z}_{\geq 0}^N}} R_{y/x}(a_1, i_1; b_1, j_1) L_x(\mathbf{I}, j_1; \mathbf{K}, j_2) L_y(\mathbf{K}, b_1; \mathbf{J}, b_2) \\ &= \sum_{\substack{b_1, j_1 \in \llbracket 0, N \rrbracket, \\ \mathbf{K} \in \mathbb{Z}_{\geq 0}^N}} L_y(\mathbf{I}, a_1; \mathbf{K}, b_1) L_x(\mathbf{K}, i_1; \mathbf{J}, j_1) R_{y/x}(b_1, j_1; b_2, j_2); \end{aligned}$$

here L_u and R_u are zero if their arguments do not satisfy colored arrow conservation.

Diagrammatically, the Yang-Baxter equation can be written as follows (we adopt a style of depiction similar to [BW22]).

$$\sum_{\substack{b_1, j_1 \in \llbracket 0, N \rrbracket, \\ \mathbf{K} \in \mathbb{Z}_{\geq 0}^N}} \begin{array}{c} \begin{array}{c} \begin{array}{c} x \rightarrow i_1 \\ y \rightarrow a_1 \end{array} \\ \begin{array}{c} \diagup \quad \diagdown \\ \diagdown \quad \diagup \end{array} \\ \begin{array}{c} b_1 \\ j_1 \end{array} \end{array} \begin{array}{c} \begin{array}{c} \uparrow \\ \uparrow \\ \uparrow \end{array} \\ \begin{array}{c} \mathbf{K} \\ \mathbf{K} \\ \mathbf{K} \end{array} \\ \begin{array}{c} \uparrow \\ \uparrow \\ \uparrow \end{array} \\ \begin{array}{c} \mathbf{I} \\ \mathbf{I} \\ \mathbf{I} \end{array} \end{array} \begin{array}{c} \begin{array}{c} \rightarrow b_2 \\ \rightarrow j_2 \end{array} \\ \begin{array}{c} \diagdown \quad \diagup \\ \diagup \quad \diagdown \end{array} \\ \begin{array}{c} b_2 \\ j_2 \end{array} \end{array} \end{array} = \sum_{\substack{b_1, j_1 \in \llbracket 0, N \rrbracket, \\ \mathbf{K} \in \mathbb{Z}_{\geq 0}^N}} \begin{array}{c} \begin{array}{c} \begin{array}{c} x \rightarrow i_1 \\ y \rightarrow a_1 \end{array} \\ \begin{array}{c} \diagdown \quad \diagup \\ \diagup \quad \diagdown \end{array} \\ \begin{array}{c} b_1 \\ j_1 \end{array} \end{array} \begin{array}{c} \begin{array}{c} \uparrow \\ \uparrow \\ \uparrow \end{array} \\ \begin{array}{c} \mathbf{K} \\ \mathbf{K} \\ \mathbf{K} \end{array} \\ \begin{array}{c} \uparrow \\ \uparrow \\ \uparrow \end{array} \\ \begin{array}{c} \mathbf{I} \\ \mathbf{I} \\ \mathbf{I} \end{array} \end{array} \begin{array}{c} \begin{array}{c} \rightarrow b_2 \\ \rightarrow j_2 \end{array} \\ \begin{array}{c} \diagup \quad \diagdown \\ \diagdown \quad \diagup \end{array} \\ \begin{array}{c} b_2 \\ j_2 \end{array} \end{array} \end{array} \quad (\text{A.1})$$

Here, the left and righthand sides mean the sum over the weights of the depicted configurations of the three vertices, and the arc between two edges indicates which of those two edges corresponds to exiting vertically (upper end of arc) and horizontally (lower end of arc). The weights of the two vertices at the intersection of the two horizontal lines and the thick vertical line are the L_u weights (so they can hold an arbitrary number of arrows) with spectral parameter u as indicated by x or y at the beginning of the line (which should be followed straight through the cross), while the weight of the vertex at the center of the cross is the R_z weights with spectral parameter $z = y/x$.

A.2. Partition function of the colored q -Boson model. With the Yang-Baxter equation in hand, we may proceed to derive the expression for the partition function of the colored q -Boson model given in (3.1). To do this we consider an augmented vertex model, as in Figure 22, by the following informal description (see the next paragraph for a more formal one). We attach a copy of an $M \times N$ rectangular grid (which we denote \mathcal{R}_1), each of whose vertices has vertex weights given by the R_z -weights (i.e., with spectral parameter z as that of the colored q -Boson model), to the left of the original domain $\mathbb{Z}_{\leq 0} \times \llbracket 1, N + M \rrbracket$ (which we denote \mathcal{R}_2). The augmented model

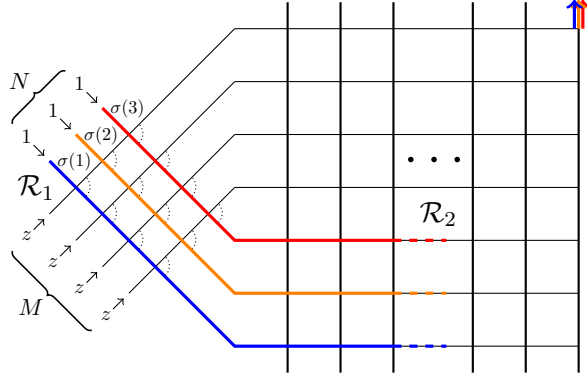


FIGURE 22. The model with the $M \times N$ rectangle of \mathbb{R}_z -weight vertices attached to the left. If any arrow tries to deviate from the configuration depicted except for finitely many columns at the right end (i.e., the portion to the right of the \dots), some arrow must travel infinitely far horizontally in the top M rows, where the weight of a single arrow moving horizontally (with no other arrows incident) across a vertex is $z \in (0, 1)$; thus any such configuration has weight zero and the depicted configuration must occur in all but finitely many columns (that is, to the left of the \dots). The arrows paths have not been shown in the region to the right of the \dots , where their trajectories are random.

has boundary conditions given by an arrow of color $\sigma(i)$ horizontally entering at the i^{th} row of the just added rectangle, no arrows vertically entering, no arrows horizontally exiting, and all arrows vertically exiting at $(0, N + M)$ in the original domain.

We are being somewhat informal in saying to attach the $M \times N$ rectangle \mathcal{R}_1 to the “left” of the semi-infinite domain \mathcal{R}_2 ; more formally, a configuration of the augmented model (with boundary condition σ) consists of an assignment of arrow configurations to the vertices of \mathcal{R}_1 as well as \mathcal{R}_2 such that (i) consistency and colored arrow conservation are satisfied within each, (ii) the entering boundary condition for \mathcal{R}_1 is given by σ , (iii) the exiting boundary condition for \mathcal{R}_2 is that $(\#\sigma^{-1}(\{j\}))_{j=1}^N$ vertically exits from $(0, N + M)$, and (iv) the exiting arrow configurations of \mathcal{R}_1 equals the boundary condition of \mathcal{R}_2 as shown in Figure 22, i.e., for all large enough K and all $y \in \llbracket 1, N + M \rrbracket$, the arrow configuration at $(-K, y) \in \mathcal{R}_2$ equals $(0^N, \tau_y; 0^N, \tau_y)$, where $\tau_y \in \llbracket 0, N \rrbracket$ is the color of the arrow exiting \mathcal{R}_1 from the y^{th} vertex on its right and top boundaries (counted counterclockwise).

We first observe that the horizontally entering arrows to \mathcal{R}_1 are forced to go horizontally straight through: if any arrow does not pass straight through, at least one arrow will enter \mathcal{R}_2 through one of the top M lines and then travel an infinite horizontal distance; any such configuration of arrows has weight zero since, under the L_z weights, the individual vertex weight of passing horizontally through a given vertex in the top M rows is $z < 1$. Thus the partition function $\mathcal{Z}_\sigma^{\text{aug}}$ of the augmented model is the partition function $\mathcal{Z}_\sigma^{\text{cB}}$ of the original colored q -Boson model (with boundary condition σ) multiplied by the weight of the configuration of arrows passing horizontally straight through \mathcal{R}_1 ; by Figure 8, the latter is $((1 - z)/(1 - qz))^{NM}$, so that

$$\mathcal{Z}_\sigma^{\text{aug}} = \left(\frac{1 - z}{1 - qz} \right)^{NM} \cdot \mathcal{Z}_\sigma^{\text{cB}}. \quad (\text{A.2})$$

Next, observe that there are MN vertices present in the rectangle \mathcal{R}_1 in the augmented model. We move each of these vertices to the right, one at a time (starting at the rightmost corner vertex of the rectangle and ending at the leftmost one), all the way across \mathcal{R}_2 . By the Yang-Baxter equation Lemma A.1 (see also (A.1)), this does not change the partition function $\mathcal{Z}_\sigma^{\text{aug}}$. Upon doing so, we obtain the situation depicted in Figure 23. Observe that again the only configuration of arrows with

non-zero weight is the one depicted, in which the arrows pass horizontally straight through (this uses that an arrow is entering at every one of the top N rows). By Figure 10, the configuration in \mathcal{R}_2 has weight 1, and from Figure 8, the empty configuration in \mathcal{R}_1 also has weight 1. Thus, for any σ ,

$$\mathcal{Z}^{\text{aug}} = 1. \quad (\text{A.3})$$

Note that the partition function was not changed between Figures 22 and 23. In other words, we can conclude from (A.2) and (A.3) that $\mathcal{Z}_\sigma^{\text{cB}} = ((1 - qz)/(1 - z))^{NM}$ for any σ , completing the proof of the claim in (3.1).

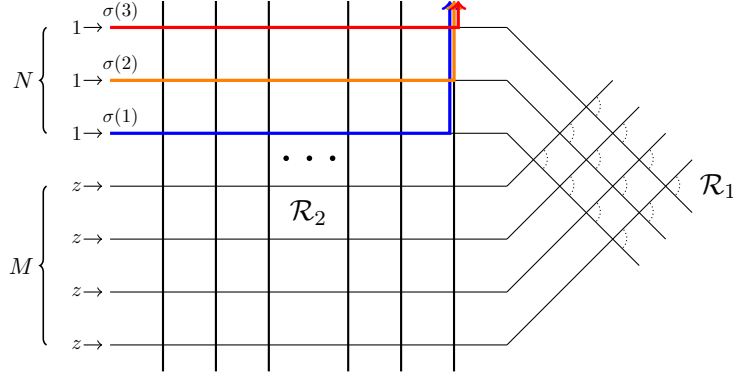


FIGURE 23. The configuration after all the crosses of \mathcal{R}_1 have been pulled all the way through \mathcal{R}_2 to the right by applying (A.1) repeatedly. We note that now, due to the location where all the arrows must exit and by the condition that at most one arrow can be present on each horizontal edge, the arrows are forced into the single configuration of moving horizontally straight through till the very last column, where they move vertically.

A.3. Proof of Proposition 3.12. Fix $M, N \in \mathbb{N}$ and a boundary condition $\sigma : \llbracket 1, N \rrbracket \rightarrow \llbracket 1, N \rrbracket$, and recall h^{S6V} from (2.12). We define a variant height function \tilde{h}^{S6V} as follows. Let $(j_v^{\text{S6V}}, b_v^{\text{S6V}})_{v \in \mathcal{R}_1}$ be sampled from the colored S6V measure on \mathcal{R}_1 with boundary condition σ , where (as in Section 2.3.1) j_v^{S6V} and b_v^{S6V} are the colors of the arrows exiting horizontally and vertically, respectively, from the vertex v . For $k \in \llbracket 1, N \rrbracket$ and $y \in \llbracket 0, N - 1 \rrbracket$, define

$$\tilde{h}^{\text{S6V}}(k; y) := \# \left\{ i > y : j_{(M, i)}^{\text{S6V}} \geq k \right\} = h^{\text{S6V}}(k, 0; y, M). \quad (\text{A.4})$$

For $k \in \llbracket 1, N \rrbracket$ and $y \in \llbracket N, N + M \rrbracket$, define

$$\tilde{h}^{\text{S6V}}(k; y) := \# \left\{ i < N + M - y : b_{(i, N)}^{\text{S6V}} \geq k \right\}.$$

In words, $\tilde{h}^{\text{S6V}}(k; y)$ counts the number of arrows of color at least k which exit from the right and top boundaries of $\llbracket 1, M \rrbracket \times \llbracket 1, N \rrbracket$ from a site which is $(y + 1)^{\text{st}}$ or later when counted counterclockwise from the bottom right corner.

Consider a sequence of Bernoulli paths $L^{(k)} : \llbracket 0, N + M \rrbracket \rightarrow \mathbb{Z}$ such that, (i) $L^{(k)}(0) = \#\sigma^{-1}(\llbracket k, N \rrbracket)$ and $L^{(k)}(N + M) = 0$, and (ii) $L^{(k)}(\cdot) - L^{(k+1)}(\cdot)$ is also a Bernoulli path. We will show that

$$\begin{aligned} \mathbb{P} \left((\tilde{h}^{\text{S6V}}(k; y))_{k \in \llbracket 1, N \rrbracket, y \in \llbracket 0, N + M \rrbracket} = (L^{(k)}(y))_{k \in \llbracket 1, N \rrbracket, y \in \llbracket 0, N + M \rrbracket} \right) \\ = \mathbb{P} \left((L_1^{\text{cHL}, (k)}(y))_{k \in \llbracket 1, N \rrbracket, y \in \llbracket 0, N + M \rrbracket} = (L^{(k)}(y))_{k \in \llbracket 1, N \rrbracket, y \in \llbracket 0, N + M \rrbracket} \right); \end{aligned} \quad (\text{A.5})$$

this implies Proposition 3.12 by a projection of y onto $\llbracket 1, N - 1 \rrbracket$ and (A.4).

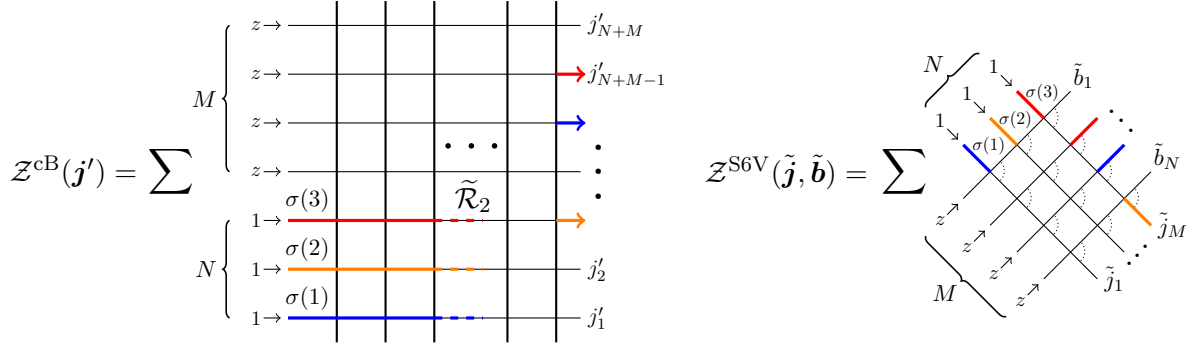


FIGURE 24. The definitions of the partition functions $\mathcal{Z}_\sigma^{\text{cB}}(\mathbf{j}')$ (left) and $\mathcal{Z}_\sigma^{\text{S6V}}(\tilde{\mathbf{b}}, \tilde{\mathbf{j}})$ (right); here the summation means to add the weights of all configurations which satisfy the depicted boundary conditions defined by σ and \mathbf{j}' in the left panel and σ , $\tilde{\mathbf{b}}$, and $\tilde{\mathbf{j}}$ in the right panel.

To establish (A.5), we first define an exiting boundary condition $(j'_{(-1,y)})_{y \in \llbracket 1, N+M \rrbracket}$ in terms of $(L^{(k)}(y))_{k \in \llbracket 1, N \rrbracket, y \in \llbracket 0, N+M \rrbracket}$ as follows: letting $\Delta(L, y) = L(y-1) - L(y) \in \{0, 1\}$ for a Bernoulli path $L : \llbracket 0, N+M \rrbracket \rightarrow \mathbb{Z}$, for $y \in \llbracket 1, N+M \rrbracket$,

$$j'_{(-1,y)} := \min \left\{ k \in \llbracket 1, N \rrbracket : \Delta(L^{(k+1)}, y) = \Delta(L^{(k)}, y) - 1 \right\},$$

where by convention $\Delta(L^{(N+1)}, y) = 0$ for all y and $\min \emptyset = 0$.

Let $(j_v^{\text{cB}})_{v \in \mathcal{R}_2}$ be sampled according to the colored q -Boson measure (as in Section 3.1.1 and Definition 3.1) with boundary condition σ . It follows from Definition 3.7 of $\mathbf{L}^{\text{cHL},(k)}$ that the righthand side of (A.5) equals

$$\mathbb{P} \left(j_{(-1,y)}^{\text{cB}} = j'_{(-1,y)} \text{ for all } y \in \llbracket 1, N+M \rrbracket \right).$$

This in turn equals the ratio of two partition functions, $\mathcal{Z}_\sigma^{\text{cB}}(\mathbf{j}') / \mathcal{Z}_\sigma^{\text{cB}}$ (see the left panel of Figure 24): the numerator is the partition function $\mathcal{Z}_\sigma^{\text{cB}}(\mathbf{j}')$ of the colored q -Boson measure with (incoming) boundary condition σ as well as the (outgoing) boundary condition $(j'_{(-1,y)} : y \in \llbracket 1, N+M \rrbracket)$ at $\{-1\} \times \llbracket 1, N+M \rrbracket$, and the denominator is the partition function $\mathcal{Z}_\sigma^{\text{cB}} = ((1-qz)/(1-z))^{NM}$ of the whole measure, as derived in Section A.2.

Recall that $(b_{(x,N)}^{\text{S6V}}, j_{(M,y)}^{\text{S6V}} : x \in \llbracket 1, M \rrbracket, y \in \llbracket 1, N \rrbracket)$ are sampled according to the colored S6V model with boundary condition σ . Let $\tilde{b}_x := j'_{(-1, N+M+1-x)}$ for $x \in \llbracket 1, M \rrbracket$ and $\tilde{j}_y := j'_{(-1,y)}$ for $y \in \llbracket 1, N \rrbracket$. Then the lefthand side of (A.5) equals

$$\mathbb{P} \left(b_{(x,N)}^{\text{S6V}} = \tilde{b}_x, j_{(M,y)}^{\text{S6V}} = \tilde{j}_y \text{ for all } x \in \llbracket 1, M \rrbracket, y \in \llbracket 1, N \rrbracket \right),$$

which in turn equals the partition function $\mathcal{Z}_\sigma^{\text{S6V}}(\tilde{\mathbf{b}}, \tilde{\mathbf{j}})$ (see the right panel of Figure 24) for colored S6V with (incoming) boundary condition σ and the (outgoing) boundary condition $((\tilde{b}_{(x,N)}, \tilde{j}_{(M,y)}) : x \in \llbracket 1, M \rrbracket, y \in \llbracket 1, N \rrbracket)$ (we do not divide by the normalization constant of the model as a whole since it is 1).

Thus, to establish (A.5), we must show that

$$\frac{\mathcal{Z}_\sigma^{\text{cB}}(\mathbf{j}')}{\mathcal{Z}_\sigma^{\text{cB}}} = \mathcal{Z}_\sigma^{\text{S6V}}(\tilde{\mathbf{b}}, \tilde{\mathbf{j}}). \quad (\text{A.6})$$

We establish this by using the Yang-Baxter equation (A.1) via a similar argument as in the last section. We start from an augmented model with \mathcal{R}_1 to the left of $\tilde{\mathcal{R}}_2 := \mathbb{Z}_{\leq -1} \times \llbracket 1, N+M \rrbracket$, with (incoming) boundary conditions σ and (outgoing) boundary conditions $(j'_{(-1,y)})_{y \in \llbracket 1, N+M \rrbracket}$; see the

left side of Figure 25. By reasoning as in Section A.2, the partition function of this model is $((1-z)/(1-qz))^{NM} \cdot \mathcal{Z}_\sigma^{\text{cB}}(\mathbf{j}') = \mathcal{Z}_\sigma^{\text{cB}}(\mathbf{j}') / \mathcal{Z}_\sigma^{\text{cB}}$.

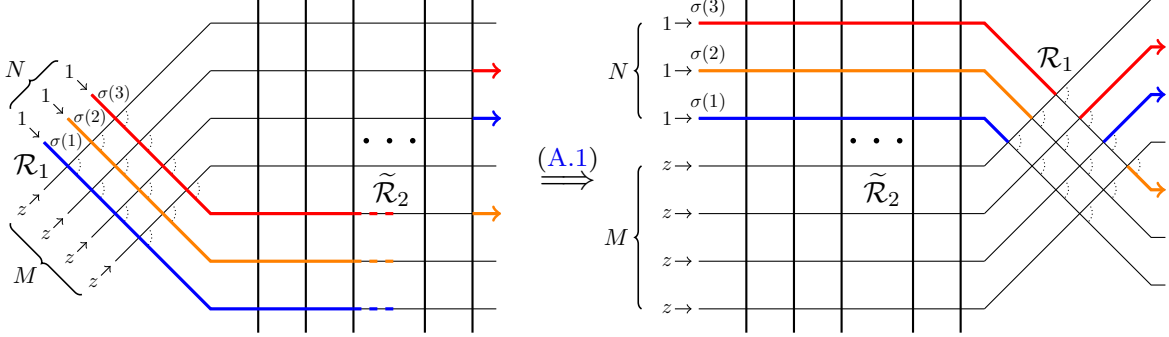


FIGURE 25. Left: The augmented model with outgoing boundary conditions. Right: the same when \mathcal{R}_1 is moved all the way through $\tilde{\mathcal{R}}_2$ using repeated applications of the Yang-Baxter equation (A.1); again, only a single configuration of arrows till \mathcal{R}_1 has non-zero weight.

Now we move the crosses in \mathcal{R}_1 to the right of $\tilde{\mathcal{R}}_2$ using (A.1) again and obtain the situation in the right side of Figure 25. Now, as depicted, there is a single configuration of non-zero weight for the arrows in $\tilde{\mathcal{R}}_2$: they go horizontally straight through and are incident on \mathcal{R}_1 in the same way as the latter having incoming boundary condition σ , and outgoing boundary condition given by $(\tilde{\mathbf{b}}, \tilde{\mathbf{j}})$. Thus the partition function of the right side of Figure 25 is simply $\mathcal{Z}_\sigma^{\text{S6V}}(\tilde{\mathbf{b}}, \tilde{\mathbf{j}})$, since the weight of the fixed configuration in the $\tilde{\mathcal{R}}_2$ region is 1. Since the partition function is not modified by applying (A.1), we obtain (A.6) and the proof is complete.

APPENDIX B. PROOFS OF MISCELLANEOUS LEMMAS

In this section we prove various miscellaneous statements in the main text whose proofs were deferred. Lemmas 5.3 and 5.4 are proved in Section B.1; Lemma 6.13 in Section B.2; Lemma 8.6 in Section B.4; Lemma 9.7 in Section B.5; and Lemma 10.4 in Section B.6. An alternative proof of Theorem 2.8 when $\alpha = 0$ (as mentioned in Remark 6.7) is given in Section B.3.

B.1. Finite speed of propagation bounds for colored ASEP and colored S6V.

Proof of Lemma 5.3. The lemma follows from the claim that, with probability at least $1 - \exp(-ct)$, no particle in colored ASEP (with packed initial condition) of color greater than $-[2t]$ is at any location to the right of $[4t]$ by time t . To see this, we merge all colors greater than or equal to $-[2t]$ to be particles and all particles of color less than $-[2t]$ to be holes, resulting in uncolored ASEP with step initial condition from location $[2t]$, in which setting we must show the probability that the rightmost particle at time t is at location greater than $[4t]$ is at most $\exp(-ct)$. By ignoring left jump attempts, and letting $(X_i)_{i=1}^{\lfloor 2t \rfloor - 1}$ be a collection of independent and identically distributed exponential rate 1 random variables, this probability is upper bounded by $\mathbb{P}(\sum_{i=1}^{\lfloor 2t \rfloor - 1} X_i < t)$, which is indeed upper bounded by $\exp(-ct)$ by standard concentration results (e.g., [Jan18, Theorem 5.1]). \square

Proof of Lemma 5.4. By monotonicity of $h^{\text{S6V}}(x, 0; \cdot, t)$ and since $h^{\text{S6V}}(x, 0; \cdot, t) \leq \lfloor \delta^{-1}t \rfloor - x + 1$ for all x , it is sufficient to prove the case $z = [4t]$. The event in the lemma with $z = [4t]$ contains the event that no arrow of color at least $-[2t]$ exits horizontally from a vertex in $I_t := \{\lfloor \delta^{-1}t \rfloor\} \times \llbracket -[2t], \lfloor \delta^{-1}t \rfloor - [4t] \rrbracket$. To lower bound the probability of this event, we first merge all arrows of color at least $-[2t]$ to color 1, and all other arrows to color 0, obtaining an

uncolored S6V model with step initial condition at $-[2t]$. Then, equivalently, we need to upper bound the probability that the lowest arrow, i.e., the one starting at $(1, -[2t])$, exits horizontally from I_t ; we call this event \mathbf{E}_t . It can be described as the bottom-most arrow traveling at least $[\delta^{-1}t]$ horizontally before traveling $[\delta^{-1}t] - [2t]$ vertically. The trajectory of the bottom-most arrow can be broken up into alternating intervals of horizontal travel and intervals of vertical travel. Note that the i^{th} interval of horizontal travel begins with a vertex configuration as in the fourth panel of Figure 8 and is followed by a random number X_i of configurations as in the third panel of Figure 8, where X_i is a geometric random variable, with distribution given by $\mathbb{P}(X_i = k) = \delta^k(1 - \delta)$ for $k \in \mathbb{Z}_{\geq 0}$; thus the i^{th} interval of horizontal travel has length $1 + X_i$. The X_i are independent for different i , and there are at most $[\delta^{-1}t] - [2t]$ many intervals of horizontal travel, so $\mathbb{P}(\mathbf{E}_t) \leq \mathbb{P}(\sum_{i=1}^{[\delta^{-1}t] - [2t]} (1 + X_i) > [\delta^{-1}t]) = \mathbb{P}(\sum_{i=1}^{[\delta^{-1}t] - [2t]} X_i > [2t])$. Using that $\mathbb{E}[\sum_{i=1}^{[\delta^{-1}t] - [2t]} X_i] = t(1 - 2\delta)/(1 - \delta) < 2t$, this is bounded by $\exp(-ct)$ for a $c > 0$ independent of δ , again by standard concentration inequalities (e.g., [Jan18, Theorem 2.1]). \square

B.2. Two-point fluctuation bound for Bernoulli random walk bridge.

Proof of Lemma 6.13. It is enough to prove the two-point bound without the supremum, i.e., to prove that there exist $C, c > 0$ such that for all $M > 0$,

$$\mathbb{P}\left(|B(x) - B(y) - p(x - y)| > M|x - y|^{1/2}\right) \leq C \exp(-cM^2).$$

From here the claim is proved by a standard chaining argument, i.e., doing a union bound over dyadically decreasing scales and using the above two point bound at each scale; e.g., we may apply [Dau23, Lemma 2.3] or imitate the proofs of Proposition 9.3 or Lemma 10.5.

Assume without loss of generality that $x > y$. Observe that $\{B(w) - B(w - 1)\}_{w=1}^n$ is a collection of pn many -1 s and $(1 - p)n$ many 0 s in uniformly random order. Clearly, $B(x) - B(y)$ is the number of -1 s lying in positions $y + 1, \dots, x$. Observe that this has the same distribution as the number of -1 s in the first $k := x - y$ positions, which is the number X of -1 s drawn without replacement in the first k draws from a collection of n numbers of which $K := pn$ are -1 s. In other words, X is a hypergeometric distribution with parameters n, K , and k . By a theorem of Hoeffding [Hoe63, Theorems 1 and 4], it follows that

$$\mathbb{P}\left(|X - pk| \geq Mk^{1/2}\right) \leq 2 \exp(-2M^2),$$

which completes the proof. \square

B.3. Alternative proof of ASEP sheet to Airy sheet convergence at $\alpha = 0$. In this subsection we provide the alternate proof of Theorem 2.8 in the case of $\alpha = 0$, that was mentioned in Remark 6.7.

Alternative proof of Theorem 2.8 for $\alpha = 0$. As in the original proof in Section 7.1, we again take $\mathcal{S}^N(x; y) = \mathcal{S}^{\text{ASEP}, \theta, \varepsilon}(-x; -y)$ as processes in (x, y) with $N = \varepsilon^{-1}$, and $\mathbf{L}^{(j), N} = \mathbf{L}^{\text{ASEP}, (j), \theta, \varepsilon}$. As in the proof of Theorem 2.8 in Section 7.1, (3.14), (7.3), and (7.4) hold and $\mathbf{L}^{(1), N}$ satisfies Assumptions 1 and 2. So by Theorem 3.18 and Proposition 6.5, $\mathfrak{L}^{(1), N}$ is tight and all subsequential limits satisfy the Brownian Gibbs property; call such a subsequential limit $\mathfrak{L}^{(1)}$. Combining Lemma 5.2 with [QS22, Theorem 2.2 (2)] yields that $\mathfrak{L}_1^{(1)} \stackrel{d}{=} \mathcal{P}_1$ (this uses $\alpha = 0$), and, since $\mathfrak{L}^{(1)}$ has the Brownian Gibbs property, [DM21, Theorem 1.1] implies that $\mathfrak{L}^{(1)} \stackrel{d}{=} \mathcal{P}$. Since every subsequential limit is the same, we obtain that $\mathfrak{L}^{(1), N} \xrightarrow{d} \mathcal{P}$. Invoking Theorem 7.1 and the fact that $\mathcal{S}(x; y) \stackrel{d}{=} \mathcal{S}(-x; -y)$, as processes on \mathbb{R}^2 , from [DV21b, Proposition 1.23] completes the proof. \square

B.4. Quantitative monotonicity for non-intersecting Bernoulli random walk bridge.

Proof of Lemma 8.6. We construct a Markov chain whose value at any time t is a pair of Bernoulli paths $(B_t^\uparrow, B_t^\downarrow)$ such that

$$B_t^\downarrow(x) \leq B_t^\uparrow(x) \leq B_t^\downarrow(x) + M \quad (\text{B.1})$$

holds almost surely and the large t marginal distributions of the chain are respectively the marginal distributions of B^\uparrow and B^\downarrow . Any subsequential limiting coupling so produced will establish the lemma. We may assume $M \geq 1$ as otherwise there is nothing to prove.

For $* \in \{\uparrow, \downarrow\}$, define B_0^* to be the minimal Bernoulli path from (a, x^*) to (b, y^*) which satisfies $g(x) \leq B_0^*(x) \leq f(x)$ for all $x \in \llbracket a, b \rrbracket$ (the assumptions guarantee at least one such path exists). We claim that (B.1) holds at $t = 0$. That the first inequality holds is immediate by minimality of the paths.

For the second inequality, suppose to the contrary that there exists $x_0 \in \llbracket a, b \rrbracket$ such that $B_0^\uparrow(x_0) = B_0^\downarrow(x_0) + M + 1$, and we take x_0 to be the smallest such point. Let $y_0 > x_0$ be the first such that $B_0^\uparrow(y_0) = B_0^\downarrow(y_0) + M$; it exists since the final separation of the paths at b is at most M and the separation changes by an element of $\{-1, 0, 1\}$ at each step. Now, by minimality of x_0 and y_0 , B^\uparrow has a flat-step starting at x_0 and a down-step starting at $y_0 - 1$. Let \tilde{B}_0^\uparrow be the path obtained from B_0^\uparrow by flipping the flat-step at x_0 to a down-step and flipping the down-step at $y_0 - 1$ to a flat-step; then \tilde{B}_0^\uparrow is lower than B_0^\uparrow and does not intersect g (as $\tilde{B}_0^\uparrow(x) \geq B_0^\downarrow(x) \geq g(x)$ for all $x \in \llbracket x_0, y_0 \rrbracket$), contradicting the minimality of B_0^\uparrow . Thus our claim is established, i.e., (B.1) holds at $t = 0$.

Now we specify the Markov dynamics. At each time $t \geq 1$, an $X \in \llbracket a, b \rrbracket$ and $\sigma \in \{0, -1\}$ are chosen independently and uniformly at random. For each $* \in \{\uparrow, \downarrow\}$, if $B_{t-1}^*(X+1) = B_{t-1}^*(X-1) - 1$ (i.e., there is a down-step followed by a flat-step or vice versa from $X - 1$ to $X + 1$ in B_{t-1}^*), we set $B_t^*(X) = B_{t-1}^*(X - 1) + \sigma$ and $B_t^*(x) = B_{t-1}^*(x)$ for all $x \neq X$, as long as the resulting B_t^* satisfies $g \leq B_t^* \leq f$; if not, no change is made.

It is easy to check that (B.1) is satisfied under these dynamics, and that the dynamics are aperiodic and irreducible. It is also straightforward that the marginal distributions of B^\uparrow and B^\downarrow are stationary for the marginal Markov chains; thus the limiting stationary distribution has the correct marginals. This completes the proof. \square

B.5. Gibbs property on a certain random interval.

Proof of Lemma 9.7. For a stochastic process $X : \llbracket a, b \rrbracket \rightarrow \mathbb{Z}$ taking values in $\Omega_{\llbracket a, b \rrbracket}$ (the space of Bernoulli paths on $\llbracket a, b \rrbracket$, as defined before Lemma 9.7), $t \in \llbracket a, b \rrbracket$, and $p \in (-1, 0)$, let $\bar{X}(x) = X(x) - px$, $a'(X) := \max\{x \in \llbracket a, t \rrbracket : \bar{X}(x) \geq m\}$, and $b'(X) := \min\{x \in \llbracket t, b \rrbracket : \bar{X}(x) \geq m\}$. With the notational convention for event names from Remark 6.16 in mind, for such a process X , define $\mathbf{E}(x, y, z_1, z_2, X) := \text{BdyVal}(x, y, z_1, z_2, X) \cap \text{IntVal}(x, y, X)$, where

$$\begin{aligned} \text{BdyVal}(x, y, z_1, z_2, X) &:= \{X(x) = z_1, X(y) = z_2\}, \quad \text{and} \\ \text{IntVal}(x, y, X) &:= \{a'(X) = x, b'(X) = y\}. \end{aligned}$$

Let $\mathcal{F}_{x,y} := \mathcal{F}_{\text{ext}}(\{k\}, \llbracket x, y \rrbracket, \mathbf{L})$, $a' := a'(L_k)$, $b' := b'(L_k)$, and $\mathbf{E}(x, y, z_1, z_2) := \mathbf{E}(x, y, z_1, z_2, L_k)$ for short. In the case that $a' = b' = t$, there is nothing to prove, so we may assume that this does not hold. By the definition of \mathcal{F} from Lemma 9.7, we must show that, for any $x \in \llbracket a, t \rrbracket$, $y \in \llbracket t, b \rrbracket$,

$z_1, z_2 \in \mathbb{Z}$, and $A \in \mathcal{F}_{x,y}$ (recalling the notation $\mathbb{E}^{z_1, z_2, \llbracket x, y \rrbracket}$ introduced just before Lemma 9.7),

$$\begin{aligned} & \mathbb{E} \left[F(L_k | \llbracket a', b' \rrbracket, a', b') \mathbb{1}_{A \cap E(x, y, z_1, z_2)} \right] \\ &= \mathbb{E} \left[\frac{\mathbb{E}^{z_1, z_2, \llbracket x, y \rrbracket} \left[F(B, x, y) W(B, L_{k-1}, L_{k+1}) \mid \overline{B}(s) < m \ \forall s \in \llbracket x+1, y-1 \rrbracket \right]}{\mathbb{E}^{z_1, z_2, \llbracket x+1, y-1 \rrbracket} \left[W(B, L_{k-1}, L_{k+1}) \mid \overline{B}(s) < m \ \forall s \in \llbracket x+1, y-1 \rrbracket \right]} \mathbb{1}_{A \cap E(x, y, z_1, z_2)} \right], \end{aligned} \quad (\text{B.2})$$

where the W factors are evaluated on the interval $\llbracket x, y \rrbracket$. First, if $z_1 - px < m$ or $z_2 - py < m$, $E(x, y, z_1, z_2) = \emptyset$ by definition of a' and b' , in which case the equality trivially holds. So we assume $z_1 - px, z_2 - py \geq m$. By conditioning on $\mathcal{F}_{x,y}$, we see that the lefthand side of the previous display equals

$$\mathbb{E} \left[\mathbb{E}_{\mathcal{F}_{x,y}} \left[F(L_k | \llbracket x, y \rrbracket, x, y) \mathbb{1}_{E(x, y, z_1, z_2)} \right] \mathbb{1}_A \right]. \quad (\text{B.3})$$

Adopt the shorthand $\text{BdyVal}(x, y, z_1, z_2) := \text{BdyVal}(x, y, z_1, z_2, L_k)$ and recall that $E(x, y, z_1, z_2) = \text{BdyVal}(x, y, z_1, z_2) \cap \text{IntVal}(x, y, z_1, z_2, L_k)$. Applying the Hall-Littlewood Gibbs property shows that the (inner) conditional expectation in (B.3) equals

$$\frac{\mathbb{E}^{z_1, z_2, \llbracket x, y \rrbracket} \left[F(B, x, y) \mathbb{1}_{\text{IntVal}(x, y, B)} W(B, L_{k-1}, L_{k+1}) \right]}{\mathbb{E}^{z_1, z_2, \llbracket x, y \rrbracket} \left[W(B, L_{k-1}, L_{k+1}) \right]} \mathbb{1}_{\text{BdyVal}(x, y, z_1, z_2)}.$$

Note that $\text{IntVal}(x, y, B) = \{\overline{B}(s) < m \ \forall s \in \llbracket x+1, y-1 \rrbracket\}$ when $\text{BdyVal}(x, y, z_1, z_2)$ holds, since $z_1 - px, z_2 - py \geq m$. Thus we can rewrite the previous display as (with the shorthand $\overline{B} < m$ for $\overline{B}(s) < m \ \forall s \in \llbracket x+1, y-1 \rrbracket$)

$$\begin{aligned} & \frac{\mathbb{E}^{z_1, z_2, \llbracket x, y \rrbracket} \left[F(B, x, y) W(B, L_{k-1}, L_{k+1}) \mid \overline{B} < m \right]}{\mathbb{E}^{z_1, z_2, \llbracket x, y \rrbracket} \left[W(B, L_{k-1}, L_{k+1}) \right]} \cdot \mathbb{P}_{\mathcal{F}}(\overline{B} < m) \mathbb{1}_{\text{BdyVal}(x, y, z_1, z_2)} \\ &= \frac{\mathbb{E}^{z_1, z_2, \llbracket x, y \rrbracket} \left[F(B, x, y) W(B, L_{k-1}, L_{k+1}) \mid \overline{B} < m \right]}{\mathbb{E}^{z_1, z_2, \llbracket x, y \rrbracket} \left[W(B, L_{k-1}, L_{k+1}) \mid \overline{B} < m \right]} \\ & \quad \times \frac{\mathbb{E}^{z_1, z_2, \llbracket x, y \rrbracket} \left[W(B, L_{k-1}, L_{k+1}) \mathbb{1}_{\overline{B} < m} \right]}{\mathbb{E}^{z_1, z_2, \llbracket x, y \rrbracket} \left[W(B, L_{k-1}, L_{k+1}) \right]} \mathbb{1}_{\text{BdyVal}(x, y, z_1, z_2)} \\ &= \frac{\mathbb{E}^{z_1, z_2, \llbracket x, y \rrbracket} \left[F(B, x, y) W(B, L_{k-1}, L_{k+1}) \mid \overline{B} < m \right]}{\mathbb{E}^{z_1, z_2, \llbracket x, y \rrbracket} \left[W(B, L_{k-1}, L_{k+1}) \mid \overline{B} < m \right]} \\ & \quad \times \mathbb{P}_{\mathcal{F}_{x,y}}(\overline{L}_k(s) < m \ \forall s \in \llbracket x, y \rrbracket) \mathbb{1}_{\text{BdyVal}(x, y, z_1, z_2)} \\ &= \frac{\mathbb{E}^{z_1, z_2, \llbracket x, y \rrbracket} \left[F(B, x, y) W(B, L_{k-1}, L_{k+1}) \mid \overline{B} < m \right]}{\mathbb{E}^{z_1, z_2, \llbracket x, y \rrbracket} \left[W(B, L_{k-1}, L_{k+1}) \mid \overline{B} < m \right]} \cdot \mathbb{P}_{\mathcal{F}_{x,y}}(\text{IntVal}(x, y, L_k)) \mathbb{1}_{\text{BdyVal}(x, y, z_1, z_2)}. \end{aligned}$$

Since all the factors outside the $\mathbb{P}_{\mathcal{F}}$ factor are $\mathcal{F}_{x,y}$ -measurable, and since by definition $E(x, y, z_1, z_2) = \text{IntVal}(x, y, L_k) \cap \text{BdyVal}(x, y, z_1, z_2)$, the tower property of conditional expectation yields that the previous display equals

$$\mathbb{E}_{\mathcal{F}_{x,y}} \left[\frac{\mathbb{E}^{z_1, z_2, \llbracket x, y \rrbracket} \left[F(B, x, y) W(B, L_{k-1}, L_{k+1}) \mid \overline{B} < m \right]}{\mathbb{E}^{z_1, z_2, \llbracket x, y \rrbracket} \left[W(B, L_{k-1}, L_{k+1}) \mid \overline{B} < m \right]} \mathbb{1}_{E(x, y, z_1, z_2)} \right].$$

Substituting this in (B.3), using the tower property again, and that A is $\mathcal{F}_{x,y}$ measurable, yields (B.2). This completes the proof. \square

B.6. Uniform separation for Brownian and random walk bridges. In this section we establish Lemma 10.4 which, recall, states that conditional on a Bernoulli random walk bridge staying above a lower boundary curve f , it will maintain some on-scale uniformly positive separation from f with high probability. The argument goes by proving a similar statement for Brownian bridges and then using the KMT coupling to obtain it for the Bernoulli case.

The Brownian bridge case is the following.

Lemma B.1 (Brownian bridge uniform separation). *Fix $M > 0$, $\sigma > 0$, $p > 0$ and $T \geq 2$. Let $U_1 \in [-2T, -\frac{3}{2}T]$ and $U_2 \in [\frac{3}{2}T, 2T]$. Let B^{Br} be a Brownian bridge from $(U_1 N^{2/3}, z_1)$ to $(U_2 N^{2/3}, z_2)$ of variance $\sigma^2 > 0$, for some z_i such that $z_i - pU_i N^{2/3} \in [-MN^{1/3}, MN^{1/3}]$ for each $i \in \{1, 2\}$. Also let $f : [U_1 N^{2/3}, U_2 N^{2/3}] \rightarrow \mathbb{R}$ be a function with $f(U_i N^{2/3}) \leq z_i$. Let $\{B^{\text{Br}} \geq f\}$ denote $\{B^{\text{Br}}(x) \geq f(x) \forall x \in [U_1, U_2]\}$ and suppose, for some $\rho > 0$, that*

$$\mathbb{P}(B^{\text{Br}} \geq f) \geq \rho.$$

Then for any $\varepsilon > 0$ there exists $\delta = \delta(\varepsilon, \rho, M, \sigma, T)$ such that

$$\mathbb{P}\left(\inf_{x \in [-TN^{2/3}, TN^{2/3}]} (B^{\text{Br}}(x) - f(x)) \leq \delta N^{1/3} \mid B^{\text{Br}} \geq f\right) \leq \varepsilon.$$

Using the previous lemma and Lemma 6.14, we give the straightforward proof of Lemma 10.4.

Proof of Lemma 10.4. We will eventually set $\delta < \omega$ and will use this fact in the coming arguments. By Lemma 6.14, there exists $N_0 = N_0(\varepsilon, \delta, T, M)$ such that there is a coupling between B^{RW} and B^{Br} (of variance lower bounded by a positive constant depending on only p) such that, for $N \geq N_0$, with probability at least $1 - \varepsilon\rho$, $\sup_{[U_1 N^{2/3}, U_2 N^{2/3}]} |B_k - B^{\text{Br}}| \leq \delta N^{1/3}$. Thus

$$\begin{aligned} & \mathbb{P}\left(\inf_{x \in [-TN^{2/3}, TN^{2/3}]} (B^{\text{RW}}(x) - f(x)) \leq \delta N^{1/3} \mid B^{\text{RW}} \geq f\right) \\ &= \frac{\mathbb{P}\left(\inf_{x \in [-TN^{2/3}, TN^{2/3}]} (B^{\text{RW}}(x) - f(x)) \leq \delta N^{1/3}, B^{\text{RW}} \geq f\right)}{\mathbb{P}(B^{\text{RW}} \geq f)} \\ &\leq \frac{\mathbb{P}\left(\inf_{x \in [-TN^{2/3}, TN^{2/3}]} (B^{\text{Br}}(x) - f(x)) \leq 2\delta N^{1/3}, B^{\text{Br}} \geq f - \delta N^{1/3}\right) + \varepsilon\rho}{\mathbb{P}(B^{\text{Br}} \geq f + \delta N^{1/3}) - \varepsilon\rho}. \end{aligned}$$

Since $\delta < \omega$, $\mathbb{P}(B^{\text{Br}} \geq f + \delta N^{1/3}) \geq \rho$ by hypothesis. So (assuming $\varepsilon < \frac{1}{2}$ without loss of generality) the previous display is upper bounded by

$$2\rho^{-1} \cdot \mathbb{P}\left(\inf_{x \in [-TN^{2/3}, TN^{2/3}]} (B^{\text{Br}}(x) - f(x)) \leq 2\delta N^{1/3}, B^{\text{Br}} \geq f - \delta N^{1/3}\right) + 2\varepsilon.$$

By Lemma B.1 we may pick $\delta < \omega$ with $\delta = \delta(\varepsilon, \rho, M, p)$ such that the probability is less than $\rho\varepsilon$, which completes the proof after relabeling ε . \square

Next we prove Lemma B.1 on the uniform on-scale separation of a Brownian bridge from its lower boundary condition. The idea is to condition on the entire bridge except for its value at zero; more precisely, one conditions on the shape of the curve so that, given the value of $B^{\text{Br}}(0)$, the whole process is determined by an affine shift. The conditional distribution of $B^{\text{Br}}(0)$ is explicit and the proof comes down to a calculation about the probability of this random variable being close to the lower edge of its support.

Similar ideas were introduced in [Ham22] and have been used in a number of subsequent works, including [CHH23, CHHM23, GHZ23].

Proof of Lemma B.1. We assume that $\sigma^2 = 1$ and $p = 0$ without loss of generality. Recall that B^{Br} is a Brownian bridge defined on $[U_1 N^{2/3}, U_2 N^{2/3}]$. For an interval $[a, b] \subseteq [U_1 N^{2/3}, U_2 N^{2/3}]$, we adopt the notation $B^{\text{Br}, [a, b]}; [a, b] \rightarrow \mathbb{R}$ to be B^{Br} affinely shifted to equal zero at a and b , i.e., for $x \in [a, b]$,

$$B^{\text{Br}, [a, b]}(x) := B^{\text{Br}}(x) - \frac{x-a}{b-a} B^{\text{Br}}(b) - \frac{b-x}{b-a} B^{\text{Br}}(a). \quad (\text{B.4})$$

We let $\tilde{\mathbb{P}}$ be the probability measure $\mathbb{P}(\cdot \mid B^{\text{Br}} \geq f)$, so that under $\tilde{\mathbb{P}}$, B^{Br} is distributed as a Brownian bridge conditioned to stay above f . We consider the σ -algebra \mathcal{F} generated by $B^{\text{Br}, [U_1 N^{2/3}, 0]}(\cdot)$ and $B^{\text{Br}, [0, U_2 N^{2/3}]}(\cdot)$. Then, conditionally on $\tilde{\mathbb{P}}_{\mathcal{F}}$, the only remaining randomness is in the value $B^{\text{Br}}(0)$. The distribution of this random variable is that of a normal random variable of mean $\mu = \frac{1}{2}(z_1 + z_2)$ and variance $\tilde{\sigma}^2 = |U_1| \cdot U_2 N^{2/3} / (U_2 + |U_1|)$ conditioned to stay above an \mathcal{F} -measurable random variable Cor (short for corner, a name given to a similar quantity in [Ham22]) defined by

$$\text{Cor} := \inf \left\{ w : B^{\text{Br}, w}(x) \geq f(x) \text{ for all } x \in [U_1 N^{2/3}, U_2 N^{2/3}] \right\},$$

where $B^{\text{Br}, w}$ is the reconstruction of B^{Br} from $B^{\text{Br}, [U_1 N^{2/3}, 0]}$ and $B^{\text{Br}, [0, U_2 N^{2/3}]}$ when $B(0) = w$, i.e.,

$$B^{\text{Br}, w}(x) := \begin{cases} \frac{U_1 - x N^{-2/3}}{U_1} w + \frac{x N^{-2/3}}{U_1} z_1 + B^{\text{Br}, [U_1 N^{2/3}, 0]}(x) & x \in [U_1 N^{2/3}, 0] \\ \frac{U_2 - x N^{-2/3}}{U_2} w + \frac{x N^{-2/3}}{U_2} z_2 + B^{\text{Br}, [0, U_2 N^{2/3}]}(x) & x \in [0, U_2 N^{2/3}]. \end{cases}$$

Notice that for any R ,

$$\begin{aligned} \tilde{\mathbb{P}} \left(\text{Cor} > RN^{1/3} \right) &\leq \tilde{\mathbb{P}} \left(B^{\text{Br}}(0) > RN^{1/3} \right) = \mathbb{P} \left(B^{\text{Br}}(0) > RN^{1/3} \mid B^{\text{Br}} \geq f \right) \\ &\leq \rho^{-1} \mathbb{P} \left(B^{\text{Br}}(0) > RN^{1/3} \right) \\ &= \rho^{-1} \mathbb{P} \left(\mathcal{N}(\mu, \tilde{\sigma}^2) > RN^{1/3} \right). \end{aligned}$$

Since $\mu \geq -MN^{1/3}$ and $\tilde{\sigma}^2 \leq TN^{2/3}$, there is $R = R(\varepsilon, \rho, M, T)$ (and since $T \geq 1$) such that the previous display is at most ε . We fix such a value of R for the rest of the proof.

Now observe that, if $w \geq \text{Cor} + 3\delta N^{1/3}$, then

$$\inf_{x \in [-TN^{2/3}, TN^{2/3}]} (B^{\text{Br}, w}(x) - f(x)) \geq \delta N^{1/3}.$$

This is because the lefthand side is at least 0 at $w = \text{Cor}$ by definition of Cor , $B^{\text{Br}, w}(x)$ increases with w , and $\frac{U_1 - x N^{-2/3}}{U_1} \cdot 3\delta N^{1/3} \geq \delta N^{1/3}$ when $x \in [-TN^{2/3}, TN^{2/3}]$ since $U_1 \in [-2T, -\frac{3}{2}T]$, and similarly for U_2 . Thus it follows that (recall \mathcal{F} from right after (B.4))

$$\begin{aligned} &\tilde{\mathbb{P}} \left(\inf_{x \in [-TN^{2/3}, TN^{2/3}]} (B^{\text{Br}}(x) - f(x)) \leq \delta N^{1/3} \right) \\ &= \tilde{\mathbb{E}} \left[\tilde{\mathbb{P}}_{\mathcal{F}} \left(\inf_{x \in [-TN^{2/3}, TN^{2/3}]} (B^{\text{Br}}(x) - f(x)) \leq \delta N^{1/3} \right) \right] \\ &\leq \tilde{\mathbb{E}} \left[\tilde{\mathbb{P}}_{\mathcal{F}} \left(B^{\text{Br}}(0) \leq \text{Cor} + 3\delta N^{1/3} \right) \right]. \end{aligned}$$

Letting $X \sim \mathcal{N}(0, 1)$, the previous display equals

$$\begin{aligned} &\tilde{\mathbb{E}} \left[\tilde{\mathbb{P}}_{\mathcal{F}} \left(\tilde{\sigma} X + \mu \leq \text{Cor} + 3\delta N^{1/3} \mid \tilde{\sigma} X + \mu \geq \text{Cor} \right) \right] \\ &\leq \tilde{\mathbb{E}} \left[\tilde{\mathbb{P}}_{\mathcal{F}} \left(X \leq \tilde{\sigma}^{-1}(\text{Cor} - \mu) + 3\tilde{\sigma}^{-1}\delta N^{1/3} \mid X \geq \tilde{\sigma}^{-1}(\text{Cor} - \mu) \right) \mathbb{1}_{\text{Cor} \leq RN^{1/3}} \right] + \varepsilon. \end{aligned}$$

Now by Lemma 8.1, the conditional probability in the previous display is upper bounded by the same with $\tilde{\sigma}^{-1}(\text{Cor} - \mu)$ replaced by an upper bound on it. Since $\tilde{\sigma}^2 \geq cTN^{2/3}$ and $\mu \geq -MN^{1/3}$, on the event $\text{Cor} \leq RN^{1/3}$, it holds that $\tilde{\sigma}^{-1}(\text{Cor} - \mu) \leq c^{-1/2}T^{-1/2}(R + M)$. By the upper bound on $\tilde{\sigma}^{-1}$, we also see that $3\tilde{\sigma}^{-1}\delta N^{1/3} \leq 3c^{-1/2}T^{-1/2}\delta$. Thus, the previous display is upper bounded (using the bound on $3\tilde{\sigma}^{-1}\delta N^{1/3}$ for the first line and Lemma 8.1 for the second) by

$$\begin{aligned} & \tilde{\mathbb{E}} \left[\tilde{\mathbb{P}}_{\mathcal{F}} \left(X \leq \tilde{\sigma}^{-1}(\text{Cor} - \mu) + 3c^{-1/2}T^{-1/2}\delta \mid X \geq \tilde{\sigma}^{-1}(\text{Cor} - \mu) \right) \mathbb{1}_{\text{Cor} \leq RN^{1/3}} \right] + \varepsilon \\ & \leq \tilde{\mathbb{E}} \left[\tilde{\mathbb{P}}_{\mathcal{F}} \left(X \leq c^{-1/2}T^{-1/2}(R + M + 3\delta) \mid X \geq c^{-1/2}T^{-1/2}(R + M) \right) \right] + \varepsilon. \end{aligned}$$

It is now clear using standard estimates on normal probabilities that, for δ small enough depending on R , M , and T (therefore on ε , ρ , M , and T), the previous display is upper bounded by 2ε . This completes the proof. \square

APPENDIX C. LPP MAXIMIZER LOCATION ASYMPTOTICS

In this section, we give the proof of Proposition 7.2. Before doing so, we set up some preliminary lemmas that will be needed. Recall the definition of Z_k^N as the maximizer of the maximum over z of (7.7).

C.1. Monotonicity properties. We need a monotonicity property of Z_k^N and of LPP values. We start with the first; its proof is the same as that of [DOV22, Lemma 3.6] and is omitted.

Lemma C.1. *For fixed N , x , and y , it almost surely holds that $Z_k^N(x, y) \geq Z_{k+1}^N(x, y)$ for all $k \in [1, N^{1/6}]$.*

Lemma C.2 ([DOV22, Lemma 3.3]). *Let $f = (f_1, \dots, f_n)$ be a sequence of continuous functions with $f_i : \mathbb{R} \rightarrow \mathbb{R}$. Then for any $x \in \mathbb{R}$,*

$$z \mapsto f[(z, k) \rightarrow (x, 1)] + f_k(z)$$

is non-increasing.

C.2. Prelimiting quantities. Define F_k^N , G_k^N and H^N by

$$\begin{aligned} F_k^N(x, z) &:= \sup_{w \leq z} \left(\mathfrak{L}_{N^{1/6}}^N(x; w) + \mathfrak{L}^{(1),N}[(w, N^{1/6} - 1) \rightarrow (z, k)] \right) - \mathfrak{L}_k^{(1),N}(z) \\ G_k^N(z, y) &:= \mathfrak{L}^{(1),N}[(z, k) \rightarrow (y, 1)] + \mathfrak{L}_k^{(1),N}(z) \\ H^N(x, y) &:= \mathcal{S}^N(x; y) = \mathfrak{L}_1^N(x; y); \end{aligned}$$

note that the definition of $G_k^N(z, y)$ requires $z \leq y$. Also define

$$\begin{aligned} G_k(z, y) &:= \mathcal{P}[(z, k) \rightarrow (y, 1)] + \mathcal{P}_k(z) \\ H(x, y) &:= \mathcal{S}(x; y). \end{aligned} \tag{C.1}$$

Observe that $G_k^N \rightarrow G^k$ (by Theorem 3.19). The quantities in (C.1) are defined in this way to obtain the monotonicity stated in Lemma C.2, i.e., $G_k(z, y)$ is non-increasing in z by Lemma C.2, a property not possessed by $\mathcal{P}[(z, k) \rightarrow (y, 1)]$.

The proof of Proposition 7.2 will also need some asymptotic information about G_k , which we record in the following lemma. We defer its proof to Section C.3 as it requires the introduction of the prelimiting model of Brownian LPP. Recall the meaning of the notation \mathfrak{o} from (7.5).

Lemma C.3. *Fix $z < y$. Then it holds that*

$$G_k \left(z\sqrt{k}, y\sqrt{k} \right) = -y^2k - \frac{\sqrt{k}}{y - z} + \mathfrak{o}(\sqrt{k}).$$

Now we give the proof of Proposition 7.2, which is an adaptation of the argument from [DOV22, Lemma 7.1].

Proof of Proposition 7.2. Note that $H^N(x, y) \stackrel{d}{=} \mathfrak{L}_1^{(1),N}(y-x)$ for fixed x, y by (7.3) and $\mathfrak{L}_1^{(1),N} \xrightarrow{d} \mathcal{P}_1$ as $N \rightarrow \infty$ by Theorem 3.19. We added $\mathfrak{L}_k^{(1),N}(z)$ in the definition of G_k^N because we will need G_k^N to converge to G^k . We subtracted the same quantity from F_k^N so that the following holds, which follows from (7.7):

$$H^N(x, y) \geq F_k^N(x, z) + G_k^N(z, y) + \mathfrak{o}(N^{-1/11}). \quad (\text{C.2})$$

Now the left hand side is tight in N and independent of k by the tightness of $\mathfrak{L}_N^{(1)}$ (Theorem 3.19). For any $\varepsilon > 0$, we claim that if $|z + \sqrt{k/2x}| > \varepsilon\sqrt{k}$, then the right hand side is at most $-\varepsilon^2\sqrt{kx}/2$. By (C.2) and the tightness of $H^N(x, y)$, thus would imply that Z_k^N , the maximizer over z , must lie within $\varepsilon\sqrt{k}$ of $-\sqrt{k/2x}$, establishing the proposition.

For z and y in a fixed compact subset independent of N (but which may depend on k), we know from Theorem 3.19 that $G_k^N(z, y) \xrightarrow{d} G_k(z, y)$ as $N \rightarrow \infty$. Further, we know from Lemma C.3 and by the convergence of G_k^N to G_k that for each fixed z and y

$$G_k^N(z\sqrt{k}, y\sqrt{k}) = -y^2k - \frac{\sqrt{k}}{y-z} + \mathfrak{o}(\sqrt{k}). \quad (\text{C.3})$$

We can use this information to obtain an upper bound on $F_k^N(x, z\sqrt{k})$. First, we know from (7.7) and the definitions of F_k^N , G_k^N , and H^N that, for all x, y, z ,

$$F_k^N(x, z\sqrt{k}) \leq H^N(x, y\sqrt{k}) - G_k^N(z\sqrt{k}, y\sqrt{k}) + \mathfrak{o}(N^{-1/11}).$$

Define

$$\tilde{F}_k^N(x, z\sqrt{k}) := \inf_y \left(H^N(x, y\sqrt{k}) - G_k^N(z\sqrt{k}, y\sqrt{k}) \right), \quad (\text{C.4})$$

so that $z \mapsto \tilde{F}_k^N(x, z\sqrt{k})$ is non-decreasing, since, by Lemma C.2, $G_k^N(z\sqrt{k}, y\sqrt{k})$ is monotonically non-increasing in z . Note also that

$$F_k^N(x, z\sqrt{k}) \leq \tilde{F}_k^N(x, z\sqrt{k}) + \mathfrak{o}(N^{-1/11}) \quad (\text{C.5})$$

for all x and z . Our next step is to upper bound $\tilde{F}_k^N(x, z\sqrt{k})$.

Since for fixed x, y we know $H^N(x, y) \xrightarrow{d} \mathcal{P}_1(y-x)$ as $N \rightarrow \infty$, $x \mapsto \mathcal{P}_1(x) + x^2$ is stationary, and exponentially decaying tail bounds for $\mathcal{P}_1(0)$ (i.e., the GUE Tracy-Widom distribution) are well-known (e.g., [AGZ10, Exercise 3.8.3]), it follows that $H^N(x, y\sqrt{k}) = -(x - y\sqrt{k})^2 + \mathfrak{o}(\sqrt{k})$. Combining this with the estimate from (C.3) of $G_k^N(z\sqrt{k}, y\sqrt{k})$ yields

$$\begin{aligned} \tilde{F}_k^N(x, z\sqrt{k}) &= \inf_y \left(-(x - y\sqrt{k})^2 - \left(-y^2k - \frac{\sqrt{k}}{y-z} \right) \right) + \mathfrak{o}(\sqrt{k}) \\ &= \inf_y \left(2xy\sqrt{k} + \frac{\sqrt{k}}{y-z} \right) + \mathfrak{o}(\sqrt{k}), \end{aligned}$$

where in the last equality we used that x is uniformly bounded, independently of k . The optimizer of the infimum is $y = z + \frac{1}{\sqrt{2x}}$. Substituting this into the previous display yields that, for each fixed x and z ,

$$\tilde{F}_k^N(x, z\sqrt{k}) \leq 2\sqrt{2kx} + 2xz\sqrt{k} + \mathfrak{o}(\sqrt{k}). \quad (\text{C.6})$$

With this information, we can show that the maximizer in (7.7) equals $-\sqrt{k/2x} + \mathfrak{o}(\sqrt{k})$. Indeed, (7.7) can be written as

$$H^N(x, y) = \sup_{z \leq y} (F_k^N(x, z) + G_k^N(z, y)) + \mathfrak{o}(N^{-1/11}).$$

Now, since x and y are bounded independently of k , the lefthand side of the previous display is $\mathfrak{o}(\sqrt{k})$ (by Theorem 3.19). So at $z = Z_k^N$ the maximizer, we must have

$$F_k^N(x, Z_k^N) + G_k^N(Z_k^N, y) = \mathfrak{o}(\sqrt{k}).$$

We will show that if $|z + \sqrt{k/2x}| > \varepsilon\sqrt{k}$, then $F_k^N(x, z) + G_k^N(z, y)$ is smaller than $-c\varepsilon^2\sqrt{k}$. More precisely, we will show that for some absolute constant $c > 0$,

$$\sup_{\substack{z: z \leq y \\ |z + \sqrt{k/2x}| > \varepsilon\sqrt{k}}} \tilde{F}_k^N(x, z) + G_k^N(z, y) \leq -c\varepsilon^2\sqrt{k} + \mathfrak{o}(\sqrt{k});$$

this suffices to establish our claim since, by (C.5), $F_k^N(x, z) \leq \tilde{F}_k^N(x, z) + \mathfrak{o}(N^{-1/11})$. Recall from just after (C.4) that $\tilde{F}_k^N(x, z\sqrt{k})$ is monotonically non-decreasing in z . We first reduce the previous display to a supremum over a finite set using the monotonicity in z of \tilde{F}_k^N and G_k^N . Letting

$$\begin{aligned} \lfloor x \rfloor_{N,k} &:= \max \left\{ w < x : w \in \frac{1}{4}\sqrt{\frac{k}{x}}\varepsilon^2\mathbb{Z} \right\} \\ \lceil x \rceil_{N,k} &:= \min \left\{ w > x : w \in \frac{1}{4}\sqrt{\frac{k}{x}}\varepsilon^2\mathbb{Z} \right\}, \end{aligned}$$

the monotonicity in z of \tilde{F}_k^N and G_k^N implies that it is sufficient to show that

$$\sup_{\substack{z: z \leq y \\ |z + \sqrt{k/2x}| > \varepsilon\sqrt{k}}} \tilde{F}_k^N(x, \lceil z \rceil_{N,k}) + G_k^N(\lfloor z \rfloor_{N,k}, y) \leq -c\varepsilon^2\sqrt{k}. \tag{C.7}$$

Combining the bounds on G_k^N and \tilde{F}_k^N from (C.3) and (C.6) respectively (taking y in the G_k^N bound to be $yk^{-1/2}$ here, and using the fact that y is bounded independently of k), we obtain, for each fixed z ,

$$\tilde{F}_k^N(x, \lceil z \rceil_{N,k}) + G_k^N(\lfloor z \rfloor_{N,k}, y) \leq 2\sqrt{2kx} + 2x(z + \frac{1}{4}\varepsilon^2x^{-1/2}\sqrt{k}) + \frac{k}{z - \frac{1}{4}\varepsilon^2\sqrt{k/x}} + \mathfrak{o}(\sqrt{k}). \tag{C.8}$$

If one substitutes $\varepsilon = 0$, the righthand side is maximized at $z = -\sqrt{k/2x}$ (under the condition $z \leq y$), at which value it equals 0. Further, by the concavity of the righthand side as a function in z (and the negativity of the third derivative) and using Taylor's theorem, if $|z + \sqrt{k/2x}| > \varepsilon\sqrt{k}$, the righthand side is at most $-c\varepsilon^2\sqrt{k}$. Since these bounds also apply simultaneously for all the finite number of z 's in (C.7), we obtain the asymptotic for Z_k^N .

The tightness of $\{Z_k^N(x, y)\}_{N=1}^\infty$ for each k follows from the asymptotic and the monotonicity property $y \geq Z_1^N(x, y) \geq Z_2^N(x, y) \geq \dots \geq Z_{N^{1/6}}^N$ from Lemma C.1. \square

Remark C.4. Let remark briefly on the difference of the above argument compared to [DOV22]. There, an analog of the F_k^N , G_k^N and H_k^N quantities were defined in a model known as Brownian last passage percolation (introduced here in Section C.3 ahead). In their context, asymptotics for F_k^N were available (via estimates for a limiting analog F_k), and these were used to derive an upper bound on G_k^N to then upper bound the analog of (C.8). Here, we do not *a priori* have such estimates for F_k^N as we do not know it weakly converges to F_k ; instead, we know the convergence of G_k^N to its analog in the parabolic Airy line ensemble, where the previously mentioned estimates for

F_k apply. These will lead to the estimates on G_k recorded in Lemma C.3, yielding the estimates for G_k^N that were used. We essentially reversed the argument in [DOV22] to obtain estimates for F_k^N that allowed us to then bound (C.8).

Remark C.5. Recall from (7.2) and (7.3) that $L_1^{N,(k)}$ is equal in law to a translation of $L_1^{N,(1)}$, which was important for our arguments in Section 7. This statement is false for the lower-indexed curves, namely, $L_j^{N,(k)}$ does not have the same law as that of the corresponding translation of $L_j^{N,(1)}$ for $j > 1$. This is closely related to the fact that, as noted in Remark 3.3, we cannot merge colors 1 and 0 in the colored q -Boson model. It can also be seen from the fact that, if such an equality in law were true, then it would imply precise asymptotics for F_k^N (since the asymptotics of $L_j^{(N)}$, converging to the j^{th} curve of the Airy line ensemble, are well understood, e.g., [DV21a, Corollary 5.3]), which are actually in disagreement with those shown in (C.5) and (C.6).

C.3. G_k asymptotics. Here we give the proof of Lemma C.3. In order to access a certain variational formula, we prove its analog in the model of Brownian LPP, and use the convergence of the latter to the Airy sheet to obtain the result for G_k itself. We briefly recall the model.

An up-right path from (x, j) to (y, k) for $x < y$ and $j > k$ is a function $\gamma : [x, y] \rightarrow \llbracket k, j \rrbracket$ which is non-increasing and càdlàg (right continuous with left-limits) with $\gamma(x) = j$ and $\gamma(y) = k$. The jump times (t_1, \dots, t_{N-1}) of a path from line N to line 1 defined by t_i being the time γ jumps from line $i + 1$ to line i , i.e., the time t such that $\gamma(t^-) = i + 1$ and $\gamma(t) = i$. A pair of up-right paths π and π' from (x, j) to (y, k) and (x', j') to (y', k') , respectively, are said to be disjoint if either $\pi(t) > \pi'(t)$ for all $t \in (x, y) \cap (x', y')$ (i.e., excluding endpoints), or $\pi(t) < \pi'(t)$ for all $t \in (x, y) \cap (x', y')$.

Let $\mathbf{B} = (B_1, \dots, B_N)$ be a collection of N independent and identically distributed Brownian motions on $[0, \infty)$. The weight of a path γ from (x, N) to $(y, 1)$ with jump times (t_1, \dots, t_{N-1}) is given by (with the convention $t_0 = y$ and $t_N = x$)

$$\mathbf{B}[\gamma] = \sum_{i=1}^N (B_i(t_{i-1}) - B_i(t_i)).$$

Let $\mathbf{WB} = (WB_1, \dots, WB_N)$ be the curves of the *watermelon*, defined by

$$\sum_{i=1}^k (WB)_i(t) = \mathbf{B}[(0, N)^k \rightarrow (t, 1)^k]$$

for each $k = 1, \dots, N$, where $\mathbf{B}[(0, N)^k \rightarrow (t, 1)^k]$ is the maximum weight over all collections of k disjoint paths $(\gamma_1, \dots, \gamma_k)$, with γ_i from $(0, N - i + 1)$ to $(t, 1)$, with the weight of a collection of paths being the sum of the weights.

Recall the LPP notation from (2.2) (which agrees with the above convention with $k = 1$). Let $x_N = 2xN^{2/3}$, and similarly for y_N and z_N . Define

$$\begin{aligned} F_k^{N,\text{Br}}(x, z) &= N^{-1/3} \left(\mathbf{WB}[(x_N, N) \rightarrow (N + z_N, k)] - (WB)_k(N + z_N) + 2xN^{2/3} \right) \\ G_k^{N,\text{Br}}(z, y) &= N^{-1/3} \left(\mathbf{WB}[(N + z_N, k) \rightarrow (N + y_N, 1)] + (WB)_k(N + z_N) - 2N - 2yN^{2/3} \right) \\ H^{N,\text{Br}}(x, y) &= N^{-1/3} \left(\mathbf{WB}[(x_N, N) \rightarrow (N + y_N, 1)] - 2N - 2(y - x)N^{2/3} \right). \end{aligned}$$

It follows from [DOV22, Proposition 2.2] or [CH14, Proposition 4.1] that $G_k^{N,\text{Br}}(z, y) \xrightarrow{d} G_k(z, y)$ for any fixed z and y (which may depend on k).

We will also need a certain stationarity property of G_k :

Lemma C.6. Fix $\varepsilon \in \mathbb{R}$ and $z < y$. Then

$$G_k(z\sqrt{k}, y\sqrt{k}) \stackrel{d}{=} G_k((z + \varepsilon)\sqrt{k}, (y + \varepsilon)\sqrt{k}) + (\varepsilon^2 + 2\varepsilon y)k.$$

Proof. Recall that $G_k(z, y) = \mathcal{P}[(z, k) \rightarrow (y, 1)] + \mathcal{P}_k(z)$ and that $\mathcal{P}_i(x) = \mathcal{A}_i(x) - x^2$ for all $i \in \mathbb{N}$ and $x \in \mathbb{R}$, where \mathcal{A} is the Airy line ensemble and is stationary. Also note that for any up-right path γ from (z, k) to $(y, 1)$, $\mathcal{P}[\gamma] = \mathcal{A}[\gamma] - y^2 + z^2$. Thus it follows that

$$\begin{aligned} G_k(z, y) &= \mathcal{A}[(z, k) \rightarrow (y, 1)] - y^2 + z^2 + \mathcal{A}_k(z) - z^2 \\ &\stackrel{d}{=} \mathcal{A}[(z + \varepsilon, k) \rightarrow (y + \varepsilon, 1)] - y^2 + \mathcal{A}_k(z + \varepsilon) \\ &= \mathcal{P}[(z + \varepsilon, k) \rightarrow (y + \varepsilon, 1)] - y^2 + (y + \varepsilon)^2 + \mathcal{P}_k(z + \varepsilon). \end{aligned}$$

This equals $G(z + \varepsilon, y + \varepsilon) + \varepsilon^2 + 2\varepsilon y$. Replacing z by $z\sqrt{k}$, y by $y\sqrt{k}$, and ε by $\varepsilon\sqrt{k}$ completes the proof. \square

Proof of Lemma C.3. In the proof we will prove the statement with z_0 in place of z as we will need to use z as a generic variable. As mentioned, we will prove that

$$G_k^{N, \text{Br}}(z_0\sqrt{k}, y\sqrt{k}) = -y^2k - \sqrt{k}/(y - z_0) + \mathfrak{o}(\sqrt{k});$$

then since $G_k^{N, \text{Br}}(z_0\sqrt{k}, y\sqrt{k}) \xrightarrow{d} G_k(z_0\sqrt{k}, y\sqrt{k})$ as $N \rightarrow \infty$, we will be done.

We know from [DOV22, Proposition 6.1] that $F_k^{N, \text{Br}}(x, z\sqrt{k}) = (2\sqrt{2x} + 2xz)\sqrt{k} + \mathfrak{o}(k^{1/2})$ for any $0 < x < z$, and from [DOV22, Theorem 1.4, Proposition 4.1] that $H^{N, \text{Br}}(x, y) \xrightarrow{d} \mathcal{S}(x; y) = -(x - y)^2 + \mathfrak{o}(\sqrt{k})$. By the variational definition of the LPP values, we also know that

$$H^{N, \text{Br}}(x, y) = \sup_{z \in \mathbb{R}} F_k^{N, \text{Br}}(x, z) + G_k^{N, \text{Br}}(z, y). \quad (\text{C.9})$$

Let $x_0 = 1/(2(y - z_0)^2)$. The previous display implies that there is a random $z_k^{*, N}$ such that

$$F_k^{N, \text{Br}}(x_0, z_k^{*, N}\sqrt{k}) + G_k^{N, \text{Br}}(z_k^{*, N}\sqrt{k}, y\sqrt{k}) = H^{N, \text{Br}}(x_0, y\sqrt{k}) = -(x_0 - y\sqrt{k})^2 + \mathfrak{o}(\sqrt{k}). \quad (\text{C.10})$$

We claim that

$$z_k^{*, N} = -\sqrt{\frac{1}{2x_0}} + y + \mathfrak{o}(1) = z_0 + \mathfrak{o}(1) \quad (\text{C.11})$$

and that $\{z_k^{*, N}\}_{N=1}^\infty$ is tight. By (C.9), we know

$$G_k^{N, \text{Br}}(z\sqrt{k}, y\sqrt{k}) \leq H^{N, \text{Br}}(x, y\sqrt{k}) - F_k^{N, \text{Br}}(x, z\sqrt{k})$$

for all x, y, z . Taking $x = 1/(2(y - z)^2)$ and the asymptotics $H^{N, \text{Br}}(x, y\sqrt{k}) = -(x - y\sqrt{k})^2 + \mathfrak{o}(\sqrt{k})$, $F_k^{N, \text{Br}}(x, z\sqrt{k}) = 2\sqrt{2kx} + 2\sqrt{kxz} + \mathfrak{o}(\sqrt{k})$ yields that

$$G_k^{N, \text{Br}}(z\sqrt{k}, y\sqrt{k}) \leq -y^2k - \frac{\sqrt{k}}{y - z} + \mathfrak{o}(\sqrt{k}); \quad (\text{C.12})$$

by taking $N \rightarrow \infty$ and using $G_k^{N, \text{Br}}(z\sqrt{k}, y\sqrt{k}) \rightarrow G_k(z\sqrt{k}, y\sqrt{k})$ in distribution we also obtain the upper bound half of the overall equality we are aiming to prove. Using this upper bound and the same asymptotics on $H^{N, \text{Br}}$ and $F_k^{N, \text{Br}}$ in (C.10) yields that the latter cannot hold if the claimed (C.11) does not hold. As with the tightness of Z_k^N in Proposition 7.2, the tightness of $z_k^{*, N}$ follows from the just established asymptotic and the monotonicity of the sequence in k from Lemma C.1.

It remains to prove a lower bound on $G_k(z\sqrt{k}, y\sqrt{k})$ matching the upper bound in (C.12). With (C.11) we see that

$$\begin{aligned} G_k^{N, \text{Br}}(z_k^{*, N}\sqrt{k}, y\sqrt{k}) &= H^{N, \text{Br}}(x_0, y\sqrt{k}) - F_k^{N, \text{Br}}(x_0, z_k^{*, N}\sqrt{k}) \\ &= -(x_0 - y\sqrt{k})^2 - (2\sqrt{2x_0} + 2x_0z_k^{*, N})\sqrt{k} + \mathfrak{o}(\sqrt{k}) \\ &= -y^2k + 2x_0y\sqrt{k} - (2\sqrt{2x_0} + 2x_0(-(2x_0)^{-1/2} + y))\sqrt{k} + \mathfrak{o}(\sqrt{k}). \end{aligned}$$

By simplifying, the previous line equals

$$G_k^{N, \text{Br}}(z_k^{*,N} \sqrt{k}, y \sqrt{k}) = -y^2 k - \sqrt{2x_0 k} + \mathfrak{o}(\sqrt{k}) = -y^2 k - \frac{\sqrt{k}}{y - z_0} + \mathfrak{o}(\sqrt{k}). \quad (\text{C.13})$$

By using the tightness of $z_k^{*,N}$ and the weak convergence of $G_k^{N, \text{Br}}$ to G_k , we obtain the existence of a z_k^* satisfying (C.11) and the previous display with G_k and z_k^* in place of their prelimiting analogs.

To go from $G_k(z_k^* \sqrt{k}, y \sqrt{k})$ to $G_k(z_0 \sqrt{k}, y \sqrt{k})$, we use that $G_k(\cdot, y)$ is monotonically decreasing by Lemma C.2, as well as the stationarity property from Lemma C.6. In the case that $z_k^* \geq z_0$, the monotonicity of $G_k(\cdot, y \sqrt{k})$ along with (C.13) immediately yields that

$$G_k(z_0 \sqrt{k}, y \sqrt{k}) \geq G_k(z_k^* \sqrt{k}, y \sqrt{k}) \geq -y^2 k - \frac{\sqrt{k}}{y - z_0} + \mathfrak{o}(\sqrt{k}). \quad (\text{C.14})$$

In the case that $z_k^* < z_0$, we know from above that $z_k^* > z_0 - \mathfrak{o}(1)$, i.e., for any $\varepsilon > 0$ it holds that $\sum_k \mathbb{P}(z_k^* < z_0 - \varepsilon) < \infty$. We fix $\varepsilon > 0$, and apply Lemma C.6 along with monotonicity of $G_k(\cdot, y \sqrt{k})$ again to obtain that, for any deterministic sequence M_k ,

$$\begin{aligned} \mathbb{P}\left(G_k(z_0 \sqrt{k}, y \sqrt{k}) < M_k - \varepsilon \sqrt{k}\right) &= \mathbb{P}\left(G_k((z_0 - \varepsilon) \sqrt{k}, (y - \varepsilon) \sqrt{k}) < M_k - (\varepsilon^2 - 2\varepsilon y)k - \varepsilon \sqrt{k}\right) \\ &\leq \mathbb{P}\left(G_k(z_k^* \sqrt{k}, (y - \varepsilon) \sqrt{k}) < M_k - (\varepsilon^2 - 2\varepsilon y)k - \varepsilon \sqrt{k}\right) \\ &\quad + \mathbb{P}(z_k^* < z_0 - \varepsilon). \end{aligned}$$

Now by (C.13), when $M_k = -(y - \varepsilon)^2 k - \sqrt{k}/(y - \varepsilon - z_0) + (\varepsilon^2 - 2\varepsilon y)k$, the first term in the previous display is summable, and we already noted that the second is also summable. We can write

$$M_k = -y^2 k - \frac{\sqrt{k}}{y - z_0} - \varepsilon \sqrt{k} \cdot \left(\frac{1}{(y - z_0)(y - z_0 - \varepsilon)} \right),$$

and the parenthetical term is positive and $O(1)$. Thus we have established that $\mathbb{P}(G_k(z_0 \sqrt{k}, y \sqrt{k}) < -y^2 k - \sqrt{k}/(y - z_0) - \varepsilon \sqrt{k})$ is summable for every $\varepsilon > 0$, i.e., $G_k(z_0 \sqrt{k}, y \sqrt{k}) \geq -y^2 k - \sqrt{k}/(y - z_0) + \mathfrak{o}(\sqrt{k})$. This, along with (C.14) and (C.12), completes the proof. \square

APPENDIX D. DIRECTED LANDSCAPE AND KPZ FIXED POINT CONVERGENCE

In this section we prove Corollaries 2.12 (ASEP) and 2.20 (S6V), using an idea communicated to us by Shalin Parekh; it was also used by him in the work [Par23] establishing joint convergence of ASEP in the weakly asymmetric regime under multiple initial conditions with the basic coupling to the KPZ equation with multiple initial conditions driven by the same noise. We prove Corollary 2.12 in Section D.1 and Corollary 2.20 in Section D.2. The latter relies on an approximate monotonicity result (Proposition D.3) which is proved in Section D.3, and a finite speed of discrepancy bound (Lemma D.4) proved in Section D.4.

D.1. ASEP to directed landscape. We start by giving a lemma on height monotonicity for ASEP under the basic coupling. Recall the definition from below (2.10) of the ASEP height function $h^{\text{ASEP}}(h_0, 0; \cdot, t)$ when started from an arbitrary height function h_0 .

Lemma D.1 (Height monotonicity of ASEP). *Let $H \in \mathbb{Z}$ be an integer and $h_0, h'_0 : \mathbb{Z} \rightarrow \mathbb{Z}$ be Bernoulli paths such that $h_0(x) + H \geq h'_0(x)$ for all $x \in \mathbb{Z}$. Then, under the basic coupling, almost surely, $h^{\text{ASEP}}(h_0, 0; x, t) + H \geq h^{\text{ASEP}}(h'_0, 0; x, t)$ for all $x \in \mathbb{Z}$ and $t > 0$.*

Proof. This follows immediately from the definitions of the basic coupling in Section 2.2.6 and $h^{\text{ASEP}}(h_0, 0; \cdot, t)$ from below (2.10). \square

We will also need to use the following basic observation, whose proof is trivial and omitted.

Lemma D.2. *Let X, Y be random variables such that $\mathbb{E}[|X|], \mathbb{E}[|Y|] < \infty$. Suppose $X \geq Y$ almost surely and $\mathbb{E}[X] = \mathbb{E}[Y]$. Then $X = Y$ almost surely.*

Proof of Corollary 2.12 (1) & (2). Corollary 2.12 (2) follows immediately from (1), so we only need to establish the latter. The convergence of $(\mathcal{L}^{\text{ASEP}, \varepsilon}(\cdot, s; \cdot, t) : (s, t) \in \mathcal{T}_{<}^2)$ to $(\mathcal{L}(\cdot, s; \cdot, t) : (s, t) \in \mathcal{T}_{<}^2)$ in the space $\mathcal{C}(\mathbb{R}^2, \mathbb{R})^{\mathcal{T}_{<}^2}$ is equivalent to the convergence

$$(\mathcal{L}^{\text{ASEP}, \varepsilon}(\cdot, s; \cdot, t) : (s, t) \in \mathcal{U}_{<}^2) \xrightarrow{d} (\mathcal{L}(\cdot, s; \cdot, t) : (s, t) \in \mathcal{U}_{<}^2) \quad (\text{D.1})$$

for every finite subset $\mathcal{U} \subseteq \mathcal{T}$. Fix such a \mathcal{U} and write $\mathcal{U} = \{s_i : i \in \llbracket 1, n \rrbracket\}$ with $0 \leq s_1 < \dots < s_n$ for some $n \in \mathbb{N}$.

We first observe that $(\mathcal{L}^{\text{ASEP}, \varepsilon}(\cdot, s; \cdot, t) : (s, t) \in \mathcal{U}_{<}^2)$ is a tight sequence in ε . This follows from combining the fact that, by Definitions 2.7 and 2.10,

$$\mathcal{L}^{\text{ASEP}, \varepsilon}(x, s; y, t) \stackrel{d}{=} (t-s)^{1/3} \mathcal{S}^{\text{ASEP}, (t-s)^{-1}\varepsilon}((t-s)^{-2/3}x; (t-s)^{-2/3}y) \quad (\text{D.2})$$

as processes in (x, y) , with Theorem 2.8 and the relation of \mathcal{L} with \mathcal{S} from Definition 2.4 (i), namely, for any $t > 0$, and as processes in x and y ,

$$\mathcal{L}(x, s; y, t) \stackrel{d}{=} (t-s)^{1/3} \mathcal{S}((t-s)^{-2/3}x, (t-s)^{-2/3}y). \quad (\text{D.3})$$

Let $(\tilde{\mathcal{L}}(\cdot, s; \cdot, t) : (s, t) \in \mathcal{U}_{<}^2)$ be any subsequential limit point of the lefthand side of (D.1). Then we further see from Theorem 2.8, (D.2), and (D.3) that, for each $(s, t) \in \mathcal{U}_{<}^2$, $\tilde{\mathcal{L}}(\cdot, s; \cdot, t) \stackrel{d}{=} \mathcal{L}(\cdot, s; \cdot, t)$. We next observe that $(\tilde{\mathcal{L}}(\cdot, s_i; \cdot, s_{i+1}) : i \in \llbracket 1, n-1 \rrbracket) \stackrel{d}{=} (\mathcal{L}(\cdot, s_i; \cdot, s_{i+1}) : i \in \llbracket 1, n-1 \rrbracket)$, since each of the components of the lefthand vector are independent, and the same for the righthand vector.

With these facts in hand, (D.1) is reduced to showing that, for any $r, s, t \in \mathcal{U}$ with $r < s < t$ fixed, almost surely, for all $x, y \in \mathbb{R}^2$,

$$\tilde{\mathcal{L}}(x, r; y, t) = \sup_{z \in \mathbb{R}} \left(\tilde{\mathcal{L}}(x, r; z, s) + \tilde{\mathcal{L}}(z, s; y, t) \right); \quad (\text{D.4})$$

this suffices since the righthand side is a deterministic function of the independent quantities $\tilde{\mathcal{L}}(\cdot, r; \cdot, s)$ and $\tilde{\mathcal{L}}(\cdot, s; \cdot, t)$ and the same relation holds with \mathcal{L} in place of $\tilde{\mathcal{L}}$. We show (D.4) by returning to the prelimit. Fix r, s, t as above. We first claim that, almost surely, for all $x, y, z \in \mathbb{Z}$ (recall $\gamma = 1 - q$),

$$\begin{aligned} h^{\text{ASEP}}(x, 2\gamma^{-1}r\varepsilon^{-1}; z, 2\gamma^{-1}s\varepsilon^{-1}) + h^{\text{ASEP}}(z, 2\gamma^{-1}s\varepsilon^{-1}; y, 2\gamma^{-1}t\varepsilon^{-1}) \\ \geq h^{\text{ASEP}}(x, 2\gamma^{-1}r\varepsilon^{-1}; y, 2\gamma^{-1}t\varepsilon^{-1}). \end{aligned} \quad (\text{D.5})$$

This holds for $z \geq y$ as both sides are equal at $z = y$, the first term on the lefthand side is non-increasing and decreases by at most 1 in going from z to $z+1$, and the second term on the lefthand side is

$$h^{\text{ASEP}}(z, 2\gamma^{-1}s\varepsilon^{-1}; y, 2\gamma^{-1}t\varepsilon^{-1}) = (z-y)\mathbb{1}_{y \leq z}$$

and so increases by 1 on going from z to $z+1$. Similarly, for $z \leq y$, we have equality in (D.5) at $z = y$, the first term on the lefthand side weakly increases on going from z to $z-1$, and the second term on the lefthand side is 0 for all $z \leq y$.

We now view (D.5) as an ordering of initial conditions: for each x, z fixed, we regard the first term $h^{\text{ASEP}}(x, 2\gamma^{-1}r\varepsilon^{-1}; z, 2\gamma^{-1}s\varepsilon^{-1})$ as a (random) constant, and $h^{\text{ASEP}}(z, 2\gamma^{-1}s\varepsilon^{-1}; \cdot, 2\gamma^{-1}t\varepsilon^{-1})$ and $h^{\text{ASEP}}(x, 2\gamma^{-1}r\varepsilon^{-1}; \cdot, 2\gamma^{-1}t\varepsilon^{-1})$ both as initial conditions. Evolving both for time $2\gamma^{-1}(t-s)\varepsilon^{-1}$ under the basic coupling, Lemma D.1 guarantees that, almost surely, for all $x, y, z \in \mathbb{Z}$,

$$\begin{aligned} h^{\text{ASEP}}(x, 2\gamma^{-1}r\varepsilon^{-1}; z, 2\gamma^{-1}s\varepsilon^{-1}) + h^{\text{ASEP}}(z, 2\gamma^{-1}s\varepsilon^{-1}; y, 2\gamma^{-1}t\varepsilon^{-1}) \\ \geq h^{\text{ASEP}}(x, 2\gamma^{-1}r\varepsilon^{-1}; y, 2\gamma^{-1}t\varepsilon^{-1}). \end{aligned}$$

Centering and rescaling according to Definition 2.10, and taking $\varepsilon \rightarrow 0$, the previous display yields that, almost surely, for all $x, y \in \mathbb{R}$,

$$\tilde{\mathcal{L}}(x, r; y, t) \geq \sup_{z \in \mathbb{R}} \left(\tilde{\mathcal{L}}(x, r; z, s) + \tilde{\mathcal{L}}(z, s; y, t) \right). \quad (\text{D.6})$$

However, we know that both sides of this inequality are marginally distributed as the corresponding expression with \mathcal{L} in place of $\tilde{\mathcal{L}}$ and, further, we know that, almost surely, for all $x, y \in \mathbb{R}$,

$$\mathcal{L}(x, r; y, t) = \sup_{z \in \mathbb{R}} \left(\mathcal{L}(x, r; z, s) + \mathcal{L}(z, s; y, t) \right). \quad (\text{D.7})$$

Thus, we know that the expectations of the lefthand and righthand sides of (D.6) are equal for every fixed x, y . Applying Lemma D.2 with (D.6) yields that (D.4) holds for all $x, y \in \mathbb{Q}^2$ on a single probability one event; since both sides are continuous in x and y , we obtain that (D.4) holds on a probability one event for all $x, y \in \mathbb{R}^2$. This completes the proof. \square

Proof of Corollary 2.12 (3). We start by recalling $\mathfrak{h}^{\text{ASEP}, \varepsilon}(h_0^{(i), \varepsilon}; \cdot, t)$ from Definition 2.11, that $\mathfrak{h}_0^{(i), \varepsilon}(x) := 2\varepsilon^{1/3}(x\varepsilon^{-2/3} - h_0^{(i), \varepsilon}(2x\varepsilon^{-2/3}))$, and that $\mathfrak{h}_0^{(i), \varepsilon} \rightarrow \mathfrak{h}_0^{(i)}$ for each $i \in \llbracket 1, k \rrbracket$ uniformly on compact sets. As in the proof of Corollary 2.12 (1) above, it is sufficient to prove that, for any finite $\mathcal{U} \subseteq \mathcal{T}$, as $\varepsilon \rightarrow 0$,

$$\left(\mathfrak{h}^{\text{ASEP}, \varepsilon}(h_0^{(i), \varepsilon}; \cdot, t) : t \in \mathcal{U} \right) \xrightarrow{d} \left(\mathfrak{h}(\mathfrak{h}_0^{(i)}; \cdot, t) : t \in \mathcal{U} \right),$$

where the righthand side is coupled via a common directed landscape \mathcal{L} as in (2.4). Fix such a \mathcal{U} . We will prove that

$$\begin{aligned} & \left(\mathfrak{h}^{\text{ASEP}, \varepsilon}(h_0^{(i), \varepsilon}; \cdot, t), \mathcal{L}^{\text{ASEP}, \varepsilon}(\cdot, 0; \cdot, t) : i \in \llbracket 1, k \rrbracket, t \in \mathcal{U} \right) \\ & \xrightarrow{d} \left(\mathfrak{h}(\mathfrak{h}_0^{(i)}; \cdot, t), \mathcal{L}(\cdot, 0; \cdot, t) : i \in \llbracket 1, k \rrbracket, t \in \mathcal{U} \right). \end{aligned} \quad (\text{D.8})$$

First, $(\mathfrak{h}^{\text{ASEP}, \varepsilon}(h_0^{(i), \varepsilon}; \cdot, t) : i \in \llbracket 1, k \rrbracket, t \in \mathcal{U})$ is a tight sequence in ε , and for each $i \in \llbracket 1, k \rrbracket, t \in \mathcal{U}$, we have the marginal convergence of $\mathfrak{h}^{\text{ASEP}, \varepsilon}(h_0^{(i), \varepsilon}; \cdot, t)$ to $\mathfrak{h}(\mathfrak{h}_0^{(i)}; \cdot, t)$; the former follows from the latter, which in turn is given by [QS22, Theorem 2.2 (2)]. We also know from Corollary 2.12 (1) that

$$\left(\mathcal{L}^{\text{ASEP}, \varepsilon}(\cdot, 0; \cdot, t) : t \in \mathcal{U} \right) \xrightarrow{d} \left(\mathcal{L}(\cdot, 0; \cdot, t) : t \in \mathcal{U} \right).$$

Let $(\tilde{\mathfrak{h}}(\mathfrak{h}_i^{(0)}; \cdot, t), \mathcal{L}(\cdot, 0; \cdot, t) : t \in \mathcal{U})$ be any subsequential limit point of the lefthand side of (D.8), so that the \mathcal{L} terms are coupled as the directed landscape and each $\tilde{\mathfrak{h}}(\mathfrak{h}_i^{(0)}; \cdot, t)$ is marginally distributed as the KPZ fixed point $\mathfrak{h}(\mathfrak{h}_0^{(i)}; \cdot, t)$ for each fixed $t \in \mathcal{U}$ and $i \in \llbracket 1, k \rrbracket$. Now, (D.8) is reduced to showing that, for any $t \in \mathcal{U}$ and $i \in \llbracket 1, k \rrbracket$ fixed, almost surely, for all $y \in \mathbb{R}^2$,

$$\tilde{\mathfrak{h}}(\mathfrak{h}_0^{(i)}; y, t) = \sup_{z \in \mathbb{R}} \left(\mathfrak{h}_0^{(i)}(z) + \mathcal{L}(z, 0; y, t) \right). \quad (\text{D.9})$$

As in the proof of Corollary 2.12 (1), we show (D.9) by returning to the prelimit. We first claim that, almost surely, for every $y, z \in \mathbb{R}$ and $i \in \llbracket 1, k \rrbracket$,

$$h_0^{(i), \varepsilon}(z) + h^{\text{ASEP}}(z, 0; y, 0) \geq h_0^{(i), \varepsilon}(y). \quad (\text{D.10})$$

As in the proof of Corollary 2.12 (1), this holds for $z \geq y$ as both sides are equal at $z = y$, the first term on the lefthand side is non-increasing and decreases by at most 1 in going from z to $z + 1$, and $h^{\text{ASEP}}(z, 0; y, 0) = (z - y)\mathbb{1}_{y \leq z}$, so the second term on the lefthand side increases by 1 on going from z to $z + 1$. Similarly, for $z \leq y$, we have equality at $z = y$, the first term on the lefthand side weakly increases on going from z to $z - 1$, and $h^{\text{ASEP}}(z, 0; y, 0) = 0$ for all such z .

We now view (D.10) as an ordering of initial conditions: for each z fixed, we regard $h_0^{(i),\varepsilon}(z)$ as a (random) constant and both $h^{\text{ASEP}}(z, 0; \cdot, 0)$ and $h_0^{(i),\varepsilon}(\cdot)$ as initial conditions. Evolving both for time $2\gamma^{-1}t\varepsilon^{-1}$ (recall $\gamma = 1 - q$) under the basic coupling, Lemma D.1 guarantees that, almost surely, for all $y, z \in \mathbb{Z}$ and $i \in \llbracket 1, k \rrbracket$,

$$h_0^{(i),\varepsilon}(z) + h^{\text{ASEP}}(z, 0; y, 2\gamma^{-1}t\varepsilon^{-1}) \geq h^{\text{ASEP}}(h_0^{(i),\varepsilon}, 0; y, 2\gamma^{-1}t\varepsilon^{-1}).$$

Centering and rescaling according to Definition 2.11, and taking $\varepsilon \rightarrow 0$, the previous display yields that, almost surely, for all $y \in \mathbb{R}$,

$$\tilde{\mathfrak{h}}(\mathfrak{h}_0^{(i)}; y, t) \geq \sup_{z \in \mathbb{R}} \left(\mathfrak{h}_0^{(i)}(z) + \mathcal{L}(z, 0; y, t) \right). \tag{D.11}$$

However, we know that both sides of this inequality are marginally distributed as $\mathfrak{h}(\mathfrak{h}_0^{(i)}; y, t)$ (for the righthand side, using (2.4)). Thus, the expectations of the lefthand and righthand sides of (D.11) are equal for every fixed y , so Lemma D.2 implies that the two sides are equal on a probability 1 event for all $y \in \mathbb{Q}$ and $i \in \llbracket 1, k \rrbracket$; since both sides are continuous in y , this yields equality for all $y \in \mathbb{R}$ and $i \in \llbracket 1, k \rrbracket$, completing the proof. \square

D.2. S6V to directed landscape. The basic coupling for S6V does not have the height monotonicity properties it does in ASEP (Lemma D.1). Nevertheless, an approximate version holds, as recorded next. It will be proved in Section D.3.

Proposition D.3 (Approximate height monotonicity of S6V). *Fix $N \in \mathbb{N}$. Let $H \in \mathbb{Z}$ and let $h_0^{(1)}, h_0^{(2)} : \llbracket -N - 1, \infty \rrbracket \rightarrow \mathbb{Z}_{\geq 0}$ be two Bernoulli paths such that $h_0^{(1)}(x) + H \geq h_0^{(2)}(x)$ for all $x \in \llbracket -N - 1, \infty \rrbracket$, and, for $i = 1, 2$, $h_0^{(i)}(-N - 1) \leq N$ and $h_0^{(i)}(x) = 0$ for all large x . There exist absolute constants $C, c > 0$ such that, for $t \in \mathbb{N}$ and under the basic coupling, the following holds. For any $M \geq (\log N)^2$, with probability at least $1 - C \exp(-cM)$, $h^{\text{S6V}}(h_0^{(1)}; x, t) + H \geq h^{\text{S6V}}(h_0^{(2)}; x, t) - M$ for all $x \in \llbracket -N - 1, \infty \rrbracket$.*

We will also need a finite speed of discrepancy estimate for the S6V model under the basic coupling. Its straightforward proof will be given in Section D.4.

Lemma D.4 (Finite speed of discrepancy). *For any real numbers $0 \leq b^\uparrow \leq b^\rhd < 1$, there exist constants $c > 0$ and $C > 1$ such that the following holds. Let $m \in \mathbb{N}$ be an integer, and for $k \in \llbracket 1, m \rrbracket$ and $i \in \{1, 2\}$, let $s_k \in \mathbb{Z}_{\geq 1}$, $N_i \in \mathbb{N}$, and $h_0^{(i),k} : \llbracket -N_i, \infty \rrbracket \rightarrow \mathbb{Z}$ be Bernoulli paths which equal 0 for all large x . Assume that $N_1 \leq N_2$ and, for $k \in \llbracket 1, m \rrbracket$, $h_0^{(1),k}(x) = h_0^{(2),k}(x)$ for all $x \in \llbracket -N_1, N_1 \rrbracket$. For $i \in \{1, 2\}$ and $k \in \llbracket 1, m \rrbracket$, let $(j_{(x,y)}^{(i),k} : (x, y) \in \llbracket -N_i, \infty \rrbracket \times \llbracket s_k, \infty \rrbracket)$ denote samples from stochastic six-vertex models with boundary conditions given by $h_0^{(i),k}$ at time s_k (recall from Section 2.3.3), all coupled via the basic coupling. Then, for any $T \in \mathbb{N}$ such that $T \leq \frac{1}{4}(1 - b^\rhd)N_1$, with probability at least $1 - Cme^{-cN_1}$, we have that $j_{(x,y)}^{(1),k} = j_{(x,y)}^{(2),k}$ for all $k \in \llbracket 1, m \rrbracket$ and $(x, y) \in \llbracket 1, T \rrbracket \times \llbracket -\lfloor \frac{1}{2}N_1 \rfloor, \lfloor \frac{1}{2}N_1 \rfloor \rrbracket$.*

With these two statements in hand, we can give the proof of Corollary 2.20 along very similar lines as the proof of Corollary 2.12 (1).

Proof of Corollary 2.20. Item (2) is an immediate consequence of (1), so we only need to prove the latter. We first claim that we may assume that $N \leq \varepsilon^{-3}$, where recall ε is the parameter in Definition 2.19 of $\mathcal{L}^{\text{S6V},\varepsilon}$. More precisely, if $N > \varepsilon^{-3}$, we may couple an ASEP landscape $\tilde{\mathcal{L}}^{\text{S6V},\varepsilon}$ with that value of N to a copy $\mathcal{L}^{\text{S6V},\varepsilon}$ with $N = \varepsilon^{-3}$ such that, with probability at least $1 - C \exp(-c\varepsilon^{-3})$, $\mathcal{L}^{\text{S6V},\varepsilon}(x, s; y, t) = \tilde{\mathcal{L}}^{\text{S6V},\varepsilon}(x, s; y, t)$ or all $|x|, |y|, |s|, |t| \leq \varepsilon^{-1/6}$. As in the proof of Theorem 2.18 in Section 7.2, the existence of this coupling amounts to a finite speed of discrepancy bound; because we need it for the basic coupling and not the colored coupling as there, we use Lemma D.4. We record

the parameters we will apply Lemma D.4 with: $T = \lceil \varepsilon^{-7/6} \rceil$, $N_1 = \varepsilon^{-3}$, N_2 the value of N associated to $\tilde{\mathcal{L}}^{\text{S6V},\varepsilon}$, and $m = T \cdot (2N_1 + 1)$. The height functions we consider are, at each time $s \in \llbracket 1, T \rrbracket$, the collection of step initial conditions starting from x for $x \in \llbracket -N_1, N_1 \rrbracket$, where the step initial condition from x means, for $i \in \{1, 2\}$ and in system i , particles at every location in $\llbracket x, N_i \rrbracket$ (note that this indeed yields m many height functions). Lemma D.4 then yields the claimed coupling. In the remainder of the proof we assume $N = \varepsilon^{-3}$ by working on the event of the above coupling holding, and we denote by $\mathcal{L}^{\text{S6V},\varepsilon}$ the associated S6V landscape. Since the probability of the coupling holding goes to 1 as $\varepsilon \rightarrow 0$, it suffices to show that $(\mathcal{L}^{\text{S6V},\varepsilon}(\cdot, s; \cdot, t) : (s, t) \in \mathcal{T}_<^2) \xrightarrow{d} (\mathcal{L}(\cdot, s; \cdot, t) : (s, t) \in \mathcal{T}_<^2)$.

Now, the convergence of $(\mathcal{L}^{\text{S6V},\varepsilon}(\cdot, s; \cdot, t) : (s, t) \in \mathcal{T}_<^2)$ to $(\mathcal{L}(\cdot, s; \cdot, t) : (s, t) \in \mathcal{T}_<^2)$ in the space $\mathcal{C}(\mathbb{R}^2, \mathbb{R})^{\mathcal{T}_<^2}$ is equivalent to the convergence

$$(\mathcal{L}^{\text{S6V},\varepsilon}(\cdot, s; \cdot, t) : (s, t) \in \mathcal{U}_<^2) \xrightarrow{d} (\mathcal{L}(\cdot, s; \cdot, t) : (s, t) \in \mathcal{U}_<^2) \quad (\text{D.12})$$

for every finite subset $\mathcal{U} \subseteq \mathcal{T}$. Fix such a \mathcal{U} and write $\mathcal{U} = \{s_i : i \in \llbracket 1, n \rrbracket\}$ with $0 \leq s_1 < \dots < s_n$ for some $n \in \mathbb{N}$.

We observe that $(\mathcal{L}^{\text{S6V},\varepsilon}(\cdot, s; \cdot, t) : (s, t) \in \mathcal{U}_<^2)$ is a tight sequence in ε . This follows from combining the fact that, by Definitions 2.17 and 2.19,

$$\mathcal{L}^{\text{S6V},\varepsilon}(x, s; y, t) \stackrel{d}{=} (t-s)^{1/3} \mathcal{S}^{\text{S6V},(t-s)^{-1}\varepsilon}((t-s)^{-2/3}x; (t-s)^{-2/3}y) \quad (\text{D.13})$$

as processes in (x, y) , with Theorem 2.18 and the relation of \mathcal{L} with \mathcal{S} noted in (D.3).

Let $(\tilde{\mathcal{L}}(\cdot, s; \cdot, t) : (s, t) \in \mathcal{U}_<^2)$ be any subsequential limit point of the lefthand side of (D.12). Then we further see from Theorem 2.18, (D.3), and (D.13) that, for each $(s, t) \in \mathcal{U}_<^2$, $\tilde{\mathcal{L}}(\cdot, s; \cdot, t) \stackrel{d}{=} \mathcal{L}(\cdot, s; \cdot, t)$. We next observe that $(\tilde{\mathcal{L}}(\cdot, s_i; \cdot, s_{i+1}) : i \in \llbracket 1, n-1 \rrbracket) \stackrel{d}{=} (\mathcal{L}(\cdot, s_i; \cdot, s_{i+1}) : i \in \llbracket 1, n-1 \rrbracket)$, since each of the components of the lefthand vector are independent, and the same for the righthand vector.

With these facts in hand, (D.12) is reduced to showing that, for any $r, s, t \in \mathcal{U}$ with $r < s < t$ fixed, almost surely, for all $x, y \in \mathbb{R}^2$,

$$\tilde{\mathcal{L}}(x, r; y, t) = \sup_{z \in \mathbb{R}} \left(\tilde{\mathcal{L}}(x, r; z, s) + \tilde{\mathcal{L}}(z, s; y, t) \right); \quad (\text{D.14})$$

this suffices since the righthand side is a deterministic function of the independent quantities $\tilde{\mathcal{L}}(\cdot, r; \cdot, s)$ and $\tilde{\mathcal{L}}(\cdot, s; \cdot, t)$ and the same relation holds with \mathcal{L} in place of $\tilde{\mathcal{L}}$. We show (D.14) by returning to the prelimit. Fix r, s, t as above. We first claim that almost surely, for all $x, y, z \in \llbracket -N-1, \infty \rrbracket$,

$$h^{\text{S6V}}(x, r\varepsilon^{-1}; z, s\varepsilon^{-1}) + h^{\text{S6V}}(z, s\varepsilon^{-1}; y, s\varepsilon^{-1}) \geq h^{\text{S6V}}(x, r\varepsilon^{-1}; y, s\varepsilon^{-1}). \quad (\text{D.15})$$

This holds for $z \geq y \geq -N-1$ as both sides are equal at $z = y$, the first term on the lefthand side is non-increasing and decreases by at most 1 in going from z to $z+1$, and the second term on the lefthand side is

$$h^{\text{S6V}}(z, s\varepsilon^{-1}; y, s\varepsilon^{-1}) = (z-y) \mathbb{1}_{-N-1 \leq y \leq z}$$

and so increases by 1 on going from z to $z+1$. Similarly, for $-N-1 \leq z \leq y$, we have equality in (D.15) at $z = y$, the first term on the lefthand side weakly increases on going from z to $z-1$, and the second term on the lefthand side is 0 for all $-N-1 \leq z \leq y$.

We now view (D.15) as an ordering of initial conditions: for each x, z fixed, we regard the first term $h^{\text{S6V}}(x, r\varepsilon^{-1}; z, s\varepsilon^{-1})$ as a (random) constant, and $h^{\text{S6V}}(z, s\varepsilon^{-1}; \cdot, s\varepsilon^{-1})$ and $h^{\text{S6V}}(x, r\varepsilon^{-1}; \cdot, s\varepsilon^{-1})$ both as initial conditions. Evolving both for time $(t-s)\varepsilon^{-1}$ under the basic coupling, Proposition D.3 and a union bound over $x, z \in \llbracket -N-1, N \rrbracket$ guarantees that there exist $c, C > 0$ such that, with probability at least $1 - C \exp(-c(\log N)^2)$, for all $x, y, z \in \llbracket -N-1, N \rrbracket$,

$$h^{\text{S6V}}(x, r\varepsilon^{-1}; z, s\varepsilon^{-1}) + h^{\text{S6V}}(z, s\varepsilon^{-1}; y, t\varepsilon^{-1}) \geq h^{\text{S6V}}(x, r\varepsilon^{-1}; y, t\varepsilon^{-1}) - (\log N)^2.$$

Next we center and rescale according to Definition 2.19 to obtain $\mathcal{L}^{\text{S6V},\varepsilon}$ and note that since $N \geq 2\alpha\varepsilon^{-1}$, the arguments of h^{S6V} still lie within the domain where the previous display holds. Recall also that the rescaling involves both sides being multiplied by $\varepsilon^{1/3}$, and that $N = \varepsilon^{-3}$; thus, the $(\log N)^2$ term vanishes in the $\varepsilon \rightarrow 0$ limit. So by taking $\varepsilon \rightarrow 0$, the previous display yields that, almost surely, for all $x, y \in \mathbb{R}$,

$$\tilde{\mathcal{L}}(x, r; y, t) \geq \sup_{z \in \mathbb{R}} \left(\tilde{\mathcal{L}}(x, r; z, s) + \tilde{\mathcal{L}}(z, s; y, t) \right).$$

However, we know that both sides of this inequality are marginally distributed as the corresponding expression with \mathcal{L} in place of $\tilde{\mathcal{L}}$, so we further know from (D.7) that the expectations of the two sides are equal. Now, Lemma D.2 yields that (D.14) holds for all $x, y \in \mathbb{Q}^2$ on a single probability one event; since both sides are continuous in x and y , we obtain that (D.14) holds on a probability one event for all $x, y \in \mathbb{R}^2$. This completes the proof. \square

D.3. Approximate monotonicity for S6V. Here we give the proof of Proposition D.3.

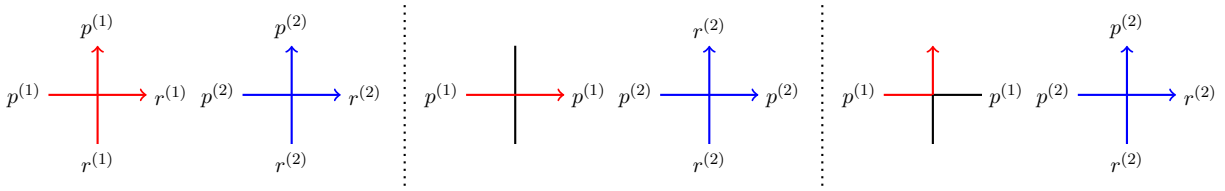


FIGURE 26. The left subfigure in each panel, with red arrows, represents a vertex in system 1, and the right subfigure, with blue arrows, represents a vertex in system 2; notice that each system is a uncolored, so here blue and red do not represent colors (in the sense of priority) associated to the arrows as in the main text of the paper. Black edges represent an absence of an arrow. For $i \in \{1, 2\}$, in system i , the label of the horizontally incoming arrow is $p^{(i)}$, and that of the vertically incoming arrow is $r^{(i)}$. The outgoing labels are assigned as depicted.

Proof of Proposition D.3. We break up the proof into a few parts. For $i \in \{1, 2\}$, we will refer to the S6V model with boundary condition $h_0^{(i)}$ as “system i ” (though note that the two systems are coupled via the basic coupling and so use the same Bernoulli random variables). Throughout this proof, we assume that $H = 0$; otherwise we may place H arrows at $+\infty$ in system 1 at time 0 if $H > 0$, or $-H$ arrows at $+\infty$ in system 2 if $H < 0$.

Specification of trajectories. Given a sample from the S6V model started from $h_0^{(1)}$ and $h_0^{(2)}$ coupled via the basic coupling, we define arrow trajectories as follows. We define them in a local way: for every pair of input and output configurations of arrows at a vertex, we define how to pair the inputs with the outputs; this extends to define arrow trajectories globally. We assume that the incoming arrows have labels, and we specify the assignment of the same labels to the outgoing arrows. For $i \in \{1, 2\}$, we use the notation $\ell_h^{(i),*}$ for $* \in \{\text{in}, \text{out}\}$ for the label of the arrow horizontally incoming and horizontally outgoing, respectively, in the i^{th} system and $\ell_v^{(i),*}$ for $* \in \{\text{in}, \text{out}\}$ for the label of the arrow vertically incoming and vertically outgoing, respectively, in the i^{th} system.

In the case that in each system a single arrow or no arrow is incident at a vertex, the pairing is obvious. If two arrows are incident at a vertex in both, then we assign $\ell_h^{(i),\text{out}} = \ell_v^{(i),\text{in}}$ and $\ell_v^{(i),\text{out}} = \ell_h^{(i),\text{in}}$ for each $i \in \{1, 2\}$; see the left panel of Figure 26. If in one system no arrows are incident at a vertex v and in the other two arrows are incident at v , we do the pairing in the latter system (system j) as in the case where two arrows are present in both systems, i.e., $\ell_h^{(j),\text{out}} = \ell_v^{(j),\text{in}}$ and $\ell_v^{(j),\text{out}} = \ell_h^{(j),\text{in}}$.

This leaves the case that one arrow is incident at a vertex v in one system and two arrows are incident at v in the other. We give the pairing in the case that the first system (with one arrow incident) is system 1 and the second system is system 2, and the analogous pairing is prescribed in the other case. If the arrow enters and exits horizontally in system 1, then we set $\ell_h^{(i),\text{out}} = \ell_h^{(i),\text{in}}$ for $i \in \{1, 2\}$ (this is the only option in the $i = 1$ case) and $\ell_v^{(2),\text{out}} = \ell_v^{(2),\text{in}}$; see middle panel of Figure 26. If the arrow enters horizontally and exits vertically in system 1, then we set $\ell_v^{(i),\text{out}} = \ell_h^{(i),\text{in}}$ for $i \in \{1, 2\}$ and $\ell_h^{(2),\text{out}} = \ell_h^{(2),\text{in}}$; see right panel of Figure 26. If the arrow in system 1 enters vertically and exits horizontally, we set $\ell_h^{(i),\text{out}} = \ell_v^{(i),\text{in}}$ for $i \in \{1, 2\}$ and $\ell_v^{(2),\text{out}} = \ell_h^{(2),\text{in}}$, and if it enters vertically and exits vertically, we set $\ell_v^{(i),\text{out}} = \ell_v^{(i),\text{in}}$ for $i \in \{1, 2\}$ and $\ell_h^{(2),\text{out}} = \ell_h^{(2),\text{in}}$.

The definition is made such that if the trajectory of an arrow in system 1 coincides at some edge with the trajectory of an arrow in system 2, then the two trajectories agree from then onwards, as can be easily checked; we will refer to this situation as the two arrows “coupling.”

Reduction to claim about arrow position ordering. For $t \in \mathbb{N}$ fixed and $i \in \{1, 2\}$, consider the set Uncoupled_i of arrows in system i which have not coupled with any arrow of the other system by time t , and let $U_i = \#\text{Uncoupled}_i$. Note that $U_1 \geq U_2$. For $s < t$, $i \in \{1, 2\}$, and $k \in \llbracket 1, U_i \rrbracket$, let us label by $X_s^{(i)}(k)$ the location at time s of the arrow in Uncoupled_i which, among arrows from the same set, is k^{th} from the bottom in the initial configuration $\eta_0^{(i)}$. Note that $X_0^{(1)}(k) \geq X_0^{(2)}(k)$ for all $k \in \llbracket 1, U_2 \rrbracket$.

We first claim that, if $X_t^{(2)}(k) \leq X_t^{(1)}(k+M)$ for all $k \in \llbracket 1, \min(U_1 - M, U_2) \rrbracket$, then $h^{\text{S6V}}(h_0^{(2)}; x, t) \leq h^{\text{S6V}}(h_0^{(1)}; x, t) + M$ for all $x \in \llbracket -N - 1, \infty \rrbracket$. Indeed, since arrows coupled by time t are counted in the height functions of both systems,

$$\begin{aligned} h^{\text{S6V}}(h_0^{(2)}; x, t) - h^{\text{S6V}}(h_0^{(1)}; x, t) &= \#\left\{k \in \llbracket 1, U_2 \rrbracket : X_t^{(2)}(k) > x\right\} - \#\left\{k \in \llbracket 1, U_1 \rrbracket : X_t^{(1)}(k) > x\right\} \\ &\leq \#\left\{k \in \llbracket 1, \min(U_1 - M, U_2) \rrbracket : X_t^{(1)}(k+M) > x\right\} \\ &\quad - \#\left\{k \in \llbracket 1, U_1 \rrbracket : X_t^{(1)}(k) > x\right\} + M \leq M. \end{aligned}$$

So it suffices to show that there exist $c > 0$ such that, for any fixed k and M ,

$$\mathbb{P}\left(X_t^{(2)}(k) > X_t^{(1)}(k+M)\right) \leq N \exp(-cM); \quad (\text{D.16})$$

indeed, then for any $M \geq (\log N)^2$ we may do a union bound over $k \in \llbracket 1, \min(U_1 - M, U_2) \rrbracket$, noting that the hypothesis that $h_0^{(i)}(-N - 1) \leq N$ for $i \in \{1, 2\}$ implies that $U_1, U_2 \leq N$ (and using that $N^2 \exp(-\frac{1}{2}c(\log N)^2)$ is bounded by an absolute constant for all N).

Reduction to overtaking event for totally uncoupled arrow. We introduce some terminology to show (D.16). We will say an arrow in system 2 “overtakes” an arrow in system 1 at a location v when the following situation occurs: v lies on the trajectory of the specified arrow in system 2 and

$$(a_v^{(1)}, i_v^{(1)}; b_v^{(1)}, j_v^{(1)}) = (0, 1; 0, 1) \quad \text{and} \quad (a_v^{(2)}, i_v^{(2)}; b_v^{(2)}, j_v^{(2)}) = (1, 0; 1, 0), \quad (\text{D.17})$$

where for $i \in \{1, 2\}$, $(a_v^{(i)}, i_v^{(i)}; b_v^{(i)}, j_v^{(i)})$ are the vertically entering, horizontally entering, vertically exiting, and horizontally exiting arrows, respectively, at vertex v in system i . Note that this implies that the arrows in both systems are uncoupled up to the point of exiting v .

We claim that, on the event in (D.16), it must be the case that at at least M vertices, the arrow in system 2 corresponding to $X_t^{(2)}(k)$ overtook an arrow in system 1. Indeed, this follows from the observation that, for any j such that $X_0^{(2)}(k) \leq X_0^{(1)}(j)$, if the arrow corresponding to $X_t^{(2)}(k)$ does not overtake the arrow corresponding to $X_t^{(1)}(j)$ at any vertex, then $X_t^{(2)}(k) \leq X_t^{(1)}(j)$; this is because uncoupled arrows cannot cross except by one overtaking the other as in (D.17).

Note that the terminology of “overtaking” does not include cases such as $(a_v^{(1)}, i_v^{(1)}; b_v^{(1)}, j_v^{(1)}) = (0, 1; 0, 1)$ and $(a_v^{(2)}, i_v^{(2)}; b_v^{(2)}, j_v^{(2)}) = (1, 1; 1, 1)$ (see, e.g., arrows labeled $p^{(1)}$ and $r^{(2)}$ in middle panel of Figure 26) or $(a_v^{(1)}, i_v^{(1)}; b_v^{(1)}, j_v^{(1)}) = (1, 1; 1, 1)$ and $(a_v^{(2)}, i_v^{(2)}; b_v^{(2)}, j_v^{(2)}) = (1, 0; 1, 0)$ which are perhaps also suggested by the terminology; this is due to the fact that such configurations correspond to the crossing of a coupled arrow with an uncoupled one, which is not relevant to our arguments (which only concern the relative orderings of the uncoupled paths in the systems).

Reduction to overtaking event for an initially uncoupled arrow. Fix an $x \in \llbracket -N, \infty \rrbracket$ such that $\eta_0^{(2)}(x) = 1$ and $\eta_0^{(1)}(x) = 0$. Consider the arrow in system 2 starting from x at time 0; in particular, the arrow is initially uncoupled (but may couple later). We will refer to it as “arrow x .” We will show the following: there exists $c > 0$ such that

$$\mathbb{P}(\exists v_1, \dots, v_M \in \mathbb{Z}_{\geq 1} \times \llbracket -N, \infty \rrbracket : \text{(D.17) occurs at each } v_i \text{ for arrow } x) \leq \exp(-cM). \quad (\text{D.18})$$

Taking a union bound over the at most N values of x with the just imposed condition will then yield (D.16), since the arrow corresponding to $X_t^{(2)}(k)$ must be arrow x for some such x .

We call a vertex v “potentially coupling” for arrow x if $(a_v^{(1)}, i_v^{(1)}) = (0, 1)$ and $(a_v^{(2)}, i_v^{(2)}) = (1, 0)$, i.e., in system 1 an arrow enters v horizontally and no arrow enters vertically, and in system 2 arrow x enters v vertically and no arrow enters horizontally. We say that arrow x in system 2 passes through a potentially coupling vertex v without coupling if v is potentially coupling for arrow x and $(B_v^\uparrow, B_v^\rightarrow) \in \{(1, 1), (0, 0)\}$, i.e, the output arrow configurations at v differ in the two systems: the arrow in system 1 exits horizontally and arrow x in system 2 exits vertically, or vice versa. Recall that if arrow x in system 2 couples at a potentially coupling vertex v , i.e., the output direction is the same at v in both systems, then for the rest of arrow x ’s trajectory it agrees with the arrow in system 1 incident at v ; in particular, it cannot overtake any further arrow in system 1 (as defined in (D.17)).

We see that the event whose probability we are bounding is contained in the event that there exist at least M potentially coupling vertices for arrow x and it does not couple at at least the first M of them; here, “first” is under the usual component-wise partial order, i.e., $w < v$ for $v, w \in \mathbb{Z}_{>0}^2$ (with $v = (v_1, v_2)$ and $w = (w_1, w_2)$) if (i) $w_1 < v_1$ or (ii) $w_1 = v_1$ and $w_2 < v_2$. Observe that the event of a given vertex v being potentially coupling for arrow x is determined by the Bernoulli random variables associated to vertices $w < v$. That is, $\{v \text{ is potentially coupling for arrow } x\} \in \sigma(\{B_w^\rightarrow, B_w^\uparrow : w < v\})$. A consequence is that, conditional on v being potentially coupling for arrow x , the random variables $(B_v^\rightarrow, B_v^\uparrow)$ are distributed as a pair of independent Bernoulli random variables of parameters b^\rightarrow and b^\uparrow , respectively (as they are independent of the random variables $(B_w^\rightarrow, B_w^\uparrow)_{w < v}$).

The probability bound. Let $\tau_1 < \tau_2 < \dots$ be the (random) coordinates of arrow x ’s potentially coupling vertices in order of appearance along its trajectory; if there is no j^{th} potentially coupling vertex, we define $\tau_j = (\infty, \infty)$. Define the σ -algebra \mathcal{F}_i by

$$\mathcal{F}_i := \left\{ \mathbb{E} \cap \{\tau_i = v\} : v \in \mathbb{Z}_{>0}^2, \mathbb{E} \in \sigma(\{B_w^\uparrow, B_w^\rightarrow : w \leq v\}) \right\}.$$

Let NC_i (short for “no coupling”) be the event that $\tau_i \neq (\infty, \infty)$ and arrow x passes through τ_i without coupling, and let $\text{NC}_{\llbracket 1, j \rrbracket} = \bigcap_{i=1}^j \text{NC}_i$ for each j . Note that $\text{NC}_i, \tau_i \in \mathcal{F}_i$ for each i . Next note that

$$\mathbb{P}(\text{NC}_1) \leq b^\rightarrow b^\uparrow + (1 - b^\rightarrow)(1 - b^\uparrow) =: \delta < 1.$$

We claim that $\mathbb{P}(\text{NC}_i \mid \text{NC}_{\llbracket 1, i-1 \rrbracket}) \leq \delta$ for each i . By the tower property of conditional expectations, this is implied by the stronger inequality

$$\mathbb{P}(\text{NC}_i \mid \mathcal{F}_{i-1}) \mathbb{1}_{\text{NC}_{\llbracket 1, i-1 \rrbracket}} \leq \delta \mathbb{1}_{\text{NC}_{\llbracket 1, i-1 \rrbracket}}.$$

The latter holds since, conditional on \mathcal{F}_{i-1} , $\{\tau_i = v\}$ is determined by the collection of random variables $\{B_w^\rightarrow, B_w^\uparrow : \tau_{i-1} \leq w < v\}$; in particular, letting \mathbf{E}_v be the event that $(B_v^\rightarrow, B_v^\uparrow) = (1, 1)$ or $(0, 0)$, we see that \mathbf{E}_v is conditionally independent of $\{\tau_i = v\}$ given \mathcal{F}_{i-1} , so

$$\begin{aligned} \mathbb{P}(\text{NC}_i \mid \mathcal{F}_{i-1}) \mathbb{1}_{\text{NC}_{[1, i-1]}} &= \sum_{v > \tau_{i-1}} \mathbb{P}(\mathbf{E}_v, \tau_i = v \mid \mathcal{F}_{i-1}) \mathbb{1}_{\text{NC}_{[1, i-1]}} \\ &= \sum_{v > \tau_{i-1}} \mathbb{P}(\mathbf{E}_v \mid \mathcal{F}_{i-1}) \cdot \mathbb{P}(\tau_i = v \mid \mathcal{F}_{i-1}) \mathbb{1}_{\text{NC}_{[1, i-1]}} \\ &= \delta \sum_{v > \tau_{i-1}} \mathbb{P}(\tau_i = v \mid \mathcal{F}_{i-1}) \mathbb{1}_{\text{NC}_{[1, i-1]}} \leq \delta \mathbb{1}_{\text{NC}_{[1, i-1]}}. \end{aligned}$$

Thus it holds that

$$\mathbb{P}(\text{NC}_{[1, M]}) = \mathbb{P}(\text{NC}_1) \cdot \prod_{i=2}^M \mathbb{P}(\text{NC}_i \mid \text{NC}_{[1, i-1]}) \leq \delta^M.$$

This establishes (D.18) and completes the proof. \square

D.4. Finite speed of discrepancy for S6V under basic coupling. Here we give the proof of Lemma D.4; it bears similarities to that of [Agg20, Proposition 2.17].

Proof of Lemma D.4. We will prove the statement for the case of $m = 1$ and use a union bound to obtain the case of general $m \in \mathbb{N}$. Since we are in the $m = 1$ case, we may assume without loss of generality that $s_1 = 1$, and we drop the second superscript in the boundary conditions and write them, for $i \in \{1, 2\}$, as $h_0^{(i)}$, and analogously we write $(j_{(x,y)}^{(i)})_{(x,y) \in \llbracket -N_i, \infty \rrbracket \times \llbracket s, \infty \rrbracket}$, for $i \in \{1, 2\}$, for the samples from the S6V models with respective boundary conditions $h_0^{(i)}$ (coupled via the basic coupling). We adopt the convention for arrow trajectories in each system (i.e., the two S6V models with initial conditions $h_0^{(1)}$ and $h_0^{(2)}$) from the beginning of the proof of Proposition D.3 from Section D.3 (recall Figure 26): in particular, all arrows in the two systems which start from the same positions (which recall we refer to as being ‘‘coupled’’) evolve first, and then the initially uncoupled arrows evolve subsequently, ‘‘bouncing’’ off of other uncoupled arrows and bouncing off or passing through coupled arrows. Recall that arrows which are uncoupled at least until a given time in their trajectories maintain their initial ordering until at least that time. Observe that all arrows which initially start in either system in $\llbracket -N_1, N_1 \rrbracket$ are coupled by assumption.

Let k be the largest value in $\llbracket -N_2, -N_1 - 1 \rrbracket$ such that there is an uncoupled arrow present at $(1, k)$ in the configuration $\eta_{h_0^{(2)}}$ corresponding to $h_0^{(2)}$ (as in (2.16)) (thus there is no arrow at $(1, k)$ in $\eta_{h_0^{(1)}}$). Now, we see that the event that $j_{(x,y)}^{(1)} \neq j_{(x,y)}^{(2)}$ for some $(x, y) \in \llbracket 1, T \rrbracket \times \llbracket -\frac{1}{2}N_1, \frac{1}{2}N_1 \rrbracket$ is contained in the event that the uncoupled arrow starting initially at $(1, k)$ in $\eta_{h_0^{(2)}}$ is incident on a vertex in $\llbracket 1, T \rrbracket \times \{-\lfloor \frac{1}{2}N_1 \rfloor\}$.

For any $y, t \in \mathbb{N}$, consider the event $\mathbf{E}_{y,t}$ that the uncoupled arrow exits horizontally from (t, x) and then exits horizontally from $(t+1, x+y')$ for some $y' \geq y$, i.e., it travels vertical distance at least y in the time step t to $t+1$. Let n be the number of coupled arrows that exit horizontally between $(t, x+1)$ and $(t, x+y-1)$ (inclusive). Now, if $\mathbf{E}_{y,t}$ occurs, it implies that all n of these coupled arrows passed straight through the vertex they horizontally entered on the vertical line $t+1$, and the uncoupled arrow passed vertically through at least $y-n-1$ many vertices which had no coupled arrow incident (it must also have not passed horizontally through $(t+1, x)$, but we will not include this in the probability upper bound). Since all these sub-events are independent, the probability of $\mathbf{E}_{y,t}$ occurring is at most $(b^\rightarrow)^n (b^\uparrow)^{y-n-1} \leq (b^\rightarrow)^{y-1}$, since $b^\uparrow \leq b^\rightarrow$.

Thus the distance the arrow starting at $(1, k)$ travels vertically in the horizontal interval $\llbracket 1, T \rrbracket$ is bounded by a sum of T independent random variables $(X_i)_{i \in \llbracket 1, T \rrbracket}$, each distributed as $\mathbb{P}(X_i \geq r) =$

$(b^-)^{r-1}$ for $r \in \mathbb{N}$. This sum has expectation $(1 - b^-)^{-1}T$. So the probability that this sum exceeds $\frac{1}{2}N_1$, under the assumed condition that $T \leq \frac{1}{4}(1 - b^-)N_1$, is bounded by $\exp(-cN_1)$ by standard concentration inequalities for sums of independent geometric random variables (e.g., [Jan18, Theorem 2.1]), completing the proof. \square

REFERENCES

- [Agg17] Amol Aggarwal. Convergence of the stochastic six-vertex model to the ASEP. *Mathematical Physics, Analysis and Geometry*, 20:1–20, 2017.
- [Agg20] Amol Aggarwal. Limit shapes and local statistics for the stochastic six-vertex model. *Communications in Mathematical Physics*, 376:681–746, 2020.
- [AB24] Amol Aggarwal and Alexei Borodin. Gibbsian line ensembles for colored stochastic vertex models. *arXiv preprint arXiv:2402.06868*, 2024.
- [ABB19] Amol Aggarwal, Alexei Borodin, and Alexey Bufetov. Stochasticization of solutions to the Yang-Baxter Equation. *Annales Henri Poincaré*, 20(8):2495–2554, August 2019.
- [AH23a] Amol Aggarwal and Jiaoyang Huang. Local statistics and concentration for non-intersecting Brownian bridges with smooth boundary data. *arXiv preprint arXiv:2308.04318*, 2023.
- [AH23b] Amol Aggarwal and Jiaoyang Huang. Strong characterization for the Airy line ensemble. *arXiv preprint arXiv:2308.11908*, 2023.
- [ANP23] Amol Aggarwal, Matthew Nicoletti, and Leonid Petrov. Colored interacting particle systems on the ring: stationary measures from Yang-Baxter equation. *arXiv preprint arXiv:2309.11865*, 2023.
- [AGZ10] Greg W. Anderson, Alice Guionnet, and Ofer Zeitouni. *An introduction to random matrices*, number 118. Cambridge university press, 2010.
- [BBS20] Márton Balázs, Ofer Busani, and Timo Seppäläinen. Non-existence of bi-infinite geodesics in the exponential corner growth model. *Forum of Mathematics, Sigma*, 8:e46, 2020.
- [BCD23] Guillaume Barraquand, Ivan Corwin, and Evgeni Dimitrov. Spatial tightness at the edge of Gibbsian line ensembles. *Communications in Mathematical Physics*, 397(3):1309–1386, 2023.
- [BGH21] Riddhipratim Basu, Shirshendu Ganguly, and Alan Hammond. Fractal geometry of Airy₂ processes coupled via the Airy sheet. *The Annals of Probability*, 49(1):485–505, 2021.
- [Baz85] Vladimir V. Bazhanov. Trigonometric solutions of triangle equations and classical Lie algebras. *Physics Letters B*, 159(4):321–324, 1985.
- [BKS85] Henk van Beijeren, Ryszard Kutner, and Herbert Spohn. Excess noise for driven diffusive systems. *Physical Review Letters*, 54(18):2026–2029, 1985.
- [BS18] Vladimir Belitsky and Gunter M Schütz. Self-duality and shock dynamics in the n-species priority asep. *Stochastic Processes and their Applications*, 128(4):1165–1207, 2018.
- [BF87] Albert Benassi and Jean-Pierre Fouque. Hydrodynamical limit for the asymmetric simple exclusion process. *The Annals of Probability*, 15(2):546–560, 1987.
- [Bill13] Patrick Billingsley. *Convergence of probability measures*. John Wiley & Sons, 2013.
- [BB21] Alexei Borodin and Alexey Bufetov. Color-position symmetry in interacting particle systems. *The Annals of Probability*, 49(4):1607–1632, 2021.
- [BBW24] Alexei Borodin, Alexey Bufetov, and Michael Wheeler. Between the stochastic six vertex model and Hall-Littlewood processes. *Journal of Combinatorial Theory, Series A*, 2024. To appear.
- [BC14] Alexei Borodin and Ivan Corwin. Macdonald processes. *Probability Theory and Related Fields*, 158(1):225–400, 2014.
- [BCG16] Alexei Borodin, Ivan Corwin, and Vadim Gorin. Stochastic six-vertex model. *Duke Mathematical Journal*, 165(3):563–624, 2016.
- [BFPS07] Alexei Borodin, Patrik Ferrari, Michael Prähofer, and Tomohiro Sasamoto. Fluctuation properties of the TASEP with periodic initial configuration. *Journal of Statistical Physics*, 129(5-6):1055–1080, 2007.
- [BGW22] Alexei Borodin, Vadim Gorin, and Michael Wheeler. Shift-invariance for vertex models and polymers. *Proceedings of the London Mathematical Society*, 124(2):182–299, 2022.
- [BO17] Alexei Borodin and Grigori Olshanski. The ASEP and determinantal point processes. *Communications in Mathematical Physics*, 353(2):853–903, 2017.
- [BW22] Alexei Borodin and Michael Wheeler. Coloured stochastic vertex models and their spectral theory. *Astérisque*, 437, 2022.
- [BW20] Alexei Borodin and Michael Wheeler. Observables of coloured stochastic vertex models and their polymer limits. *Probability and Mathematical Physics*, 1(1):205–265, 2020.

- [BK21] Alexey Bufetov and Sergei Korotkikh. Observables of stochastic colored vertex models and local relation. *Communications in Mathematical Physics*, 386(3):1881–1936, September 2021.
- [BMP21] Alexey Bufetov, Matteo Mucciconi, and Leonid Petrov. Yang-Baxter random fields and stochastic vertex models. *Advances in Mathematics*, 388:107865, 2021.
- [BP19] Alexey Bufetov and Leonid Petrov. Yang-Baxter field for spin Hall-Littlewood symmetric functions. *Forum of Mathematics, Sigma*, 7:Paper No. e39, 70, 2019.
- [Bus24] Ofer Busani. Diffusive scaling limit of the Busemann process in last passage percolation. *Annals of Probability*, 2024. To appear.
- [BSS23] Ofer Busani, Timo Seppäläinen, and Evan Sorensen. Scaling limit of multi-type invariant measures via the directed landscape. *arXiv preprint arXiv:2310.09284*, 2023.
- [BSS22] Ofer Busani, Timo Seppäläinen, and Evan Sorensen. Scaling limit of the TASEP speed process. *arXiv preprint arXiv:2211.04651*, 2022.
- [BSS24] Ofer Busani, Timo Seppäläinen, and Evan Sorensen. The stationary horizon and semi-infinite geodesics in the directed landscape. *The Annals of Probability*, 52(1):1–66, 2024.
- [CHH23] Jacob Calvert, Alan Hammond, and Milind Hegde. Brownian structure in the KPZ fixed point. *Astérisque*, 441, 2023.
- [CGW15] Luigi Cantini, Jan de Gier, and Michael Wheeler. Matrix product formula for Macdonald polynomials. *Journal of Physics A: Mathematical and Theoretical*, 48(38):384001, August 2015.
- [CGHSU22] Zeying Chen, Jan de Gier, Iori Hiki, Tomohiro Sasamoto, and Masato Usui. Limiting current distribution for a two species asymmetric exclusion process. *Communications in Mathematical Physics*, 395(1):59–142, October 2022.
- [CGW20] Zeying Chen, Jan de Gier, and Michael Wheeler. Integrable stochastic dualities and the deformed knizhnik–zamolodchikov equation. *International Mathematics Research Notices*, 2020(19):5872–5925, 2020.
- [CEP00] Henry Cohn, Noam Elkies, and James Propp. Local statistics for random domino tilings of the Aztec diamond. *arXiv preprint math/0008243*, 2000.
- [CMW22] Sylvie Corteel, Olya Mandelshtam, and Lauren Williams. From multiline queues to macdonald polynomials via the exclusion process. *American Journal of Mathematics*, 144(2):395–436, 2022.
- [Cor12] Ivan Corwin. The Kardar–Parisi–Zhang equation and universality class. *Random matrices: Theory and applications*, 1(01):1130001, 2012.
- [CD18] Ivan Corwin and Evgeni Dimitrov. Transversal fluctuations of the ASEP, stochastic six vertex model, and Hall-Littlewood Gibbsian line ensembles. *Communications in Mathematical Physics*, 363:435–501, 2018.
- [CH14] Ivan Corwin and Alan Hammond. Brownian Gibbs property for Airy line ensembles. *Inventiones mathematicae*, 195(2):441–508, 2014.
- [CH16] Ivan Corwin and Alan Hammond. KPZ line ensemble. *Probability Theory and Related Fields*, 166(1):67–185, 2016.
- [CHHM23] Ivan Corwin, Alan Hammond, Milind Hegde, and Konstantin Matetski. Exceptional times when the KPZ fixed point violates Johansson’s conjecture on maximizer uniqueness. *Electronic Journal of Probability*, 28:1–81, 2023.
- [Dau23] Duncan Dauvergne. Wiener densities for the Airy line ensemble. *arXiv preprint arXiv:2302.00097*, 2023.
- [DNV23] Duncan Dauvergne, Mihai Nica, and Bálint Virág. Uniform convergence to the Airy line ensemble. *Annales de l’Institut Henri Poincaré, Probabilités et Statistiques*, 59(4):2220–2256, 2023.
- [DOV22] Duncan Dauvergne, Janosch Ortmann, and Bálint Virág. The directed landscape. *Acta Mathematica*, 229(2):201–285, 2022.
- [DV21a] Duncan Dauvergne and Bálint Virág. Bulk properties of the Airy line ensemble. *The Annals of Probability*, 49(4):1738–1777, 2021.
- [DV21b] Duncan Dauvergne and Bálint Virág. The scaling limit of the longest increasing subsequence. *arXiv preprint arXiv:2104.08210*, 2021.
- [Dim18] Evgeni Dimitrov. KPZ and Airy limits of Hall-Littlewood random plane partitions. *Annales de l’Institut Henri Poincaré Probabilités et Statistiques*, 54(2):640–693, 2018.
- [Dim23] Evgeni Dimitrov. Two-point convergence of the stochastic six-vertex model to the Airy process. *Communications in Mathematical Physics*, 398(3):925–1027, 2023.
- [DFF⁺21] Evgeni Dimitrov, Xiang Fang, Lukas Fesser, Christian Serio, Carson Teitler, Angela Wang, and Weitao Zhu. Tightness of Bernoulli Gibbsian line ensembles. *Electronic Journal of Probability*, 26:1–93, 2021.
- [DM21] Evgeni Dimitrov and Konstantin Matetski. Characterization of Brownian Gibbsian line ensembles. *The Annals of Probability*, 49(5):2477–2529, 2021.

- [EPM09] Martin R. Evans, Sylvain Prolhac, and Kirone Mallick. The matrix product solution of the multi-species partially asymmetric exclusion process. *Journal of Physics A: Mathematical and Theoretical*, 42(16):165004, 2009.
- [FM07] Pablo A. Ferrari and James B. Martin. Stationary distributions of multi-type totally asymmetric exclusion processes. *The Annals of Probability*, 35(3):807–832, 2007.
- [FW13] Omar Foda and Michael Wheeler. Colour-independent partition functions in coloured vertex models. *Nuclear Physics B*, 871(2):330–361, 2013.
- [Gal21] Pavel Galashin. Symmetries of stochastic colored vertex models. *The Annals of Probability*, 49(5):2175–2219, 2021.
- [GH23] Shirshendu Ganguly and Milind Hegde. Local and global comparisons of the Airy difference profile to Brownian local time. *Annales de l’Institut Henri Poincaré, Probabilités et Statistiques*, 59(3):1342–1374, 2023.
- [GHZ23] Shirshendu Ganguly, Milind Hegde, and Lingfu Zhang. Brownian bridge limit of path measures in the upper tail of KPZ models. *arXiv preprint arXiv:2311.12009*, 2023.
- [GMW23] Jan de Gier, William Mead, and Michael Wheeler. Transition probability and total crossing events in the multi-species asymmetric exclusion process. *Journal of Physics A: Mathematical and Theoretical*, 56(25):255204, June 2023.
- [GS92] Leh-Hun Gwa and Herbert Spohn. Six-vertex model, roughened surfaces, and an asymmetric spin Hamiltonian. *Physical Review Letters*, 68:725–728, 6, February 1992.
- [Ham22] Alan Hammond. Brownian regularity for the Airy line ensemble, and multi-polymer watermelons in Brownian last passage percolation. *Memoirs of the American Mathematical Society*, 277(1363), 2022.
- [Har78] Theodore E. Harris. Additive set-valued Markov processes and graphical methods. *The Annals of Probability*, 6(3):355–378, 1978.
- [Hoe63] Wassily Hoeffding. Probability inequalities for sums of bounded random variables. *Journal of the American Statistical Association*, 58(301):13–30, 1963.
- [Jan18] Svante Janson. Tail bounds for sums of geometric and exponential variables. *Statistics & Probability Letters*, 135:1–6, 2018.
- [Jim86] Michio Jimbo. Quantum R matrix for the generalized Toda system. *Communications in Mathematical Physics*, 102(4):537–547, December 1986.
- [Joh03] Kurt Johansson. Discrete polynuclear growth and determinantal processes. *Communications in Mathematical Physics*, 242(1):277–329, November 2003.
- [Joh00] Kurt Johansson. Shape fluctuations and random matrices. *Communications in Mathematical Physics*, 209(2):437–476, 2000.
- [Kal21] Olav Kallenberg. *Foundations of modern probability*, volume 99 of *Probability Theory and Stochastic Modelling*. Springer, 2021, pages xii+946. Third edition.
- [KPZ86] Mehran Kardar, Giorgio Parisi, and Yi-Cheng Zhang. Dynamic scaling of growing interfaces. *Physical Review Letters*, 56(9):889, 1986.
- [Kua18] Jeffrey Kuan. An algebraic construction of duality functions for the stochastic $u_q(a_n(1))$ vertex model and its degenerations. *Communications in Mathematical Physics*, 359:121–187, 2018.
- [KRS81] Piotr P. Kulish, Nicolai Yu. Reshetikhin, and Evgeny K. Sklyanin. Yang-Baxter equation and representation theory: I. *Letters in Mathematical Physics*, 5(5):393–403, September 1981.
- [KMMO16] Atsuo Kuniba, Vladimir V. Mangazeev, Shouya Maruyama, and Masato Okado. Stochastic R matrix for $U_q(A_n^{(1)})$. *Nuclear Physics B*, 913:248–277, 2016.
- [Lig76] Thomas M. Liggett. Coupling the simple exclusion process. *The Annals of Probability*, 4(3):339–356, 1976.
- [MGP68] Carolyn T. MacDonald, Julian H. Gibbs, and Allen C. Pipkin. Kinetics of biopolymerization on nucleic acid templates. *Biopolymers*, 6(1):1–5, 1968.
- [Mar20] James B. Martin. Stationary distributions of the multi-type ASEP. *Electronic Journal of Probability*, 25(43):1–41, 2020.
- [MQR21] Konstantin Matetski, Jeremy Quastel, and Daniel Remenik. The KPZ fixed point. *Acta Mathematica*, 227(1):115–203, 2021.
- [NQR20] Mihai Nica, Jeremy Quastel, and Daniel Remenik. One-sided reflected Brownian motions and the KPZ fixed point. *Forum of Mathematics, Sigma*, 8:e63, 2020.
- [NY04] Masatoshi Noumi and Yasuhiko Yamada. Tropical Robinson-Schensted-Knuth correspondence and birational Weyl group actions. *Advanced Studies in Pure Mathematics*, 40:371–442, 2004.

- [OR03] Andrei Okounkov and Nikolai Reshetikhin. Correlation function of Schur process with application to local geometry of a random 3-dimensional Young diagram. *Journal of the American Mathematical Society*:581–603, 2003.
- [Par23] Shalin Parekh. Convergence of ASEP to KPZ with basic coupling of the dynamics. *Stochastic Processes and their Applications*, 160:351–370, 2023.
- [Pau35] Linus Pauling. The structure and entropy of ice and of other crystals with some randomness of atomic arrangement. *Journal of the American Chemical Society*, 57(12):2680–2684, 1935.
- [PS02] Michael Prähofer and Herbert Spohn. Scale invariance of the PNG droplet and the Airy process. *Journal of Statistical Physics*, 108(5-6):1071–1106, 2002. Dedicated to David Ruelle and Yasha Sinai on the occasion of their 65th birthdays.
- [QS22] Jeremy Quastel and Sourav Sarkar. Convergence of exclusion processes and the KPZ equation to the KPZ fixed point. *Journal of the American Mathematical Society*, 2022.
- [QS15] Jeremy Quastel and Herbert Spohn. The one-dimensional KPZ equation and its universality class. *Journal of Statistical Physics*, 160:965–984, 2015.
- [Rez91] Fraydoun Rezakhanlou. Hydrodynamic limit for attractive particle systems on \mathbf{Z}^d . *Communications in Mathematical Physics*, 140(3):417–448, 1991.
- [Ros81] Hermann Rost. Nonequilibrium behaviour of a many particle process: density profile and local equilibria. *Zeitschrift für Wahrscheinlichkeitstheorie und Verwandte Gebiete*, 58(1):41–53, 1981.
- [Spi70] Frank Spitzer. Interaction of Markov processes. *Advances in Mathematics*, 5(2):246–290, 1970.
- [Spo14a] Herbert Spohn. KPZ scaling theory and the semi-discrete polymer model. *Random Matrix Theory, Interacting Particle Systems and Integrable Systems*, 65(4.3), 2014.
- [Spo14b] Herbert Spohn. Nonlinear fluctuating hydrodynamics for anharmonic chains. *Journal of Statistical Physics*, 154(5):1191–1227, March 2014.
- [TW09] Craig A. Tracy and Harold Widom. Asymptotics in ASEP with step initial condition. *Communications in Mathematical Physics*, 290:129–154, 2009.
- [TW94] Craig A. Tracy and Harold Widom. Level-spacing distributions and the Airy kernel. *Communications in Mathematical Physics*, 159(1):151–174, 1994.
- [Vir20] Bálint Virág. The heat and the landscape I. *arXiv preprint arXiv:2008.07241*, 2020.
- [Wu23] Xuan Wu. The KPZ equation and the directed landscape. *arXiv preprint arXiv:2301.00547*, 2023.
- [Zha23] Lingfu Zhang. Shift-invariance of the colored TASEP and finishing times of the oriented swap process. *Advances in Mathematics*, 415:Paper No. 108884, 60, 2023.